# Investigations on Machining Aspects of Inconel 718 during Wire Electro-Discharge Machining (WEDM): Experimental and Numerical analysis

**Anshuman Kumar**

Department of Mechanical Engineering
**National Institute of Technology Rourkela**

# Investigations on Machining Aspects of Inconel 718 during Wire Electro-Discharge Machining (WEDM): Experimental and Numerical analysis

*Dissertation submitted to the*

***National Institute of Technology Rourkela***

*in partial fulfillment of the requirements*

*of the degree of*

***Doctor of Philosophy***

*in*

***Mechanical Engineering***

*by*

***Anshuman Kumar***
(Roll Number: 512ME115)

*under the supervision of*

***Prof. K.P.Maity***

November 2016

Department of Mechanical Engineering
**National Institute of Technology Rourkela**

Department of Mechanical Engineering
**National Institute of Technology Rourkela**

# Certificate of Examination

Roll Number: *512ME115*

Name: *Anshuman Kumar*

Title of Dissertation: *Investigations on Machining Aspects of Inconel 718 during Wire Electro-Discharge Machining (WEDM): Experimental and Numerical analysis.*

We the below signed, after checking the dissertation mentioned above and the official record book (s) of the student, hereby state our approval of the dissertation submitted in partial fulfillment of the requirements of the degree of *Doctor of Philosophy* in *Mechanical Engineering* at *National Institute of Technology Rourkela*. We are satisfied with the volume, quality, correctness, and originality of the work.

Prof. K.P.Maity
Principal Supervisor

Prof. B.B.Biswal
Chairman , DSC Member

Prof. A.K.Mondal
Member, DSC

Prof. D.P.Mohapatra
Member, DSC

Prof. S.K.Sahoo
Member, DSC

Department of Mechanical Engineering
**National Institute of Technology Rourkela**

**Prof. K.P.Maity**

Professor

November 26, 2016

# Supervisors' Certificate

This is to certify that the work presented in the dissertation entitled "*Investigations on Machining Aspects of Inconel 718 during Wire Electro-Discharge Machining (WEDM): Experimental and Numerical Analysis" submitted* by ***Anshuman Kumar***, Roll Number **512me115** is a record of original research carried out by my under my supervision and guidance in partial fulfillment of the requirements of the degree of *Doctor of Philosophy* in *Mechanical Engineering*. Neither this dissertation nor any part of it has been submitted earlier for any degree or diploma to any institute or university in India or abroad.

Prof. K.P.Maity
Professor
Department of Mechanical Engineering
National Institute of Technology, Rourkela

*Dedicated*

*to*

*My Family*

# Declaration of Originality

I, *Anshuman Kumar*, Roll Number *512ME115* hereby declare that this dissertation entitled "*Investigations on Machining Aspects of Inconel 718 during Wire Electro-Discharge Machining (WEDM): Experimental and Numerical analysis"* presents my original work carried out as a doctoral student of NIT Rourkela and, to the best of my knowledge, contains no material previously published or written by another person, nor any material presented by me for the award of any degree or diploma of NIT Rourkela or any other institution. Any contribution made to this research by others, with whom I have worked at NIT Rourkela or elsewhere, is explicitly acknowledged in the dissertation. Works of other authors cited in this dissertation have been duly acknowledged under the sections "Reference" or "Bibliography". I have also submitted my original research records to the scrutiny committee for evaluation of my dissertation.

I am fully aware that in case of any non-compliance detected in future, the Senate of NIT Rourkela may withdraw the degree awarded to me on the basis of the present dissertation.

November 26, 2016

NIT Rourkela *Anshuman Kumar*

# Acknowledgment

I take the opportunity to express my first thanks and sincere gratitude to my supervisor, **Prof. Kalipada Maity**, Mechanical Engineering Department, National Institute of Technology, Rourkela for his insistent help and guidance, constructive suggestions from early stage of this research and providing me extraordinary experiences throughout the work. It has been a benediction for me to spend many opportune moments under the guidance of the perfectionist at the acme of professionalism. The present work is a testimony to his alacrity, inspiration and ardent personal interest, taken by him during the course of this thesis work in its present form.

I am grateful to **Prof. Siba Sankar Mahapatra**, Head of department, Mechanical Engineering Department, National Institute of Technology, Rourkela for providing facilities to carry out the investigations..

I am grateful to **Prof. A. Biswas**, Director, National Institute of Technology, Rourkela, for his timely support and encouragement during the academic requirements.

I express my thankfulness to the faculty and staff members of the Department of Mechanical Engineering for providing valuable suggestions concerning this research work.

I would like to thank I am indebted to our respected sir **Dr. Saurav Datta**, Assistant Professor, Department of Mechanical Engineering and my colleagues **Mr. Swastik Pradhan, Dr. Sambit Kumar Mohapatra**, **Mr. Himanshu Mishra, Mr. Himadri Majumdar, Mr. Sarat Chaini**, **Ms. Munmun Bhaumik, Mr. Akhtar Khan**, **Mr. Asit Parida, Dr. Kumar Abhishek**, **Mr. Suman Chatterjee** and **Mr. Chandramani Upadhaya** for their support and co-operation which is difficult to express in words. The time spent with them will remain in my memory for years to come

November 26, 2016
NIT Rourkela

*Anshuman Kumar*
Roll Number: 512ME115

# Abstract

Wire electro- discharge machining (WEDM) is known as unique cutting in manufacturing industries, especially in the good tolerance with intricate shape geometry in die industry. In this study the workpiece has been chosen as Inconel 718. Inconel 718 super alloy is widely used in aerospace industries. This nickel based super alloy has excellent resistance to high temperature, mechanical and chemical degradations with toughness and work hardening characteristics materials. Due to these properties, the machinability studies of this material have been carried-out in this study. The machining of Inconel 718 using variation of wire electrode material (brass wire electrode and zinc coated brass wire) with diameter equal to 0.20mm has been carried out. The objective of this study is mainly to investigate the various WEDM process parameters and performance of wire electrodes materials on Inconel 718 with various types of cutting. The optimal process parameter setting for each of wire electrode material has been obtained for multi-objective response. The kerf width, Material Removal Rate (MRR) and surface finish, corner error, corner deviation and angular error are the responses which are function of process variables viz. pulse-on time, discharge current, wire speed, flushing pressure and taper angle. The non-linear regression analysis has been developed for relationship between the process parameter and process characteristics. The optimal parameters setting have been carried out using multi-objective nature-inspired meta-heuristic optimization algorithm such as Whale Optimization Algorithm (WOA) and Gray Wolf Optimizer (GWO). Lastly numerical model analysis has been carried out to determine MRR and residual stress using ANSYS software and MRR model validated with the experimental results. The overlapping approach has been adopted for solving the multi-spark problem and validate with the experimental results.

**Keywords**: Wire electrical discharge machining (WEDM); Inconel 718; brass wire; zinc coated brass wire; Taper cutting; Whale Optimization Algorithm (WOA); Gray Wolf Optimizer (GWO).

# Contents

# List of Figures

# List of Tables

# Chapter 1

## 1. Introduction

WEDM is considered as a unique conventional machining process, which uses a wire electrode to initialize the sparking process. This non-traditional machining method is commonly used for very hard materials that would be difficult to machine with conventional technique. It has been extensively used, especially for cutting intricate contours or delicate cavities which would be difficult to produce with conventional machining methods.

In this process a continuously travelling wire electrode with different wire materials like, brass, copper, tungsten of diameter varing from 0.05 to 0.30mm, which can cut intricate shape and sharp corner radii. The wire should have constant tension using CNC program for achieving good parts shapes. During the machining process, there have been no direct contacts between the workpiece and tool (wire).

WEDM process has incredible potential in its applicability in the present scenario in the manufacturing sector for achieving a good surface finish, dimensional accuracy etc. of the products. The difficulties encountered in the die sinking EDM are avoided by WEDM, because intricate shape tool is switched by moving wire and relative movement of wire guides.

Wire electrical discharge machining (WEDM) is widely accepted non-traditional material removal process used to manufacture components with intricate shapes, close tolerance and precision. The first numerically controlled CNC wire cut machine was developed in the year 1969. The development was a modification to the die sinking process. In 1974, D.H.Dulebohn applied the optical line follower system to automatically control the shape of the component to be machined by the WEDM process. By 1975, its popularity was rapidly increasing, as the process and its capabilities were better understood by the industry. It was only towards the end of the 1970s, when computer numerical control (CNC) system was added to WEDM and brought about a major evolution of the machining process. Die-sinking electrical discharge machining (EDM) process possesses some limitations of cutting, but in WEDM process the wire (Tool) can move in different directions to produce intricate cutting. To obtain fine accuracy and complex shape of super hard materials dimension obtained; WEDM is more unique machining process.

Without the WEDM process the fabrication of precision workpieces gives high production cost for surface grinding and polish [1, 2]. Due to its increasing demand in the manufacturing sector, many investigators have carried out research to study different aspect of WEDM process. [3-5]

### 1.1.1 Process principle of WEDM

The pulse generator unit has generated a series of electrical pulse, which is applied in material removing from the workpiece (anode) with the help of continuous travelling wire electrode (cathode) separated by a stream of dielectric fluid which continuously pass through machining zone with the help of nozzle (Figure. 1.1) and converted it into thermal-energy at temperature of around $8000^{o}C$ – $12000^{o}C$ [6].

As the process proceeds, the controller moves the worktable carrying the workpiece transversely along a programmed path in the controller. The WEDM machine tool comprises of a main worktable (X-Y) on which the work piece is clamped; an auxiliary table (U-V) and wire drive mechanism. The main table moves along X and Y axes and it is driven by the DV servo motors. The spool supplies and renews the cutting tool that performs the work. The wire collection bin that holds the used wire must be emptied at regular intervals and with the constant wire tension between the pair of wire guide located at the opposite sides of the workpiece. The lower guide is having important role of intricate cutting in this process. The ranges of gap between the wire and the workpiece have been 0.025 to 0.075mm and constantly maintained by a CNC controller system.

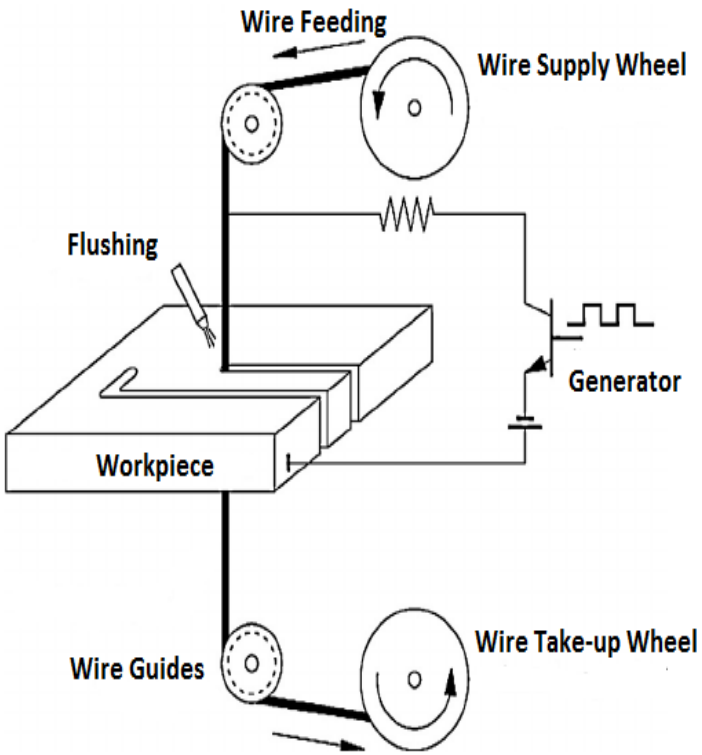


Figure 1.1: Working principle of WEDM process.

[7]

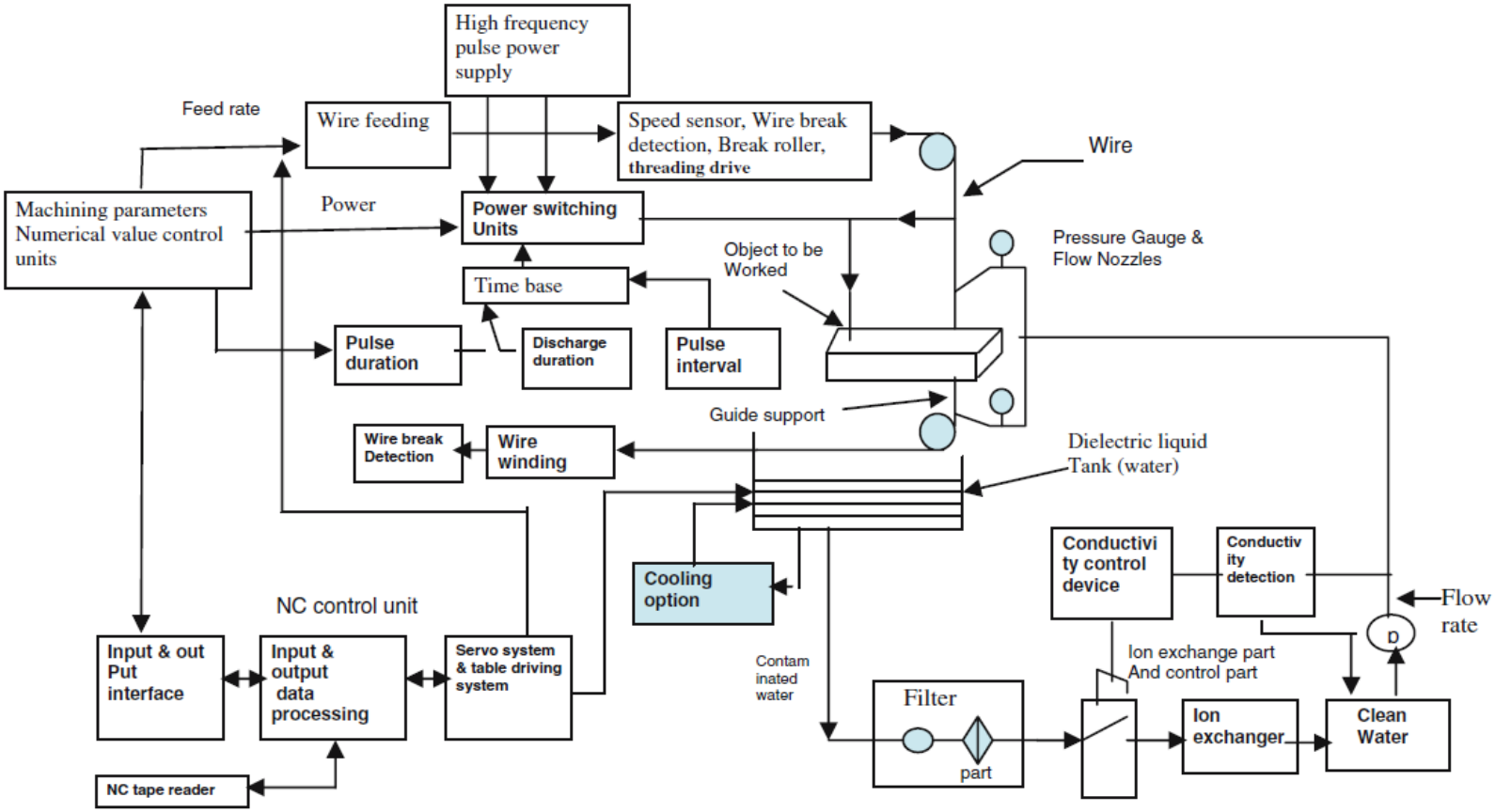


Figure 1.2: Schematic diagram of WEDM. [8]

### 1.1.2 Important machining process parameters of WEDM

The researcher has shown that EDM parameters consist of two functional groups [9]

i. *Electrical parameters*, e.g., polarity, peak current, pulse duration, and powder supply voltage, and
ii. *Non-electrical parameters*, e.g., rotational speed of the electrode, injection flushing pressure of the dielectric fluid.

According the [10] categorized the parameters into five groups:

i. *Dielectric fluid* - Type of dielectric, temperature, pressure, flushing system
ii. *Machining responses*- Servo system and stability stiffness, thermal stability and accuracy
iii. *Tool*- Material, shape, accuracy
*iv.* *Workpiece*
v. *Controllable parameters* - Discharge current, gap voltage, pulse duration, polarity, charge frequency, capacitance and tool materials

Different investigators have studied the significance of machining parameters of WEDM that affect the machining responses. Mandal et al. [11] studied the model and optimization of machining Nimonic C-263 super alloy using multi-cut strategy in WEDM. The pulse-on time, pulse-off time, voltage, and flushing pressure were the machining controllable parameters and the machining responses were chosen as cutting rate, surface roughness, spark gap and wire wear ratio. The electrical parameters are more significant parameters on the machining responses than the non-electrical parameters.

Gökler and Ozanözgü (2000) presented an investigation of the effect and optimization of machining controllable parameters on machining responses such as kerf width and MRR in WEDM operation. The most significant parameters on both the machining responses have been found as open circuit voltage and pulse-on time wire and flushing pressure has been observed less effective parameter. Previous researchers had also indicated that electrical parameters were more significant than that of the non-electrical parameters for getting the machining responses.

### 1.1.3 Electrical parameter of WEDM Operation

The selection of proper machining process is desirable prior to operation for accuracy and productivity. WEDM process is affected by various electrical parameters such as pulse-on time, pulse-off time, servo voltage, discharge current and pulse frequency and non-electrical parameters such as flushing pressure, wire speed, wire tension, cutting angle and taper angle. Part thickness in work material and wire material, diameter of wire electrode in wire electrode materials are the basic parameters in WEDM process. Some of the important parameters, which influence the machining responses in WEDM process, are discuss below:

***Pulse-on time***: The time duration of successive pulse during of the machining process performed during the pulse-on time. The erosion rates are mainly affected by pulse parameter. The longer pulse-on time increases the material removal rate from the existing workpiece but deteriorate the surface finish [12]. The unit of pulse-on time is in micro-second (µs)

***Pulse-off time:*** During the machining time, the time duration of two successive pulses has been called pulse-off time. Graphically presentation has been shown in Figure. 1.3. During this time the re-ionization of the dielectric takes place, which can affect the speed of the operation in a large way. The pulse-off time also governs the stability of the process. An insufficient pulse-off time can lead to irregular cycling and retraction of the advancing servo thereby slowing down the operation cycle [13]. Moreover, pulse-off time also provides the time to clear the eroded material and also prevents from the re-cast layer and the wire brakeage. Too short pulse interval will increase the relative wear ratio and will deteriorate the surface finish of the WEDMed surface [14].

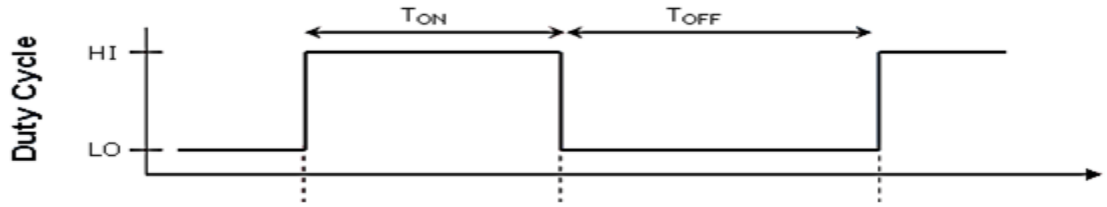


Figure 1.3 Graphical Representation of Sparking Cycles

***Duty factor***: It is a ratio of pulse-on time to total spark time. It controls the number of sparks per unit time.

$$Duty\ Factor = \frac{Pulse\ on\ time\ (T_{on})}{Pulse\ on\ time\ (T_{on}) + Pulse\ off\ time\ (T_{off})}$$

***Discharge current***: This is also an important primary process parameter of WEDM process. The stronger discharge current increases MRR, over cut and surface roughness. Proper selection of discharge current minimizes the electrode wear rate [15], [14].

### 1.1.4 Non-electrical parameters of WEDM

**1.1.4.1 Flushing pressure**: It is one of the non-electrical process parameter. The flushing pressure may effect on the machining responses like surface roughness and electrode wear rate during the WEDM. The proper flushing flow would give the better debris removal from the workpiece during the machining, thus improving the machining efficiency and surface finish. The unit of flushing pressure is in bar.

**1.1.4.2 Spark gap*:*** The spark gap is also important non-electrical parameters. The gap between the workpiece and wire electrode represented by anode and cathode which is separated by a controlled gap which constantly controlled by the machine. The schematic representation of spark gap is shown in Figure 1.4.

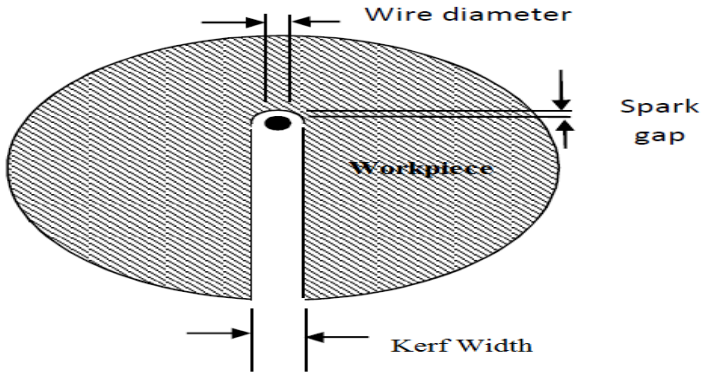


Figure 1.4 schematic Representation of spark gap [16]

This overcut is in the range of 0.020 – 0.050 mm [17]. The most common sparking gap is 0.03 mm. Once cutting condition has been established for a given cut, the overcut remains fairly constant and predictable.

### 1.1.5 Electrode Parameter

**1.1.5.1 Wire speed**: It is the speed of the wire spool in the WEDM process. Higher wire speed gives the machining stability and prevents from the wire brakeage. It's represented in mm/s.

**1.1.5.2 Wire tension**: It is the stretch between the upper guide and the lower guide of wire during the machining process. It also indicates the stability during the machining process. The proper selection of wire tension gives accuracy in cutting, especially in sharp corner cut and also prevent from the wire breakage.

#### 1.1.5.3 Wire electrode materials

The development of wire electrodes used in WEDM owing to the evolution of new materials exerts a significant influence and has helped their use for high speed production applications [18],[19]. For productivity improvement of electrode dies and achieving high quality there is demand for high performance wire electrodes [20].

The electrical properties are expressed by its electrical resistance. These properties minimizes the energy loses with the help of two current contacts and selecting high conductivity tool electrode material like, brass, copper, aluminum with proper selection of machining process parameter. The tool conductivity shows how readily the energy is transferred from power feed to the actual point of cutting [20].

Brass wire had been introduced in the WEDM process in half of the 1970s, with the replacement of pure copper. The zinc coated copper were first used for high cutting speed in 1980, this zinc coated brass wire electrode is having high tensile strength and good weldability nature.

High performance wires such as coated, composite, and diffusion-annealed wires are characterized by high conductivity and spark ability. These are generally zinc-coated wires with a copper-brass alloy or steel core; the brass contains either a small amount of chromium or high concentration of zinc.

From the last decay researchers were using brass wire as electrode material in WEDM process [21], [22], [23] . Brass wire electrode is widely used in industries due to its good

machining properties and can be die casted or extruded for specialized application. It's having tensile strength, good electrical conductivity and wire durability to close tolerances.

The different investigators [8, 24, 25] used coated wire electrodes to investigate WEDM machining performance. The coated brass wire also produces good surface finish. Prohaszka et al. [26] observed that there were increased of cutting speed by 50% with the use of coated brass wire.

Figure 1.4 shows the desirable properties of wire electrode for WEDM operation. The properties required for the wire electrode are (i) electrical properties (ii) geometrical properties, (iii) physical properties and (iv) mechanical properties [27].

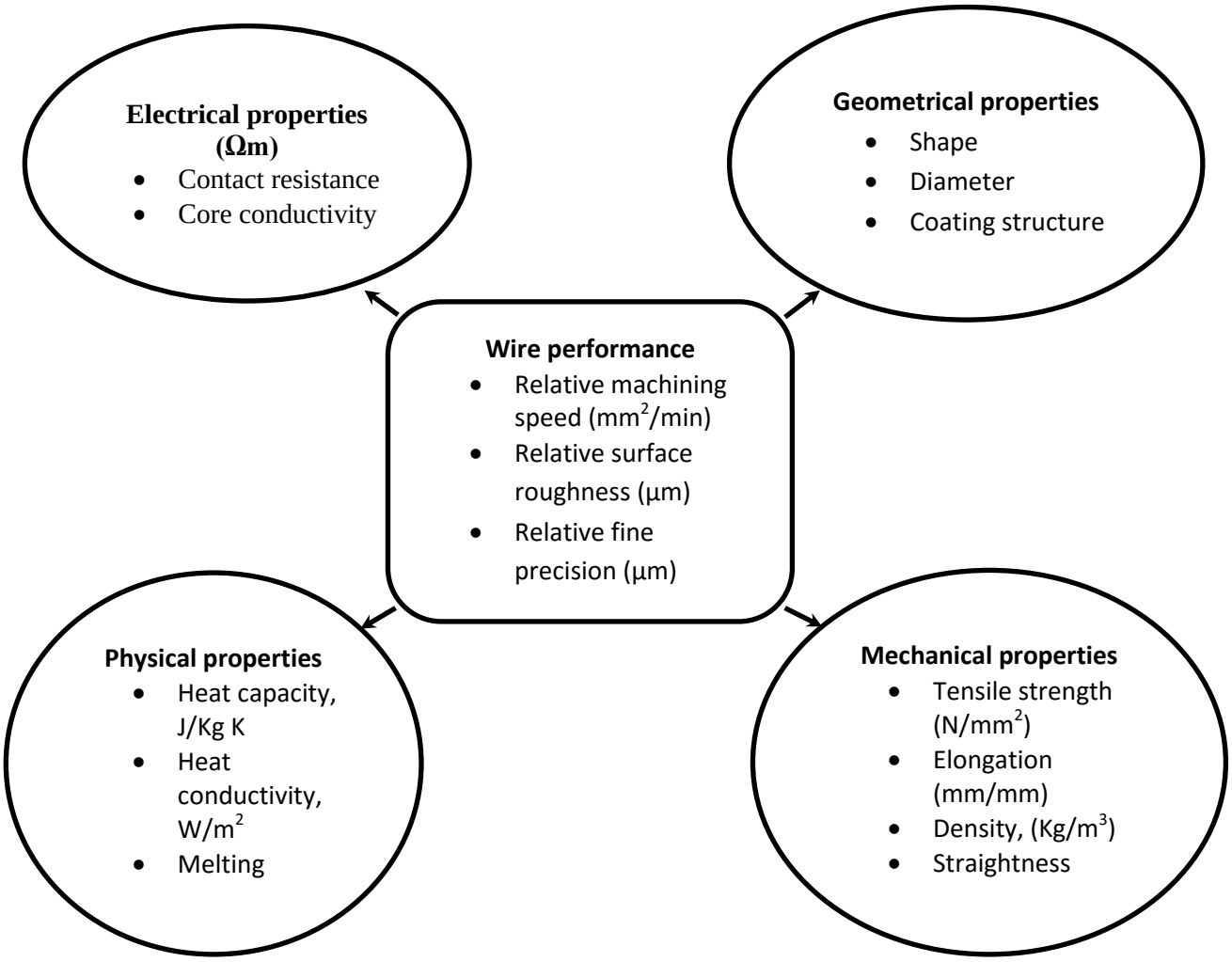


Figure 1.5 Wire electrode performance for WEDM process [28]

### 1.1.5.3.1 Copper Wire

Copper was the first material used in WEDM operation. Copper having excellent conductivity, low tensile strength, high melting point and low vapor pressure severely limited its application. Due to predominant the electro-thermal condition during WEDM operation, copper wire wears rapidly and its tension ability is rather poor, resulting, therefore, in machining instabilities, due to high degree of short circuits, especially in the machining of small curvature. The schematic diagram has been shown in Figure. 1.6

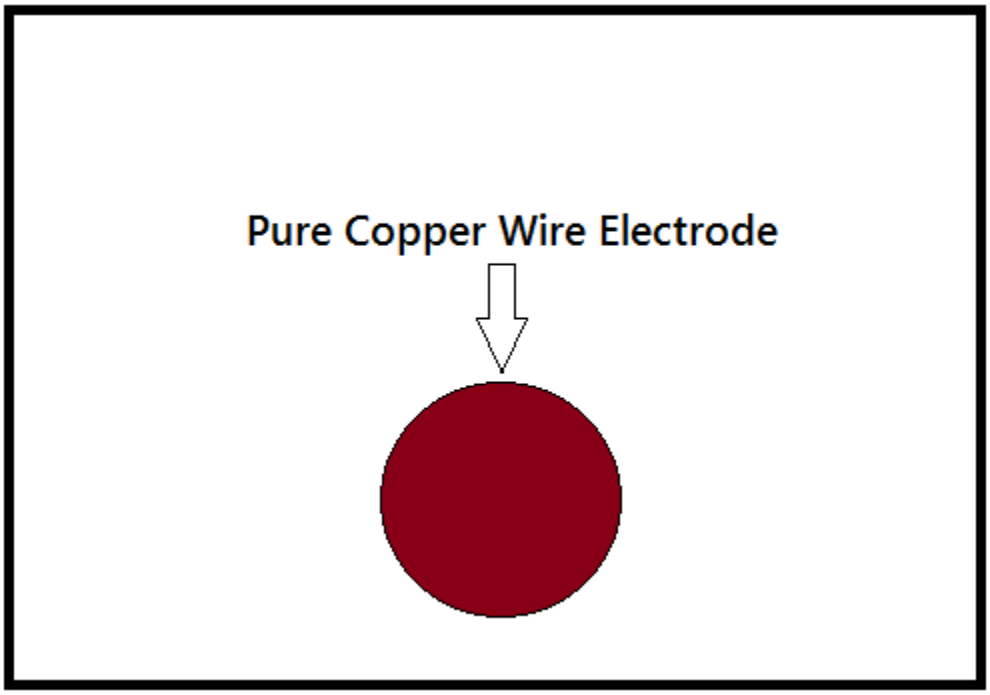


Figure 1.6 Pure Copper wire electrode

### 1.1.5.3 .2 Brass wire

Bass was the first good alternative to copper when researchers were looking for better performance. Brass wire electrode is a combination of copper and zinc, typically alloyed in the range of 63%-65% Cu and 35%-37% Zn [29].

Brass wire having addition zinc element provides significantly higher tensile strength, lower melting point and higher vapor pressure, which offsets the relative losses in conductivity. The zinc in brass wire electrode vaporizes during the cutting process, which helps the wire cool and delivers more energy to the workpiece. Brass wire becomes the most widely used electrode

material for general-purpose wire. Now a day, it is commercially available in a wide range of tensile strengths and hardness. ([30]). The schematic has been shown in Figure. 1.7

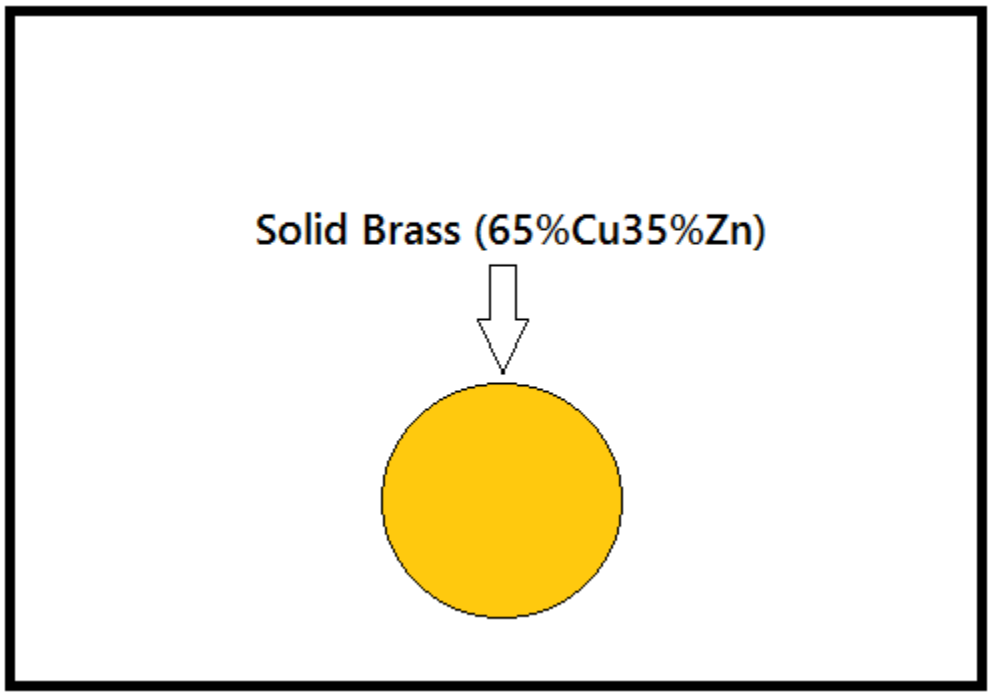


Figure 1.7 Brass wire electrode

### 1.1.5.3.3 Coated wire

Coated wire is commonly working in WEDM process to increase substantially the cutting speed and cutting precision. Since brass wires cannot be efficiently fabricated with any higher concentration of zinc, the logical next step is the development of coated wires, sometimes called plated or "stratified" wire. They typically have a core of brass or copper, for conductivity and tensile strength, and are electroplated with a coating of pure or diffused zinc for enhanced spark formation and flush characteristics.

Originally called "speed wire" due to their ability to cut at significantly higher metal removal rates [26], coated wires are now available in a wide variety of core materials, coating materials, coating depths and tensile strengths, to suit the various applications and machine requirements. Although more expensive than brass, coated wires currently represent the optimum choice for top all-around performance, and their relative economics are covered in a later section. Table 1.1 indicates the designation of these coated wire and their applications. The schematic diagram has been shown in Figure. 1.8

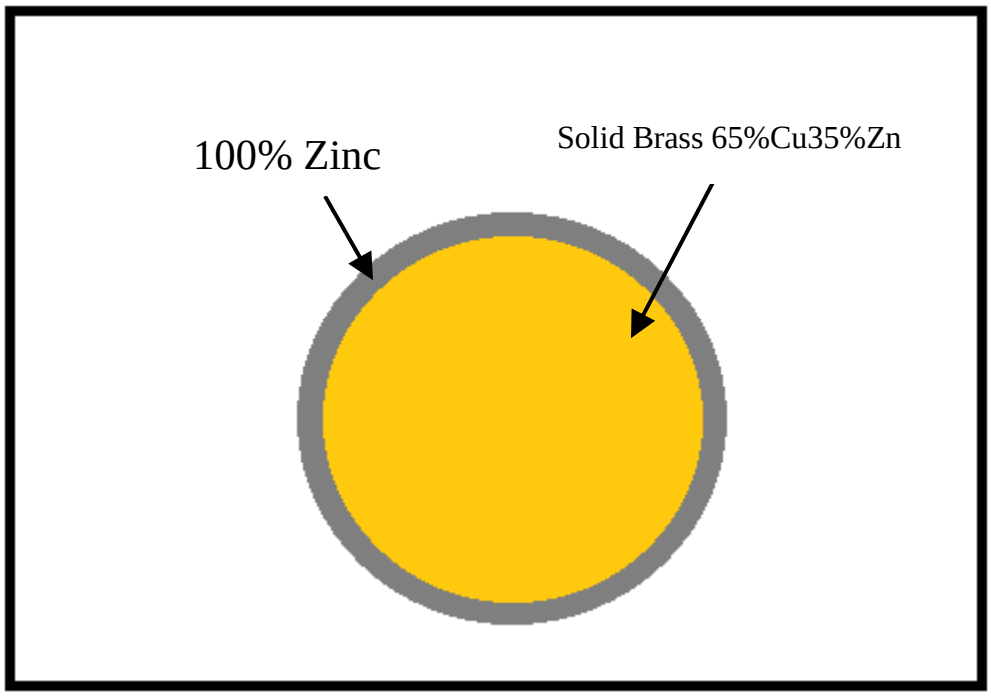


Figure 1.8 Zinc coated brass wire electrode

Table 1.1: Types of coated wire and their applications

| | Type of Wire (Charmilles Machine) | Diameter of wire (mm) | Basic Material | Applications |
|---|---|---|---|---|
| 1 | Zinc coated brass wire (half hard zinc coated brass) | 0.20-0.25 | CuZn37 | Characteristic and application similar to those of half hard brass wire |
| 2 | Diffused zinc coated copper, XS25-XS30 | 0.25-0.30 | Cu | Better usage for cylindrical cut, 1 roughness and 2 finishing Passes |
| 3 | Brass coated with special alloy | 0.30 -0.07 | Special alloy | Allows high wire tensions making it possible to produce high precision punches and dies with fines detail. |

### 1.1.4 Important Performance Measures Characteristics of the Process

WEDM performance is mainly measured by the material removal rate (MRR), surface roughness, kerf width, dimensional deviation, corner error and angular error (Taper cutting) during the different type of cutting in WEDM process. Theses machining responses characteristics have been identified by the previous researchers as the most significant criteria that can influence of WEDM performance.

#### 1.1.4.1 Material Removal in WEDM Process

The mechanisms of material removal rate in WEDM are similar to EDM operation. The Material removal Rate in WEDM mainly depends on speed and accuracy. Speed should be expressed in terms of length divided by time. The unit of MRR is in $mm^3$/min. A good numbers of research works have been carried out to maximize the MRR and cutting speed because these factors can considerably increase production as well as economic benefits of WEDM operation.

MRR is calculated by using the formula that can be expressed as: [31]:

$$MRR = K \times t \times C_s \times \rho \quad (1.1)$$

Here K is the kerf width (mm), t is the thickness (mm), Cs cutting speed (mm/min) and ρ is the density of the workpiece material. The MRR depends on amount of current of each discharge, frequency of the discharge, wire material, workpiece material and dielectric flushing condition. Material removal from the workpiece is due to melting and vaporization caused by the electric spark discharge generated by a pulsating direct current power supply between the electrodes. The sparks have been initiated between the tool and the workpiece which separated by dielectric fluid. Distilled water has been used as dielectric in WEDM process, because its having low viscosity and rapid cooling characteristics [2]. Discharge current, pulse duration and dielectric flow rate and their interaction play significant roles in rough cutting operations for maximization of MRR [32].

#### 1.1.4.2 Surface roughness

Surface roughness also known as surface texture are terms used to describe the general quality of machined surface, which is concerned with the geometric irregularities and the quality of a surface. The surface quality of a machined surface has an important response to full fill the customers demand, longevity and reliability.

Surface roughness is significantly affected by the pulse-on time, peak current and cutting speed. There is an inverse relationship between cutting speed and surface roughness. Pulse-on time is the most significant factor that affects surface roughness, and its increase causes an increase of surface roughness because of "double sparking" phenomenon which produces a poor surface finish [33]. The process parameters affect the craters size (diameter and depth) on wire electrode. Large sizes of craters on the wire increase the risk of wire rupture and also result in deteriorating the surface finish on the workpiece with decrease in machining accuracy. Roughness can be measured by a profile-meter that can be in contact or optical type.

### 1.1.4.3 Kerf Width

Kerf width is illustrated in Figure. 1.4. It is used to determine the dimensional accuracy of the finishing part of the machined product in WEDM process. Parashar et al. [34] investigated the effect of process parameters on kerf width using SS304L stainless steel as workpiece. The results shows that pulse-on time and flushing pressure are the most significant parameters and gap voltage, pulse-off time and wire feed are insignificant parameters on kerf width. Tosun et al. [14] shows the performance of process parameters on kerf width and claims that the pulse-on time and gap voltage are the most significant parameters whereas flushing pressure and wire speed are the insignificant parameters.

### 1.1.4.4 Dimensional Deviation

WEDM is mainly used for intricate shapes with good dimensional accuracy. Wire lag can create geometrical inaccuracy in the final machined product and it's important to minimize it. Now-a-days the most of investigations about wire lag can improve the accuracy in corner cutting with wire EDM. Sarkar et al. [35] illustrated about the sharp cutting or curve profile cutting. The corner error at the die is much higher than the punch. Selvakumar et al. [36] discussed the strategies to improve the corner accuracy. First strategy is to modify the process parameter (pulse-on time, pulse-off time, peak current etc.) in order to reduce the wire deflection. Second strategy is to modify the wire path to compensate the geometrical accuracy in an online manner. Furthermore, wire tension has the greatest effect on three dimensional accuracy characteristics in WEDM.

### 1.1.4.5 Angular error in Taper cutting

Taper cutting involves the generation of inclined ruled surfaces, and it is especially important in the manufacturing of tooling requiring draft angles. In taper cutting, cutting angle is greater than $5^{o}$. The angle is achieved by applying relative displacement of taper and lower guides in WEDM as shown Figure. 1.9.

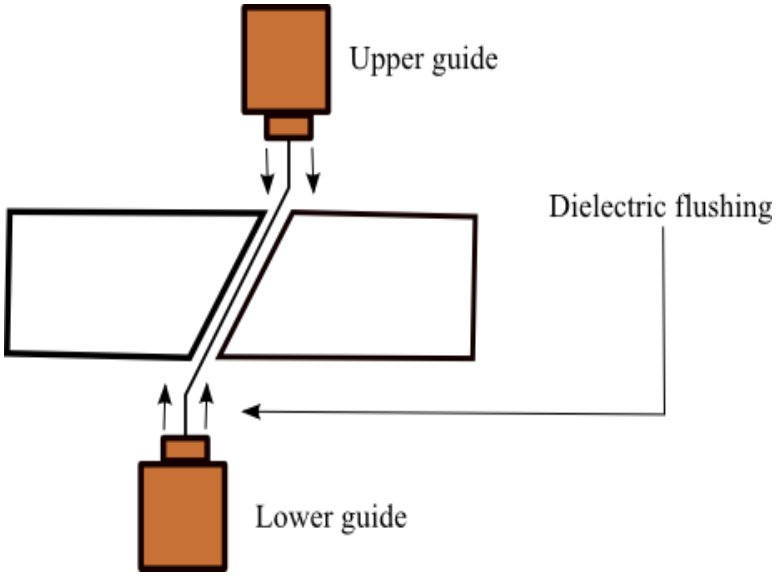


Figure 1.9 Relative displacement of taper and lower guides in WEDM taper-cutting

Taper cutting has been a very unique capability of WEDM process which any drafted parts can be produced. Nonetheless, little attempt has been made on the taper cutting by the past researchers. Generally, all type of dies are having some taper angle to avoid eventual part sticking and facilitate ejection [37]. In the taper cutting, the deformation caused by the rigidity of the wire in generation of a given angle is also of primary importance. The wire deformation during cutting leads to deviations in the inclination angle of machined parts. This fact causes dimensional errors and loss of tolerances that can lead to the rejection of high added value tooling. In the machining of taper cut, the value of error depends on aspects such as the distance between upper and lower guides, the stiffness of the wire, in geometry of the guides and the forces exerted during the cutting process.

### 1.1.6 Workpiece

#### 1.1.6.1 Nickel based super alloy Inconel 718

Inconel is a relatively recent alloy as its industrial use started in 1965 [38]. These materials having extensively used in high temperature applications such as nuclear reactors, electrical power generation equipment, gas turbine, aerospace industries and high temperature chemical vessels etc. The nickel based alloys contain at least 50% nickel and are characterized by the high phase stability of the FCC austenitic (γ) matrix. Many nickel based alloys contain 10–20% of chromium, up to 8% of aluminum and titanium combined 5–15% of cobalt, and small amounts of boron, zirconium, hafnium and carbon. The super alloys are the most difficult to machine material by the conventional machining, because their low thermal conductivities cause high temperatures during machining. The combination of high strength, toughness, and ductility impairs chip segmentation, while the presence of abrasive carbide particles accelerates tool wear. This alloys have to rapidly work harden which can create a hardened surface layer that degrades the surface integrity and can lead to lower fatigue life. It is used by 50% of weight only in aircraft turbojet engines in the form of major parts of discs, blades and casing of high pressure part of compressor and discs and blades of turbines. It is also used in rocket engines and cryogenic conditions as it offers high toughness and secures components from brittle transformation. However, non-conventional machining is the best options, to machine these alloy, among the all non-conventional machining WEDM is the good options because of its feasibility of cutting of different types of profile. WEDM is having the best capability for cutting and it's a backbone of manufacturing from last decades.

Inconel 718 super alloy is the most common and widely used in different industries. This is having high nickel material content super-alloy possessing high strength at elevated temperatures and resistance to oxidation and corrosion.

Inconel 718 super-alloy is very difficult to be machined. This alloy can be machined by WEDM, and this process is widely used for machining them [39].

### 1.1.6.2 Characteristics of Inconel 718 [40]

i. Rapid work hardening during machining
ii. Retention of high strength levels at elevated temperature
iii. Low thermal conductivities

### 1.1.6.3 Physical and mechanical properties of Inconel 718

This is widely used alloy which has creep-rupture strength at high temperatures up to 700ºC. This is used in gas turbines, rocket motors, spacecraft, nuclear reactors, pumps and tooling [40].The chemical composition of Inconel 718 has been shown in Table 1.2.

Table 1.2: Chemical composition of Inconel 718 [41]

| **Element** | **Ni+Co** | **Cr** | **Fe** | **Nb+Ta** | **Mo** | **Ti** | **Al** |
|---|---|---|---|---|---|---|---|
| Content wt. (%) | 50-55 | 17-21 | Bal | 4.45-5.5 | 2.8-3.3 | 0.65-1.15 | 0.2-0.8 |

Table 1.3: Physical properties of Inconel 718

| **Properties** | **Unit** | **Value** |
|---|---|---|
| Density | $kg/m^3$ | 8190 |
| Melting point | K | 1609 |
| Specific heat | J/kg.K | 435 |
| Thermal conductivity | W/m.K | 11.4 |
| Coefficient of thermal expansion | µm/m.K | 13.0 |

Table 1.4: Mechanical properties of Inconel 718

| **Properties (at room temperature)** | **Unit** | **value** |
|---|---|---|
| Young's Modulus | GPa | 205 |
| Poisson's Ratio | - | 0.29 |
| Yield strength | MPa | 1036 |
| Ultimate tensile strength | MPa | 1240 |
| Elastic modulus | GPa | 211 |

# Chapter 2

## 2. State of Art

### 2.1 Introduction

WEDM is the most popular non-conventional machining operation in the manufacturing sectors or industries, for manufacture of product with intricate shape, precision and accuracy. Many investigators have attempted for improving the machining responses such as Material Removal Rate (MRR), surface roughness (Ra), dimensional accuracy etc. and wire electrode properties of WEDM process. However, the selection of cutting parameters for obtaining higher cutting efficiency or accuracy in WEDM is still not fully solved, even with the most up-to-date WEDM machine. This is mainly due to the nature of the complex stochastic process mechanisms in WEDM [42].

This chapter deals with details of development and problem associated with various aspect of WEDM process.

### 2.1 Influence of Process parameters on various machining responses

Considerable research has been carried out on the influence of different process parameters on the different factors affecting the WEDM process discussed as follows:

#### 2.1.1 Effects of the machining parameters on the Material Removal Rate

Scott et al. [43] investigated the effect of process parameter using a factorial design of experiment. It was observed that the discharge current, pulse-on time and pulse frequencies were the significant parameters of MRR and surface roughness while wire tension wire speed and flushing pressure were the insignificant parameters. Ramakrishnan et al. [39] studied the effect of various process parameter such as pulse-on time, wire feed speed, delay time and ignition current during machining of Inconel 718. It was observed that pulse-on time and ignition current

were the most significant process parameters for MRR. Singh et al. [32] investigated the effects of process parameters (i.e., pulse-on time, pulse off time, gap voltage, peak current wire feed and wire tension) on response parameter as MRR of hot die steel (H-11) using WEDM operation. With the increase of the pulse-on time and peak current, the MRR increased. While increasing the pulse-off time and servo voltage, MRR was decreasing. Liao et al. [44] studied an approach of process parameter based on the Taguchi quality design method and ANOVA (analysis of variance). It was observed that pulse-on time and table feed rate were more effective on MRR and surface roughness. The pulse-on time and table feed rate controlled the discharge frequency to protect the wire breakage. Goswami et al. [45] studied a multi response optimization method using utility concept using WEDM of Nimonic-80A alloy. The machining responses were investigated as MRR and surface roughness along with surface topography of machined surface. It was observed that MRR increased with increased in pulse-on time and decreased with increase in pulse-off time. Huang et al. [46] used the use of Grey Relational Analysis (GRA) optimization technique and observed that MRR was more influenced by pulse-on time and feed rate. Rajurkar et al. [5] carried out experimental investigation to analyse the MRR and surface roughness which increased with increase in pulse-on time. Thermal model was developed to analyse the wire breakage. Singh et al. [32] investigated the effects of various process parameters such as pulse-on time, pulse-off time, gap voltage, peak current, wire feed and wire tension on the performance of wire EDM operation using H-11 hot die steel. Mahapatra et al. [47] optimized wire EDM operation using Taguchi's method.. The process parameters like pulse-on time, discharge current and dielectric flow were used to maximize the MRR and to minimize surface roughness. Torres et al. [48] investigated the effect of process parameter through response surface methodology. The process parameters such as pulse-on time, current intensity and duty cycle are the most significant parameters for MRR. They also observed that positive polarity increased MRR whereas negative polarity decreased surface roughness. Va et al. [49] demonstrated with machining responses based on grey-Taguchi method and ANOVA. It was observed that the process parameters such as gap voltage and pulse-on time were more influencing MRR. Kozak et al. [50] observed that actual MRR was dependent on machining geometry and relative position of wire electrode with respect to champing. Sadeghi et al. [51] investigated the influence of process parameters on the MRR and surface roughness using design of experiment due to Taguchi's. Modeling was carried out with the help of regression analysis and the analysis of

variance techniques. It was concluded that discharge current and pulse interval were having the most significant on MRR and surface roughness. Yuan et al. [52] discusses the development of multi-optimization based on Gaussian process regression (GPR). It was observed that pulse-on time and discharge current were the most significant on MRR while pulse-off time and pulse-on time were significant on surface roughness. Scott et al. [43] observed that the discharge current, pulse duration and pulse frequency were the most significant control factors affecting the MRR and SR, while the wire speed, wire tension and dielectric flow rate were having the least effect. Dabade et al. [53] analyzed the machining conditions for MRR, surface roughness kerf width and dimensional deviation during WEDM of Inconel 718 using $L_8$, orthogonal array. The pulse-on time, pulse-off time, peak current, wire feed, wire tension and spark gap set voltage were taken as the responses. It was observed that the pulse-on time was the most influential factor for all the responses.

### 2.1.2 Effects of the process parameters on the surface finish

Gökler et al. [54] investigated selection of the combination of the most suitable machining process parameters and offset parameters for required surface roughness. The results had been found that wire speed and flushing press were the most significant process parameter for surface roughness. Tosun et al. [55] studied the effect of process parameters such as pulse-on time, open circuit voltage, wire speed and flushing pressure on machining surface. It was found that increase in flushing pressure decreased the surface roughness whereas increase in the pulse-on time, open circuit voltage and wire speed increased the surface roughness. Anand [56] used an orthogonal array design of experiment to determine the most desirable process parameters for affecting the better dimensional accuracy and surface roughness. Kumar et al. [57] investigated WEDM operation for pure titanium. The pure titanium has low thermal conductivity having reactivity with cobalt in tool material. This work was mainly focused on microstructure analysis in terms of process parameters such as pulse-on time, pulse-off time, peak current, spark gap using energy-dispersive x-ray, scanning electron microscope and z-ray diffraction techniques. The results revealed that pulse-on time and peak current significantly deteriorated the microstructure of WEDMed surface, which produced the deeper, wider overlapping craters, pockmarks, globules of debris and micro-cracks. Spedding et al. [58] used the artificial neural network model for

obtaining the best combination of process parameter for the machined surfaces. Williams et al. [59] investigated the effect of process parameters on the machined surfaces using scanning electron microscope (SEM) images. Spedding et al. [58] developed a mathematical modeling of the WEDM process using Response Surface Methodology (RSM) and ANN. Based on central composite and a back propagation neural network. The pulse width, pulse-on time, wire tension and flushing pressure were selected as controllable factors. The surface roughness and surface waviness were considered as the responses. Liao et al. [60] observed that a low conductivity of dielectric should be incorporated for the discharge spark to take place for reducing surface roughness. Han et al. [61] investigated that decrease in pulse-on time and discharge current improved the surface finish. Kanlayasiri et al. [4] studied the influence of process parameters on affecting the surface roughness based on variance technique. The variables the peak current pulse-on time were significant to surface roughness. Tosun et al. [55] carried out experimental investigation of WEDM operation and used the variance technique for analysis. With increase in pulse-on time, wire speed and voltage the surface roughness increased. Kanlayasiri et al. [62] studied the influence of process parameter such as taper angle, peak current, pulse-on time, pulse-off time, wire tension and dielectric flow rate. Form the variance technique the taper angle and pulse-on time were observed to be the most significant parameters for surface roughness and MRR combined. Pasam et al. [63] obtained optimal process parameter for minimizing the surface roughness using design of experiment due to Taguchi. Ramakrishnan et al. [64] studied the surface waviness, form accuracy and surface flatness of workpiece using WEDM operation and other non-conventional process. Gökler et al. [54] obtained the most suitable cutting and offset parameter combination to get the desired surface roughness value for the WEDMed surface. It was observed that the thickness of workpiece played the important role to achieve the better surface finish. Saha et al. [65] developed the mathematical model using multi-variable regression and BPNN (Back-Progression Neural Network) based on experimental dataset. Increase in peak current and capacitance increased cutting speed and surface roughness. Sarkar et al. [33] obtained an optimal parameter condition for predicting surface roughness, cutting speed and wire offset with different process parameters. Gong et al. [66] focused on surface integrity of Low-Speed wire electrical discharge machining (LS-WEDM) in machining TC4 (Ti-6Al-4V) by multiple cut followed by rim cuts. The brass is considered as electrode material with possible polarity deionized water is considered as dielectric. The machine response was surface

roughness. The surface microstructure, spherical droplets, irregular droplets, cracks, craters and micro-void had been examined using scanning electron microscopy (SEM).

### 2.1.3 Effects of the process parameters on dimensional deviations

Hsue et al. [67] studied the fundamental geometry properties of WEDM process in cutting. A mathematical model was derived by analytical geometry to get the concept of discharge angle. The model was developed to estimate MRR in geometrical cutting by considering wire deflection with transformed exponential trajectory of wire center. Corner cutting was physically interpreted with increase in gap-voltage and decrease in sparking frequency. Muthuraman et al. [68] conducted experiments on O1 steel in WEDM process using Taguchi's L32 orthogonal array at different process parameters of pulse-on time, pulse-off time, wire feed, flow rate, wire tension and voltage and analyzed their machining responses such as material removal rate, wire wear ratio, surface roughness and dimensional deviation. Padhi et al. [69] reported that an optimization technique using face centered central composite design of RSM was used to develop the empirical model for relationship between process parameters (pulse-on-time, pulse-off-time, wire tension, spark gap set voltage and servo feed) and responses (cutting rate, surface roughness and dimensional deviation) in WEDM operation of EN-31 steel considered as workpiece material with an objective to maximize cutting speed and minimize of surface roughness and dimensional deviation combined. Selvakumar et al. [70] analysed the corner accuracy achievable through trim cutting operation. Pulse-on time, pulse-off time peak current and servo-voltage were considered as process parameters and MRR, surface roughness and dimensional shift were considered as the responses.

### 2.1.4 Variations of electrodes affecting the performance measures

Chalisgaonkar et al. [71] presented the finish cutting operation of WEDM for commercially pure titanium. The wire type (zinc coated brass wire and uncoated brass wire) has been selected as tool materials. The process parameters selected as pulse-on time pulse-off time, peak current, wire feed servo voltage and wire offset were investigated on responses like cutting speed, surface roughness and surface integrity after finish cut operation. From the ANOVA table, it was observed that wire material, pulse-on time and wire offset were influencing cutting speed and surface roughness during the trim cutting. It was observed that lower pulse-on time, peak current and wire offset obtained good surface finish using uncoated brass wire. The X-ray diffraction

investigation indicated that peak intensity got lowered down due to increase of pulse discharge energy. Galindo-Fernandez et al. [72] investigated of WEDM operation of Polycrystalline Diamond (PCD). To understand the reactions of PCD on process parameters (i.e., pulse-on time , pulse-off time and servo voltage wire tension, wire unspooling speed and injection pressure) and to determine if there was a relationship between the response parameters and surface finish and cutting speed. ANOVA table has been used to predict the significant process parameters and develop a regression equation to model the response parameters. Different types of coated wires (Cu, CuZn36 and CuZn 63/37 and zinc diffused and zinc rich brass double layer) were used. The results showed that coated wires increased cutting speed to a value of 4.7mm/min without affecting surface roughness drastically. Golshan et al. [73] focused on comparing the performance of different types of wire electrodes (i.e., brass wire and zinc coated brass wire) in WEDM process, which is widely used in specially industries. The pulse-on time, pulse-off time and peak current were considered as process parameters. MRR, spark gap and white layer thickness were considered as the responses. Kozak et al. [50] experimented WEDM operation of less conductive material. The electrical resistance between the tool and workpiece, and tool was varying during the machining depending upon the clamping position. Product quality had been improved by varying the resistance during WEDM operation.

### 2.1.5 Optimizing the process variables

Scott et al. [43] presented a formulation and solution of multi-objective optimization problem for the selection of process parameters on the WEDM process. The MRR and surface finish were considered as responses. A factorial design model was selected to predict the best combination of a variety of process parameters settings to achieve the responses. A non-dominated point had been introduced for the best combination of process parameters settings. Tosun et al. [3] investigated the effect of process parameters such as pulse-on time, open circuit voltage, wire speed and flushing pressure on the kerf width and MRR in WEDM operations using Taguchi experimental design method and ANOVA. They had also developed a regression model to study the variation of kerf width and MRR on process parameters. Spedding et al. [74] observed that a combination of electro-dynamic, thermal-dynamic electromagnetic and hydro-dynamic actions, exhibited a complex and stochastic nature. An optimization technique was adopted to optimize the controllable parameter using Artificial Neural Networks (ANN). The WEDMed surface was

characterized through time series techniques. Puri et al. [75] performed an experimental investigation with various machine control parameters as well as to propose optimum parametric combinations for various machining requirements. Puertas et al. [76] focused on aspects related to surface quality and dimensional precision. A mathematical model was adopted for finding the optimum parameter setting to improve machinability criteria with a lower process time. Sarkar et al. [33] presented an investigation on WEDM of γ-titanium Aluminide alloy. In this study authors have found the optimum process parameters to get the desired cutting speed, surface finish and dimensional accuracy. Lastly, the optimum process parameters for different machining condition arising from productivity requirement were synthesized. Wang et al. [77] compared all mathematical models based on thermal, physical, electrical, and material properties of the work and the tool pertinent process parameters. The results were in good agreement with the experimental verifications. Lin et al. [78] had used a new approach for optimization of the process parameter with multiple performance characteristics viz. MRR, surface roughness tool wear. Lin et al. [79] investigated an optimization method using orthogonal array with fuzzy logic and Grey relation analysis (GRA) method for optimizing the multi-response, viz MRR, tool wear and surface roughness. GRA gave better optimization result than the fuzzy-based Taguchi method. Tosun et al. [55] studied the variation of surface roughness with varying pulse duration, open circuit voltage, wire speed and dielectric fluid pressure experimentally investigated in WEDM operation. The level of importance of the machining parameters on the workpiece surface roughness has been determined by analysis of variance (ANOVA) table. Hewidy et al.[80] developed a mathematical model using response surface methodology (RSM) for correlating the inter-relationships of various WEDM, process parameters (i.e., peak current, duty factor, wire tension and water pressure) of Inconel 601 selected as workpiece. The responses of the machining in terms of MRR wear ratio and surface roughness were investigated. Kuriakose et al. [81] reported that a regression model was made to represent relationship between process parameters (i.e., voltage, ignition pulse current, pulse off time, pulse duration, servo control reference mean voltage, servo speed variation, wire speed, wire tension and injection pressure) and responses variables (cutting velocity and surface roughness) and established a multi-objective optimization model using Non-Dominated Sorting Algorithm (NSGA) to optimized the WEDM process. Mahapatra et al. [8] developed a model of rough cutting operation in WEDM for improving machining performance measures viz. MRR, surface roughness and cutting width.

Using Taguchi's parameter design, significant process parameters affecting the performance measures were identified as pulse-on time, pulse-off time wire speed, wire tension and dielectric flow. Finally, Genetic Algorithm (GA) had been implemented to optimize the WEDM process with multiple objectives. It was observed that WEDM process parameters were adjusted to achieve better MRR surface roughness and cutting width simultaneously. Kanlayasiri et al. [4] investigated of the effects of machining variable on the surface roughness of WEDMed and selected DC53 die steel as a workpiece. ANOVA table has been used for analysis of variables method for determination of residual stress. From the analysis it was observed that pulse-on time and pulse peak current were significant variables for the surface roughness. Finally, a mathematical model was developed using regression method to formulate the pulse-on time and pulse-peak current on effects of surface roughness. Kung et al. [24] studied the effects and optimization of four process parameters such as peak current, pulse on time, duty factor, and wire speed, on the performance characteristics of MRR and surface roughness using face centered central composite design (CCD) for conducting the experiment on aluminum oxide based ceramic material ($Al_2O_3$+TiC) in WEDM process. They have also developed empirical models using Response Surface Methodology (RSM) to investigate the influence of process parameters on material removal rate (MRR) and surface roughness (SR). Kumar et al. [82] carried out experimented investigation to study the effect of various process parameters on MRR and surface roughness. Mathematical models were established and optimized using Non-Dominated Sorting Genetic Algorithm (NSGA-II). Mukherjee et al. [83] attempted to apply six most popular population based non-traditional optimization algorithm i.e., genetic algorithm, particle swarm optimization, sheep flock algorithm, ant colony optimization of two WEDM processes. It was observed that biogeography-based optimization algorithm outperformed the others. Saha et al. [65] adopted Taguchi's $L_{27}$ orthogonal array to study the effects of seven process parameters on machining responses characteristics such as material removal rate, kerf and surface roughness of tungsten carbide as workpiece during WEDM operation. ANOVA table had been used for obtaining the responses to determine the significant factors. Ikram et al. [84] carried out an optimization of process parameters such as wire feed velocity, dielectric pressure, pulse on-time, pulse off-time, open voltage, wire tension and servo voltage on MRR and surface roughness and kerf width in WEDM process for tool steel D2. ANOVA signal- to noise (S/N) ration had been used to identify the significant process parameters and to achieve

optimum levels respectively. Muthukumar et al. [85] developed the mathematical model using accelerated particle swarm optimization algorithm to optimize the process parameters that led to optimum setting for maximum MRR, minimum surface roughness and kerf width on WEDM process. Shayan et al. [86] developed to create relationships between the process parameter and machining responses by considering variance technique. The two approaches had been utilized for optimization of dry WEDM operation. First approach was based on mathematical model and desirability function and second approach was designed based on neural network and particle swarm optimization. The back progression neural network and particle swarm optimization (BPNN-PSO) approach was more efficient in optimization process. Kumar et al. [87] presented the relationship of process parameters such as pulse-on time, pulse off time peak current, spark gap voltage, wire feed and wire tension on the responses like MRR wire wear ration and surface roughness on pure titanium using WEDM process. Box-Behnken design had been used for design of experiment and RSM was implemented for mathematical model. Multi-objective optimization of process parameters was used using desirability approach. The sample was examined by using energy-dispersive X-ray, SEM and X-ray diffraction techniques. Mandal et al. [11] examined the influence of the WEDM process parameters on different performance measures during machining of Nimonic C-263 super alloy. A mathematical model has been developed for relations between performance measure (cutting rate, surface roughness, spark gap and wire wear ratio) and process parameters (pulse-on time, pulse off time, servo reference voltage and dielectric flow rate) using response surface methodology (RSM). A mathematical model had been used to find the optimal process parameter setting for maximum cutting speed at optimum surface finish and higher value of wire wear ratio using single cut and multi-cut strategies. Soundararajan et al. [88] studied on new fabricated A413 alloy produced by squeeze casting route using WEDM process. The experiments were carried out by adapting central composite rotatable design approach of RSM to find out the effect of machining process parameters such as pulse-on time, pulse-off time and peak current on the responses like MRR and surface roughness. ANOVA tables were developed to check the significance of the models. Through the additively test, a mathematical models were developed to predict the results of agreeable average error for MRR and surface roughness. Desirability faction approach was used to determine the optimal process parametric combinations for multi-objective optimization and

successful machining of the castings. Better casting properties and machining quality were observed on squeeze casting and WEDM process parameter of A412 alloy.

Ayesta et al.[89] examined the capabilities of WEDM operation for manufacture of fatigue specimens on Inconel 718. The process parameters used for fatigue specimen are current intensity, pulse off time, voltage and servo voltage for WEDM operation. The grinding wheel type (5SG46G12VXP), grinding wheel material (aluminum oxide), depth of cut, grinding wheel speed and workpiece speed for grinding process were used. It was observed that conducting the WEDM process with the new generation of machines having a detrimental effect at high fatigue cycles, reducing fatigue strength by approximately 10% in comparison with ground specimens. However, there were no significant differences between the ground and WEDM samples. Sanchez et al. [90] presented a computer simulation for error analysis of taper cutting in WEDM operation. Computer simulation results and experimental results have been compared with those obtained by the classical trial and error method. Plaza et al. [91] discussed about the two models for the prediction of angular error of taper cutting first mechanical behavior of the wire related to its mechanical properties and second geometrical definition of the problem defined by the distance between the upper and lower guides and desired angle. Selvakumar et al. [37] proposed a method to optimize the process parameters such as pulse-on time, peak current, wire tension and taper angles of WEDM process. The performance responses were selected as cutting speed, surface roughness and taper error on AISI D3 selected as workpiece. $L_9$ orthogonal array was used for design of experiment. The results revealed that pulse-on time had the most influencing factor for the cutting speed and surface roughness. The taper angle was the most influencing factor for taper error on the workpiece.

### 2.1.6 Wire lag and wire vibration

Liao et al. [60] observed that there was difficulty in obtaining the finishing process because due to occurrence of short circuit attributed to wire deflection and vibration when the energy was gradually decreasing. Kunieda et al. [92] described the development of a new dry WEDM method, which was conducted in a gas atmosphere without using dielectric liquid to improve the accuracy of finish cutting. Gong et al. [93] reported low speed wire electrical discharge machining (LS-WEDM). This is a process to manufacture inticate shapes with proper dimensional accuracy and surface quality. $L_{16}$ orthogonal array for design of experiment for

optimum parametric setting for multiple cuts were designed and the experimental work had established that the acute angle convex corners machined by LS-WEDM. The wire deflection model based on unilateral discharge mechanism was built to improve the machining accuracy. The kerf was obtained with close accuracy lead better surface micro-structure. The cracks, voids and spherical droplets were decreasing.

### 2.1.7 Research objective

The performance measures of the WEDM process are Material Removal Rate (MRR), surface quality (Ra), angular error, corner error, and dimensional accuracy for Inconel 718 as work material using statistical approach for different type of cutting. For cost effective machining, it is essential to identify and estimate the changes those are taking place within wire electrode materials. The wire electrode materials play a very important role in manufacture sectors for increasing the economic cutting, surface quality and productivity. The wire electrode has one time use only because of high wear rate of electrode material during the machining time which may increase the machining cost. The different wire materials have been used to enhance the productivity of the process with better surface quality. Different type optimization have been applied to predict the performance measures during the process to reduce the experimental cost and errors associated to provide guidelines for the tool engineers in selection of optimum set of process parameters prior to machining. The following objectives are set on the basis on literature gap for this research work.

1. An experimental investigations to study the effect of the various process parameters on machining performance measures for machining performance measures for straight cut using Inconel 718 as workpiece.
2. Experimental investigations to study the process parameters for fabrication of corner in Inconel 718.
3. Experimental investigation to analyse the effect of process parameters of WEDM for manufacture of V-Shape cutting in Inconel 718.
4. Experimental study to analyse the influence of wire electrode material on machining performance measures during WEDM process.

5. Experimental investigation of taper cutting in Inconel 718 using WEDM operation and obtain the performance measure using metaheuristic search algorithm
6. To develop the mathematical models of the process parameter and various machining performance measures for the best machining process using nature-inspired meta-heuristic optimization algorithm.
7. To develop thermo-mechanical model for predicting the MRR and validate with experiment.

### 2.1.8 Organization of thesis

The thesis consists of five chapters. A brief discussion of each chapter is made as follows:

First chapter introduce the concept of WEDM operation including basic working principles and its applications. This phase provides the justification, motivation and need for present research work.

In the second chapter, extensive literature review related to different aspects of WEDM operation have been carried out. Based on literature survey, the objectives of the present investigation have been defined.

Experimental investigation of WEDM operation uses Inconel 718 as work material and different wire materials have been carried out in this chapter. This chapter has been divided into three phases. This chapter deals with different type of cutting with variation of wire electrode material in Inconel 718 using WEDM process.

- First phase deals with machining performance analysis of straight cut WEDM in Inconel 718.
- The second phase of this chapter proposes a machining performance analysis of corner-cut WEDM in Inconel 718.
- Third phase of this chapter exhibits a machining performance analysis of V-shape cutting WEDM in Inconel 718.

In the fourth chapter, parametric optimization of WEDM operation for different type of cuts have been carried out.

- The first phase of this chapter is based on optimization of machining parameters for Inconel 718 with variation of wire material by using a meta-heuristic approach known as Grey Wolf optimizer (GWO) and nonlinear regression. The performance of the proposed

optimization module has been compared to that of Genetic Algorithm (GA) and Taguchi's robust optimization philosophy.

- The second phase focuses on experimental attempt that has been made to analyze the influence of wire electrode on Material Removal Rate (MRR), Corner deviation and surface roughness (Ra) in Wire Electrode Discharge Machining (WEDM) process of Inconel 718. Finally, the process model is optimized by using a latest meta-heuristic approach known as Whale Optimization Algorithm (WOA) approach to obtain the optimum machining parameter settings. The results of WOA have been compared to that of Genetic Algorithm (GA).

Fifth chapter deals with thermo-mechanical model based in finite element method (FEM) to predict the thermal profile of Inconel 718 as workpiece material in WEDM operation. MRR was estimated from the numerical model and was validate with experiments. The coupled thermos-mechanical model was developed to determine residual stress.

Sixth chapter deals with summary of the investigation, recommendations and scope for the future work.

# Chapter 3

## 3. Experimental investigations on Wire Electro Discharge Machining (WEDM): Effect of variation of Electrode materials for straight cut, corner cut, V-cut using Inconel 718

### 3.1 Machining Performance Analysis of Straight-Cut WEDM on Inconel 718

## 3.1.1 Coverage

In the present study, an attempt has been made to study the performance of (Brass wire electrode and zinc coated brass wire electrode) wire electrodes in relation to Material Removal Rate (MRR), kerf width and surface roughness of machined Inconel 718 obtained by wire electro discharge machining (WEDM) process. Experiments have been conducted using $L_{16}$ orthogonal array with two different types of wire electrodes and by tuning the following controllable process parameters; discharge current, flushing pressure, wire tension, and pulse-on time. It has been observed that zinc coated brass wire produces lesser kerf width as well as surface roughness; higher MRR as compared to brass wire electrode. The pluse-on time is found to be the most singnificant factor on influencing MRR for all electrodes types. Pulse on time and discharge current is found to be very singnificant on affecting Kerf width for all electrodes types .

## 3.1.2 Problem Definition

Inconel 718 is a nickel based super alloy processing high strength and thermal resistance. Due to its uniqueness in properties, this alloy is mainly used in the aerospace industries. Due to extreme toughness and work-hardening characteristic of Inconel 718, the problem of machining this alloy possesses a great challenge [94]. Machining of Inconel 718 with conventional process tends to

be tedious job where tool wears. Since the nonconventional machining process like WEDM process exhibits better machinability; it is felt very important to understand process behavior for improving overall machining performance.

The most important performance measures in WEDM are Material Removal Rate (MRR), kerf width and surface finish [95]. Aforesaid responses depend on machining parameters like discharge current, pulse on time, wire speed, wire tension and dielectric flow rate.

Substantial volume of research has been carried out by pioneers to improve surface roughness of WEDMed component [55, 64, 96]. In this context, an attempt has been made to compare surface roughness of the end product obtained by using two different wire electrode materials for improving overall machining performance.

Mohanty et al. [41] discussed about the performance of three tool electrodes such as copper, brass and graphite on affecting machining characteristic of EDM process on Inconel 718. Authors claimed that selection of electrode material is highly responsible for better machining performance. Aggarwal et al. [97] attempted parametric optimization and modeling for WEDM of Inconel 718 with brass wire electrode using Response Surface Methodology (RSM). The input parameters were selected such as pulse-on time, pulse-off time, peak current spark gap voltage, wire feed rate and wire tension; the responses considered were cutting rate and surface roughness. The pulse on time was found to be the most influencing factor for cutting rate and surface roughness. Ramakrishnan et al. [98] studied the performance of WEDM of Inconel 718, the authors attempted mathematical modeling and multi-response optimization to predict and select the best cutting parameters for WEDM process using a bass wire. The effects of various machining parameter such as pulse on time, wire feed speed, delay time and ignition current were studied on influencing the responses. Kuppan et al. [99] reported the effect of process parameters (peak current, pulse on time duty factor, electrode speed) on material removal rate and surface roughness in EDM drilling of Inconel 718 using graphite electrode. The results exhibited that graphite electrode produced moderate MRR and good surface finish as compared to copper electrode. Abdulkareem et al. [100] reported the effect of electrode cooling on electrode wear during the EDM of titanium alloy (Ti-6Al-4V). Current, pulse-on time, pulse-off time and gap voltage were considered as the machining parameters considering electrode wear as the response. Golshan et al. [73] focused on comparing the performance of brass wire and zinc coated brass wire. An evolutionary computation method was presented based on Non-

Dominated Sorting Genetic Algorithm (NSGA) in order to find an optimal parameters setting for improving machining performance on the Ti-6Al-4V titanium alloy. Current, pulse on time and pulse off time were considered as the machining parameters. The zinc coated brass wire was found more effective to a reliable extent response. Prohaszka et al. [26] examined material requirement for fabrication of WEDM electrode for improving WEDM performance. Experiments were carried out regarding the choice of suitable WEDM method. The effect of the materials properties of the wire on the machinability in WEDM was discussed. Muthuramalingam et al. [101] explained the erosion process to analyze the effects of tool electrode like copper, brass and tungsten on machinability of AISI 202 stainless steel during WEDM. Kapoor et al. [20] discussed the effect of wire electrodes used in WEDM operation.

From the literature survey, owing to the fact that proper selection of electrode material leads to the enhancement of machining performance during WEDM on Inconel 718 in this context. In the present work an attempt has been made to compare the performance of brass wire electrode and zinc coated brass wire electrode in consideration with MRR, kerf width and surface roughness of the WEDMed end product. It has been noted that lesser extent of work has been performed so far in this particular directions [8, 102]. Literature seemed sparse to discuss the effects of various process parameters on performance measures in the WEDM process with different wire electrodes material.

## 3.1.3 Experimental details

In the present study, experiments have been conducted on a CNC WEDM machine, [AGIE, SWITZERLAND] as shown in Figure. 3.1 Inconel 718 has been selected as work material with dimension (50 × 20 × 1) $mm^3$.


Figure 3.1 CNC-Wire Cut EDM Machine (AC Progress V2**)**

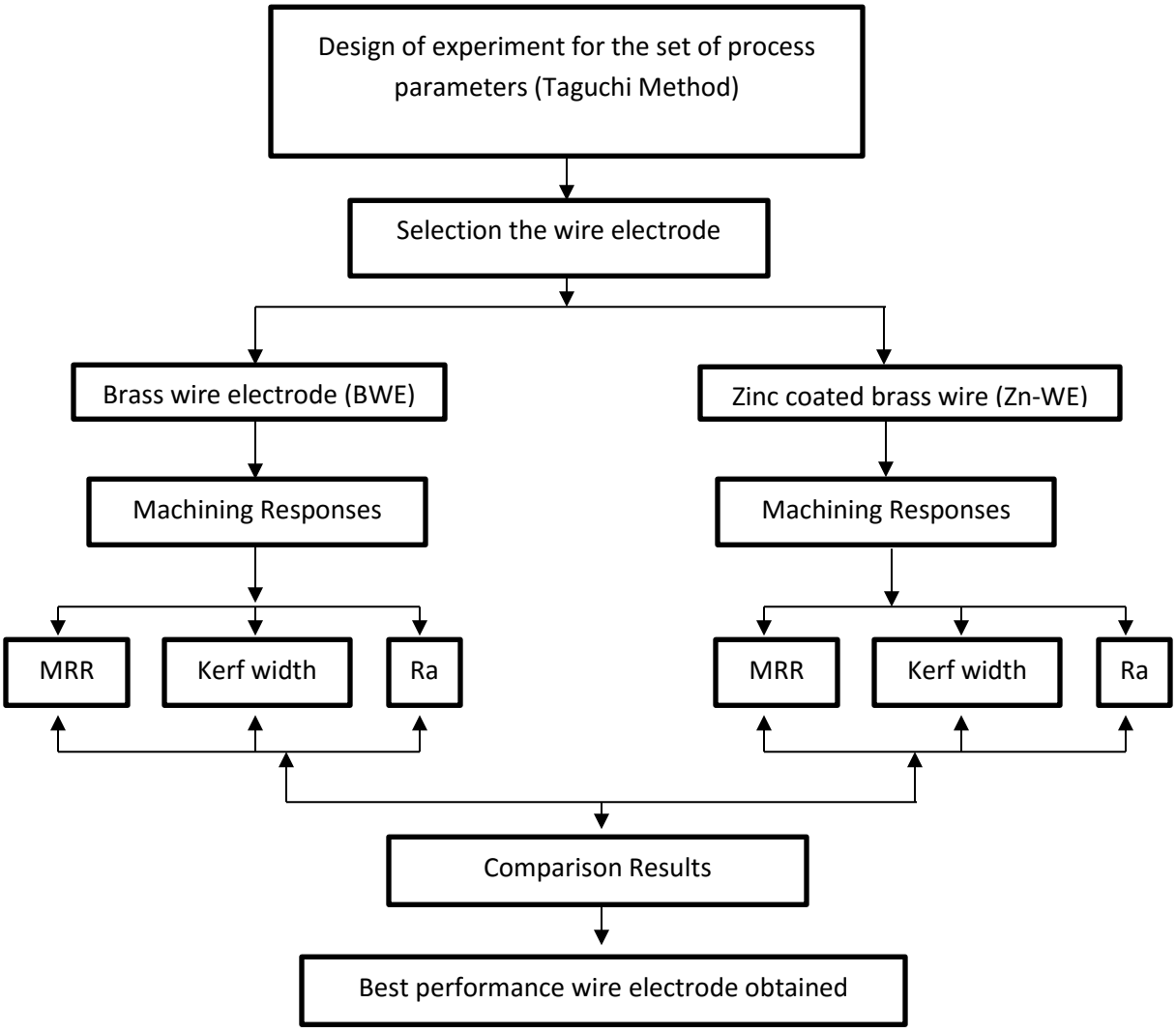


Figure 3.2 Experimental strategy

### 3.1.3.1 Selection of process parameters

The selection of process factor has been given in Table 3.1. The experiments have been conducted to investigate the significant contribution of process parameters on machinability (in terms of MRR, Kerf width and Surface finish) during WEDM process. Pulse-on time, flushing pressure, wire tension and discharge current have been chosen as input process parameters. Deionized water has been used as dielectric fluid. The pulse-off time and dielectric flow rate have been kept fixed as 50μs and 1.2 bars, respectively, throughout the experiments.

Table 3.1 Process factors and domain of variation

| Control factor | Code | Unit | Level I | Level II | Level III | Level VI |
|---|---|---|---|---|---|---|
| Pulse on time | A | [μs] | 26 | 28 | 30 | 32 |
| Flushing Pressure | B | [kg/mm$^2$] | 8 | 12 | 16 | 20 |
| Wire tension | C | [N] | 6 | 8 | 10 | 12 |
| Discharge Current | D | [A] | 10 | 12 | 14 | 16 |

### 3.1.3.2 Design of experiments

A 4-factor-4-level, $L_{16}$ orthogonal array has been selected for the present study as shown in Table 3.1. Based on the orthogonal array, a total of 16 numbers of experimental runs have been conducted using WEDM operation. Table 3.2 shows the $L_{16}$ design of experiment.

Table 3.2 Design of experiment (L16) Orthogonal Array (factors are in coded form)

| Experiment no. | A | B | C | D |
|---|---|---|---|---|
| 1 | 1 | 1 | 1 | 1 |
| 2 | 1 | 2 | 2 | 2 |
| 3 | 1 | 3 | 3 | 3 |
| 4 | 1 | 4 | 4 | 4 |
| 5 | 2 | 1 | 2 | 3 |
| 6 | 2 | 2 | 1 | 4 |
| 7 | 2 | 3 | 4 | 1 |
| 8 | 2 | 4 | 3 | 2 |
| 9 | 3 | 1 | 3 | 4 |
| 10 | 3 | 2 | 4 | 3 |
| 11 | 3 | 3 | 1 | 2 |
| 12 | 3 | 4 | 2 | 1 |
| 13 | 4 | 1 | 4 | 2 |
| 14 | 4 | 2 | 3 | 1 |
| 15 | 4 | 3 | 2 | 4 |
| 16 | 4 | 4 | 1 | 3 |

### 3.1.3.3 Selection of wire electrode materials: properties and requirements

Two different types electrode i.e., brass wire electrode and zinc coated brass wire electrode (ϕ 0.20) have been used in the present study. The properties of the wire electrodes have been given in Table 3.3

Table 3.3 Properties of wire Electrodes

| Properties | Unit | Brass wire electrode | Zinc coated brass wire electrode |
|---|---|---|---|
| Melting point | [$^{o}$C] | 927 | 419 |
| Tensile Strength | [N/mm$^{2}$] | 980 | 964 |

A brass alloy wire, consisting of 63% Cu and 37% Zn, was developed in the early 70s in order to improve cutting speed. Brass is a relatively good conductor (29 IACS). It yields satisfactory surface finish in WEDM applications and it is characterized by sufficient mechanical properties and tension ability and commonly used in various industries [26]. Zinc coated brass wire possesses high performance and has conductivity (IACS 84). Brass core with ZnO layer of 25µm thickness has been used. The outer coated layer of these electrodes is characterized by a lower melting temperature in relation to the core material. When a pulse is applied the wire coating is overheated and then evaporated. Therefore, a 'heat sink' effect on the wire is created and thus a cooling of the core material is obtained [27]. The zinc coated brass wire improves the cutting performance and cutting speed [18]. Figure 3.3 shows the Inconel 718 specimens before and after machining along with various wire electrodes.

i) Inconel 718 alloy workpiece specimen

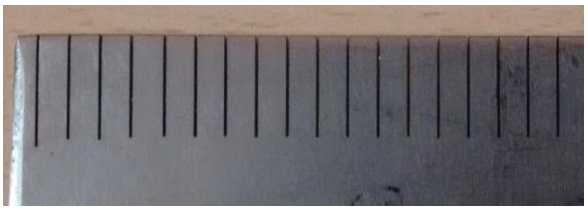

ii) Workpiece specimen after machining

a) Brass wire electrode

b) Zinc coated brass wire electrode

Figure 3.3 Inconel 718 work piece specimen (i) before machining and (ii) after machining process. Various wire electrodes (a) Brass wire and (b) zinc coated brass wire

## 3.1.4 Selection Process Responses

The MRR, kerf width and surface roughness are the dominated performance responses in the WEDM process; those responses have been selected for the present study. The machining length has been fixed at 10mm for each experiment run. MRR is calculated by using the Equation 1.1 in chapter no. 1:

Kerf width (Figure. 3.4) represents the overcut occurred in the workpiece during machining process. Surface roughness determines the quality of the machined surface and it is generally represented by Ra. Kerf width is defined as the width of workpiece material which is removed by machining process [8]. Kerf width can be used to determine the dimensional accuracy of the end product. The kerf value has been here expressed as the average of five measurements made from the workpiece with 2mm increment along the length. The cutting speed ($C_s$) has been directly obtained from the computer monitor of WEDM machine. The kerf width of all machined specimens has been measured using Optical Microscope (CARL ZEISS JENA, Germany). The surface images of magnification of 5000X of machined Inconel 718 have been acquired using Field Emission Scanning Electron Microscopy (FESEM) (NOVA NANO SEM 450).

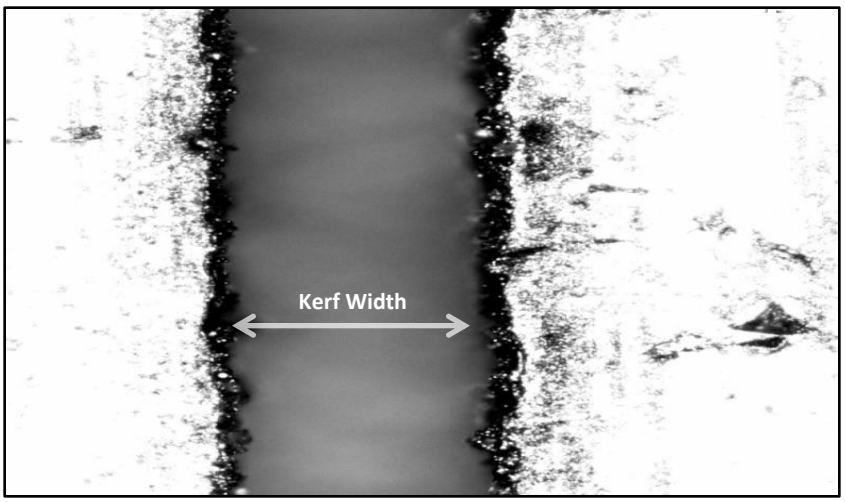


Figure 3.4 Measurement of Kerf width

Experimental data have been furnished in Table 3.4.

## 3.1.5 Results and discussions

Experimental data have been explored to study effects of electrode material along with process parameters on various machining performance characteristics. For different combination of input parameters the material removal rate and kerf width are given in Table 3.4. The snapshot images of machined specimen are given in Fig.3.5 to indicate kerf width.

Table 3.4 Experimental data

| Ex. No | A | B | C | D | MRR (g/min) | | Kerf Width (mm) | |
|---|---|---|---|---|---|---|---|---|
| | [µs] | [kg/mm$^2$] | [N] | [A] | Zn-WE | BWE | Zn-WE | BWE |
| 1 | 26 | 8 | 6 | 10 | 0.010699 | 0.005149 | 0.2465 | 0.2535 |
| 2 | 26 | 12 | 8 | 12 | 0.018350 | 0.008424 | 0.2420 | 0.2571 |
| 3 | 26 | 16 | 10 | 14 | 0.024200 | 0.012608 | 0.2432 | 0.2483 |
| 4 | 26 | 20 | 12 | 16 | 0.025424 | 0.018803 | 0.2503 | 0.2551 |
| 5 | 28 | 8 | 8 | 14 | 0.025420 | 0.012462 | 0.2483 | 0.2507 |
| 6 | 28 | 12 | 6 | 16 | 0.032746 | 0.020144 | 0.2531 | 0.2595 |
| 7 | 28 | 16 | 12 | 10 | 0.009642 | 0.003614 | 0.2422 | 0.2451 |
| 8 | 28 | 20 | 10 | 12 | 0.020109 | 0.008336 | 0.2526 | 0.2583 |
| 9 | 30 | 8 | 10 | 16 | 0.040616 | 0.021431 | 0.2610 | 0.2670 |

| | | | | | | | | |
|---|---|---|---|---|---|---|---|---|
| 10 | 30 | 12 | 12 | 14 | 0.026681 | 0.014828 | 0.2670 | 0.2727 |
| 11 | 30 | 16 | 6 | 12 | 0.014083 | 0.007208 | 0.2422 | 0.2515 |
| 12 | 30 | 20 | 8 | 10 | 0.008993 | 0.004630 | 0.2440 | 0.2570 |
| 13 | 32 | 8 | 12 | 12 | 0.017149 | 0.011719 | 0.2327 | 0.2409 |
| 14 | 32 | 12 | 10 | 10 | 0.013252 | 0.007958 | 0.2279 | 0.2358 |
| 15 | 32 | 16 | 8 | 16 | 0.033277 | 0.014409 | 0.2390 | 0.2454 |
| 16 | 32 | 20 | 6 | 14 | 0.024626 | 0.014910 | 0.2506 | 0.2564 |

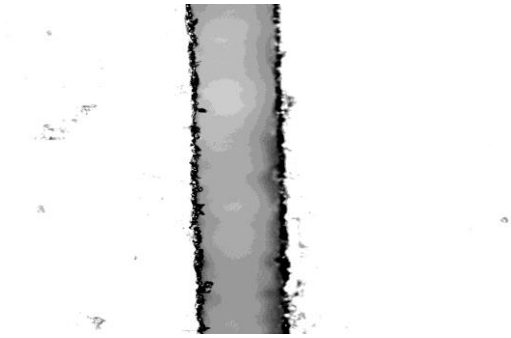

(a) Run no. 3

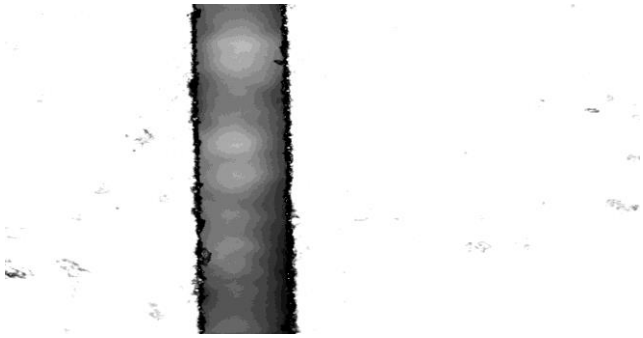

(b) Run no. 3

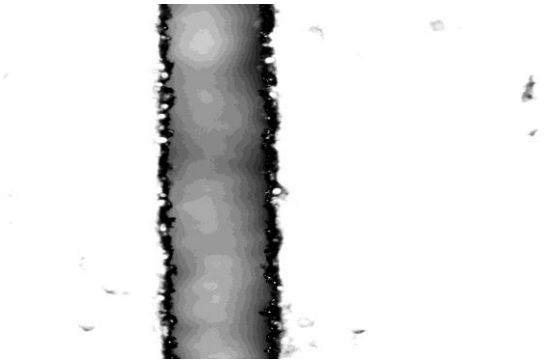

(c) Run no. 13

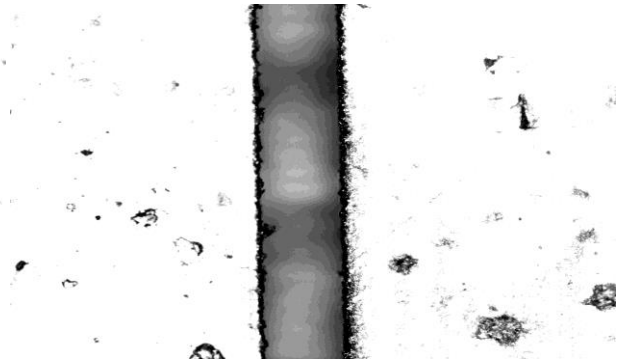

(d) Run no.13

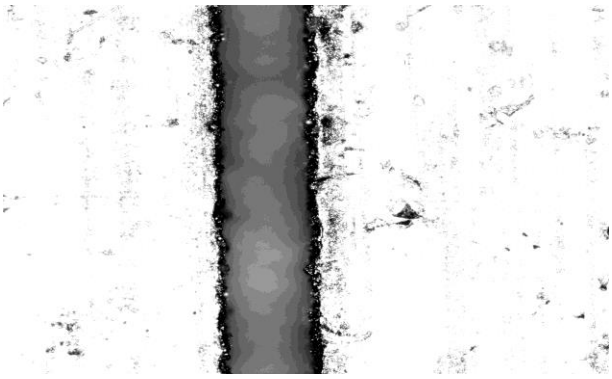

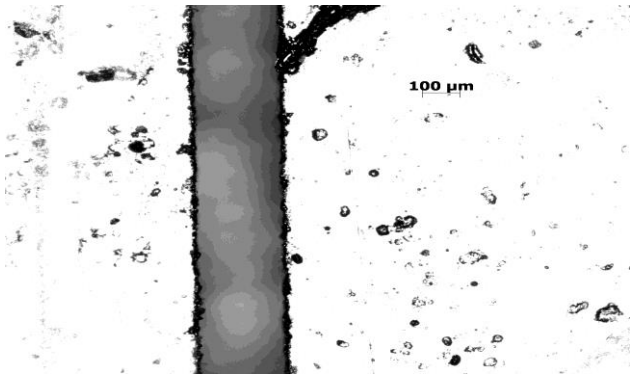

(e) Run no. 15 (f) Run no. 15

Figure 3.5 Kerf width after machining [ a,c and e kerfs are from uncoated brass electrode; b,d and f kerfs are from zinc coated brass wire]

Figure. 3.6 shows the effect of electrode materials on MRR obtained during WEDM of Inconel 718. It has been observed that for all 16 settings experimented in this work, MRR value appears higher in case of zinc coated brass wire electrodes as compared to brass wire electrode. As MRR corresponds to "Higher-is- Better" (HB) criteria (from productivity view-point); higher MRR obtained in zinc coated brass wire exhibits superiority in performance as compared to brass wire. Therefore, according to different researcher, the cutting speed of the zinc-coated brass wire is approximately twice to that of brass wire because the exterior zinc coating possesses a lower melting temperature than of that of the core material (brass). In zinc coated brass wire; the zinc is overheated and evaporated during the pulses. The evaporation acts as a heat sink, which helps to reduce the wire temperature and improve the effectiveness of the WEDM process [26].

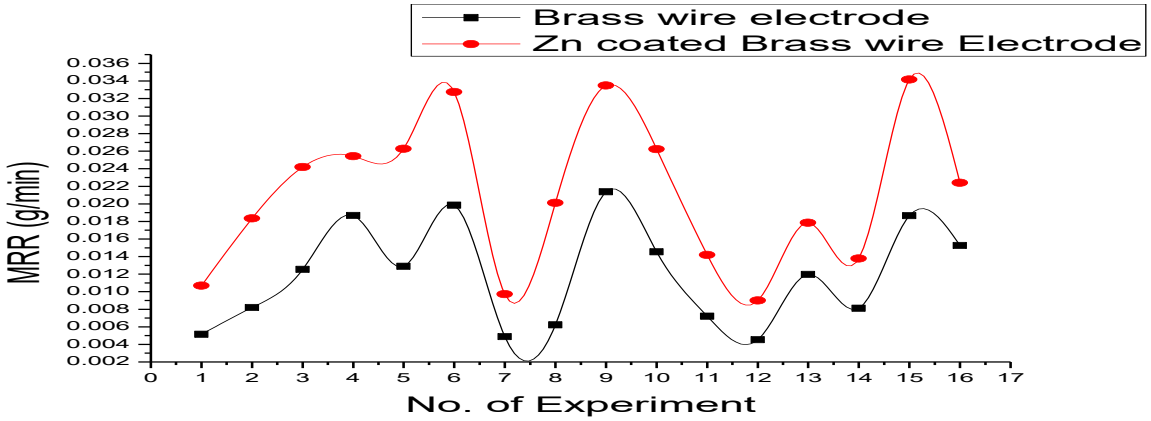


Figure 3.6 Effects of wire electrode on MRR

Figure 3.7 shows effect of electrode material on Kerf width obtained during WEDM of Inconel 718. It has been observed that for all 16 settings experimented in this work. Kerf width value appears lower in case of zinc coated brass wire electrodes as compared to plain brass wire electrode. As Kerf width corresponds to "Lower-is-Better" (LB) criteria (from quality view-point); lower Kerf width obtained in zinc coated brass wire exhibits its superiority in

performance over plain brass wire. Zinc coated brass wire having its heat sink capability, helps to reduce the wire temperature and improve the effectiveness by insuring minimum karf width.

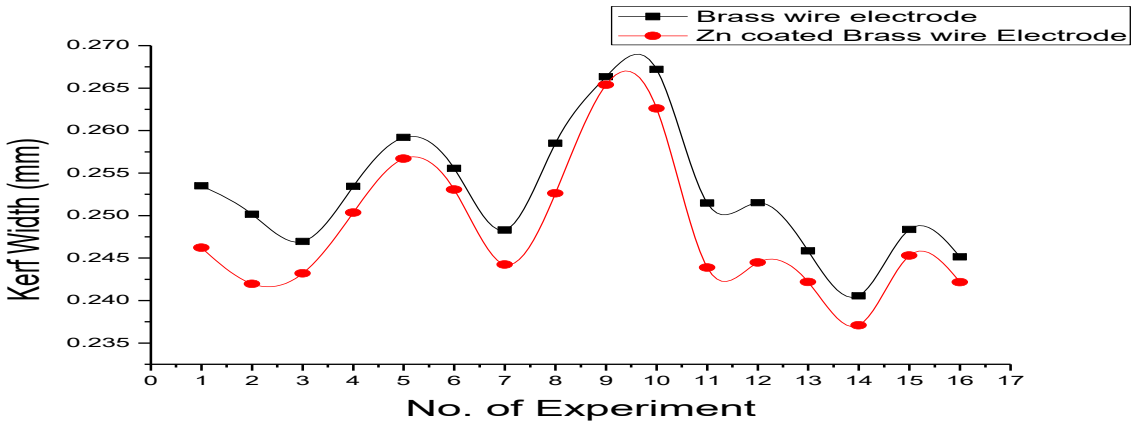


Figure 3.7 Effects of wire electrode on Kerf width

Figure. 3.8 show the effect of electrode material on surface roughness of WEDMed Inconel 718. In this analysis some few samples have been selected to analyse the surface roughness. Literature depicts that the surface of the workpiece is a replica from of a wire electrode at every instant in the spark erosion process. Surface roughness is indirectly proportional to the melting point of the wire tool electrode material [101]. Surface roughness is characterized by the crater size and tool surface at any instant. Outer layer of zinc having the lower melting point in the zinc coated brass wire than the internal brass wire electrode; during the machining process the outer layer of zinc cools the wire temperature and converts the more usable energy to the working zone [18]. The zinc coated brass wire electrode has developed lower surface roughness value than the brass wire electrode for Inconel 718 (Figure.3.8). Because, the coating evaporation increases the gap size, which results in better debris removal that can reduce the surface roughness [27]. In the brass wire, the non-uniform thermal load is due to non-uniform spark formation and inefficient flushing characteristics. Improper flushing can also cause arc formation, which can further deteriorate the surface finish [102].

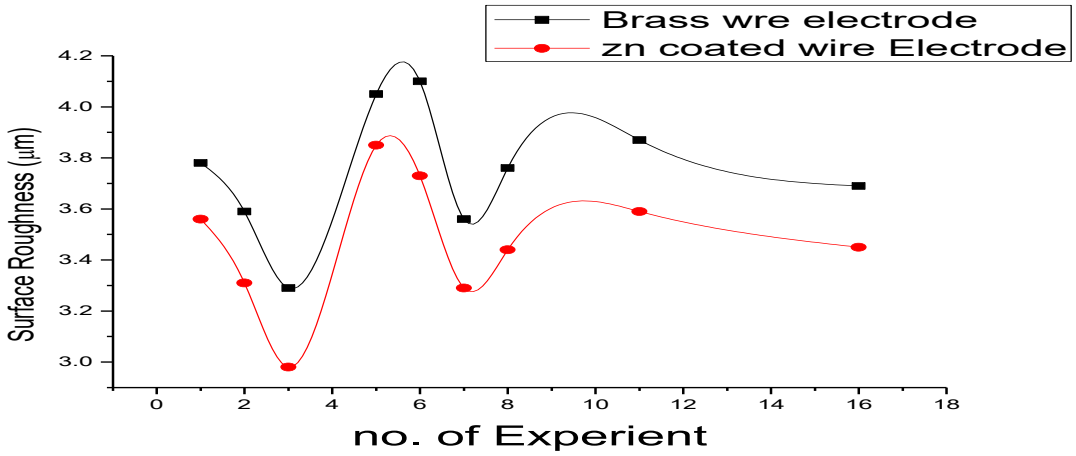


Figure 3.8: effect of wire electrode on surface roughness

Figure. 3.9 (a-d) show snapshots of various wire electrode peripheral surface before and after the machining process. During cutting process, the zinc layer (in case of zinc coated brass wire) actually boils off, or vaporizes; which helps to cool down the wire and delivers more usable energy to the work zone [103]. Literature also provides the information that zinc coated brass electrode possesses higher flushability nature [104].

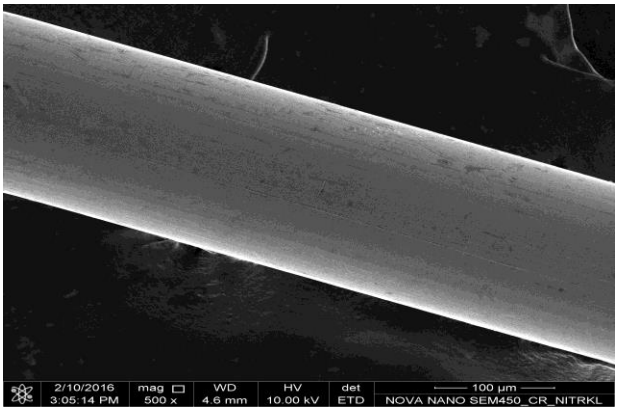


a) Before Machining

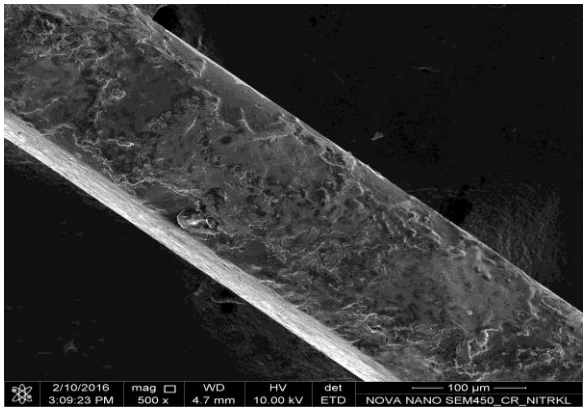


b) After Machining

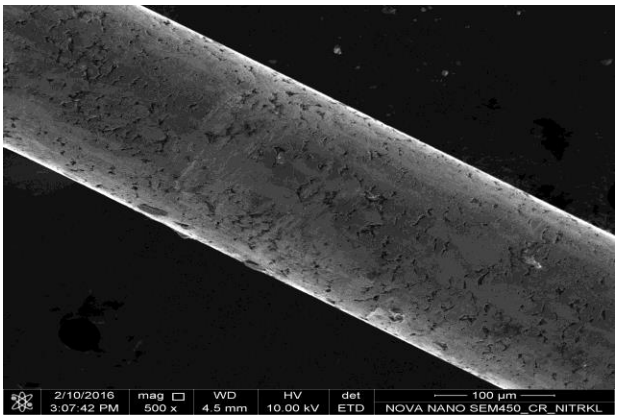


c) Before Machining

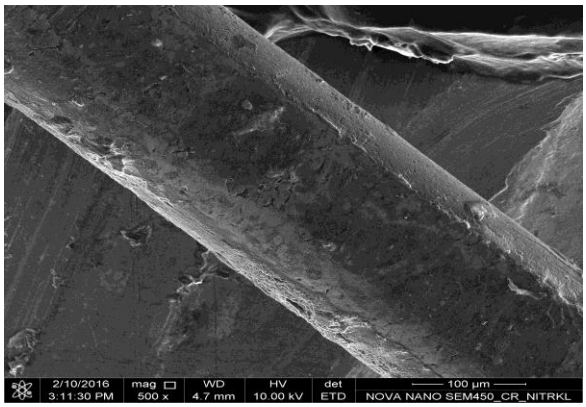


d) After Machining

Figure 3.9: FESEM image of wire electrode before and after machining process. Brass wire electrode (a) before machining (b) after machining. Zinc coated brass wire (c) before machining (d) after machining

Figure 3.10 (a-b) shows the FESEM image revealing machined surface of WEDMed Inconel 718 using different wire electrodes. Literatures say that crater size is directly proportional to the surface roughness. It has been observed that zinc coated wire electrode has produced good surface profile than the brass wire electrode. This may be due to the fact that, zinc content in coating alloys provides a better cooling ability and flushability than conventional brass wire electrode [18]. Flushability of the wire electrode surface indicates the ability of removing more material from the machining zone. Prohaszka et al. [26] reported that the zinc coated brass wire electrode surface could be easily discharged due to due spark energy in the machining process. Referring to Figure 3.10 (a-b) it has been observed that the micro-cracks have been developed more on the machined surface. The formation of micro-cracks is generally accompanied by rapid cooling and heating cycle. In brass wire, the non-uniform thermal load and insufficient flushing characteristics increases yield stress of the part component as a consequence the material plastically deforms during heating that build up the tensile stresses leading to crack formation. In zinc coated brass wire, a heat sink characteristic and modified flushability can help to reduce the wire temperature, which tends to minimize the crack formation.

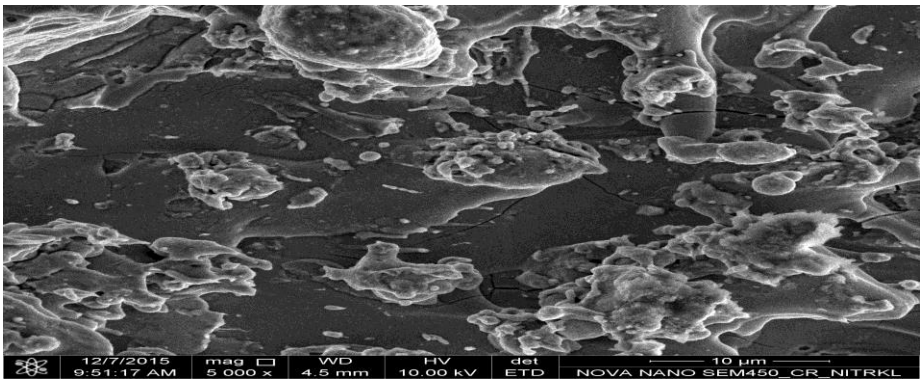


(a) FESEM image of Machined surface of workpiece using Zinc coated brass wire (5000x)

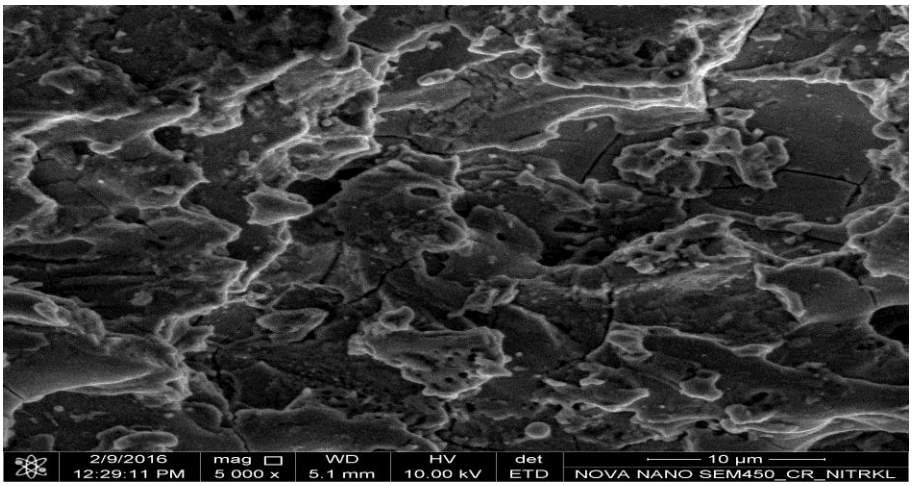


(b) FESEM image Machined surface of workpiece using brass wire electrode (5000x)

Figure 3.10: FESEM image Machined surface of workpiece using different wire electrode with input parameters (A = 32µs, B = 20kg/mm2, C = 6N, D = 14A)

The mean effect analysis of MRR obtained from $L_{16}$ orthogonal array experimentally is shown in Figures. 3.11. The main effects of the controllable process parameters on MRR for both wire types have been are shown in Figure 3.11 (a-d). MRR increases as the discharge current increases. Figure 3.11 (a) shows that MRR is partially increasing with increases in the pulse-on time for both the wire electrodes. While pulse-on time is increased, the power available between the anode and cathode becomes greater. Hence high energy input facilitates the melting and evaporation of materials [105].

Referring to Figure 3.11 (b), it is evident that as flushing pressure increases the MRR tends to decreases. This can be a conflicted due to the fact that the cooling effect increases with increase in the flushing pressure on the workpiece, which results in lower MRR. Figure 3.11 (c) shows

that as wire tension increases the MRR tends to increase for both the wires; because, wire tension is a factor that influences stability of wire during the discharge process. During discharge process, the wire is subjected to disturbances caused by external as well as internal sources [106]. The wire undergoes complex oscillation, which influences the discharge process itself, since the gap is changing continuously. Figure 3.11 (d) indicate that MRR increases with an increase in the discharge current with both the wire electrodes. Increasing the discharge current caused more electrical discharge energy to be conducted into the machining gap with increase in the MRR [51]. With high discharge current stability was obtained in the machining condition and effective material removal was achieved. It has been noted that discharge current is the most significant parameter for MRR using both the wire electrodes.

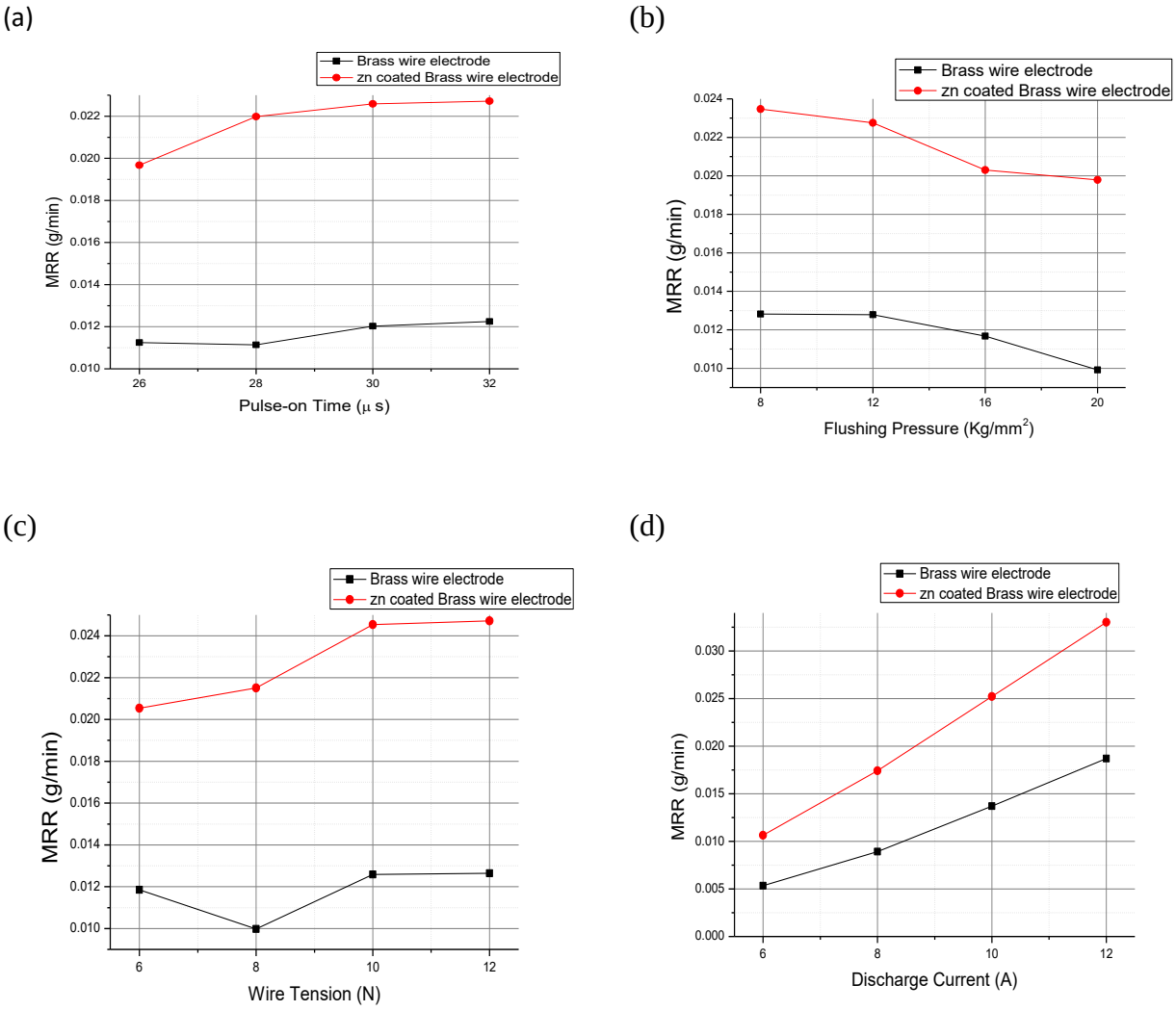


Figure 3.11: Main effect plot on MRR with various wire Electrodes

Figure 3.12 (a-d) shows effects of process parameters on kerf width obtained during WEDM of Inconel 718 using two electrode materials. Referring to Figure 3.12 (a) it can be seen that the kerf width increases with increase in pulse-on time but decreases with wire tension (Figure 3.12 (c)). The increase in the wire tension reduces wire vibration amplitude, which decreases the kerf width [107]. Figure 3.12(d) shows that, kerf width increases with increase in the discharge current with both the electrode. Increasing the discharge current also increases the energy of every discharge, which leads to producing wider kerf width. Some conclusion can also be drawn of from the mean effect analysis of kerf width. It has also been observed that pulse on time and discharge current are the most significant parameters for kerf width using both the wire electrodes. Referring to Figure 3.12 (b) it has been observed that with increase in flushing pressure, kerf width assumes first increasing trends then decreases. However literature depicts, kerf width is inversely proportional to flushing pressure. The experimental data that have been plotted herein found inadequate to capture the real trend. This may be due to experimental error or lack of insufficient data since orthogonal array has been used. The cooling effect increases with increase in the flushing pressure on the workpiece. Higher heat transfer rate from the work surface results in smaller kerf width [55]. Maximum kerf width has been obtained with the brass wire electrode as compared to zinc coated brass wire.

(a)

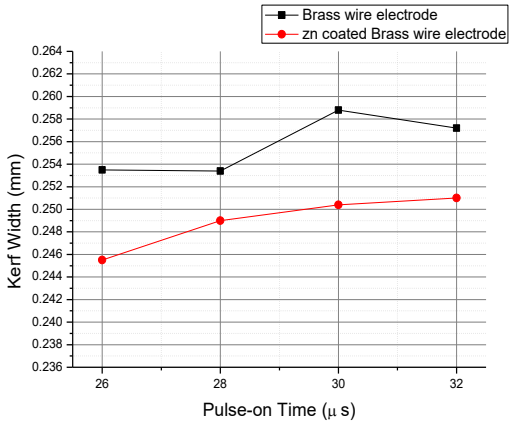


(b)

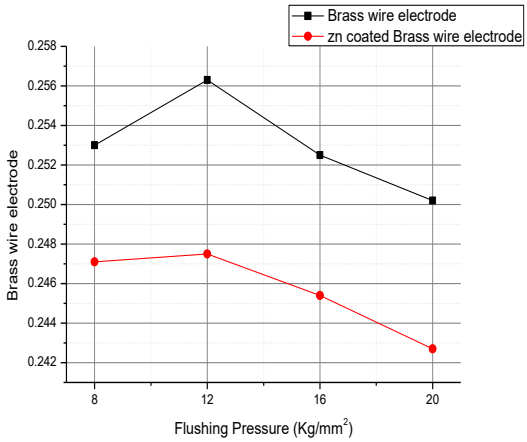

(c)

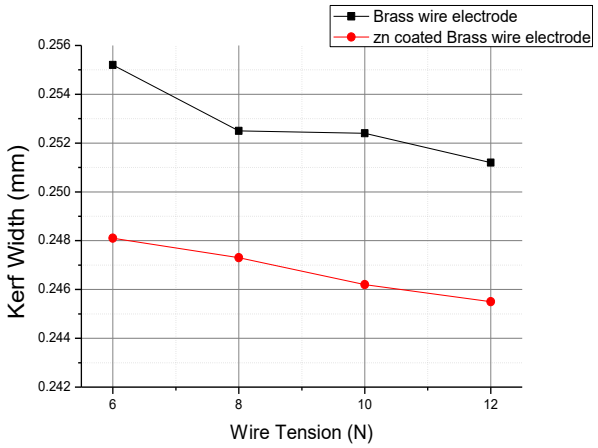


(d)

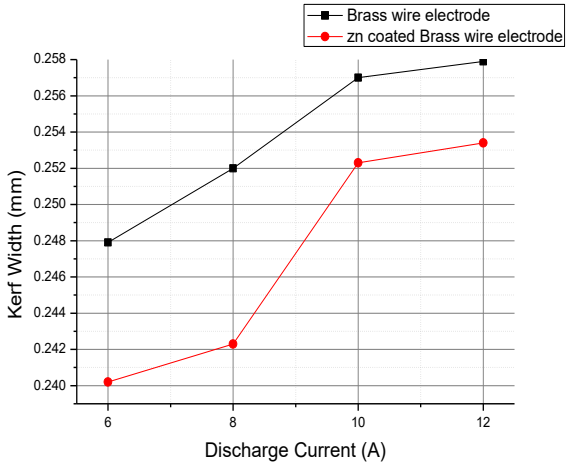


Figure 3.12 Main effect plot on kerf width with various wire Electrode

## 3.1.6. Concluding Remarks

From the experiment the following conclusions have been made.

1. Wire electrode material has considerable contribution on determining performance variable such as MRR, Kerf width and Surface roughness during machining of Inconel 718.
2. The zinc coated brass wire electrode has produced the higher MRR, lesser kerf width and surface roughness as compared to brass wire electrode during machining of Inconel 718.
3. The discharge current is considered the most significant factor for MRR during WEDM on Inconel 718 uses two wire types.
4. The pulse-on time and discharge current have been found to be the most singnificant factor on influsing kerf width for both electrode types.

## 3.2 Machining Performance Analysis of Corner-Cut WEDM in Inconel 718

### 3.2.1 Coverage

This study presents an experimental investigation aiming at analyzing the effect of tool electrode material on machinability of Inconel 718 in terms of Material Removal Rate (MRR), surface roughness and corner deviation during Wire Electrical Discharge Machining (WEDM) operation. Two different electrodes wire viz. uncoated and coated (Zinc) wires, respectively, have been used as tool electrodes with different combinations of controllable process parameters like discharge current, flushing pressure, wire tension and pulse-on time, as per $L_{16}$ orthogonal array design of experiment. The electrode material imposes significant effect on determining WEDM performance on Inconel 718. It has also been observed that zinc coated brass wire shows better performance on MRR, surface roughness and corner deviation, as compared to uncoated brass wire.

### 3.2.2 Problem definition

WEDM is a spark erosion process through electrically conductive wire electrode specially recommended for machining of aerospace material to produce intricate profile with good dimensional accuracy. The workpiece along with the wire electrode are flushed with or immersed in a dielectric fluid. The spark is generated between the workpiece and wire electrode. Good dimensional accuracy of the workpiece is obtained herein with good surface finish.

The machining accuracy, especially at corner position, may be affected during WEDM, because, of some phenomena such as wire defect, vibration, etc. The accuracy of the corner cuts may be improved by modifying the cutting parameters and the wire path [31].

Ramakrishanan et al. [98] developed mathematical models and attempted multi response optimization to predict and select the best cutting parameters for WEDM process on Inconel 718 with brass wire electrode. The effects of various machining parameters such as pulse on time, wire feed speed, delay time and ignition current were studied on the MRR and surface roughness. It was identified that the pulse-on time, delay time and ignition current were influenced more than the wire feed speed on the performance characteristics considered.

Ramakrishnan et al. [39] highlighted optimization of multiple performance characteristics using multi-response Signal to Noise (MRSN) ratio, to achieve high material removal rate and good surface finish, simultaneously. It was observed that increase in pulse-on time and ignition current, resulted improved MRR with brass wire electrode. Hsue et al. [67] studied the fundamental geometrical properties of WEDM process in corner cutting. A model was developed to estimate the MRR in geometrical cutting by considering wire deflection with transformed exponential trajectory of wire center. The observed phenomenon of increased gap-voltage and decreased sparking frequency in corner cutting were physically interpreted. Han et al. [108] discussed about corner error simulation of rough cutting in WEDM operation. A model has been developed to shows the relation between the wire electrode path and the NC path in roughing of sharp corners in order to predict the actual path of the wire electrode. Sanchez et al. [109] discussed about corner geometry generated by successive cuts (roughing and finishing) with brass wire electrode. Errors at different zones of the corner were identified in relation to the material removed during each cut. It was also inferred that MRR depended on factors such as workpiece thickness, corner radius and number of finishing cuts. Han et al. [110] presented that increase in wire tension could improve corner accuracy due to reduced wire deformation, in the meantime, the difference in corner radii in its middle and the edges of thickness was found; to be decreased using brass wire electrode. Dodun et al. [111] described the condition in which sharp corners and small corner radius size could be generated in workpieces with small thickness by using WEDM operation. Yang et al. [31] explored Analysis of Variance (ANOVA) to find out significant factors for the WEDM process amongst (pulse-on time, pulse off time, arc off time, servo voltage, wire feed rate, wire tension and water pressure) on influencing MRR, surface roughness and corner deviation for cutting tungsten using brass wire electrode. It was observed that higher pulse-on time resulted an increase in MRR as well as the wire tension; whilst it decreased the corner deviation. Ghodsiyeh et al. [112] studied the behavior of four major control parameters including pulse-on time, pulse-off time, peak current and servo voltage to find out their effect on the surface roughness, sparking gap, wire lag, wire wear ratio and white layer thickness during WEDM of titanium alloy using zinc coated brass wire electrode. Golshan et al. [73] focused on comparing the performance of brass wire and zinc coated brass wire along with effects of process parameters ( pulse on time, pulse off time and peak current) on the process output i.e., MRR, sparking gap and white layer thickness. Poros et al. [113] found that increase

in discharge time resulted increment of cutting speed as well as MRR almost twice using zinc coated brass wire as compared to brass wire electrode. Because, the exterior zinc coating of the electrode possessed a lower melting temperature than the core material (brass). Hence, the zinc was found overheated and evaporated in the presence of a pulse.

From the literature survey, it has been observed that proper selection of electrode material leads to enhancement of machining performance during WEDM. In the present work, an attempt has been made to compare performance of uncoated brass wire electrode and zinc coated brass wire electrode in terms of MRR, corner deviation (CD) and surface roughness of the WEDMed end product. It has been noted that literature contains very limited studies focusing on comparing performance of different the wires materials [25, 26, 73, 104, 113]. To this end, in the present study, an attempt has been made to discuss the effect to discuss the effect of various process parameters along with varying electrode materials on corner errors measures during WEDM on Inconel 718. Attempt has also been made to analyze the influence of the wire electrode on MRR, CD and surface roughness in WEDM process using various wire electrodes such as uncoated brass electrode and zinc coated brass on Inconel 718.

### 3.2.3 Experimentation

Inconel 718 was taken as a work material in form of rectangular plate with dimension 50.18mm × 20.08mm × 5.29mm. The chemical and the physical properties are given in Table 1.2-1.4 in Chapter no 1. The experiments were performed on (AGIE, SWITZERLAND) CNC WEDM machine (Figure 3.1). Experiments were cut with a prefixed length of 10mm and orthogonal length of 10mm for each experimental run. Zinc coated brass wire and uncoated brass wire having 0.20mm diameter were used in these experiments. Relevant properties of brass wire and zinc coated brass wire have been shown in Table 3.5.

Table 3.5 Properties of wire electrodes

| Properties | Zinc coated brass wire | Brass wire |
|---|---|---|
| Electrode diameter | 0.20 | 0.20 |
| Electrode dia tolerance (mm) | ±0.001 | ±0.001 |
| Minimum tensile strength (MPa) | 964 | 980 |
| Melting point ($^{o}$C) | 419 | 927 |

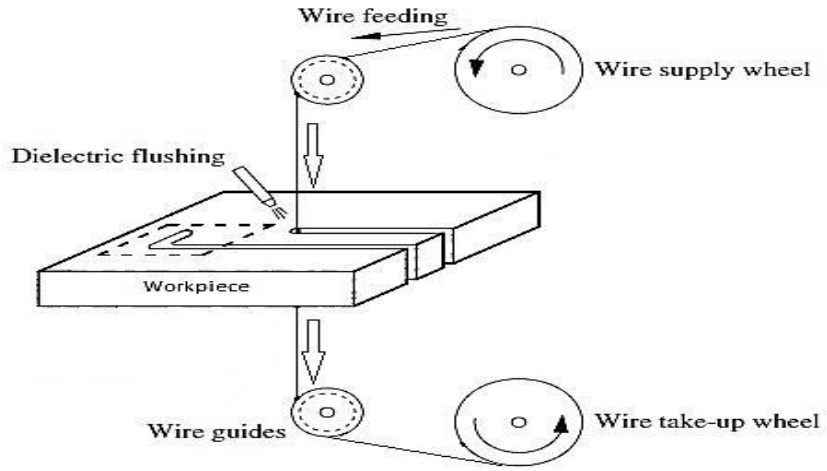


Figure 3.13 Scheme of the WEDM process

The selection of controllable process factors has been given in Table 3.6. The parametric selection in rough cut stage is targeted to achieve highest cutting speed irrespective of surface finish. Pulse on time, flushing pressure, wire tension and discharge current have been chosen as the input parameters. The pulse-off time (50µs) and dielectric flow rate (1.2 bars) were kept fixed throughout the experiments as show in Figure 3.13. Deionized water has been used as dielectric fluid. The schematic for methodology of the experiments were depicted in Figure 3.15. The following responses viz. MRR, surface average roughness and corner deviation have been investigated.

Table 3.6 Process control factors and domain of experiments

| Control factors | Code | Unit | Level I | Level II | Level III | Level VI |
|---|---|---|---|---|---|---|
| Pulse on time | A | [µs] | 26 | 28 | 30 | 32 |
| Flushing Pressure | B | [kg/mm$^2$] | 8 | 12 | 16 | 20 |
| Wire tension | C | [N] | 6 | 8 | 10 | 12 |
| Discharge Current | D | [A] | 10 | 12 | 14 | 16 |

The cutting speed ($C_s$) has been directly obtained from the computer monitor of WEDM machine. The surface roughness (Ra) of WEDMed surface of Inconel 718 has been measured using Talysurf (Talysurf 50 Taylor hobson Ltd., UK). The surface texture and the finishing mechanism after WEDM process have been observed through FE-SEM (NOVA NANO SEM 450).

The corner deviation has been defined as the geometrical contour error on the outer corner by orthogonal cutting and enlargement of corner deviation as shown in Figure. 3.14.

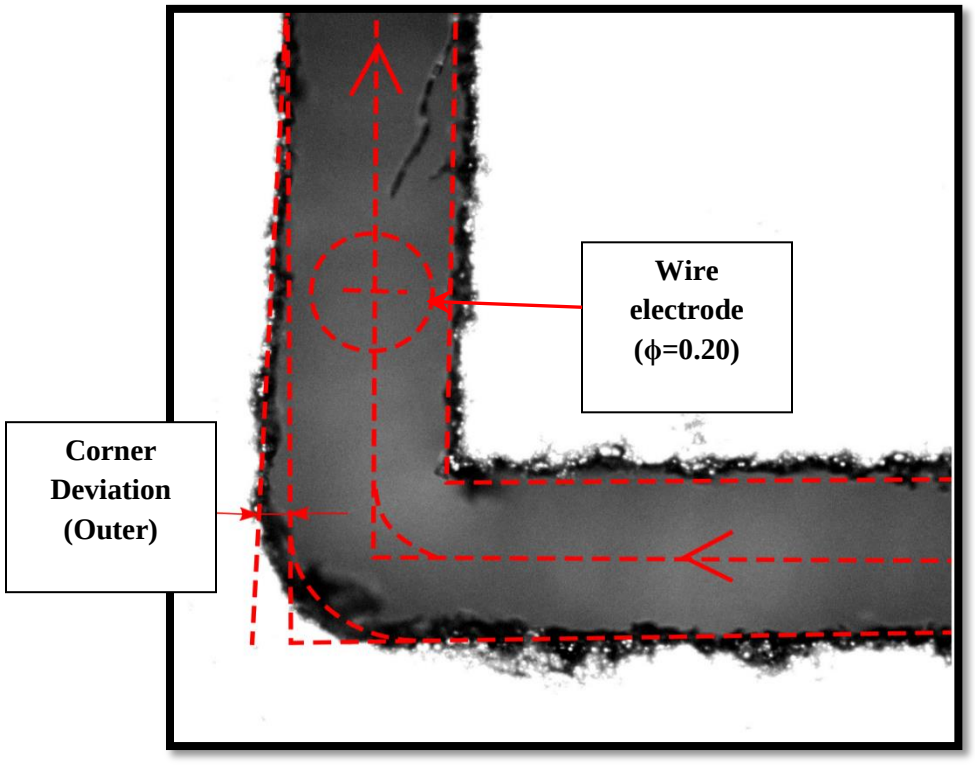


Figure 3.14 Enlargement of corner deviation by WEDM

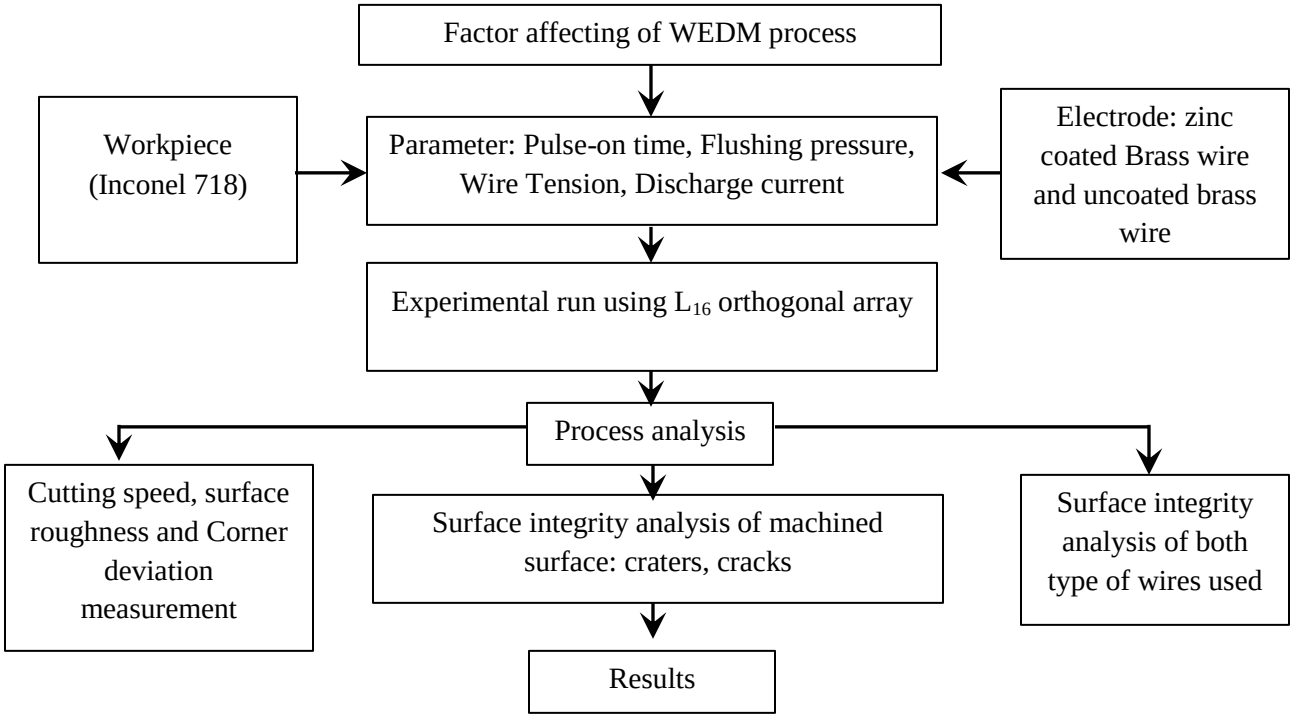


Figure 3.15 Experimental strategy

The experimental strategy has been depicted in Figure 3.15. During experiments, it has been observed that due to low thermal conductivity of Inconel 718, high flushing pressure has been found absolutely necessary for rough machining; otherwise, the short-circuit phenomenon might have caused to wire breakage.

Table 3.7: design of experiment and collection response data **(in coded form)**

| | Design of Experiment | | | | Responses data | | | | | |
|---|---|---|---|---|---|---|---|---|---|---|
| Ex. No | A [µs] | B [kg/mm$^2$] | C [N] | D [A] | Cutting Speed (mm/min) | | Corner deviation [mm] | | Surface roughness [µm] | |
| | | | | | Zn-WE | BWE | Zn-WE | BWE | Zn-WE | BWE |
| 1 | 1 | 1 | 1 | 1 | 05.30 | 02.48 | 0.0351 | 0.0435 | 2.58 | 3.12 |
| 2 | 1 | 2 | 2 | 2 | 09.26 | 04.00 | 0.0351 | 0.0381 | 3.12 | 3.53 |
| 3 | 1 | 3 | 3 | 3 | 12.10 | 06.20 | 0.0406 | 0.0442 | 3.30 | 3.60 |
| 4 | 1 | 4 | 4 | 4 | 12.40 | 09.00 | 0.0355 | 0.0393 | 3.10 | 3.59 |
| 5 | 2 | 1 | 2 | 3 | 15.50 | 06.07 | 0.0374 | 0.0435 | 3.19 | 3.85 |
| 6 | 2 | 2 | 1 | 4 | 15.80 | 06.48 | 0.0783 | 0.0844 | 4.40 | 4.80 |
| 7 | 2 | 3 | 4 | 1 | 04.86 | 04.80 | 0.0320 | 0.0366 | 3.29 | 3.88 |

| | | | | | | | | | | |
|---|---|---|---|---|---|---|---|---|---|---|
| 8 | 2 | 4 | 3 | 2 | 09.72 | 03.40 | 0.0258 | 0.0286 | 3.50 | 3.80 |
| 9 | 3 | 1 | 3 | 4 | 15.00 | 06.80 | 0.0381 | 0.0408 | 4.08 | 4.32 |
| 10 | 3 | 2 | 4 | 3 | 12.20 | 06.64 | 0.0311 | 0.0367 | 3.40 | 3.62 |
| 11 | 3 | 3 | 1 | 2 | 07.10 | 03.50 | 0.0376 | 0.0408 | 3.42 | 3.87 |
| 12 | 3 | 4 | 2 | 1 | 04.50 | 02.20 | 0.0218 | 0.0537 | 3.67 | 3.83 |
| 13 | 4 | 1 | 4 | 2 | 09.00 | 05.94 | 0.0279 | 0.0313 | 3.40 | 3.70 |
| 14 | 4 | 2 | 3 | 1 | 07.10 | 04.12 | 0.0218 | 0.0347 | 3.78 | 4.10 |
| 15 | 4 | 3 | 2 | 4 | 15.10 | 07.97 | 0.0314 | 0.0583 | 4.40 | 4.80 |
| 16 | 4 | 4 | 1 | 3 | 12.00 | 07.10 | 0.0469 | 0.0442 | 3.80 | 4.20 |

**Zn-WE:** Zinc coated brass wire, **BWE:** uncoated brass wire

A 4-factor-4-level, $L_{16}$ orthogonal array has been selected for conduction of experiments and experimental data have been furnished as shown in Table 3.7

## 3.2.4 Results and Discussions

### 3.2.4.1 Effects of variation of electrode material on different response measures

Table 3.7 depicts the experimental results of Cutting speed, corner deviation and surface roughness. Figure 3.16 evident from mean effect plot that zinc coated wire provides higher cutting speed as compared to uncoated brass wire because of its capability to sustain high discharge energy and improve flushability in nature. As Cutting speed corresponds to “Higher-is-Better” (HB) criteria (from productivity viewpoint); higher cutting speed obtained in zinc coated brass wire exhibits superiority in performance as compared to plain brass wire. This is in support with previous literature which say that, cutting speed of the zinc-coated brass wire is almost twice with respect to uncoated brass wire [26]. On run no 7 suddenly goes down to minimum cutting speed, this may because of high flushing pressure and low discharge current, decrease the conductivity in the machining zone.

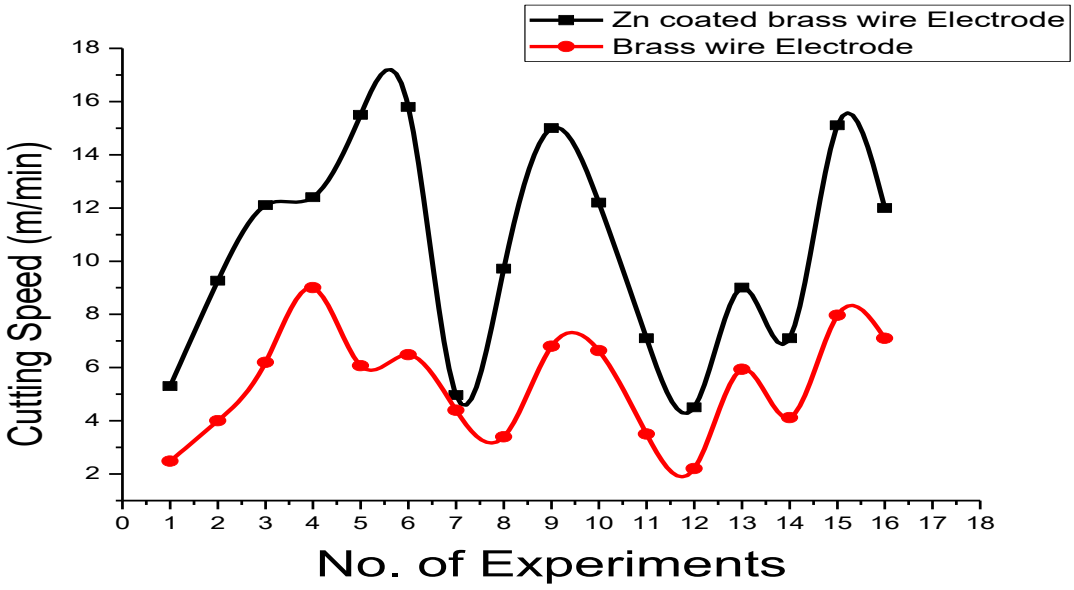


Figure 3.16 Effects of wire electrode on Cutting Speed

Figure 3.17 illustrates that surface finish is improved with zinc coated brass wire compared to uncoated brass wire. This may be because of the superior flushing characteristics of zinc coated brass wire as compared to uncoated brass wire. Superior flushing in the machining zone enables development of high rate of discharge energy which results in rougher surface. In case of brass wire, the non-uniform thermal load is due to non-uniform spark formation and inefficient flushing characteristics. Improper flushing can also cause arc formation, which can further deteriorate surface finish [102]. This phenomenon has also been confirmed through SEM image analysis. Literature depicts that the surface of the workpiece is a replica from of a wire electrode at every instant in the spark erosion process. Surface roughness is indirectly proportional to the melting point of the wire tool electrode material [101].

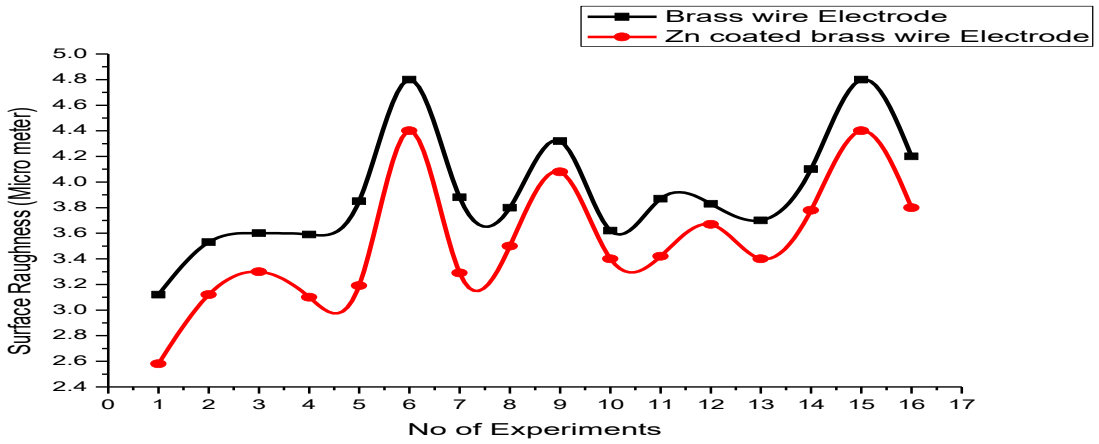


Figure 3.17 Effect of wire electrode on surface roughness

Figure 3.18 shows the effect of electrode material on corner deviation obtained during WEDM of Inconel 718. It has been observed that for all 16 settings experimented in this work; corner deviation value appears lower in case of zinc coated brass wire electrodes as compared to plain brass wire electrode. As corner deviation corresponds to "Lower-is-Better" (LB) criteria (from quality view point); lower corner deviation obtained in zinc coated brass wire exhibits its application feasibility in terms of dimension accuracy as compared to plain brass wire. Zinc coated brass wire having its heat sink capability helps to reduce the wire temperature and thus improve extent of corner deviation

.

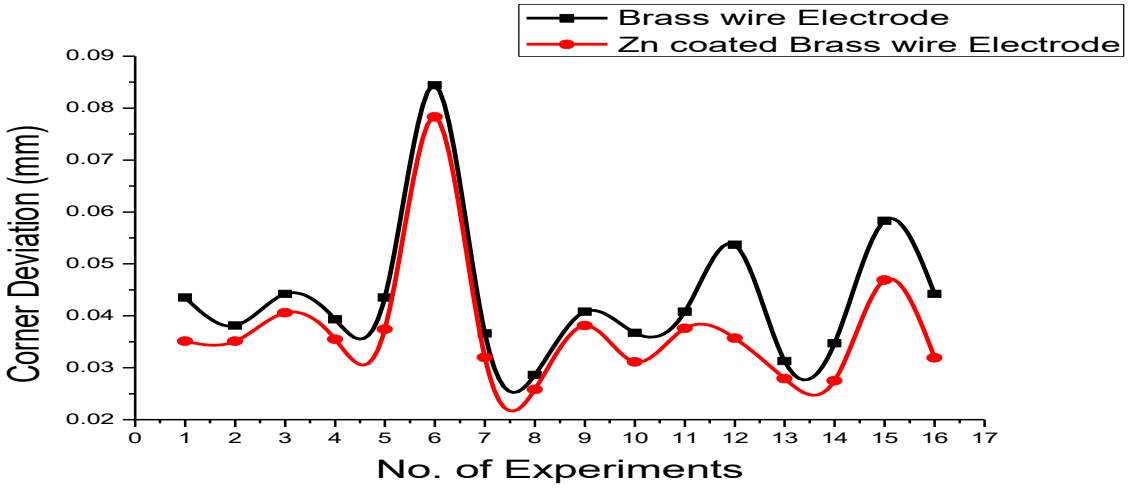


Figure 3.18: Effects of wire electrode on Corner deviation

### 3.2.4.2 Influence of cutting condition on the Corner Deviation

To study the influence of the wire electrode of the corner cut. The measurements of kerf width and corner deviation (CD) of all machined specimens have been measured using tool maker microscope (CARL ZEISS JENA, Germany). Han et al. [108] showed how to obtain the coefficient for the change of the wire deformation during cut machining die to the change of the discharge area.

By measuring the corner cutting radius of results of the above experiments, it is possible to get a relation between the corner cutting radius and process parameters with variation of wire electrode. A comparison of Figure 3.19 (a) and (b) reveals that corner deviation obtained for zinc coated brass wire and uncoated brass wire for different combination of parameters. It has been obtained from specimens machined by zinc coated brass wire observed that better results compared to uncoated brass wire electrode. The obtained profiles for machined surfaces by uncoated brass wire results from the non-uniform thermal load on the workpiece. This non-uniform spark formation and inefficient flushing characteristics of uncoated brass wire electrode. Improper flushing can also cause arc formation, which can further damage the corners. The most of the cases, maximum peak intensity values are considerably low for workpiece machined using uncoated wire.

From the analysis, it is clear that, WEDMed of Inconel 718, zinc coated brass wire preferred over uncoated brass wire.

The measurements of outer corner deviation by orthogonal cutting denoted and depicted in Figure 3.19. All machined specimens have been measured using Optical Microscope (CARL ZEISS JENA, Germany). From the measurements it's having been observed that corner deviation decreases with using of zinc coated brass wire with compared with uncoated brass wire electrode. The snapshot of machined slots have shown for Run nos. 1,8 and 16. These sets of run no. have been selected for variation of most significant parameter which highly affected on corner deviations.

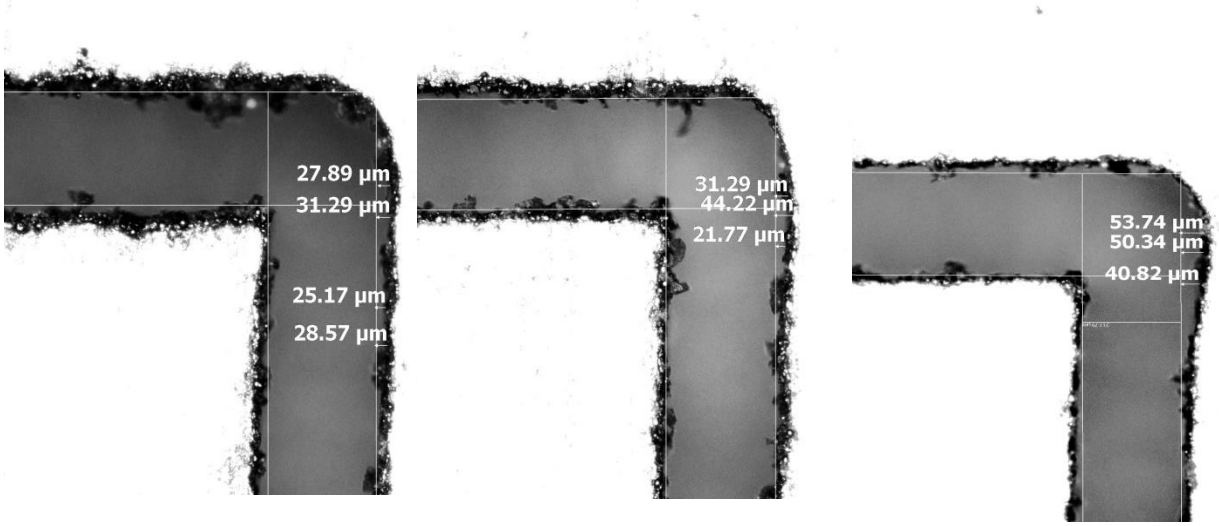


(a) Run no 1 Run no 8 Run no 16

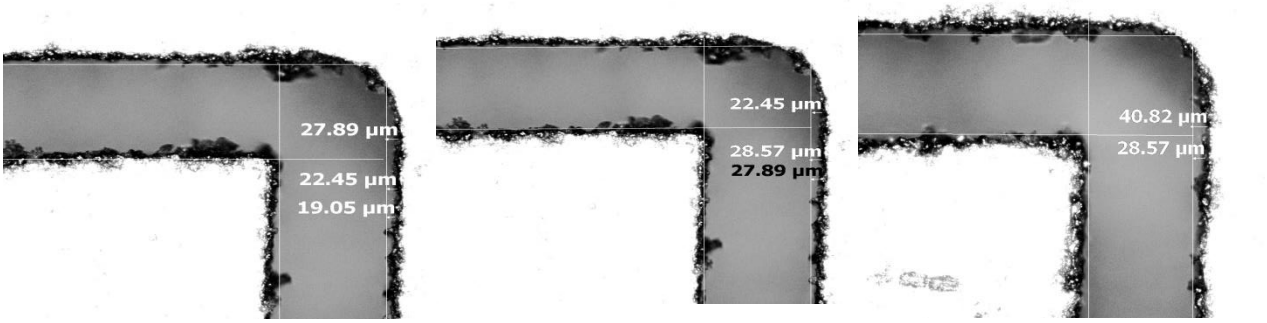


(b) Run no 1 Run no 8 Run no 16

Figure 3.19 Experimental image after machining and measurements. (a) Uncoated brass wire electrode (b) Zinc coated brass wire electrode.

### 3.2.4.3 SEM Analysis revealing surface characteristics of work surface for varying process parameters.

*Surface analysis of the work surface using SEM images*

Figure 3.20(a-b) shows the FESEM image revealing machined surface of WEDMed Inconel 718 using zinc coated brass wire electrodes. Figure 3.20(a) depicts that more number of craters and re-solidified debris compared to figure 3.20 (b). This is because of higher pulse-on

time and discharge current was used on run no 15 compared to run no 1. Figure 3.20(c-d) represented the SEM image revealing machined surface of WEDMed Inconel 718 using uncoated brass wire electrodes. Figure 3.20 (c) depicts that more number of craters, re-solidified debris and spherical droplets compared to figure 3.20 (d). The improved surface finish due to lower pulse discharge energy and pulse-on time. This agreement with another study reported on trim cut WEDM operation [114]. Prohaszka et al. [26] reported that the surface of the zinc coated brass wire can easily be discharged due to spark energy in the machining process referring.

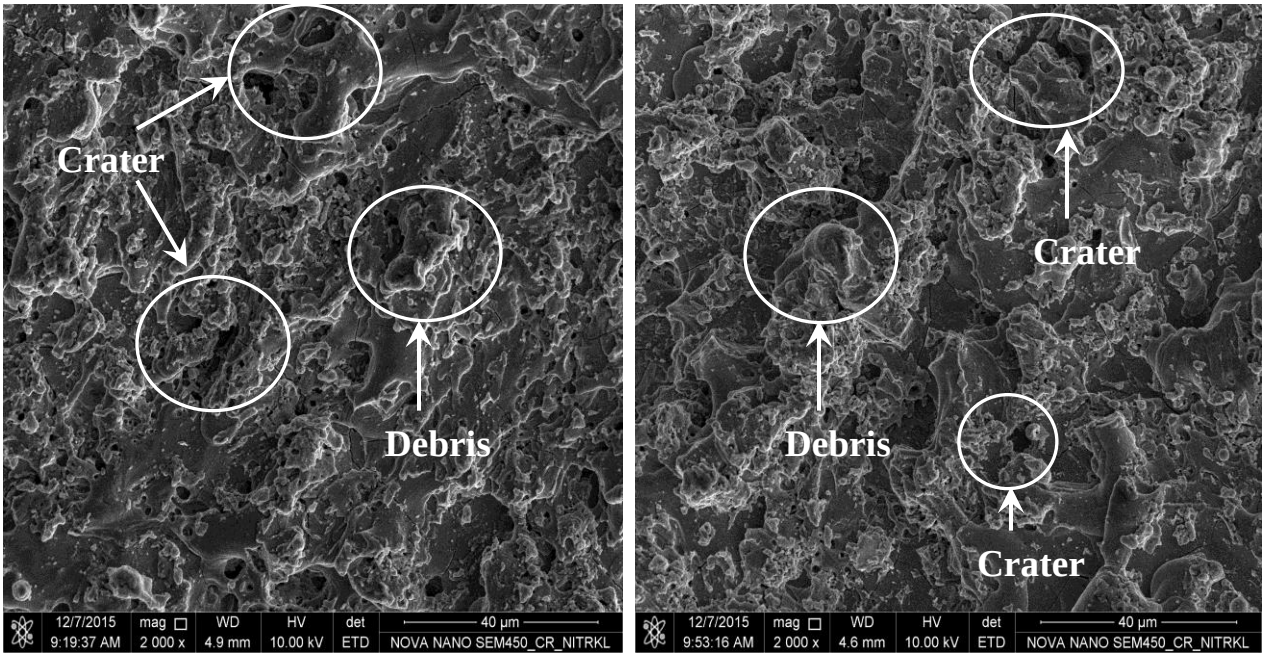


(a) Run no 1 from zinc coated brass wire (b) Run no 15 from zinc coated brass wire

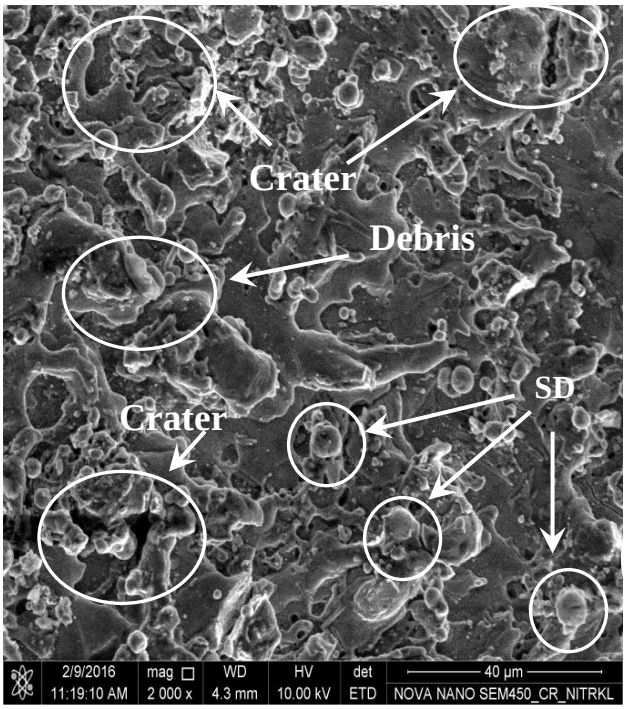


(c) Run no 15 from brass wire electrode

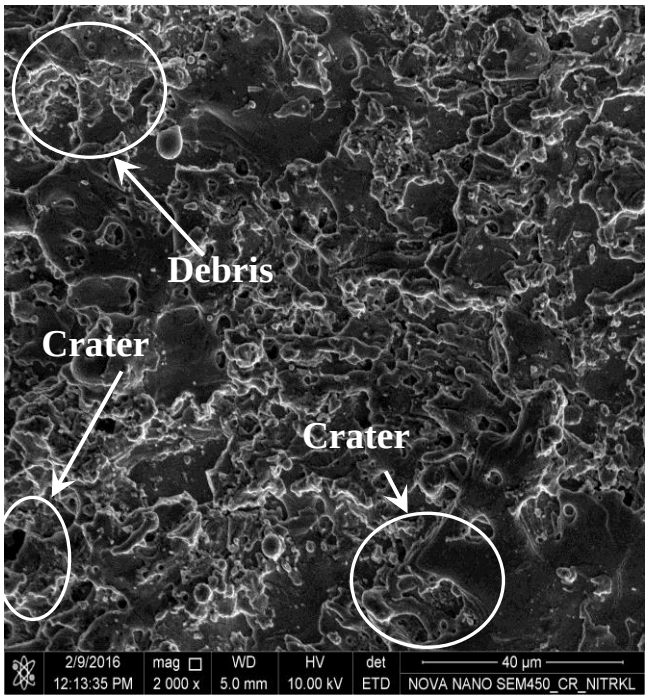


(d) Run no 1 from brass wire electrode

Figure 3.20: FESEM images of the machined surface of WEDMed Inconel using different wire electrode with input parameters, (a) and (b) for zinc coated brass wire and (c) and (d) for uncoated brass wire.

### *Microstructure analysis of the wire electrode surface*

Figure 3.21 (a-d) shows peripheral surface of various wire electrodes before and after the machining process. During cutting process, the zinc layer in case of zinc coated brass wire actually boils off, or vaporizes, which helps to cool down the wire and delivers more usable energy to the work zone [103]. Figure 3.21 (c) the uncoated brass wire exhibited sever degradation as compared to zinc coated wire it is evident that higher amount of debris, cracks and craters were observed on uncoated wire as compared to zinc coated brass wire under similar parametric setting. Figure 3.21 (b) depicts that in case of zinc coated brass wire the wire surface exhibits a smooth surface, without any presence of crack, debris or recast material in run no 15. It may be the because of to the impact of higher pulse on time and discharge current.

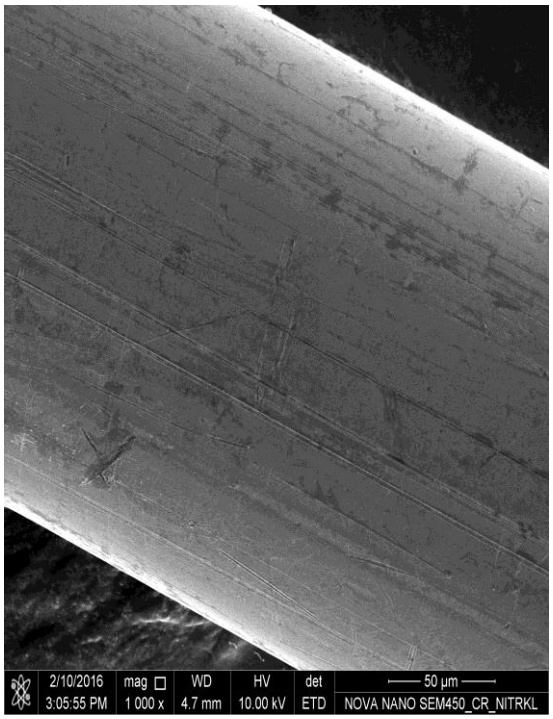


(a) Before Machining

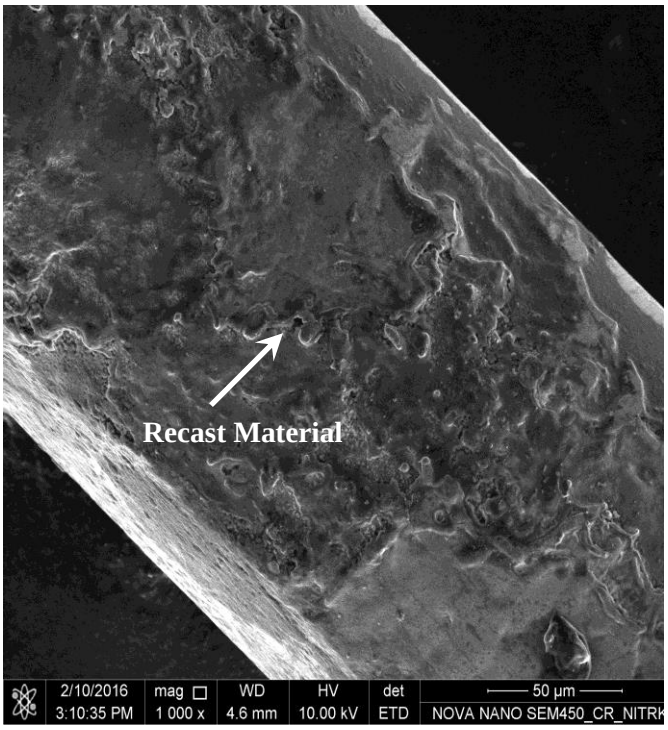


(b) After Machining

Brass wire Electrode (Magnification 1000x)

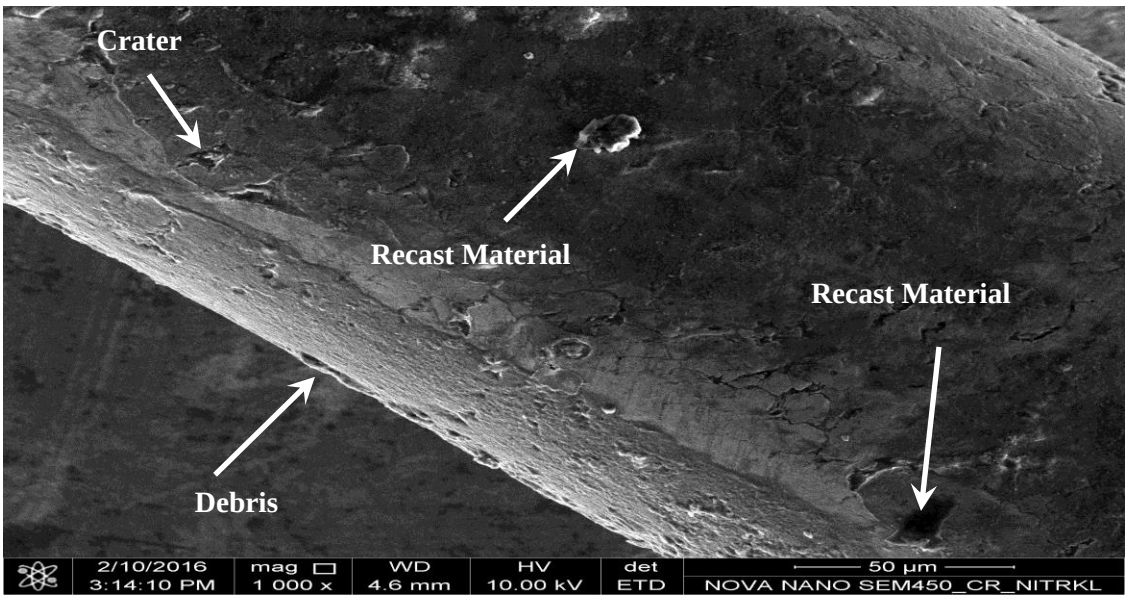


(c) After Machining

Zinc coated Brass wire Electrode (Magnification 1000x)

Figure 3.21: FESEM images of wire electrode (before and after machining process). Brass wire (a) Before machining (b) After Machining. Zinc coated brass wire (c) After machining.

*Analysis of effect of wire Electrode material on workpiece material*

The effects of electrodes on run no. 1 and run no. 15 from Table no. 3.7. It was observed from the inspection of surface texture exhibited in figure 3.20 that zinc coated brass wire yielded a good surface texture that the uncoated brass wire electrode. As the coated wire contains a 5µm thin layer of zinc on the core brass wire, the low melting layer of zinc particles vaporize quickly following spark ignition and contribute to increased gap conductivity and therefore, enable use of higher working gap between the wire electrodes, provides a better cooling ability and flushability than conventional brass wire electrode [18]. Additionally, the vaporization of zinc coated helps to maintain lower temperature of core material of wire electrode which gives more intensive pulse power and results in increased cutting speed [71].

*Electrodes effects on recast layer*

Comparing the recast layer for run no 1 and run no 15 from Table 3.7, it has been observed that brass wire electrode creates of thicker recast layer in WEDMed surface. This variation in the surface texture for WEDMed surface by uncoated brass wire results from the non-uniform thermal load on the workpiece. This non-uniform thermal load is due to non-uniform spark formation and inefficient flushing characteristics. Improper flushing can also cause arc formation, which can further damage the surface.

From the above analysis, it is clear that, for machining of Inconel 718 , zinc coated wire electrode preferred over uncoated brass wire.

### 3.2.4.4 Effect of controllable Process parameters on Cutting Speed, CD, Ra

The main effects of the controllable process parameters on Cutting speed for both wire type have been shown in Figure 3.22 (a-d). The zinc coated wire provides higher cutting as compared to uncoated brass wire because of its capability to sustain high discharge energy and improved flushing ability. Due to low melting and evaporation temperature of zinc layer, the conductivity in the machining zone increases and results in improved flushability. Wire tension play a very important role during the corner cutting of WEDM since wire tension is a deviation between programmed path and actual path taken by wire. Wire tension increases creates a stronger forces acting on the wire, responsible for wire stability during the discharge process [31]. During

discharge, the wire is subjected to disturbances caused by external as well as internal sources [106]. It is apparent that higher wire tension yield higher cutting speed the gap between wire path and actual workpiece profile is increased, which results in lesser pronounced effect of pulse energy in high cutting speed. Increased pulse-on time and discharge current causes higher intensity of discharge energy in machining zone leading increased cutting speed. It can be conclude from above analysis that zinc coated brass wire used with higher values of pulse-on time discharge and wire tension yields higher cutting speed.

(a)

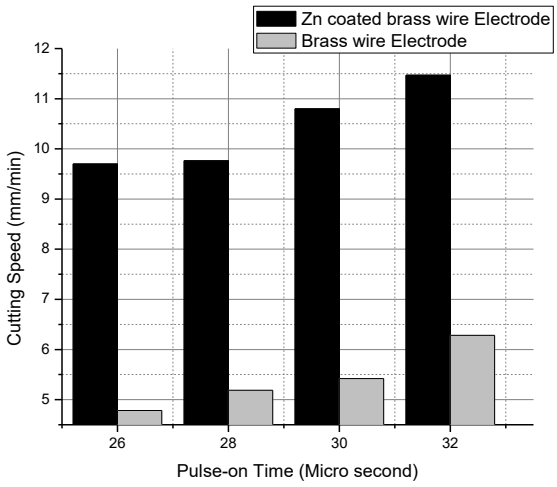


(b)

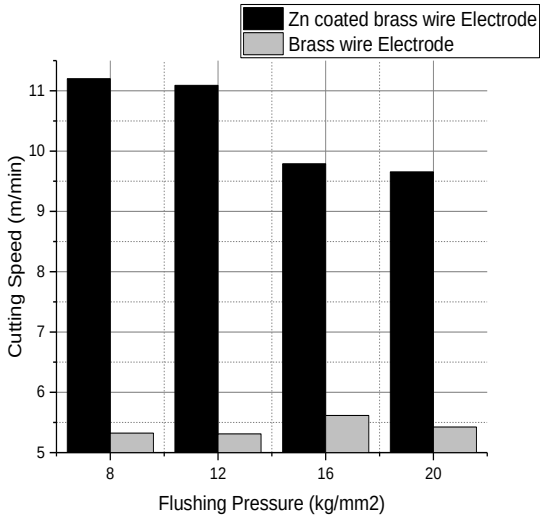

(c)

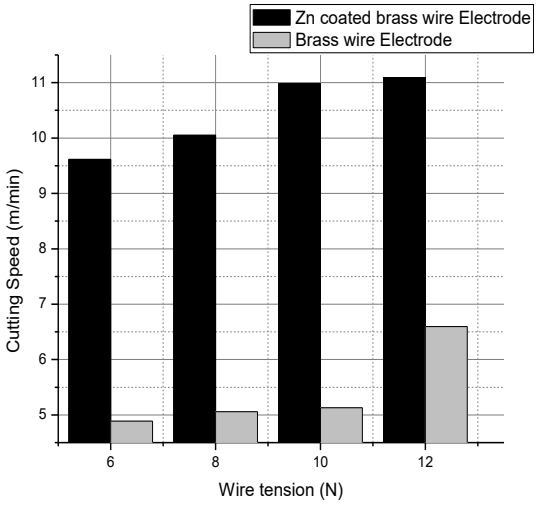


(d)

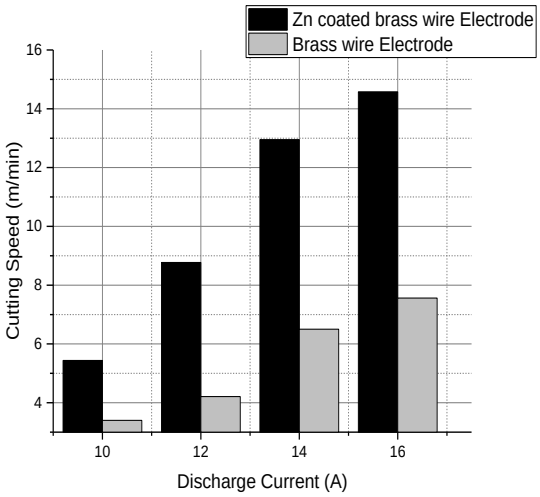


Figure 3.22: Main effect plots for controllable process parameters on influencing MRR with various wire electrodes

Figure 3.23 illustrate that surface finish in improve while zinc coated brass wire is used as compared to brass wire electrode. This might be attributed to the low melting point of zinc layer and superior flushing in the machining zone enables provides good discharge energy which results in smoother surface compared to uncoated brass wire electrode. Parametric effect was investigated through main effects plot on surface roughness. As pulse on time increased and wire tension due to fact that increases in pulse-on time causes increase in the amount of discharge energy resulting in increased vibration of the wire. It also observed that surface roughness decreases with increase in flushing pressure. With higher flushing pressure, it was observed that the surface roughness of the WEDMed Inconel 718 also has increased. Literature delineates, as flushing pressure increases, the surface roughness also decreases. The experimental data that have been plotted herein found deficient to acquire the real trend. This error may be due to the experimental error or insufficient data since orthogonal array has been used. As flushing pressure increases the surface roughness decreases, this may be due to the cooling effect and effective flushing on the working zone leading to good surface finish. So, it can be observed from above investigation that use of zinc coated brass wire along with lower pulse-on time, discharge current and high wire tension will generate lower surface roughness.

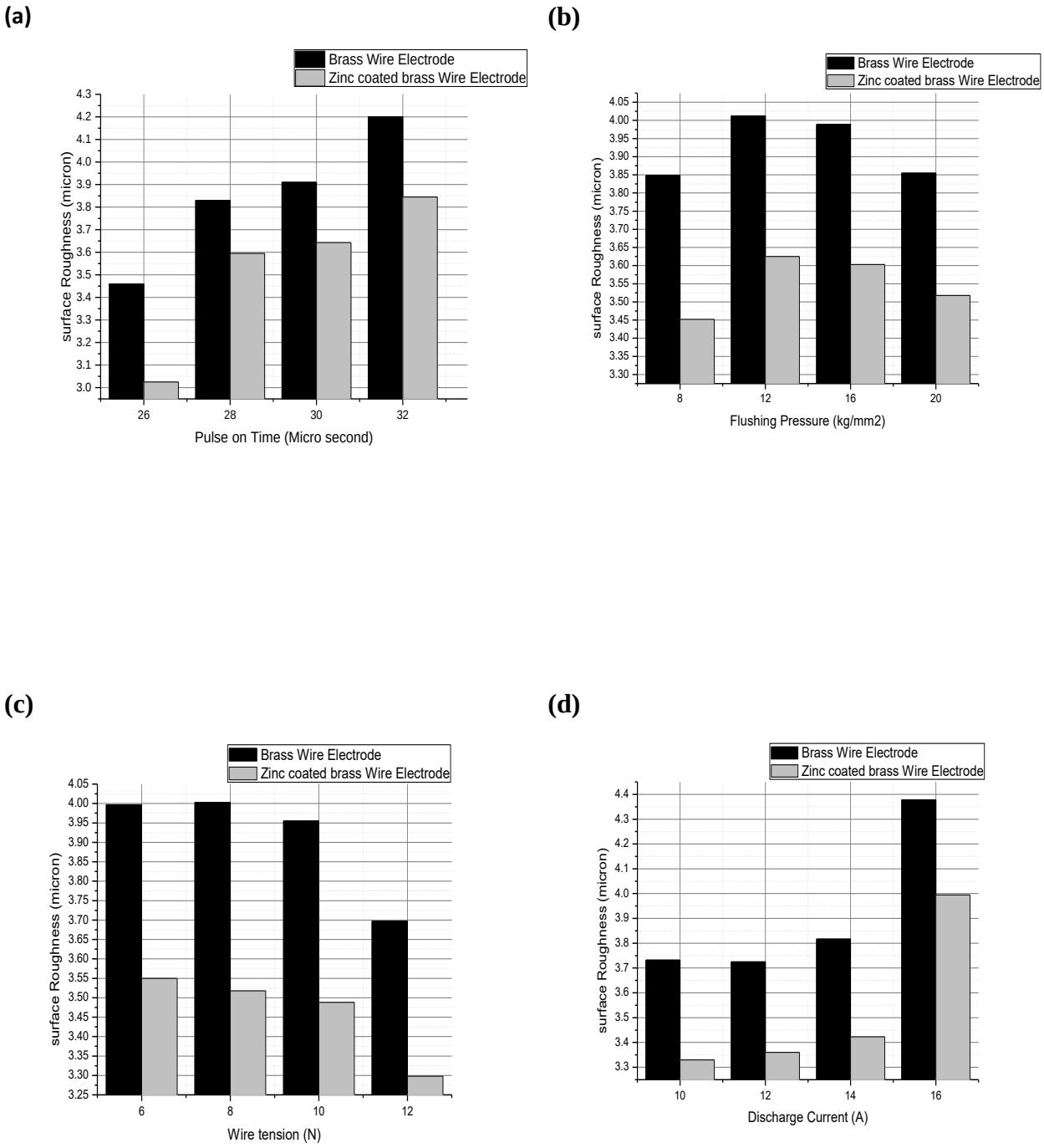


Figure 3.23 Main effect plot on surface roughness with various wire Electrode

Figure 3.24 (a-d) shows effects of process parameters on corner deviation obtained during WEDM of Inconel 718 using two electrode materials. From Figure 3.23 (a) it has been observed that with increase in pulse-on time, corner deviation assumes first increasing trends, and then tends to decreases. However, literature depicts that, corner deviation is inversely proportional to

the pulse on time. The experimental data that have been plotted herein found inadequate to capture the real trend. This may be due to experimental error or lack of insufficient data since orthogonal array has been used. The corner deviation is decreasing trend with increase in pulse on time; this may be due to the fact that, with increase in pulse-on time, discharge energy increases. During every single spark, the wire experiences an impact force, which acts in the reverse direction of the discharge occurrence. Thus, corner deviation decreases [115].

Figure 3.24 (b) shows that with increase in flushing pressure corner deviation first observe an increasing trend then follows decrease. However, literatures illustrate, corner deviation is inversely proportional to flushing pressure. The, inexact trend retrieved herein may be due to lack of insufficient data or experimental error since orthogonal array has been used. The cooling effect increases with increase in flushing pressure on the workpiece which results in smaller corner deviation.

Figure 3.24(c) clearly indicates that corner deviation decreases with increase in wire tension. A higher wire tension produces in stronger forces acting on the wire, responsible for which seems decreasing wire deformation. Therefore, corner deviation reduces. It is clear form Figure 3.24 (d) that with increase in discharge current; corner deviation also increases. This phenomenon may attribute due to the fact that with increase in discharge energy (with increase the discharge current) leads to produce maximum corner deviation. Some conclusion regarding degree of significance of process parameters on corner deviation can also be drawn of from the mean effect analysis. It has also been observed that wire tension and discharge current are the most significant parameters affecting for corner deviation for both wire electrodes.

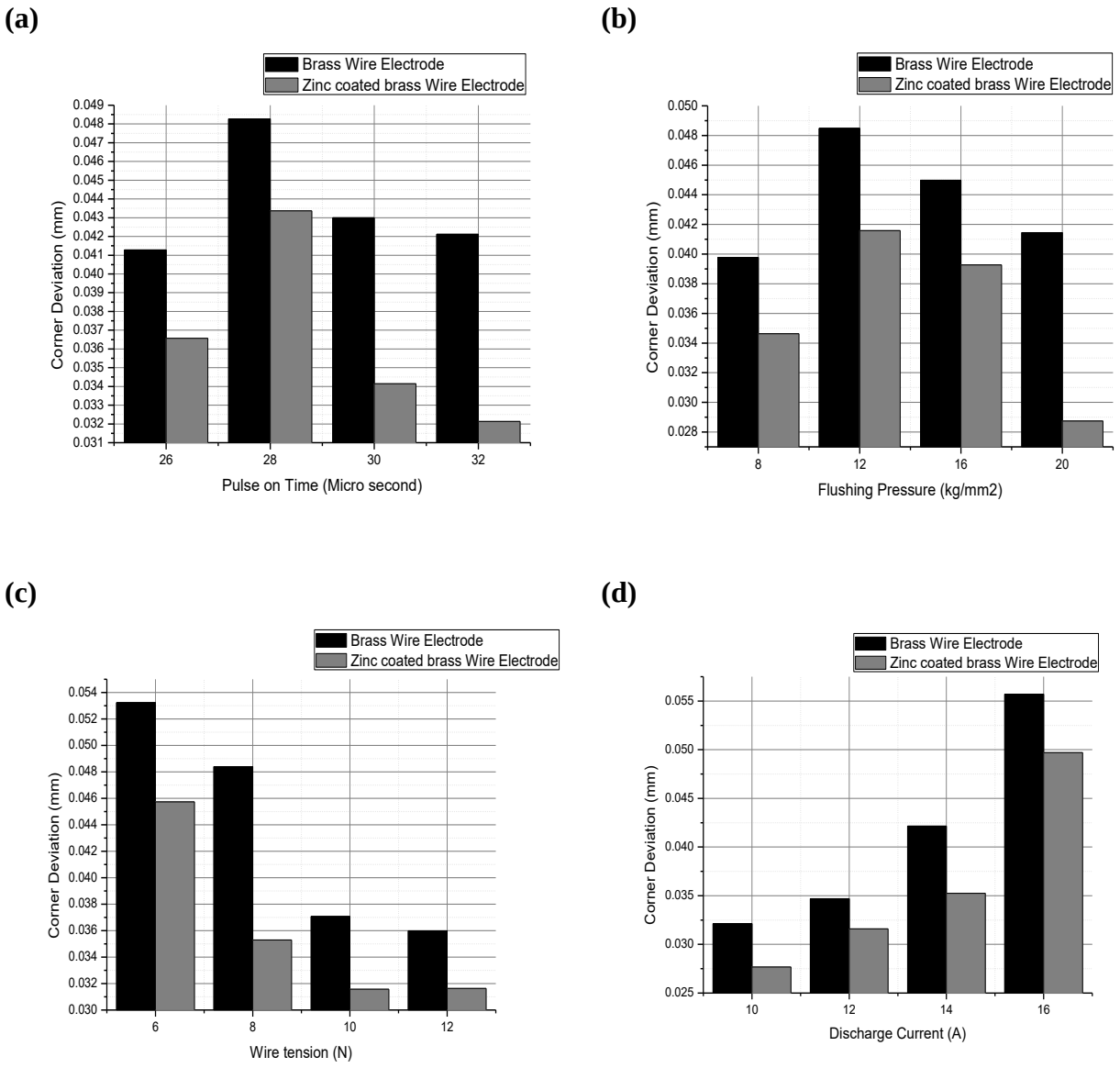


Figure 3.24 Main effect plot on Corner deviation with various wire Electrode

## 3.2.5 Concluding Remarks

The influence of different tool electrode (zinc coated brass wire and uncoated brass wire) on machinability of Inconel 718 has been experimentally investigated. Based on the aforesaid research the following conclusions have been drawn.

a. Selection of appropriate electrode material is very important on enhancing performance in terms of cutting speed, surface roughness and corner deviation during WEDM on Inconel 718.
b. The combination of lower pule-on time, wire tension and zinc coated brass wire yields good surface finish as compared to uncoated brass wire electrode after corner cut WEDM operation of Inconel 718. Cutting speed has been found to be improved with the use of higher value of pulse-on time, discharge and wire tension.
c. The surface texture of the WEDMed surface indicated that uncoated brass wire produce more number of craters, re-solidified debris and spherical droplets compared zinc coated brass wire electrode under similar pulse discharge energy conditions.
d. Comparing the both wire electrodes, large number of recast layer were found on uncoated brass wire electrode. Overall, zinc coated brass wire produce better results for surface finish and recast layer.
e. The zinc coated brass wire has produced the minimum corner deviation as compared to uncoated brass wire electrode.
f. The surface roughness is significantly affected by the pulse on time and discharge current.

## 3.3 Machining Performance Analysis of wire die corner accuracy using V-cut WEDM in Inconel 718

### 3.3.1 Coverage

In present investigation the effects of tool electrode on machinability of Inconel 718 using wire electrical discharge machining for V-cut has been analysed. An $L_{16}$ orthogonal array has been used for experimentation by considering machine controllable factors (i.e. pulse on time, wire speed, flushing pressure and discharge current). The influence of the process parameters on the responses, such as Material Removal Rate (MRR), surface Roughness and die error were studied. From the results, it has been observed that tool material has the significant nature on determining performance variables. It has been also observed that zinc coated brass wire have better performance on MRR, surface roughness and die error than the uncoated brass wire.

### 3.3.2 Problem Definition

Wire electrical discharge machining (WEDM) is a thermos-electrical process in which material is eroded by a series of sparks between the working zone (workpiece and the wire electrode). The workpiece and wire electrode flushed with or immersed in a dielectric fluid. Fine accuracy and complex shape of super hard materials dimension obtained; WEDM is more unique machining process. Without the WEDM process the fabrication of precision workpieces gives high production cost for surface grinding and polish.

In the WEDM process, the material removal rate (MRR) mechanism is a complex stochastic and time varying process involving many variables that make it extremely difficult for setting an optimal parameter setting. Many researchers have been attempted to solve this problem. Selvakumar et al. [36] had attempted an experimentation by considering machine controllable factors (i.e. wire tension, pulse-on time, pulse frequency, peak current and servo voltage) as process parameters on Monel 400 alloy. The process parameters on the responses, such as MRR, surface roughness, corner error, were studied. The impact of pulse parameters modification in

corner accuracy improvement has been analyzed and also an additive model prediction and Pareto optimality approach has been used. Sanchez et al. [109] has been studied on the corner geometry generated by the successive cut (roughing and finishing) on AISI D2 tool steel. Errors at different zones of the corner are identified and related to the MRR during each cut. The main conclusion is that a corner accuracy optimization procedure must consider the errors generated by the previous cuts. Sarkar et al. [116] calculate the wire off-set parameter has been included in the process modeling in order to achieve the dimension accuracy on γ-TiAl plate as workpiece. Puri et al.[75] had discussed that effect the different machining criteria, such as average cutting speed, surface roughness values and the geometrical inaccuracy caused due to wire lag. Hsue et al.[67] proposed the fundamental geometry properties in corner cutting and the concept of discharge angle in introduced its mathematical expression. Yan and Huang [117] introduce a closed loop wire tension control system to improve the machining accuracy. The developed system can obtain fast transient response and small steady-state error of wire tension than an open loop control system and comparison with them. Han et al.[108] analyzed the wire electrode vibration due to the reaction force acting on the wire electrode during machining and compression between the actual versus predicted under the different cutting parameters. Golshan et al [73] attempt to develop a mathematical model and analyze extensively the impacts of the dominant input process parameters on Ti-6Al-4V titanium alloy with the different wire electrode. Kauriakose et al. [102] studied the essentially thermal process and the nature of surface produced by different cutting parameter with different wire electrodes. Antar et al.[25] ideate on the workpiece productivity and integrity of the wire EDMed nickel based super-alloy, and it was found that an increase in productivity of about 40% for nickel based alloy and about 70% for titanium was possible with replacing uncoated brass wire with Cu core coated wires diffusion annealed under the same cutting parameters.

From the literatures, on single pass rough cutting operation, it has been inferred that the total deflection of the wire i.e. wire lag is highly dependent upon the workpiece thickness, spark gap, wire tension and the gap force intensity [67, 70, 75, 117, 118]. During the corner cutting (sharp corner or curve profile), the mismatch match between the defined position and wire guide position leads to huge geometrical and corner inaccuracies. Nonetheless, little or no attempt has been conducted to analyze the influence of wire electrode such as zinc coated brass wire and uncoated brass wire on controllable characteristics in the WEDM process on Inconel 718 as a

workpiece. It has been noted that analysis for the influences of those electrodes on the machining characteristics such as material removal rate (MRR), surface finish, and die corner error has been carried out. Further, from the literatures, it has been observed that two type of strategies have chiefly has been used to improve. First strategy, to improve die accuracy is that to modify the controllable parameters (pulse-on time, pulse-off time, discharge current etc.) in order to control the wire deflection [75, 109, 117]. The second strategy is to modify the wire path to satisfy the geometrical accuracy in online manner. But, most of WEDM manufacturing has been supported the first strategy, i.e., modify the controllable parameters. However, to achieve excellent corner die accuracy, MRR and roughness, an attempt has been made to analyze the influence of the wire electrodes (i.e., zinc coated brass wire and uncoated brass wire) with controllable parameters modification in the WEDM process for rough cutting.

## 3.3.3 Experimental Details

In the present study, experiments have been conducted on a CNC WEDM machine, [AGIE, SWITZERLAND]. Inconel 718 has been selected as work material with dimension (50.1mm× 20.25mm × 3.20mm).

### 3.3.3.1 Selection of process parameters

The selection of process factors has been given in Table 3.8. The experiments have been conducted to investigate the significant contribution of process parameters on machinability (in terms of MRR, surface finish and corner error) during WEDM process. Pulse-on time, flushing pressure, wire tension and discharge current have been chosen as input process parameters. Deionized water has been used as dielectric fluid. The pulse-off time and dielectric flow rate have been kept fixed as 60µs and 1.4 bars, respectively, throughout the experiments.

Table 3.8: Process factors and domain of variation

| Control factor | Code | Unit | Level I | Level II | Level III | Level IV |
|---|---|---|---|---|---|---|
| Pulse on time | A | [μs] | 26 | 28 | 30 | 32 |
| Flushing Pressure | B | [kg/mm$^2$] | 4 | 8 | 12 | 16 |
| Wire tension | C | [N] | 6 | 8 | 10 | 12 |
| Discharge Current | D | [A] | 10 | 12 | 14 | 16 |
| Wire speed | C | [mm/s] | 95 | 115 | 135 | 150 |

During the experiment it is observed that the measurement of corner area (μm$^2$), measured the uncut corner area is more for the smaller corner angle due to die diameter. Therefore, to minimize these corner error, corner angles has been considered as 30$^o$ with different wire electrode (i.e., uncoated brass wire and zinc coated brass wire) to see the effects of wire electrode on die corners error and controllable factors (pulse-on time, flushing Pressure, wire tension and discharge current) has been selected by suitable modifying for rough cutting. The schematic diagram of the operation is shown in Figure. 3.25.

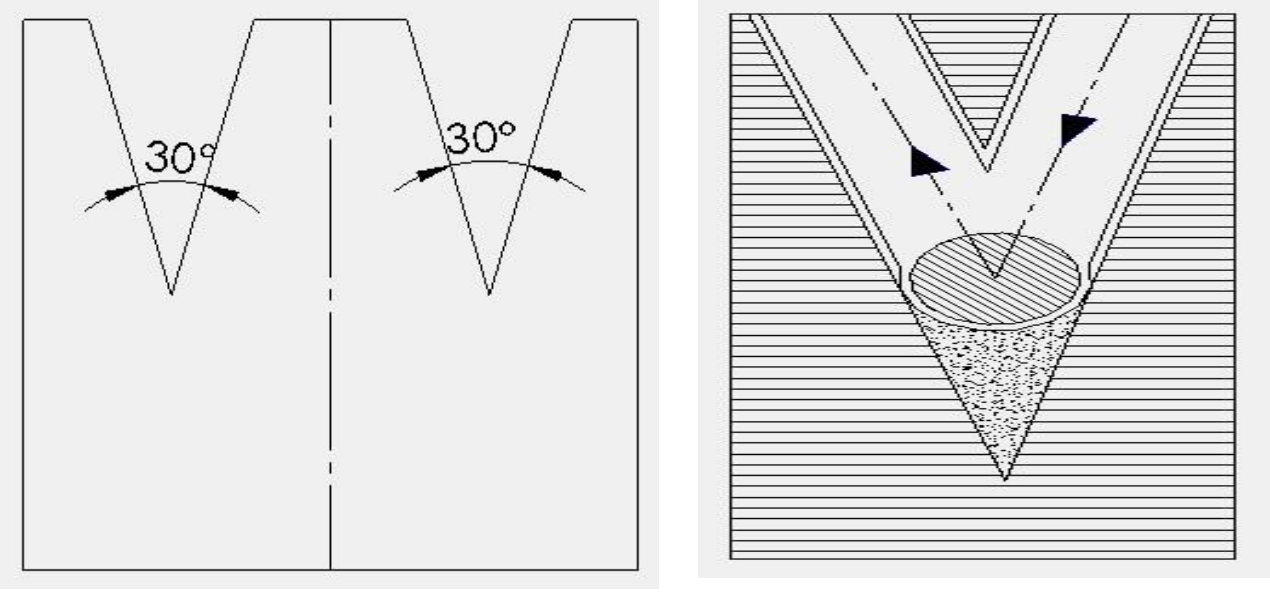


Figure 3.25 Job profile with corner angle

## 3.3.4 Results and discussions

This work, $L_{16}$ orthogonal array has been used for experimentation as it can used 4-level 4 factors in this design.

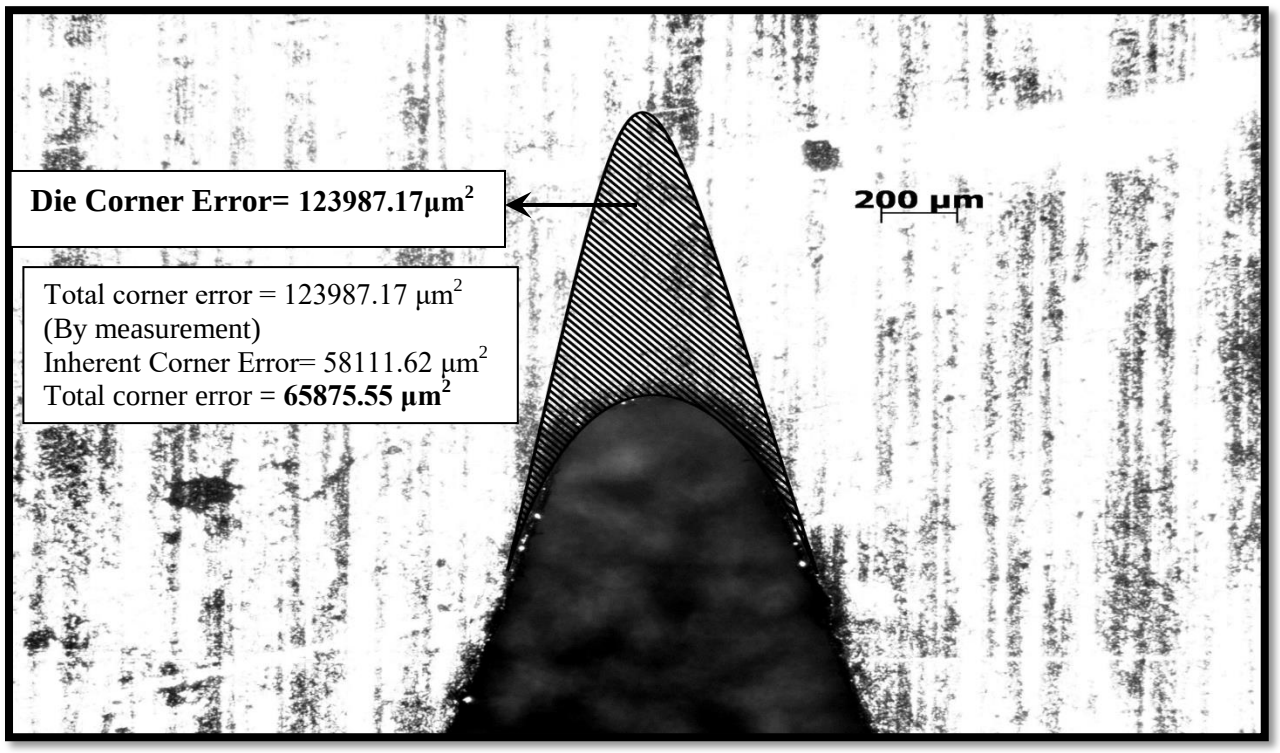


Figure 3.26: die Corner error measurement

The single pass cutting operation is known as rough cutting operation. In this operation high pulse-energy setting has been passed in required job profile. In this rough cutting operation is good for getting high cutting speed and high MRR as compared to trim cutting. In this work a single pass roughness cutting in view of improving dies corner accuracy. Experiment data have been explored to study effects of electrode material along with process parameters on various machining performance characteristics. The cutting speed (mm/min) has been directly obtained from the computer monitor of WEDM machine. MRR is calculated by using Equation 1.1 in chapter 1

Under proportional mode, the cutting speed has been expressed as [70]

Cutting speed ($C_s$) = $k(V_0 - S_0)$ (3.1)

Where $k$ =constant, $V_0$ = gap voltage, and $S_0$ = spark gap set voltage $(V_0 - S_0)$ = error voltage.

The $C_s$ has been proportional to the error voltage $(V_0 - S_0)$. The constant $k$ has been introduced to equate $C_s$ with the error voltage. Constant $k$ is depending on the make and model of the WEDM. The roughness was measured using TALYSURF.

The measurement of corner die error comprises of two components, namely inherent corner error and the corner error due to the wire lag. Figure 3.26 shows the imaginary position of the wire by dashed circle. Figure 3.26 is the inherent corner error which cannot be eliminated by any other strategies. The magnitude of the inherent corner error can be calculated by analysing the corner geometry. For illustrative purposes, the calculation inherent corner error for $30^0$ corner angle is shown below.

$$Inherent\ corner\ error = \text{Area}\ of\ wire - Area\ of\ uncut\ area\ by\ wire\ due\ to\ wire\ lag.$$

The unit inherent corner error is $\mu m^2$ and radius of the wire is 100μm.

The uncut area (hatched area) as shown in Figure 3.26 illustrated the corner error due to wire lag. This corner area (hatched area) has been reduced by zinc coated brass wire electrode because its capability to sustain high discharge energy and improved flushability. Due to low melting and evaporation temperature zinc layer, conductivity in the machining zone increases and results in improved flushability.

Profile of the die corner error illustrated as Figure 3.25. The die corner error was measured Optical Microscope (CARL ZEISS JENA, Germany). The surface images of magnification of 5000X of machined Inconel 718 have been acquired using Field Emission Scanning Electron Microscopy (FESEM) (NOVA NANO SEM 450). Corner error was the average of 3 measurements made from the snapshot to avoid the uncertainty. The corner die error due to wire lag hatched area has been shown in Table 3.9.

Table 3.9: Experimental data **(Coded Form)**

| Ex. No | A [µs] | B [kg/mm$^2$] | C [N] | D [A] | Corner Error (µm$^2$) | | MRR (g/min) | | Surface roughness (µm) | |
|---|---|---|---|---|---|---|---|---|---|---|
| | | | | | Zn-WE | BWE | Zn-WE | BWE | Zn-WE | Zn-WE |
| 1 | 1 | 1 | 1 | 1 | 66542.21 | 83998.10 | 0.1158 | 0.0642 | 3.49 | 3.80 |
| 2 | 1 | 2 | 2 | 2 | 53251.33 | 92008.13 | 0.1806 | 0.0905 | 3.32 | 3.60 |
| 3 | 1 | 3 | 3 | 3 | 73428.74 | 90491.53 | 0.2268 | 0.1291 | 2.98 | 3.31 |
| 4 | 1 | 4 | 4 | 4 | 55230.40 | 78629.42 | 0.2603 | 0.1900 | 3.12 | 3.64 |
| 5 | 2 | 1 | 2 | 3 | 65875.55 | 90379.18 | 0.2666 | 0.1272 | 3.83 | 4.08 |
| 6 | 2 | 2 | 1 | 4 | 80248.52 | 90624.38 | 0.3173 | 0.1232 | 3.68 | 4.12 |
| 7 | 2 | 3 | 4 | 1 | 72854.23 | 90301.5 | 0.1058 | 0.0989 | 3.33 | 3.55 |
| 8 | 2 | 4 | 3 | 2 | 88458.55 | 90149.79 | 0.2093 | 0.0660 | 3.46 | 3.77 |
| 9 | 3 | 1 | 3 | 4 | 68478.88 | 87917.25 | 0.3983 | 0.1975 | 4.09 | 4.31 |
| 10 | 3 | 2 | 4 | 3 | 66847.75 | 85568.02 | 0.2669 | 0.1505 | 3.86 | 3.91 |
| 11 | 3 | 3 | 1 | 2 | 98254.23 | 142481.3 | 0.1483 | 0.0742 | 3.62 | 3.89 |
| 12 | 3 | 4 | 2 | 1 | 94366.54 | 105196.4 | 0.0941 | 0.0614 | 3.69 | 3.85 |
| 13 | 4 | 1 | 4 | 2 | 96589.65 | 138487.9 | 0.1747 | 0.1217 | 4.60 | 4.72 |
| 14 | 4 | 2 | 3 | 1 | 97458.88 | 124267.6 | 0.1357 | 0.0870 | 3.82 | 4.25 |
| 15 | 4 | 3 | 2 | 4 | 92554.78 | 115699.6 | 0.3448 | 0.1471 | 3.85 | 4.04 |
| 16 | 4 | 4 | 1 | 3 | 93489.55 | 119626 | 0.2540 | 0.1419 | 3.48 | 3.74 |

**Zn-WE**: Zinc coated brass wire, **BWE**: Uncoated brass wire

The comparison of the results for WEDM of Inconel 718, applying zinc coated brass wire and uncoated brass wire electrodes, are shown in Figure 3.27. In zinc coated brass wire; the zinc is overheated and evaporated during the pulses. The evaporation acts as a heat sink, which helps to reduce the wire temperature and improve the effectiveness of the WEDM process [26]. Because of these characteristics of zinc coated brass wire, its decreases the gap voltage. The decrease in gap voltage ends up with a decrease in gap width of corners which minimizes the corner die errors during cutting.

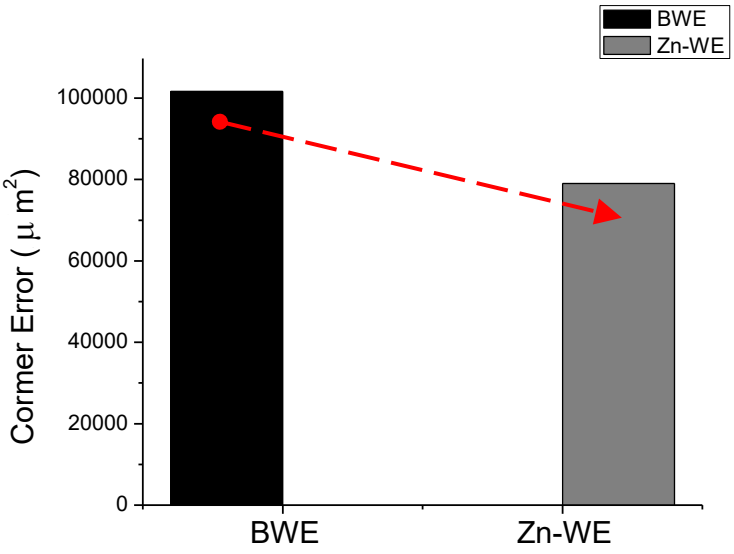


Figure 3.27: Effects of wire electrode on Corner Die Error

In comparison with the models (Figure 3.28) which have appeared previously in the literature observations by different researchers the cutting speed of the zinc-coated brass wire is approximately twice to that of uncoated brass wire because the exterior zinc coating possesses a lower melting temperature than of the core material (brass). It depicts in present study also, the zinc coated brass wire is almost twice than the uncoated brass wire electrode. Because of high cutting rate of zinc coated brass wire, MRR also reaches it twice value form the uncoated brass wire electrode.

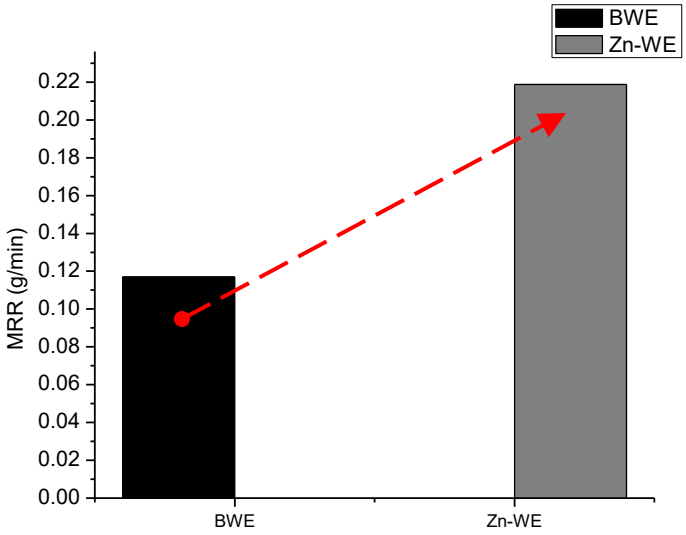


Figure 3.28: Effects of wire electrode on MRR

Literature illustrates that the surface of the workpiece is a replica from of a wire electrode at every instant in the spark erosion process. Surface roughness is indirectly proportional to the melting point of the wire tool electrode material [101]. Surface roughness is characterized by the crater size and tool surface at any instant. In case of zinc coated brass wire; outer layer of zinc having the lower melting point than the internal brass wire electrode; during the machining process the outer layer of zinc cools the wire temperature and converts the more usable energy to the working zone [18]. The zinc coated brass wire electrode has developed lower surface roughness value than the uncoated brass wire electrode for Inconel 718 (Figure. 3.29). Because, the coating evaporation increases the gap size, which results in better debris removal that can reduce the surface roughness [27]. In the brass wire, the non-uniform thermal load is due to non-uniform spark formation and inefficient flushing characteristics. Improper flushing can also cause arc formation, which can further deteriorate the surface finish [102].

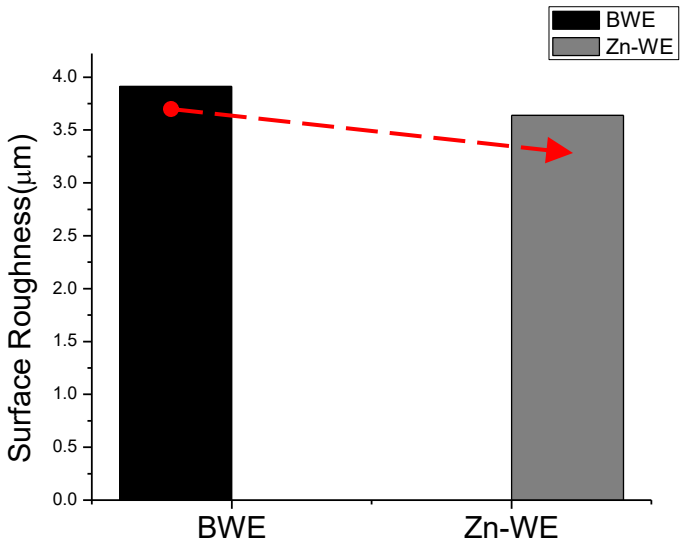


Figure 3.29: the effect of wire electrode on surface roughness

Figure 3.30 (a-d) show FESEM images of surface of various wires electrode surface before and after the machining process. In case of zinc coated brass wire, during the machining process, the zinc layer actually boils off, or vaporizes; which helps to cool down the wire and delivers more usable energy to the work zone [103]. Literature also provides the information that zinc coated brass electrode possesses improved flushability nature [104].

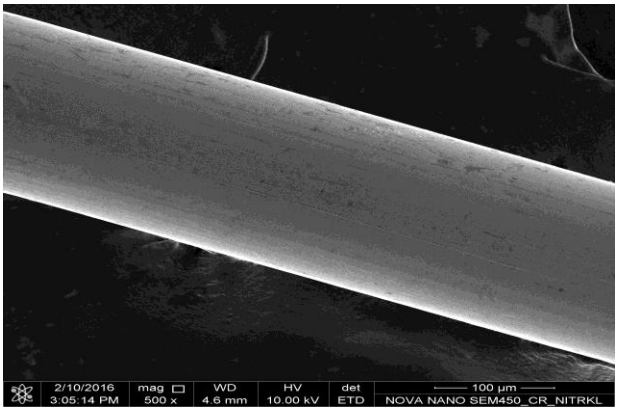


(a) Before Machining

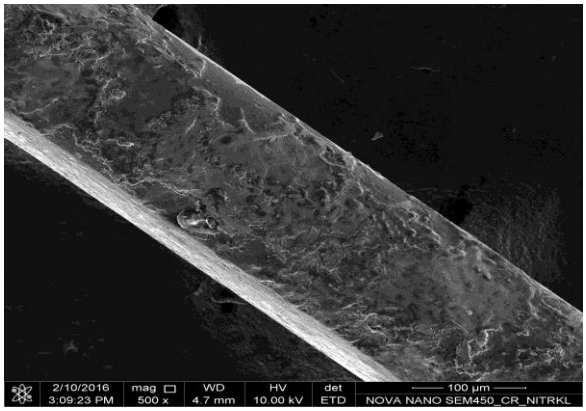


(b) After Machining

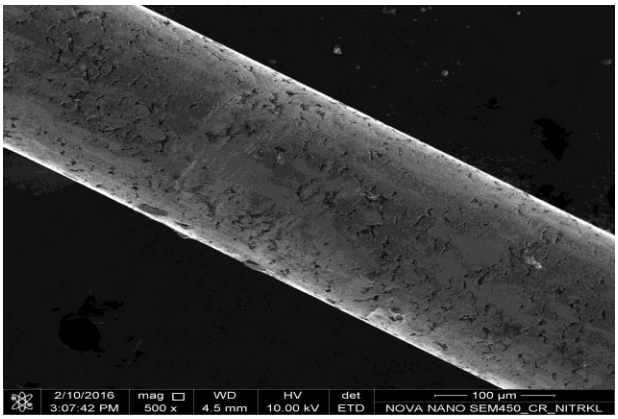


(c) Before Machining

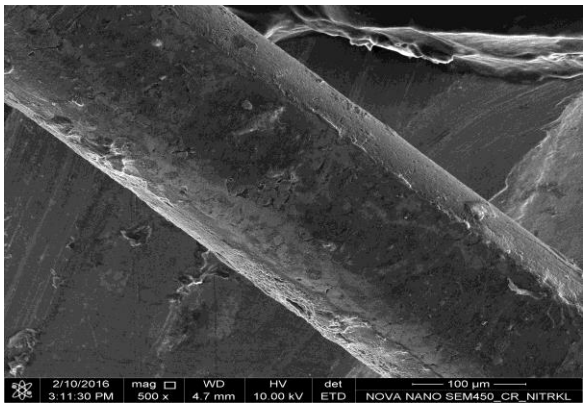


(d) After Machining

Figure 3.30: FESEM image of wire electrode before and after machining process. Brass wire (a) before machining (b) after machining. Zinc coated brass wire (c) before machining (d) after machining

From the Figure 3.31 the pulse-on time (30 µs), flushing pressure (4 kg/mm$^2$) wire tension (10 N) and discharge current (16A). Figure 3.31 (a) shows that large no of spherical shape particles was observed on the WEDMed surface. These observations were obtained with uncoated brass wire. Similar observation was found by comparing Figure 3.31 (b) depicts of WEDMed surface using zinc coated brass wire. In zinc coated brass wire, zinc content in coating alloys provides a better cooling ability and flushability than conventional brass wire electrode [18]. It also observed that form investigation that use of zinc coated and uncoated brass wire along with lower pulse-on time, discharge current and wire tension result in improve surface for both the wire electrode and generate lower surface roughness

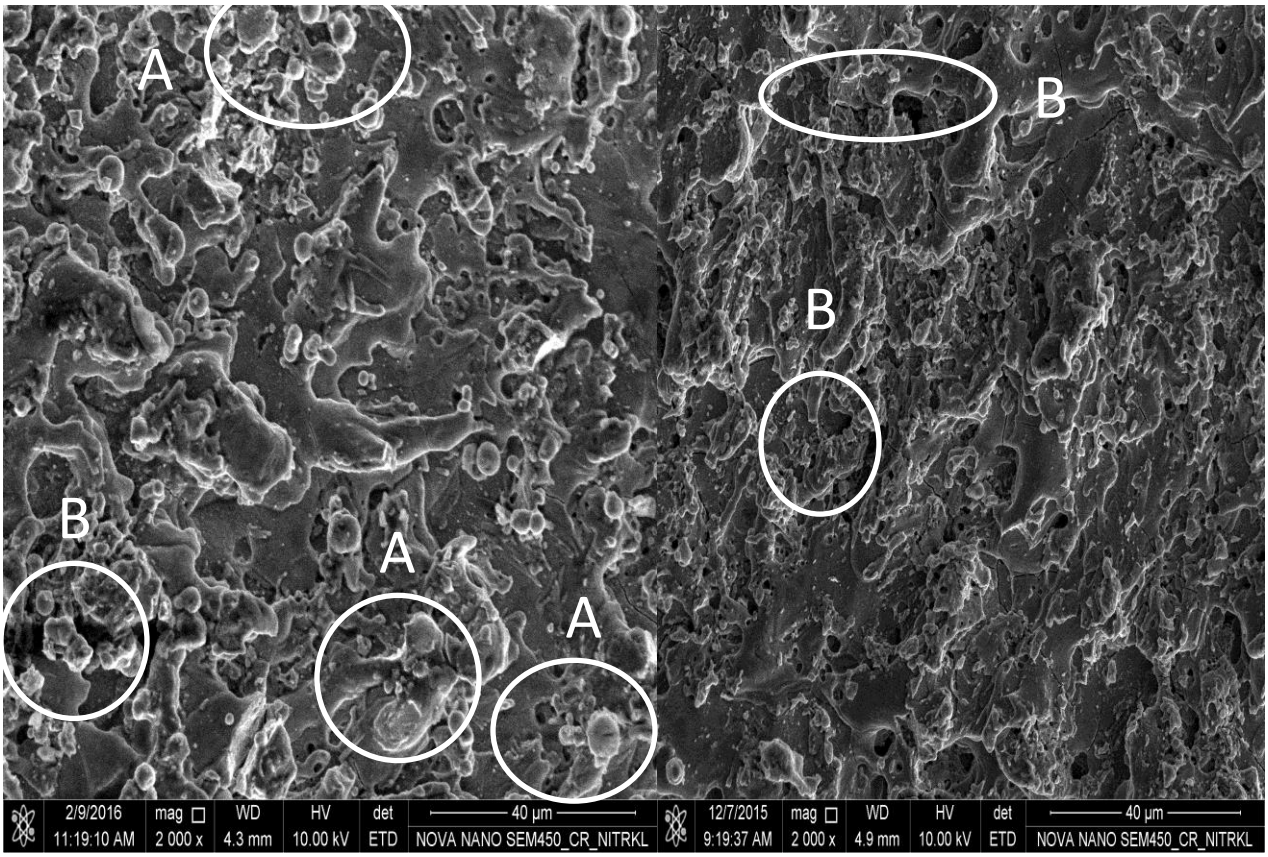


(a) Uncoated Brass wire electrode (b) Zinc coated brass wire electrode

Figure 3.31: FESEM image of WEDMed surface of with less number of craters, and no cracks were formed at lower peak current and pulse on time at $A_1B_1C_1D_1$. A= spherical nodules, B= Crater Rims

From Figure. 3.32 (a) large craters size, re-solidified debris and large no of spherical nodules are protruding as compared to 3.32 (b), which may happen due to higher pulse on time (32µs), discharge current (16 A), at the higher discharge current (16 A), the impact of discharge energy on the surface of work piece using both wire electrodes becomes greater, and thus, resulting erosion leads to the increase in deterioration of surface roughness. Figure 3.32 (b), observed that small craters protruding particles using the zinc coated brass wire compared to brass wire electrode were observed. It may be the modified flushing ability of zinc coated brass wire.

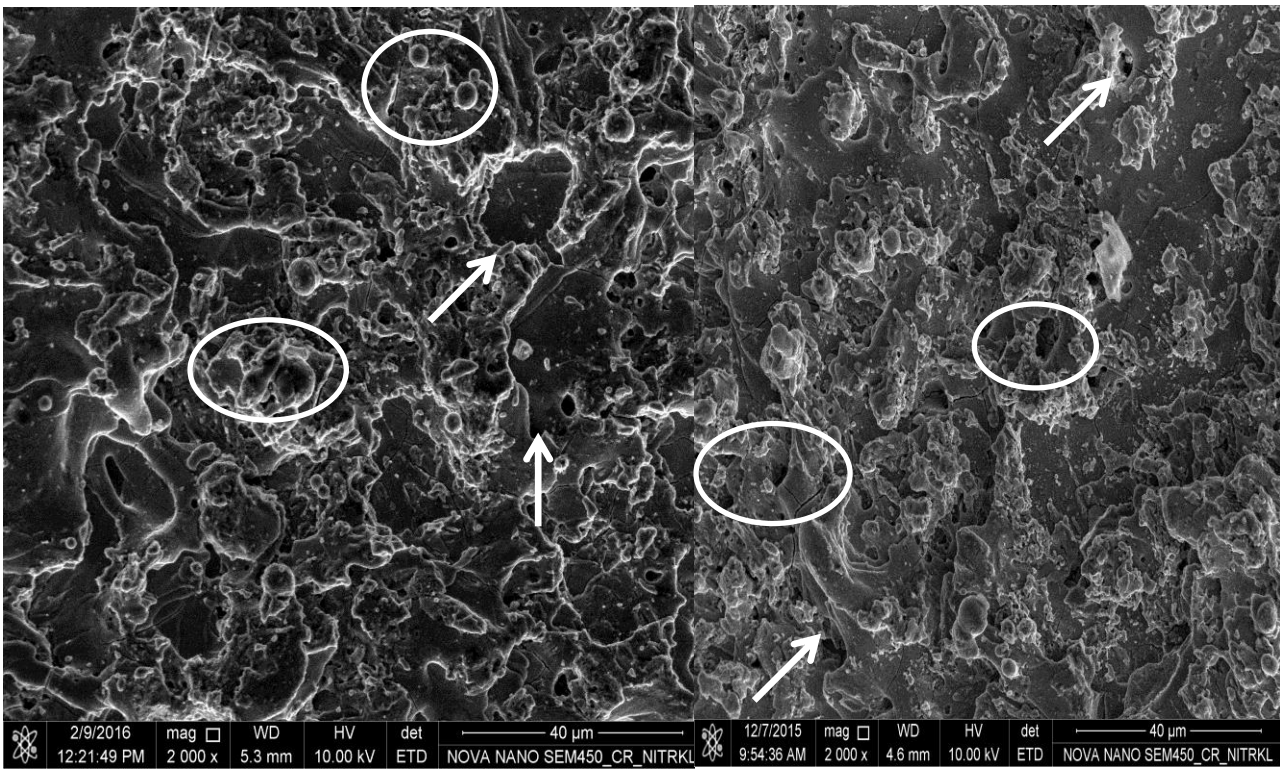


(a) Brass wire electrode (b) Zinc coated brass wire electrode

Figure 3.32 FESEM image of WEDMed surface of melted and re-solidified lumps of debris with few micro-cracks at $A_4B_3C_3D_4$

The surface roughness mainly depends upon per pulse energy and the efficiency with which pulse energy is utilized to form crater. The pulse energy is the ratio between the energy observed by the workpiece to the sum of energy observed by the workpiece and dielectric medium. However from Figure 3.33 (a-b), observed that the minimum dielectric flushing pressure is causes more deteriorate the surface finish of uncoated brass wire electrode as compared to zinc coated brass wire. So, dielectric flushing pressure is the most important parameter to achieve good surface finish of machined surfaces.

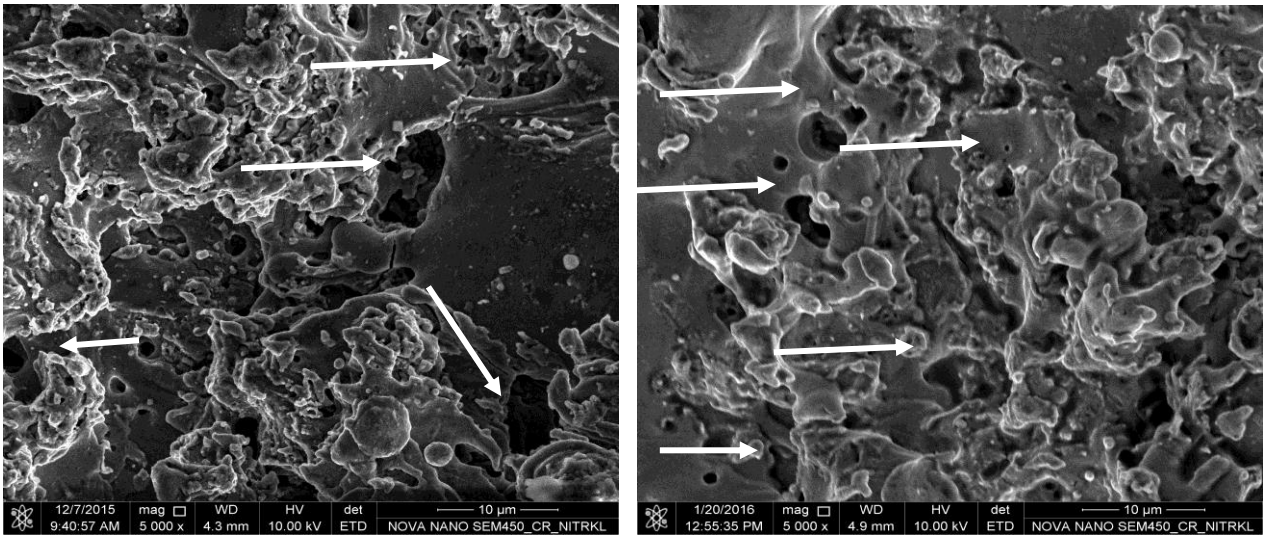


(a)Brass wire electrode (b)Zinc coated brass wire electrode

Figure 3.33: FESEM image of WEDMed surface of protruding particles, at $A_4B_1C_2D_4$

Figure 3.34(a-d) shows effects of process parameters on corner error obtained during WEDM of Inconel 718 using two electrode materials. Improper flushing produces a higher wire vibration and wire lag, these are the primary causes for corner error [36]. An increase in pulse-on time or discharge current will produce higher energy pulse which turns result in more intense bubble generation in the inter-electrode gap [70] and this will cause a larger amount of wire deflection. This is because of an increase in pulse-on time and discharge current exhibits increasing trends of corner die error. The corner error produce in the rough cutting operation increases with the increase in pulse parameter setting.

(a)

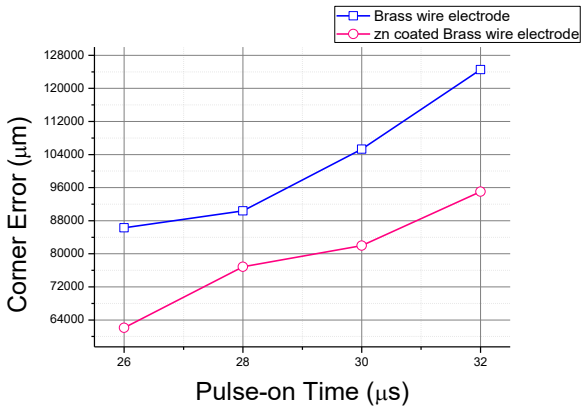


(b)

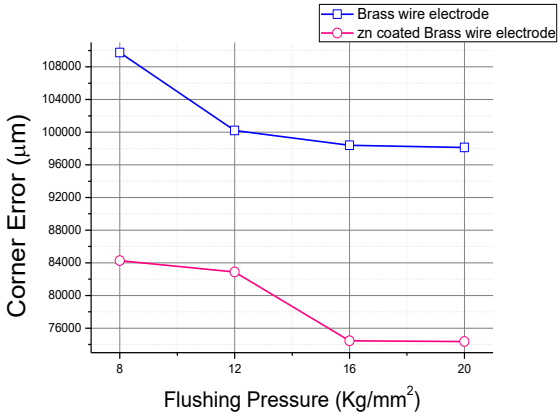

(c) (d)

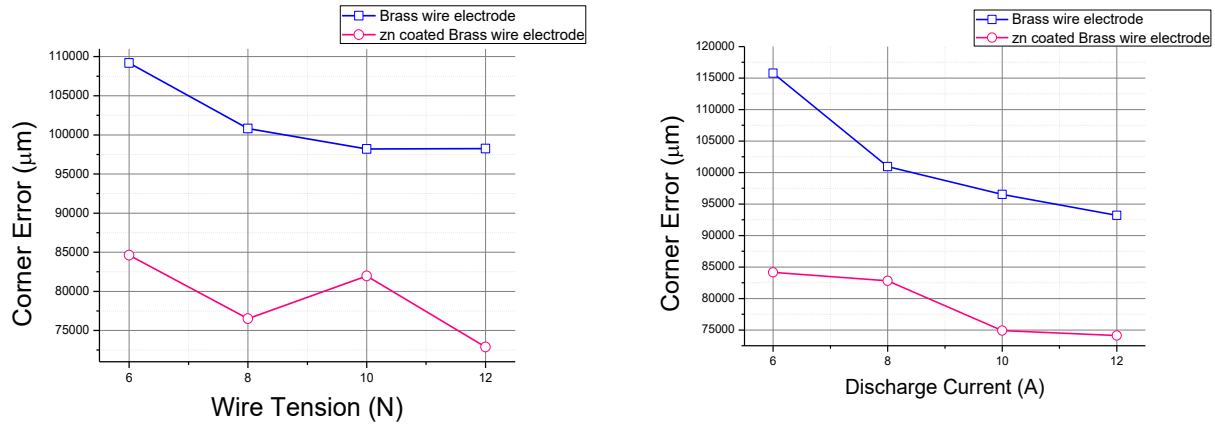


Figure 3.34: Main effect plot on corner error with various wire Electrodes

From the mean effect analysis of MRR was obtained from $L_{16}$ orthogonal array experimentally. The main effects of the controllable process parameters on MRR for both wire type have been are shown in Figure 3.35(a-d). Figure 3.35 (a) illustrate that MRR is partially increasing with increase in the pulse-on time for both the wire electrode. While pulse-on time is increased, the power available between the anode and cathode becomes greater, hence high energy input facilitates the melting and evaporation of materials [105]. In case of uncoated brass wire, MRR is first decreasing and then increases. However literature depicts, MRR increases with increases pulse-on time. The experimental data that have plotted herein found inadequate to capture the real trend which may happen due to machining error or lack of insufficient data since orthogonal array has been used. A Figure 3.35 (b) shows that as flushing pressure increases MRR tends to decrease. Which may happen due to, fact that the cooling effect increases with increases the flushing pressure on working zone during machining time. A Figure 3.35 (c) shows that as wire tension increasing the MRR is also increasing for both the wire electrodes; because, wire tension is a factor that influences stability of wire during the discharge process. During discharge process, the wire is subjected to disturbances caused by external as well as internal sources, since the gap is changing continuously [106]. But in case of zinc coated brass wire, MRR first increases but at the end goes to decreases, this may happen due to experimental error. Figure 3.35(d) indicates that MRR tends to increases with increases the discharge current using both the wire electrode Increasing the discharge current caused more electrical discharge energy to conducted into the machining gap and increasing the MRR [51]. With high discharge current has

been stable the machining condition and effective material removal was achieved. It has noted that discharge current is the most significant parameter for MRR using both the wire electrodes.

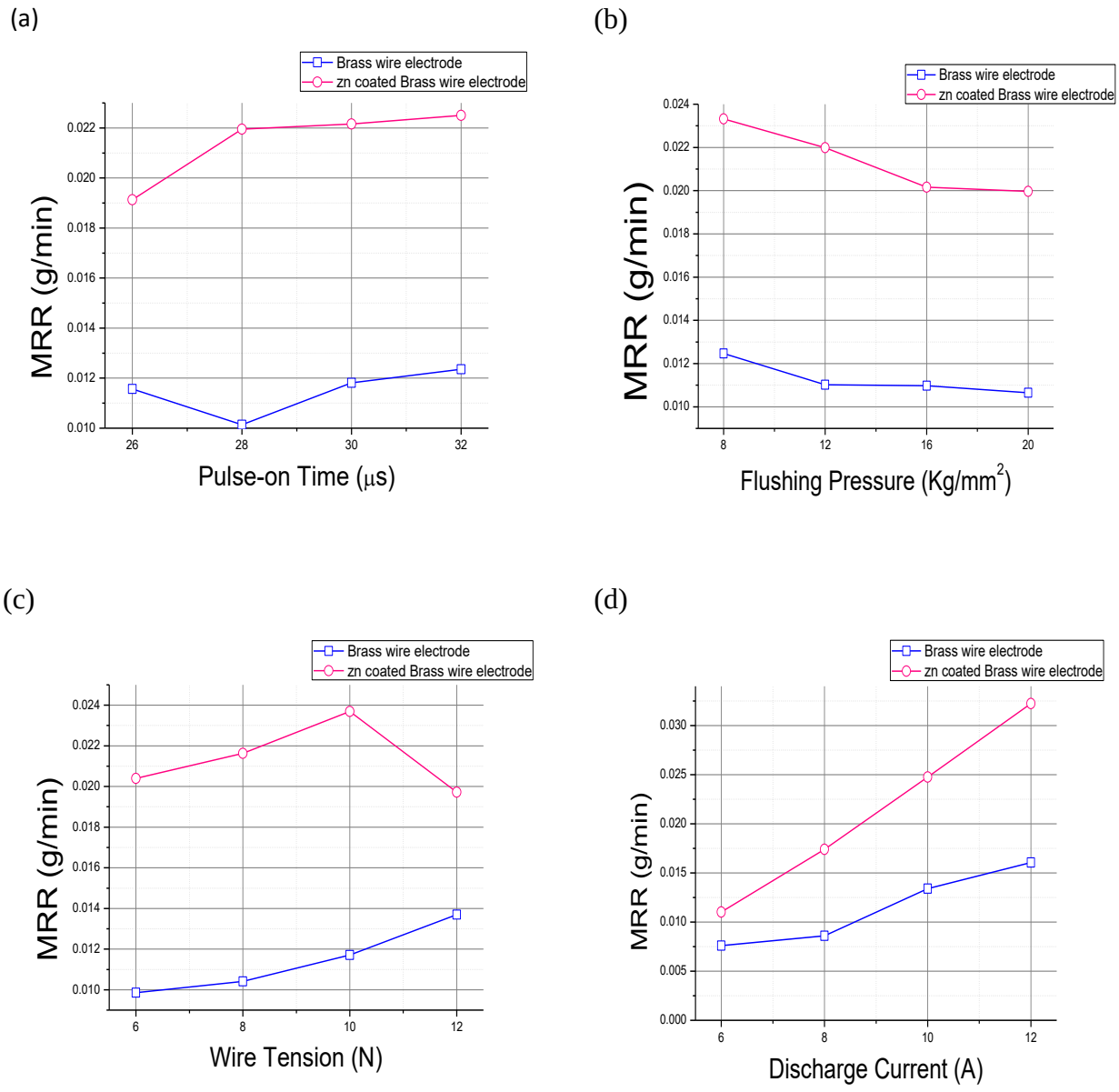


Figure 3.35: Main effect plot on MRR with various wire Electrodes

Figure 3.36(a-d) shows effects of process parameters on surface roughness obtained during WEDM of Inconel 718 using two electrode materials. Figure 3.36 (a) it can be seen that the surface roughness increases with increase in pulse-on time but decreases with wire tension (Figure 3.36(c)). The reason for increasing the wire tension reduced wire vibration amplitude and influence stability of wire during discharge process may become active. On the working zone, the impingement of spark may become stable, i.e., succeeding spark may be cutting a portion of workpiece smoothly, which decreases the surface roughness [107]. Figure 3.36 (b) it has been observed that with increasing flushing pressure, surface roughness assumes decreases this is because of the cooling effect increases with increase in the flushing pressure on the workpiece. Higher heat transfer rate from the work surface results in smaller kerf width [55]. Maximum surface roughness was obtained with the plain brass wire electrode as compare to zinc coated brass wire. Figure 3.36 (d) it has been observed that with increasing discharge current, surface roughness assumes increasing decreases trends using both wire electrodes. Literature delineate, discharge current increases the surface roughness decreases. The experimental data that have plotted herein found deficient to acquire the real trend. This error may be due to experimental error or machining error or insufficient data since orthogonal array has been used. Increasing the discharge current also increases the energy of every discharge, which leads to deteriorate the surface finish. Some conclusion can also be drawn of from the mean effect analysis of surface roughness that pulse on time and discharge current are the most significant parameters for surface roughness using both wire electrodes.

(a)

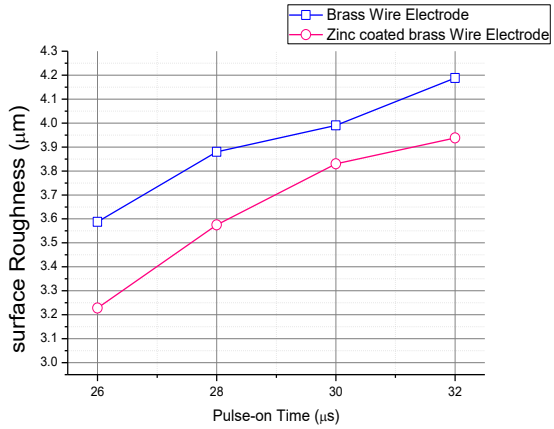


(b)

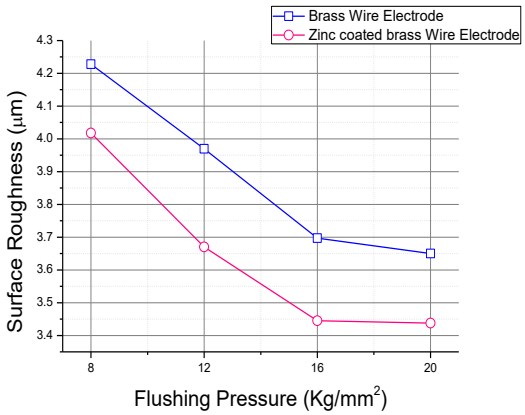


(c)

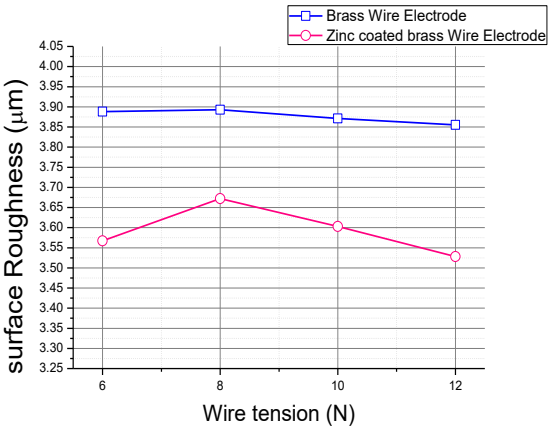


(d)

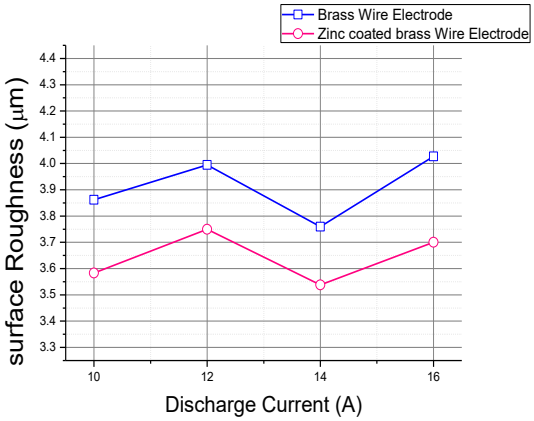


Figure 3.36: Main effect plot on Surface Roughness with various wire Electrodes

## 3.3.5 Concluding Remarks

In the present study, focuses on comparing the performance of uncoated brass wire and zinc coated brass wire in WEDM process of Inconel 718 using experimental results. The following conclusions were drawn from this study.

1. Selection of appropriate electrode material is very important on enhancing in terms of MRR, Surface roughness and corner error during WEDM on Inconel 718.
2. Zinc coated brass wire has been significantly improve in terms of MRR, surface roughness and corner error compare to uncoated brass wire on Inconel 718.
3. The pulse-on time and discharge current are the most important parameter that influences the response variables. The pulse-on time and discharge current have been most affecting parameter on MRR. Pulse-on time and flushing pressure have been most affecting parameters on surface roughness. The corner accuracy has been almost independent of sparking factors. Wire tension has been most affecting parameter on corner accuracy.

4. The application of zinc coated brass wire as electrode material leads to significant reduction in corner error by 21.89% as compare to uncoated brass wire. The zinc coated brass electrode due to its improved flushability nature.

# Chapter 4

# 4 Parametric optimization during WEDM

## 4.1 Machining Responses and Optimization of process parameters using WOA

### 4.1.1 Coverage

In the present study, the experimental attempt has been made to analyze the influence of wire electrode material on Material Removal Rate (MRR), Corner deviation and surface roughness (Ra) in Wire Electrode Discharge Machining (WEDM) process of Inconel 718 alloy has been chosen as the workpiece material. An $L_{16}$ orthogonal array has been used for both wire electrodes (i.e. zinc coated brass wire and uncoated brass wire) experimentation by tuning the machining controllable factors (i.e. Pulse-on time, Flushing pressure, Wire tension, and Discharge current). From the experimental results, it has been observed that, zinc coated brass wire perform better as compare to uncoated brass wire. Additionally, initially develop mathematical models by using nonlinear regression equation for comparing various controllable process parameters with respect to the process responses. In the next stage, the optimization results for both the wires have been demonstrated the most recently developed optimization Whale Optimization Algorithm (WOA) approach to obtain the optimum machining parameter settings. The results of WOA have been compared to that of Genetic Algorithm (GA). It has been observe that WOA appears good results compare GA on the machining of Inconel 718.

### 4.1.2 Problem Definition

Wire Electrical Discharge Machining (WEDM) has become an important non-conventional machining technique for producing complete cutouts through very hard to machine material specially, aerospace material with précised dimensional accuracy. WEDM is a thermo-electrical process used to produce complex shape, through electrically conductive material by using wire. In this process MRR occurs from initiation of repetitive spark discharges between the gap of workpiece and the wire electrode connected in an electrical circuit. A dielectric is continuously passes through gap provided by workpiece and the wire electrode. The wire electrode diameter ranges from 0.05 to 0.3 mm is applied. The gap of 0.025-0.05, between the wire electrode and workpiece is maintained constantly by the control system [58, 106]. Since, using the flexible wire in WEDM as a tool electrode, which is subject to deform due to reaction forces such as explosive force and the electrostatic force between the wire electrode and workpiece, a geometry error has been occurs on the machined surface [108]. The improving the corner cut area accuracy is a significant area of study for all researchers interested in WEDM. The corner inaccuracy has been happened not only due to geometry error along the direction of the wire electrode, but, also happening due to electrode wire lags (measured between the position of the guides (programed) and the deformed wire (actual)), which is strongly dependent upon the workpiece thickness, gap force intensity etc.

Antar et al. [25] studied on the workpiece productivity and integrity when WEDMing nickel based super-alloy and titanium alloy, and it was found that up to 40% increase in productivity was possible in super alloy as and approximately 70% increase in titanium alloy in productivity was possible as compare to uncoated brass wire with using Cu core coated wire electrode with the same controllable parameter setting. Golshan et al.[73] focused on comparing the performance of uncoated brass wire and zinc coated brass wire electrode of WEDM on titanium alloy. In the study the effects of three controllable process parameter via pulse-on time, pulse-off time and peak current on the process responses, i.e., MRR, spark gap and white layer thickness have been investigated. The result obtained that zinc coated brass wire was more predictable responses in the experimental compared to uncoated brass wire electrode. Kuriakose et al. [102] observed that, more uniform surface characteristics in a specimen of Ti6Al4V were achieved by

the zinc coated electrode compared to uncoated brass wire. Among the process parameter i.e., time between two pulses, pulse duration, injection pressure wire speed and wire tension, which have more influence on the surface characteristics. The time between two pulses was found to be the most significant process parameter. Sanchez et al. [109] presented a study on corner geometry generated by successive cuts (roughing and finishing). Errors at different zones of corner are identified and related to the MRR during each cut. Yang et al. [31] analyzed the responses like, MRR, Ra and Corner Deviation (CD) depending on controllable parameters of Wire EDM, simultaneously, Response Surface Methodology (RSM) and simulated annealing algorithm (SAA) were proposed to find out an appropriate cutting parameter setting. Hsue et al. [119] described a concept of discharge contact-angle. Based on the analysis of MRR in corner cutting, a strategy of discharge power control together with the adjustment of wire has been proposed. From the experimental result shows that not only the contour accuracy, but also the vertical straightness of the workpiece at corner edge can be improve significantly. Sanchez et al. [118] investigated the WEDM corner accuracy. A hybrid computer-integrated system for the improvement knowledge of the process and numerical simulation were described. They selected the optimum cutting strategy by wire path modification when high accuracy is required. Padhi et al. [69] optimized the cutting rate, surface roughness and Dimensional Deviation (DD) in WEDM, through RSM and Genetic Algorithm (GA) weighted sum method. Dabade et al. [53] attempted to analyze the machining conditions for MRR, Ra, kerf width and DD during WEDM of Inconel 718 using Taguchi methodology. Dey et al. [120] describe a simulation method for WEDM of MRR, Ra, DD and wire wear ratio. In the simulation, they analyzed the ANN based on six WEDM process parameters, such as pulse-on time, pulse-off time, peak current, spark gap voltage, wire feed and wire tension through forward mapping.

Literature depicts that, two strategies have mainly been used to improve the corner accuracy. The first one is to modify the controllable parameters like pulse-on time, pulse-off time, peak current etc. in order to control wire deflection [75, 109]. The second one is to modify the wire path to achieve the geometrical accuracy [109, 111]. The most of the WEDM manufacturer are highly suggested the first strategy for improvement of corner accuracy. From the literatures observation, it has been concluded that less or no literature has been discussed to analyze the influence of wire electrodes such as zinc coated brass wire and uncoated brass wire on corner cutting in the WEDM process using Inconel 718 as a workpiece. In the present study, an attempt has been

made to analyse the influence of wire electrode on MRR, Ra and corner deviation in WEDM process using zinc coated brass wire and uncoated brass wire. Finally, WOA is used to obtain optimal process parameter setting for both the wire electrodes.

### 4.1.3 Experimentation

In this study, Inconel 718 alloy has been selected as the workpiece. The experiment has been conducted on CNC WEDM machine, [AGIE, SWITZERLAND] (Figure 3.1). A zinc coated brass wire and uncoated brass wire were used as tool electrodes with 0.20mm diameter and compared to each other. The properties of zinc coated brass wire and uncoated brass wire as shown in Table 4.1. The pulse-off time and dielectric flow rate have been kept fixed at 50µs and 1.2 bars, respectively, throughout the experiments. Deionized water has been used as dielectric fluid.

Table 4.1: Properties of wire electrodes [73]

| Properties | Zinc coated brass wire | Brass wire |
|---|---|---|
| Electrode dia tolerance (mm) | ±0.001 | ±0.001 |
| Minimum tensile strength (MPa) | 964 | 980 |
| Melting point ($^{o}$C) | 419 | 927 |

Table 4.2: Process factors and domain of variation

| Control factor | Code | Unit | Level I | Level II | Level III | Level VI |
|---|---|---|---|---|---|---|
| Pulse-on time | A | [µs] | 26 | 28 | 30 | 32 |
| Flushing Pressure | B | [kg/mm$^2$] | 8 | 12 | 16 | 20 |
| Wire tension | C | [N] | 6 | 8 | 10 | 12 |
| Discharge Current | D | [A] | 10 | 12 | 14 | 16 |

The controllable parameters have been selected based on machining parameters. The experiments were conducted according to $L_{16}$ orthogonal array. 4-level-4-factor design has been

selected in the rough machining process for this present study: pulse-on time, flushing pressure, wire tension and discharge current as shown in Table 4.2.

In each experimental run, the MRR, Surface roughness and corner deviation were measured. In each run continuous cutting with a straight length of 10mm and orthogonal length of 10 mm was made on 1mm thickness of the workpiece. MRR is calculated by using the formula in Equation 1.1 (Chapter 1)

The kerf width and corner deviation of the workpiece after the WEDM experimental run were measured using optical microscope (CARL ZEISS JENA, Germany). The roughness average (Ra) of the surface after WEDM was measured using Talysurf (Talysurf 50 Taylor hobson Ltd., UK). A field emission scanning electron microscope (FESEM) (NOVA NANO SEM 450) has been used to investigate the surface texture on the workpiece after the WEDM process. The experimental layout and results have been shown in Table 4.3.

Corner deviation is a geometrical contour error occurs in the inner corner of the workpiece during orthogonal cutting. It has been shown that enlargement image of the corner deviation by WEDM operation $A_1B_3C_3D_3$ (Run no. 4 of Table 4.3) has been shown in Figure 4.1.

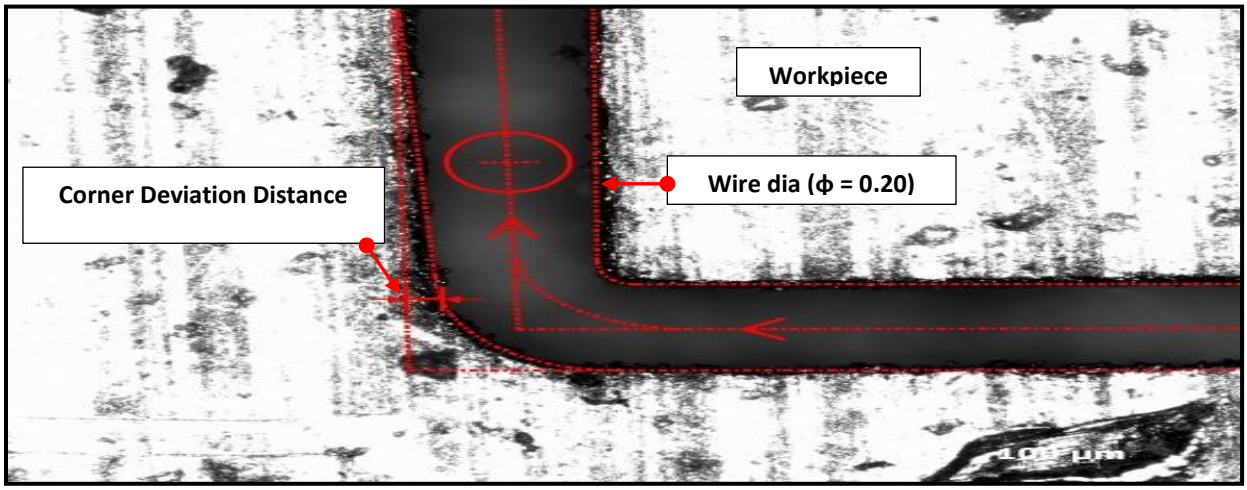


Figure 4.1 Corner cutting by WEDM operation under the conditions A1B3C3D3 (Run no. 4) using uncoated Brass wire electrode

Table 4.3: design of experiment and collection response data.

| Design of Experiment | | | | | Responses data | | | | | |
|---|---|---|---|---|---|---|---|---|---|---|
| Ex. No | A [µs] | B [kg/mm2] | C [N] | D [A] | MRR [g/min] | | Corner deviation [mm] | | Surface roughness [µm] | |
| | | | | | Zn-WE | BWE | Zn-WE | BWE | Zn-WE | BWE |
| 1 | 26 | 8 | 6 | 10 | 0.0107 | 0.0051 | 0.0351 | 0.0435 | 2.58 | 3.12 |
| 2 | 26 | 12 | 8 | 12 | 0.0183 | 0.0082 | 0.0351 | 0.0381 | 3.12 | 3.53 |
| 3 | 26 | 16 | 10 | 14 | 0.0242 | 0.0125 | 0.0406 | 0.0442 | 3.30 | 3.60 |
| 4 | 26 | 20 | 12 | 16 | 0.0254 | 0.0187 | 0.0355 | 0.0393 | 3.10 | 3.59 |
| 5 | 28 | 8 | 8 | 14 | 0.0263 | 0.0129 | 0.0374 | 0.0435 | 3.19 | 3.85 |
| 6 | 28 | 12 | 6 | 16 | 0.0327 | 0.0198 | 0.0783 | 0.0844 | 4.40 | 4.80 |
| 7 | 28 | 16 | 12 | 10 | 0.0097 | 0.0049 | 0.0320 | 0.0366 | 3.29 | 3.88 |
| 8 | 28 | 20 | 10 | 12 | 0.0201 | 0.0062 | 0.0258 | 0.0286 | 3.50 | 3.80 |
| 9 | 30 | 8 | 10 | 16 | 0.0335 | 0.0214 | 0.0381 | 0.0408 | 4.08 | 4.32 |
| 10 | 30 | 12 | 12 | 14 | 0.0262 | 0.0145 | 0.0311 | 0.0367 | 3.40 | 3.62 |
| 11 | 30 | 16 | 6 | 12 | 0.0142 | 0.0072 | 0.0376 | 0.0408 | 3.42 | 3.87 |
| 12 | 30 | 20 | 8 | 10 | 0.0090 | 0.0045 | 0.0216 | 0.0537 | 3.67 | 3.83 |
| 13 | 32 | 8 | 12 | 12 | 0.0179 | 0.0120 | 0.0279 | 0.0313 | 3.40 | 3.70 |
| 14 | 32 | 12 | 10 | 10 | 0.0138 | 0.0081 | 0.0218 | 0.0347 | 3.78 | 4.10 |
| 15 | 32 | 16 | 8 | 16 | 0.0342 | 0.0187 | 0.0469 | 0.0583 | 4.40 | 4.80 |
| 16 | 32 | 20 | 6 | 14 | 0.0224 | 0.0153 | 0.0319 | 0.0442 | 3.80 | 4.20 |

**Zn-WE**: Zinc coated brass wire, **BWE**: Uncoated brass wire

### 4.1.3.1 Effects of Wire Electrodes on Different Responses Measures

Figure 4.2 demonstrated the interval plot of response factors from uncoated brass wire to zinc coated brass wire using all 16 settings experimented in this work (Table 4.3). Referring to Figure 4.2(A) Demonstrates that the mean MRRs using zinc coated brass wire and uncoated brass wire have 0.021 and 0.012 g/min, respectively. Thus, MRR mean from uncoated brass wire to zinc coated brass wire have been increased +56.1%. Likewise, the percentage increase of corner deviation and surface roughness (Figure 4.2 (B-C)) from uncoated brass wire to zinc coated brass

wire are -21.11% and -10.1 %, respectively. It has been seen that MRR obtained using the zinc coated brass wire is more than that of the uncoated brass wire. This may be, because of outer layer of zinc coating of the zinc coated brass wire electrode has a lower melting temperature than the core brass material. Therefore, zinc is overheated and evaporated in the presence of pulse. Accordingly, the cutting speed has also been increased by approximately 50% as more intense thermal flows are enabled [26].

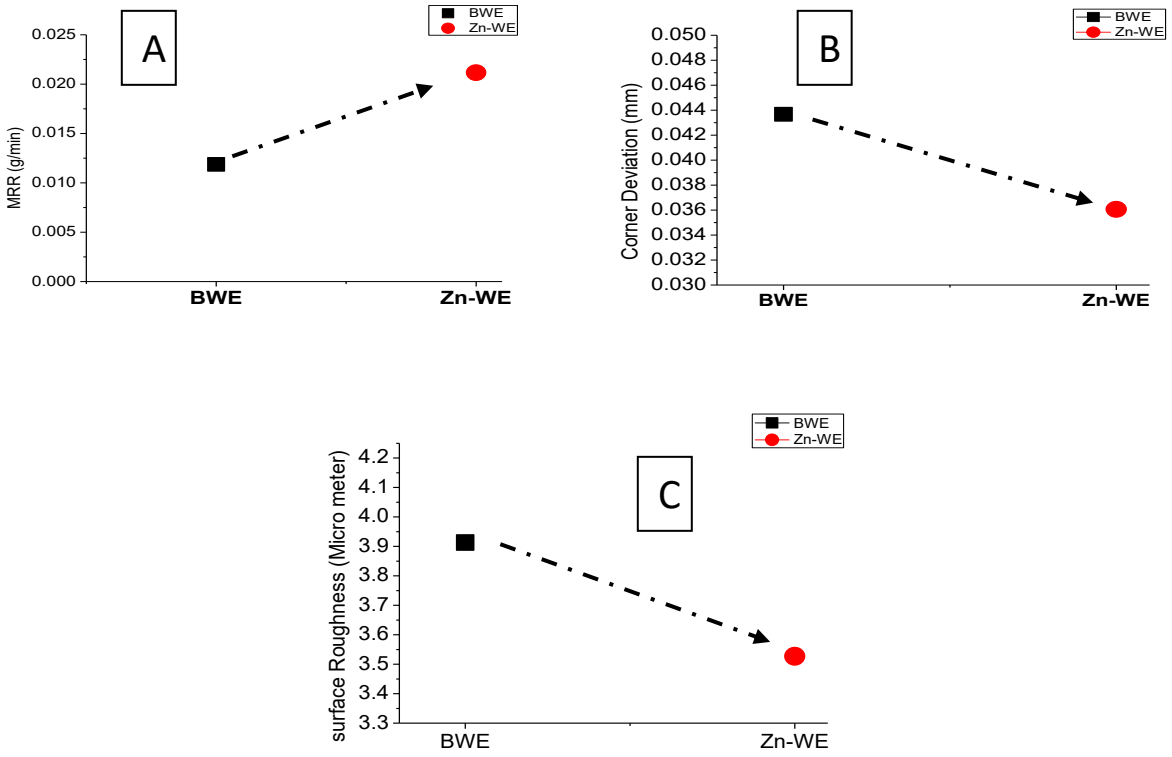


Figure 4.2: Interval plot of response factors from uncoated brass wire to zinc coated brass wire.

Moreover, coating evaporation increases the gap size between wire electrode and workpiece, which results in good debris removal, which can decrease the surface roughness. The coated wire thus produces minimum corner deviation as compare to uncoated brass wire. This may be because of zinc coated brass wire having its heat sink capability, which helps to reduce the wire temperature and thus reduce of die corner error. Kapoor et al. [20] discussed that, coated zinc in zinc coated brass wire, provided a higher tensile strength, lower melting point, higher vapor pressure rating and improve flushability, which resulted in increase in cutting speed, good dimension accuracy and good surface finish.

The main effects plot of the machine parameters on the MRR, Corner deviation and Surface roughness for both wires are shown in Figure 4.3. Figure 4.3 (a) demonstrates that, MRR increases with increases in pulse-on time and discharge current. Likewise discharge current is the most significant controllable parameter for both the wire electrodes. With increases pulse-on time, the power between wire electrode and the workpiece becomes greater, which facilitates the melting and evaporating of the workpiece [121]. In addition increasing the discharge current caused more electrical discharge energy to be generated on the working zone (between wire electrode and workpiece) and increasing the MRR. Some conclusion can also be drawn from the mean effect analysis of MRR that effective material removal has been achieved at high discharge current [51].

Referring to Figure 4.3 (b), it has been observed that corner deviation decreases with an increase in wire tension with constant pulse-on time, which illustrates that a higher wire tension has resulted in strong force acting on the wire, which seems decreasing wire deformation, therefore, reduction in the corner deviation.

From Figure 4.3 (c), clearly indicates that discharge current and pulse-on time is the most significant controllable parameters on surface roughness compare to flushing pressure and wire tension for both the wire electrodes. It can be seen that increase in pulse-on time or discharge current, increases surface roughness. This may be because of the discharge energy becomes more intense with increased pulse-on time or discharge current; the more powerful discharge energy is the explosion which deteriorates the surface finish.

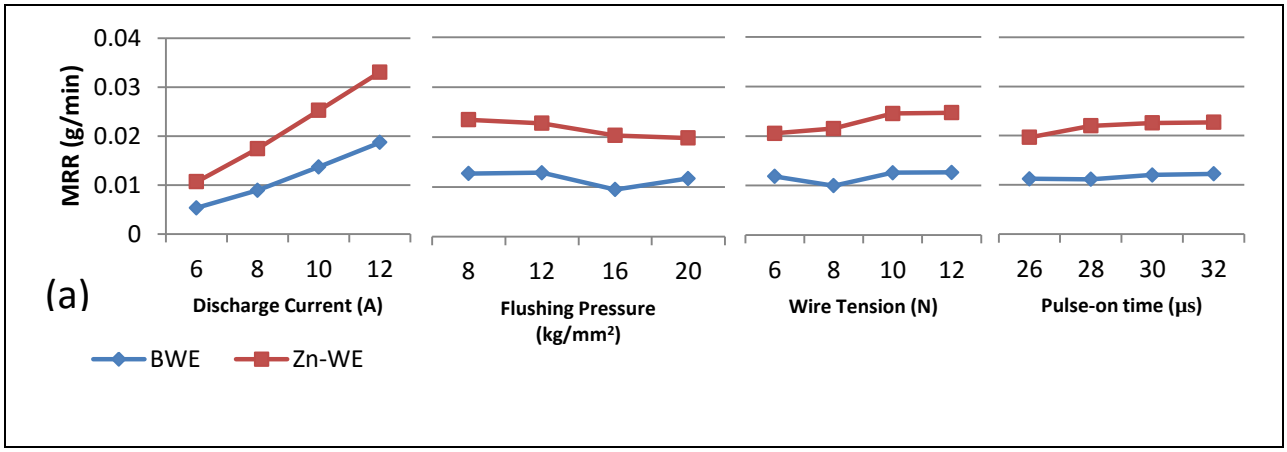

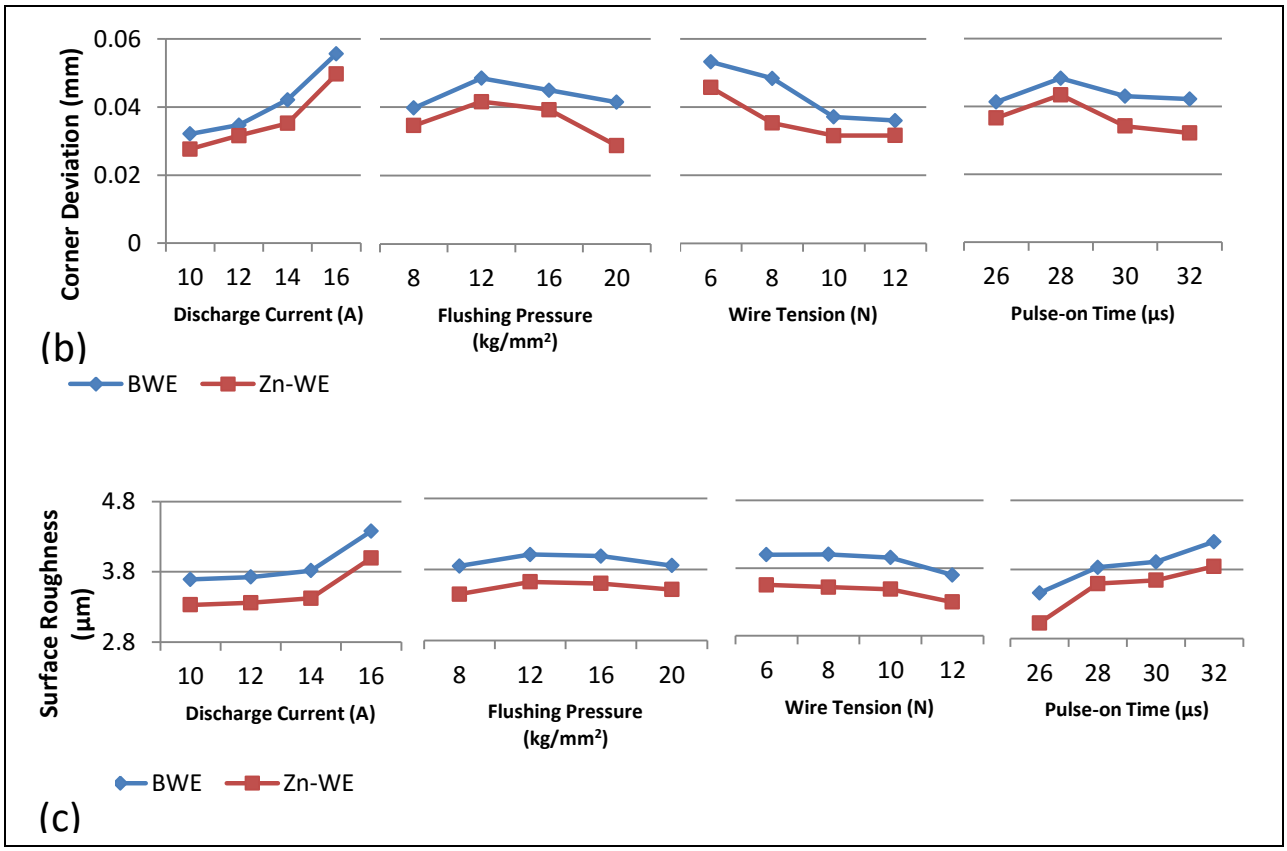


Figure 4.3: Main effect plots for controllable process parameters on influencing (a) MRR (b) corner deviation (c) Ra with various wire electrodes.

## 4.1.3.2 Development of Mathematical model

Non-linear regression is a method of search using a nonlinear model by a function which is a nonlinear combination between the dependent variable and a set of independent variable(s) [122] [123]. The data are fitted by successive approximations method. Nonlinear regression plays an important role to finding out the complex interrelationship between the variables.

Proper execution of experiments is indeed essential for developing an adequate mathematical model based upon the experimental data. In this present study, mathematical models have been developed using the nonlinear regression model based on experimental data of both the wire electrodes. The proposed mathematical model for each response is shown as below:

$$Y_i = C \times X_1^a \times X_2^b \times X_3^c \times X_4^d \quad (4.1)$$

Where, C represent as constant; $X_1$ represent as pulse-on time; $X_2$ represent as flushing pressure ; $X_3$ represent as wire tension ; $X_4$ represent as discharge current. $a, b, c, d$ are the estimated coefficients of the said regression model

## 4.1.3.3 The Whale Optimization Algorithm (WOA)

Mirjalili et al. [124] proposed a novel nature-inspired meta-heuristic optimization algorithm called Whale Optimization Algorithm (WOA). WOA is working on the hunting behavior with random or the best search agent to chase to prey and the use of a spiral to simulate bubble-net attacking mechanism of humpback whales. There are three main phase i.e. encircling prey, bubble-net attacking method (exploitation phase) and search for prey (exploration phase). It has been tested with 29 mathematical problem and 6 structural design problem. Flow chart has depicted in Figure 4.4.

### 4.1.3.3.1 *Mathematical Model*

#### 4.1.3.3.1.1 *Encircling prey*

Humpback whales can recognize the location of prey and encircle them. This algorithm targeting the current best solutions i.e., prey or are close to optimum. After the best search agent is defined, the other search agents, try to upgrade their position towards the best search agent. This behavior can be defined from the following equation:

$$\vec{D} = \left|\vec{C}.\vec{X}^{*}(t) - \vec{X}(t)\right| \tag{4.2}$$

$$\vec{X}(t+1) = \vec{X}^{*}(t) - \vec{A}.\vec{D} \tag{4.3}$$

The vectors $\vec{A}$ and $\vec{C}$ are calculated by following equation:

$$\vec{A} = 2\vec{a}.\vec{r} - \vec{a} \tag{4.4}$$

$$\vec{C} = 2.\vec{r} \tag{4.4}$$

Where $t$ is current iteration $\vec{A}$ and $\vec{C}$ are coefficient vectors, $X*$ is the position vector of the updated best solution. $\vec{X}$ is the position vector. $\vec{a}$ is linearly decreased from 2 to 0 over the course of iterations (in both exploration and exploitation phase) and $\vec{r}$ is a random vector in [0,1]. Where $X*$ should be updated at every iteration to find is a better solution.

#### **4.1.3.3.1.2** *Bubble-net attacking method (Exploitation phase)*

In this section a mathematically model the bubble-net behavior humpback whales, can define via two approaches.

*i) Shrinking encircling mechanism*:

This behavior has been achieved by decreasing the value of $\vec{a}$ in equation 5 where $a$ is decreased from 2 to 0 in each set of iterations. Setting random values for $\vec{A}$ in [-1, 1], search the new position of a search agent can be define anywhere between original position of the agent and position of current best agent.

*i) Spiral updating position*:

In this position, calculate the distance between the whale position and prey located of whale. A spiral equation is then created between the position of whale and prey to mimic the helix shaped movement of humpback whales as follows:

$$\vec{X}(t+1) = \vec{D}'.e^{bl}.\cos(2\pi l) + \vec{X}^*(t) \tag{4.5}$$

Where $\vec{D}' = \left|\vec{X}^*(t) - \vec{X}(t)\right|$ and define the distance of the $i^{th}$ whale to the prey (best solution obtained till now), $b$ is a constant for shape of logarithmic spiral, $l$ is a random no. in [-1, 1].

#### **4.1.3.3.1.3** *Search for prey (exploration phase)*

This approach is based on variation of the $\vec{A}$ vector; it can be utilized to search for prey (exploration). $\vec{A}$ vector's value can be defined with the random values greater than 1 or less than -1 to force search agent to move far away from a reference whale. During this approach, updating the position of search agent in exploration phase according to a randomly selecting

select search agent instead of the best search agent found. This mechanism and $\left|\vec{A}\right| > 1$ emphasize exploration and allow the WOA algorithm to perform a global search. The mathematical model as show as follows:

$$\vec{D} = \left|\vec{C}.\vec{X}_{rand} - \vec{X}\right| \tag{4.6}$$

$$\vec{X}(t+1) = \left|\vec{X}_{rand} - \vec{A}.\vec{D}\right| \tag{4.7}$$

where $\vec{X}_{rand}$ is a random position vector (a random whale) selected from the current population.

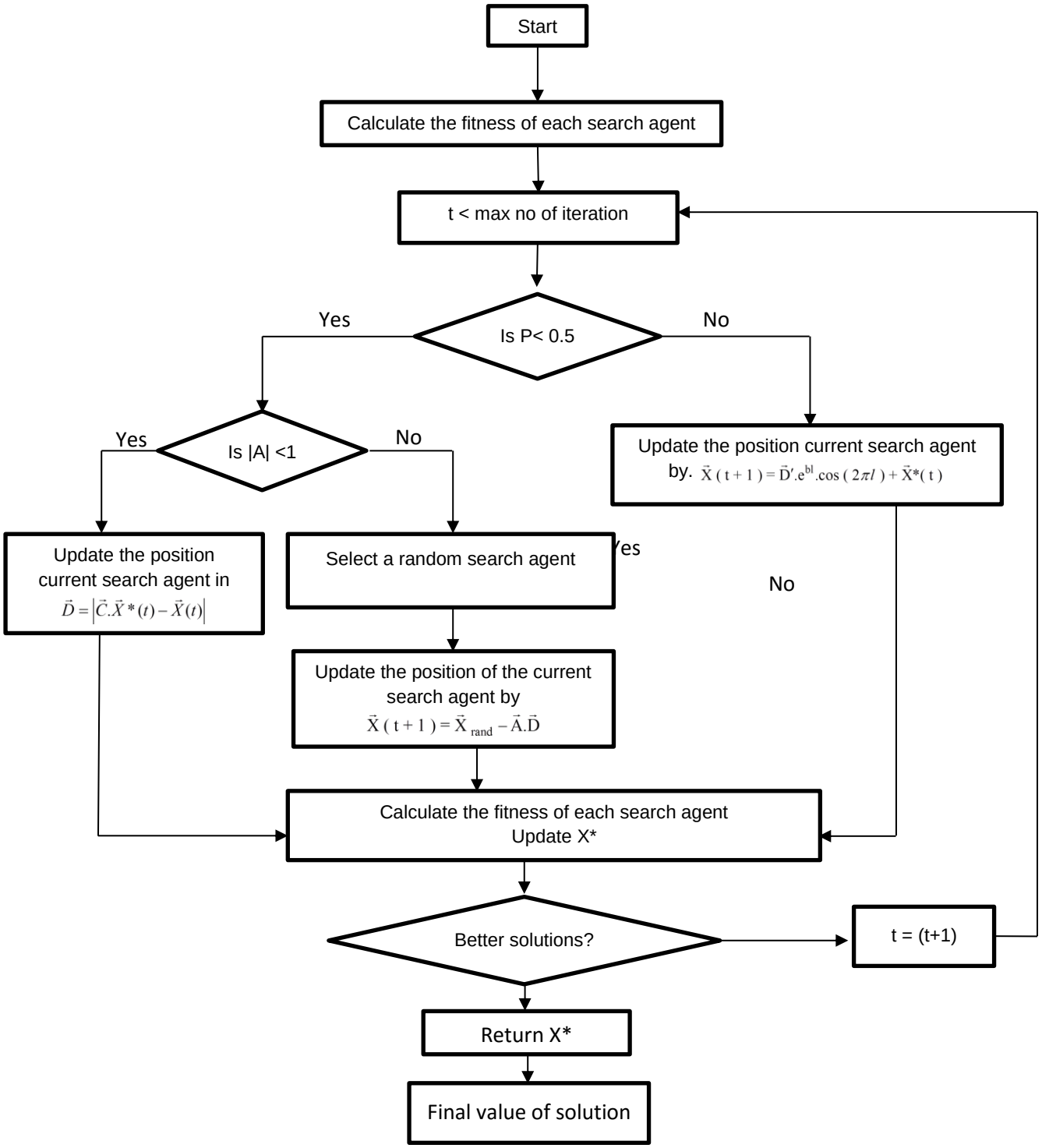


Figure 4.4: Flow diagram of WOA algorithm

## 4.1.3.4 Mathematical Modelling of MRR, Corner Deviation and surface Roughness (Ra)

In the present study, Gauss-Newton algorithm has been used to generate the coefficients by using SYSTAT 7.0 software package.

***For Zinc coated Brass Wire***

$$\text{Corner Deviation } (Z_1) = 0.432947 \times X_1^{(-1.3379)} \times X_2^{(-0.1233)} \times X_3^{(-0.7682)} \times X_4^{(1.5398)} \quad (4.8)$$

$$\text{Ra } (Z_2) = 0.04867 \times X_1^{(0.9987)} \times X_2^{(0.050486)} \times X_3^{(-0.06554)} \times X_4^{(0.36446)} \quad (4.9)$$

$$\text{MRR } (Z_3) = 0.00003 \times X_1^{(0.42814)} \times X_2^{(-0.14826)} \times X_3^{(-0.00851)} \times X_4^{(2.15758)} \quad (4.10)$$

***For Uncoated Brass Wire***

$$\text{Corner Deviation } (Z_4) = 0.074965 \times X_1^{(-0.3908)} \times X_2^{(0.0012)} \times X_3^{(-0.6763)} \times X_4^{(0.8645)} \quad (4.11)$$

$$\text{Ra } (Z_5) = 0.160929 \times X_1^{(0.7379)} \times X_2^{(0.0307)} \times X_3^{(-0.0974)} \times X_4^{(0.3281)} \quad (4.12)$$

$$\text{MRR } (Z_6) = 0.000001 \times X_1^{(0.7089)} \times X_2^{(-0.1275)} \times X_3^{(0.0938)} \times X_4^{(2.7353)} \quad (4.13)$$

Where, MRR are in g/min, Corner Deviation are in mm and Ra are in μm

### 4.1.3.3.1 *Model accuracy test for MRR, Corner deviation and Ra*

The first step of this present work, responses have been derived (for individual: MRR, corner deviation and Surface roughness) using non-linear regression analysis. The mathematical models have been based on controllable parameters. These models have been optimized individually using WOA algorithm in the selected parametric search space.

### 4.1.3.3.2 *Optimization of Inconel 718 machining parameters*

Careful examination of Figures 4.2-4. 3 reveals that the best level of significant factor for MRR, corner deviation and surface roughness for uncoated brass wire are $A_3B_1C_3D_4$, $A_2B_4C_3D_2$ and $A_1B_1C_1D_1$ and for zinc coated brass wire are $A_3B_1C_3D_4$, $A_3B_4C_3D_2$ and $A_1B_1C_1D_1$ respectively.

From these results, it has been confirmed that the level of significant parameter setting for MRR, corner deviation and Ra are completely contradictory. Therefore, there is no single parameter setting for optimal choice for all the responses. Hence, there is a requirement to explore a suitable strategy for optimization of this process.

This work focuses on application of WOA to evaluate optimal solution in WEDM of Inconel 718. The WOA discussed above uses (Equation 4.8-4.13), as objective functions to maximize the MRR and minimize corner deviation and surface roughness (Ra), respectively. The controllable parameter bonds have been listed as follows:

| | |
|---|---|
| $26 \le A \le 32$ | *Pulse-on time* |
| $8 \le B \le 20$ | *Flushing pressure* |
| $6 \le C \le 12$ | *Wire Tension* |
| $10 \le D \le 16$ | *Discharge current* |

Both single and multi-objective optimization have been performed and result obtained as shown in Tables (4.4 - 4.5). For multi-objective optimization, equal weightage has been assigned for the each response. Multi-objective optimization, the decision variable and bonds are the same as signal objective optimization. The normalize combined objective functions ($Z_{Zn-WE}$, $Z_{BWE}$) for zinc coated brass wire and uncoated brass wire respectively, have been formulated by considering different weightages to all objectives as given by the following equation:

$$Z_{Zn-WE} = \frac{W_1 Z_1}{Z_{1\min}} + \frac{W_2 Z_2}{Z_{2\min}} - \frac{W_3 Z_3}{Z_{3\max}} \tag{4.14}$$

$$Z_{BWE} = \frac{W_4 Z_4}{Z_{4\min}} + \frac{W_5 Z_5}{Z_{5\min}} - \frac{W_6 Z_6}{Z_{6\max}} \tag{4.15}$$

$Z_{Zn-WE}$ = normalize combined objective function for zinc coated brass wire.

$Z_{BWE}$ = normalize combined objective function for uncoated brass wire

$Z_{1\min}$ = minimum value of corner deviation (0.0149 mm) obtained when the single objective optimization problem considering only corner deviation as an objective.

$Z_{2\min}$ = minimum value of Ra (2.7530 μm) obtained when the single objective optimization problem considering only Ra as an objective.

$Z_{3\max}$ = minimum value of MRR (0.0381 g/min) obtained when the single objective optimization problem considering only MRR as an objective.

$Z_{4\min}$ = minimum value of corner deviation (0.0284 mm) obtained when the single objective optimization problem considering only corner deviation as an objective.

$Z_{5\min}$ = minimum value of corner deviation (3.1734 μm) obtained when the single objective optimization problem considering only corner deviation as an objective.

$Z_{6\max}$ = minimum value of corner deviation (0.0231 g/min) obtained when the single objective optimization problem considering only corner deviation as an objective.

$W_1, W_2$ and $W_3$ = weight assigned to the objective functions $Z_1, Z_2$ and $Z_3$ respectively for zinc coated brass wire and $W_4, W_5$ and $W_6$ = weight assigned to the objective functions $Z_4, Z_5$ and $Z_6$ respectively for uncoated brass wire.

The WOA convergence plots for optimizing MRR, corner deviation and surface roughness for both the wire electrode have been shown in Figures. 4.5-4.6 respectively. The WOA convergence plots for combine objective functions for both wire electrodes (Z) have been depicted in Figure 4.7.

The normalized combined objective functions for zinc coated brass wire electrode and uncoated brass wire electrode have been found to be minimal at 0.4921 and 1.0276. The optimal parametric combination for multi-objective optimization have been used to find out the MRR, corner deviation and surface roughness for zinc coated brass wire and uncoated brass wire electrode, which have been shown in Tables 4.6 - 4.7. For optimal setting, no. of search agent =50, maximum no. of iteration= 50 has been considered.

Table 4.4: Results of single objective and multi-objective optimization for Zinc coated brass wire

| Optimization for | A | B | C | D | $Z_{Zn-WE}$ |
|---|---|---|---|---|---|
| Maximizing the MRR | 32 | 8 | 6 | 16 | 0.0381 |
| Minimize the corner deviation | 32 | 20 | 12 | 10 | 0.0144 |
| Minimize the surface roughness | 28 | 8 | 12 | 10 | 2.7527 |
| Multi-objective optimization | 32 | 20 | 12 | 10 | 1.9735 |

Table 4.5: Results of single objective and multi-objective optimization for uncoated brass wire.

| Optimization for | A | B | C | D | $Z_{BWE}$ |
|---|---|---|---|---|---|
| Maximizing the MRR | 32 | 8 | 12 | 16 | 0.0284 |
| Minimize the corner deviation | 32 | 8 | 12 | 10 | 0.0278 |
| Minimize the surface roughness | 26 | 8 | 12 | 10 | 3.1724 |
| Multi-objective optimization | 26 | 8 | 12 | 10 | 1.8462 |

(a)

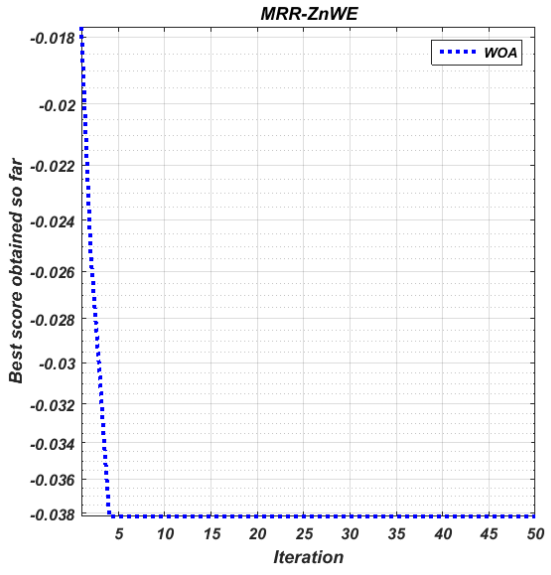


(b)

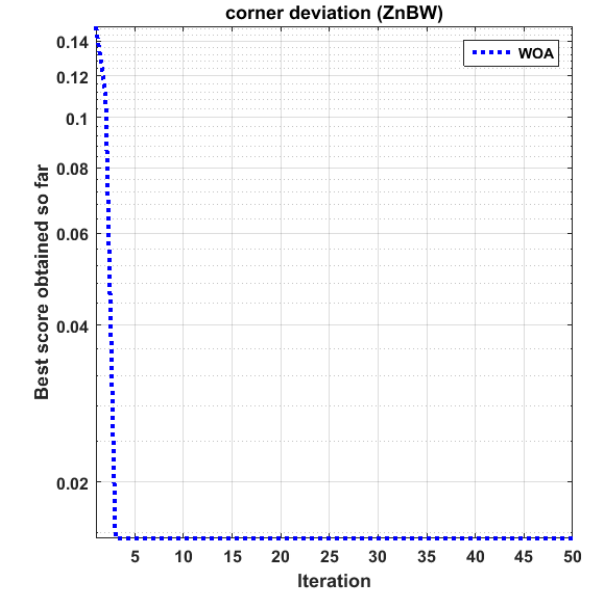

(c)

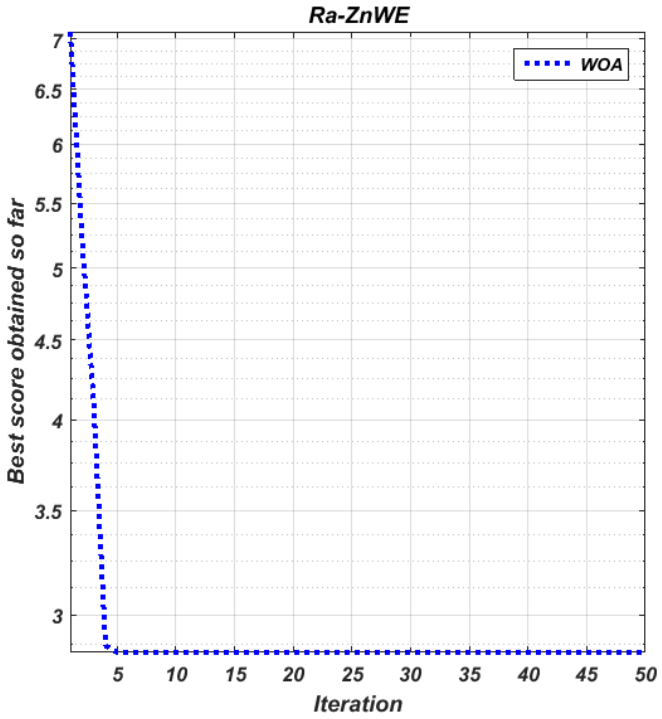


Figure 4.5: Convergence plot for optimizing using WOA for Zinc coated brass wire (a) MRR (b) corner deviation (c) Surface roughness.

(a)

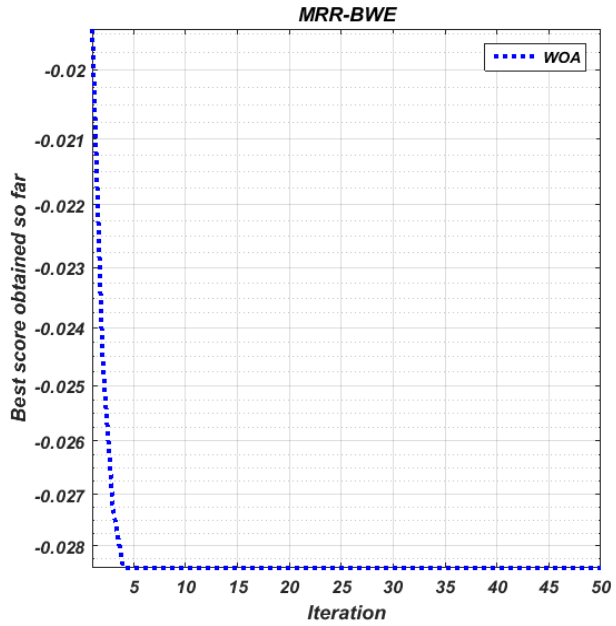


(b)

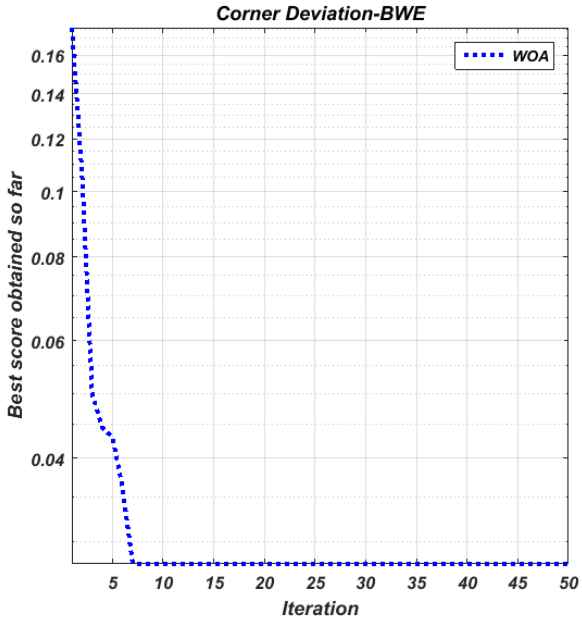

(c)

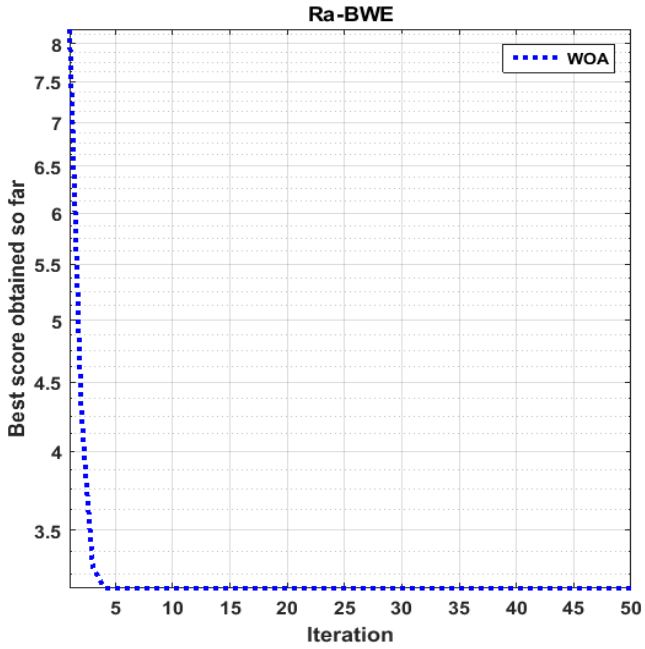


Figure 4.6: Convergence plot for optimizing using WOA for uncoated brass wire (a) MRR (b) corner deviation (c) Surface roughness.

Table 4.6: Results of different output response at optimal parametric combination for zinc coated brass wire.

| A | B | C | D | $Z_{Zn-WE}$ | Corner deviation | Surface roughness | MRR |
|---|---|---|---|---|---|---|---|
| 32 | 20 | 12 | 10 | 1.9735 | 0.0146 | 2.7530 | 0.01778 |

Table 4.7: Results of different output response at optimal parametric combination for uncoated brass wire.

| A | B | C | D | $Z_{BWE}$ | Corner deviation | Surface roughness | MRR |
|---|---|---|---|---|---|---|---|
| 26 | 8 | 12 | 10 | 1.8462 | 0.0277 | 3.181 | 0.01009 |

(a) (b)

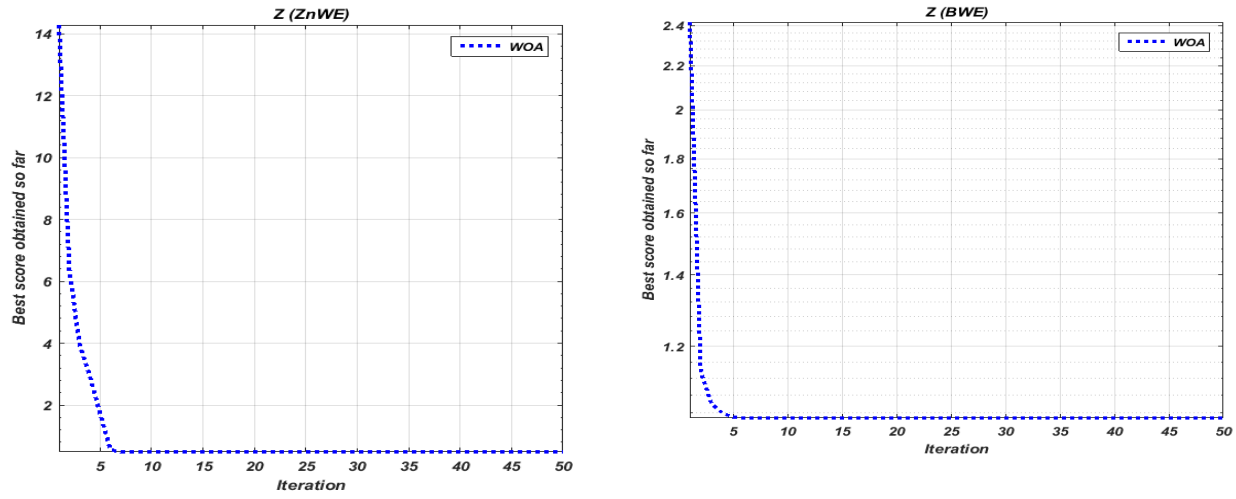


Figure 4.7: Convergence plot for optimizing multi-objective combined function using WOA for (a) Zinc coated brass wire (b) uncoated brass wire electrode.

Table 4.8: Comparisons of performance between GA and WOA using Zinc coated brass wire:

| Algorithm | Responses | Optimization parametric combination | | | | Fitness value |
|---|---|---|---|---|---|---|
| | | Pulse-on time | Flushing pressure | Wire tension | Discharge current | |
| Genetic algorithm | Corner deviation | 32 | 8 | 12 | 10 | 0.0149 |
| | Surface roughness | 26 | 8 | 12 | 10 | 2.7575 |
| | MRR | 32 | 8 | 6 | 16 | 0.0360 |
| | $Z_{Zn-WE}$ | 32 | 20 | 12 | 10 | 2.6067 |
| WOA | Corner deviation | 32 | 20 | 12 | 10 | 0.0144 |
| | Surface roughness | 28 | 8 | 12 | 10 | 2.7527 |
| | MRR | 32 | 8 | 6 | 16 | 0.0381 |
| | $Z_{Zn-WE}$ | 26 | 20 | 12 | 10 | 1.9735 |

Table 4.9: Comparisons of performance between GA and WOA using uncoated brass wire

| Algorithm | Responses | Optimization parametric combination | | | | Fitness value |
|---|---|---|---|---|---|---|
| | | Pulse-on time | Flushing pressure | Wire tension | Discharge current | |
| Genetic algorithm | Corner deviation | 32 | 20 | 12 | 10 | 0.0285 |
| | Surface roughness | 26 | 8 | 12 | 10 | 3.1744 |
| | MRR | 32 | 8 | 12 | 16 | 0.02308 |
| | $Z_{BWE}$ | 26 | 8 | 12 | 10 | 1.8471 |
| WOA | Corner deviation | 32 | 8 | 12 | 10 | 0.0278 |
| | Surface roughness | 26 | 8 | 12 | 10 | 3.1724 |
| | MRR | 32 | 8 | 6 | 16 | 0.0284 |
| | $Z_{BWE}$ | 26 | 20 | 12 | 10 | 1.8462 |

(a)

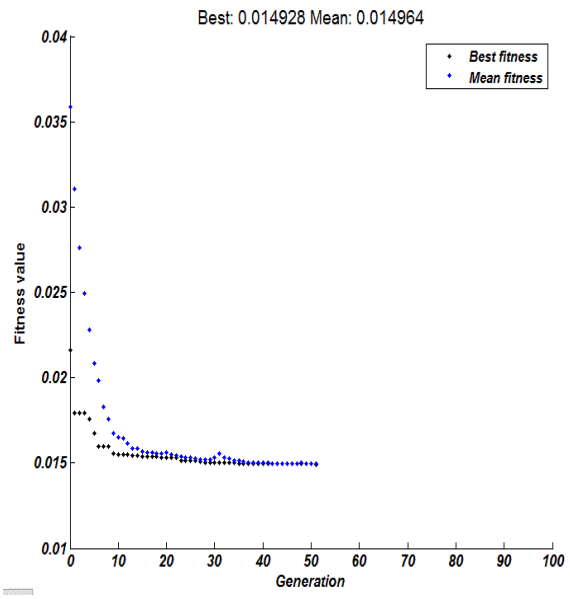


(b)

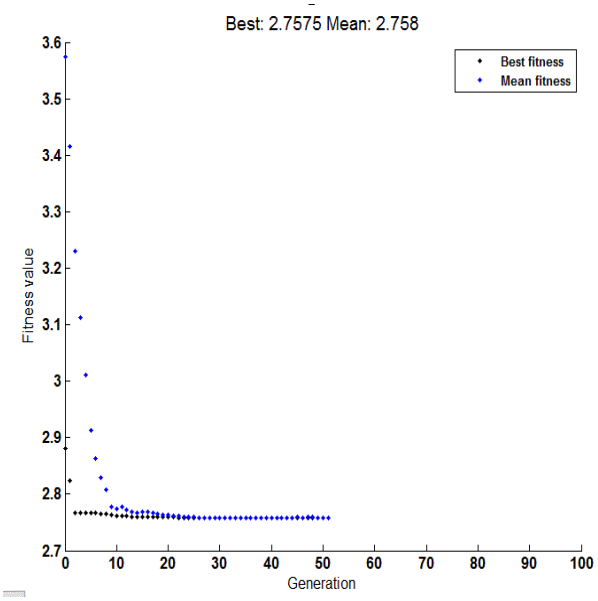

(c)

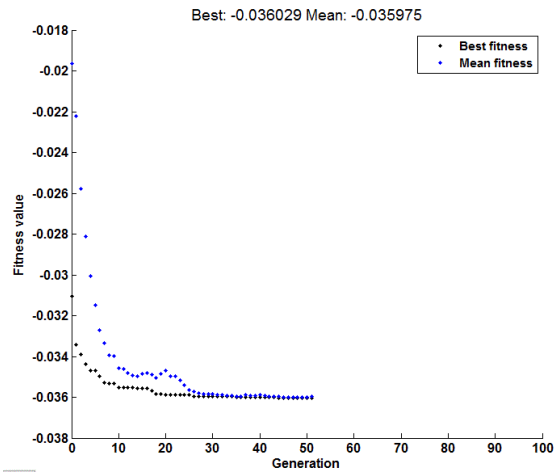


(d)

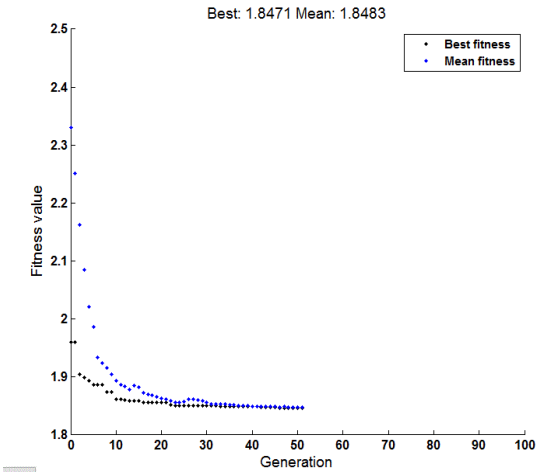


Figure 4.8: Convergence curve of fitness function using GA (zinc coated brass wire) for (a) Corner deviation (b) Surface roughness (c) MRR (d)

(a)

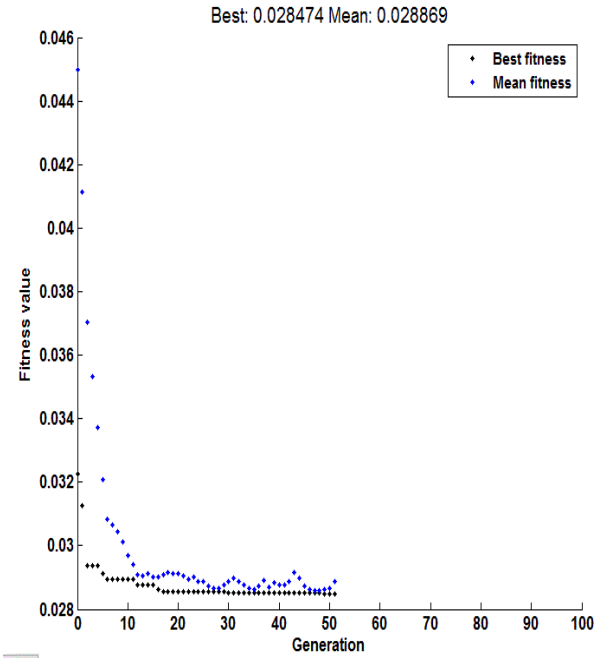


(b)

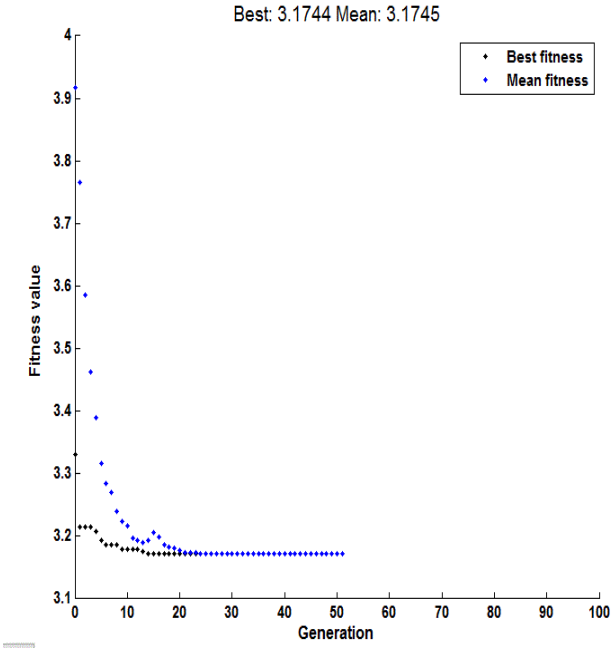

(c)

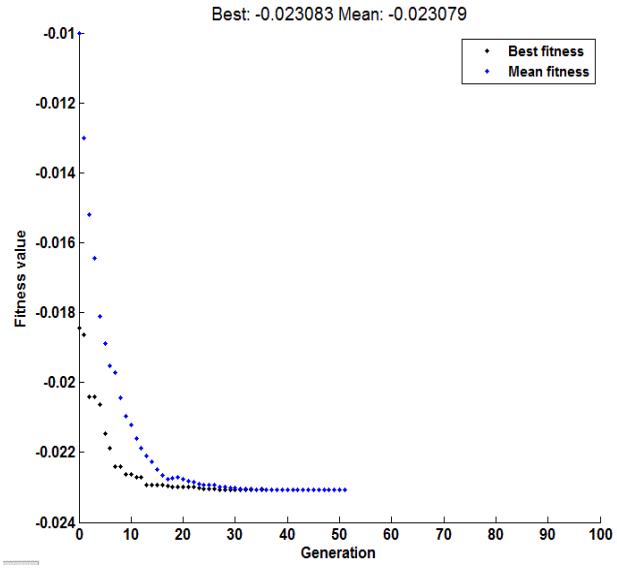


(d)

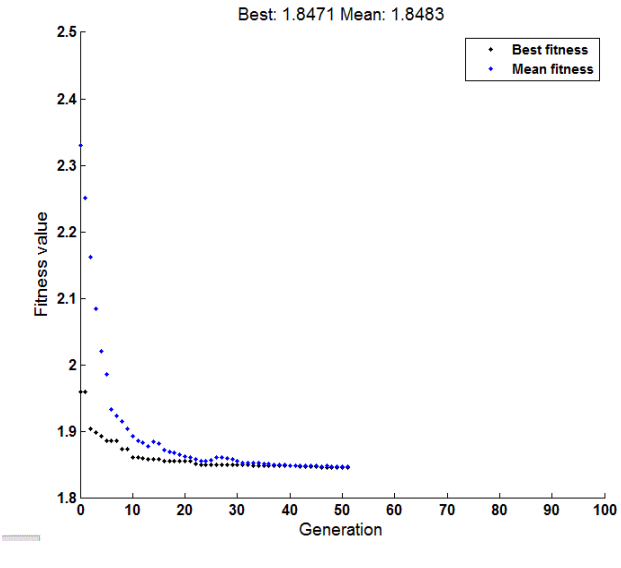


Figure 4.9: Convergence curve of fitness function using GA (uncoated brass wire) for (a) Corner deviation (b) Surface roughness (c) MRR (d)

The performance of WOA has been compared with that of Genetic Algorithm (GA). The results have been shown in Tables (4.8-4.9) for both the wire electrodes. The best fitness function for convergence curves of Corner deviation; Ra, MRR and multi-objective have been shown in Figures 4.8-4.9 respectively. The best optimal value of the objective function found by WOA for Corner deviation, Ra, MRR and multi-objective function 0.0144, 2.7527, 0.0381 and 1.9735 respectively for zinc coated brass wire and 0.0278, 3.1724, 0.0284 and 1.8462 for uncoated brass wire; whereas, objective function value found by GA for Corner deviation, Ra, MRR and multi-objective function 0.0149, 2.7575, 0.0360 and 2.6067 for zinc coated brass wire and 0.0285, 3.1744, 0.02308 and 1.8471 for uncoated brass wire as shown in Tables (4.8-4.9); while considering initial parameter setting of GA as depicted in Table 4.10. From the value it has been observed that WOA provides better result compared to GA.

Table 4.10: Initial parameter setting for GA.

| Population size | 50 |
|---|---|
| Maximum no. of generation | 100 |
| Crossover fraction | 0.8 |
| Mutation function | Constraint dependent |
| Selection function | Stochastic uniform |
| Crossover function | Scattered |
| Migration fraction | 0.2 |
| Elite count | 2 |

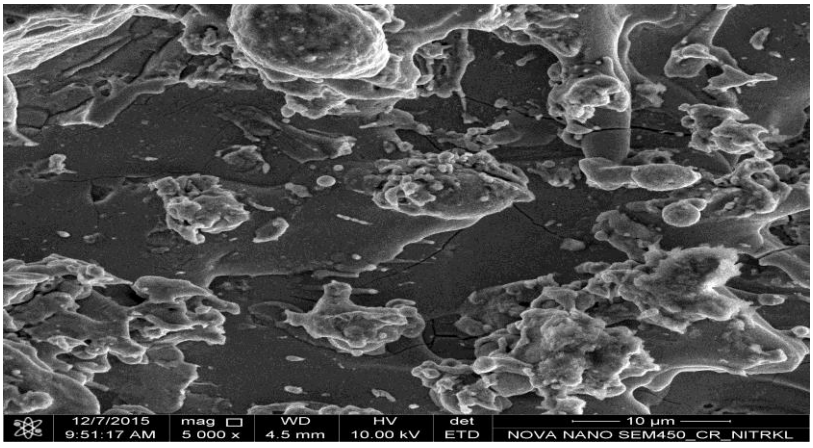


(a) FESEM image of the WEDMed Inconel 718 using Zinc coated brass wire (5000x)

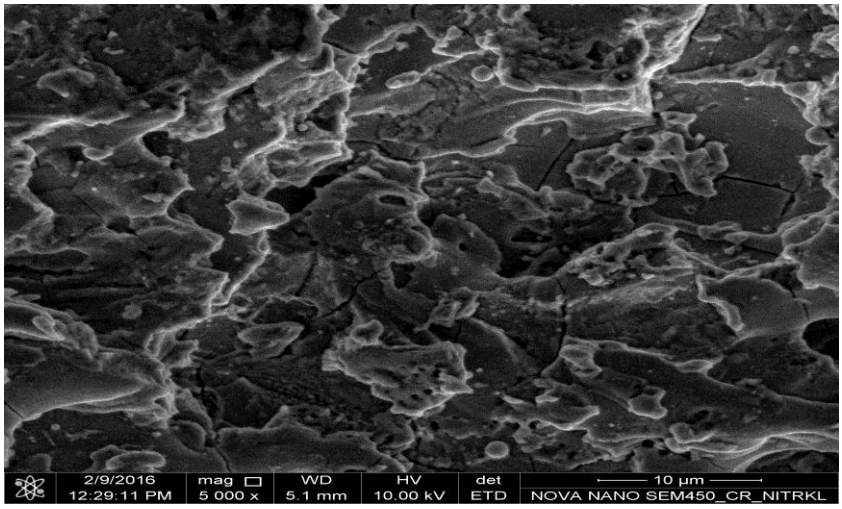


(b) FESEM image the WEDMed Inconel 718 using uncoated brass wire electrode (5000x)

Figure 4.10: (a-b). FESEM images of the machined surface of WEDMed Inconel 718 using different wire electrode with input parameters (A = 32µs, B = 20kg/mm2, C = 6N, D = 14A)

Figure 4.10 (a-b) shows the micrograph of Inconel 718 of using different wire electrode by field emission scanning electron microscope (FESEM) (NOVA NANO SEM 450). It has been observed that the good surface profile is produced on machined surface using zinc coated brass wire compared to using uncoated brass wire. This may be due to fact that, the zinc coating alloy on zinc coated brass wire provided a better cooling effect and flushability nature compared to conventional uncoated brass wire [18]. The flushability nature of the wire electrode indicated the ability of removing maximum material from the machining zone. It can also be observed that, maximum micro-cracks have been generated on machined surface using uncoated brass wire compared to zinc coated brass wire. This is because of brass wire having non-uniform thermal load and lack of flushing characteristics, results increase in yield stress on machined surface; as a outcomes the material plastically deform during heating that builds up tensile stresses leading to crack formation. In case of zinc coated brass wire, the flushability nature and a heat sink characteristic, which helps to decrease the wire temperature during the machining, which cause, minimizes the crack formation on the machined surface.

The meta-heuristic methods are becoming more popular in engineering application, because it's easy to implement do not require gradient information and cover wide range of problems. Some popular methods are GA, Group Search Optimizer (GSA), Social-Based Algorithm (SBA), etc. The major drawback by meta-heuristics is of trapping at local optimum of traditional optimization methods has been solved to a large extent. GA requires high computational time and also more algorithmic parameters settings. On other hand WOA is easy to understand as mimicking the hunting behavior of humpback whales. Also, only three parameters setting required for WOA whereas GA, PSO etc. need more parameters setting and computational time.

In this investigation, attempts have been made by WOA algorithm, to determine the optimal machining parameters settings in view of different process performance yields in the context of WEDMed of Inconel 718. Initially attempts for considering individual responses feature like MRR, corner deviation and Ra respectively for both the wire electrodes. After the next step, aforesaid aggregated all the responses features to obtained the combined objective functions for zinc coated brass wire ( $Z_{Zn-WE}$ ) and for uncoated brass wire ( $Z_{BWE}$ ) and finally optimized using WOA. WOA results have also been compared with GA. From the results of WOA and GA, it has been observed that WOA showed better performance compare to GA for both the wire electrodes.

## 4.1.4 Concluding Remarks

The present research focuses on investigating the influence of different tool electrode (zinc coated brass wire and uncoated brass wire) on machinability of Inconel 718 along with optimization of machining parameters (process variable). Mathematical model has been developed using nonlinear regression model equation for analysis the effect of process parameters such as pulse-on time, flushing pressure, wire tension and discharge current. MRR, corner deviation and surface roughness have been considered for evaluation of machining performance characteristics. The study also illustrates the feasibility of the relatively new optimization algorithm i.e. WOA for obtaining the optimal solution. Based on the aforesaid investigation the following conclusions have been made.

i. The proper selection of electrode material is very important on improving the performance in terms of MRR, corner deviation and surface roughness during WEDM on Inconel 718.
ii. The zinc coated brass wire electrode has produced the higher MRR, good surface finish and minimum corner deviation as compared to uncoated brass wire electrode.
iii. Pulse-on time, wire tension and discharge current are found to be the most important parameters that influence the output responses considered herein for both the wire electrodes.
iv. The optimization results demonstrate that WOA is very competitive compare to GA.

# 4.1 Machining Response and Optimization of WEDM process parameters by using GWO

## 4.2.1 Coverage

This study focuses an experimental investigation of Inconel 718 by using zinc coated brass wire as tool electrode in wire electrical discharge machining (WEDM) process for taper cutting. Experiments have been conducted using $L_{27}$ orthogonal array by process parameters (such as taper angle, pulse on time, wire speed, wire tension and discharge current) to obtained the machining performance yields viz. angular error and surface roughness. Initially, a process model has been developed by using non-linear regression analysis for correlating various process parameters with respect to the output responses. Finally, new advance optimization technique; Grey Wolf Optimizer (GWO) in order find the optimal machining parameter setting (the most favourable combination) of process parameters for achieving satisfactory machining performances. The results of GWO have been compared with Genetic Algorithm (GA), and its shown good performance for GWO in the context of this study concern on machining of Inconel 718.

## 4.2.2 Problem Definition

Wire electrical-discharge machining (WEDM) is a non-conventional machining process in which material is eroded by the sparks between the workpiece and electrode (wire). It is used to manufacture conductive hard metal components with intricate shape with precise and good tolerance limit. In this process, there is no contact between tool and workpiece; therefore, any hard materials can be cut easily. WEDM employs a continuous travelling electrode in form of wire. The wire electrode has made of different materials (brass, copper, zinc coated etc.) of diameter from 0.05 to 0.35mm. The travelling of wire controlled by CNC (Computer Numerically controlled) program to achieve desire shape and size of the workpiece. That can

make WEDM more popular precision machining process and the best choice for super hard material with intricate shape. In case of taper-cutting, a common application of the WEDM process, the objective is the generation of inclined surfaces. This is achieved by applying a relative displacement between the upper guide and lower guide of the wire as shown in Figure. 4.11. If the wire had no stiffness it would exactly adapt the geometry of the guide [91]. In this ideal case, α would be the programmed angle; this angle is the actual cutting angle in the machined part as shown in Figure. 4.12. However, the deviation of the wire with respect to actual shape happens due to change in stiffness of wire

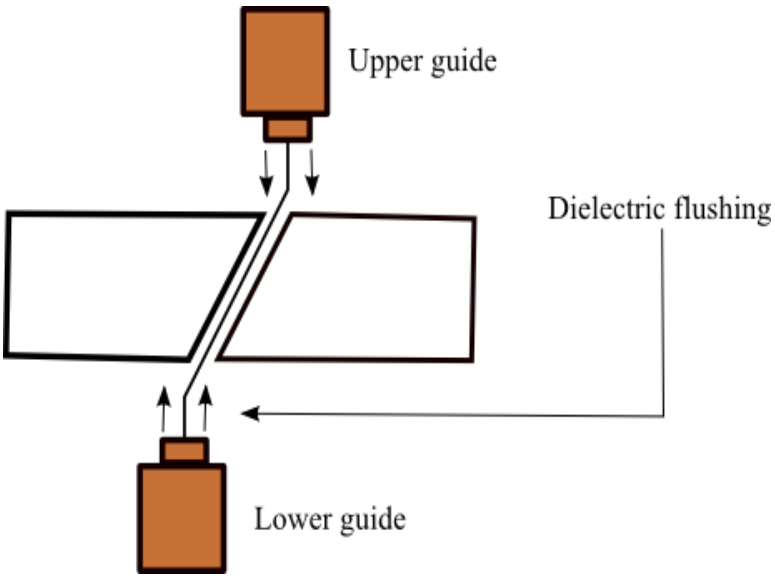


Figure 4.11 Relative displacement of taper and lower guides in WEDM taper-cutting

From the Figure. 4.12, angle β represents the angular error induced by this effect and its shown in minutes. The errors may be occurs in different aspects such as the stiffness of the wire, distance between the upper and lower guide and the force exerted during the cutting process etc. As a result, the machined part loses its precision.

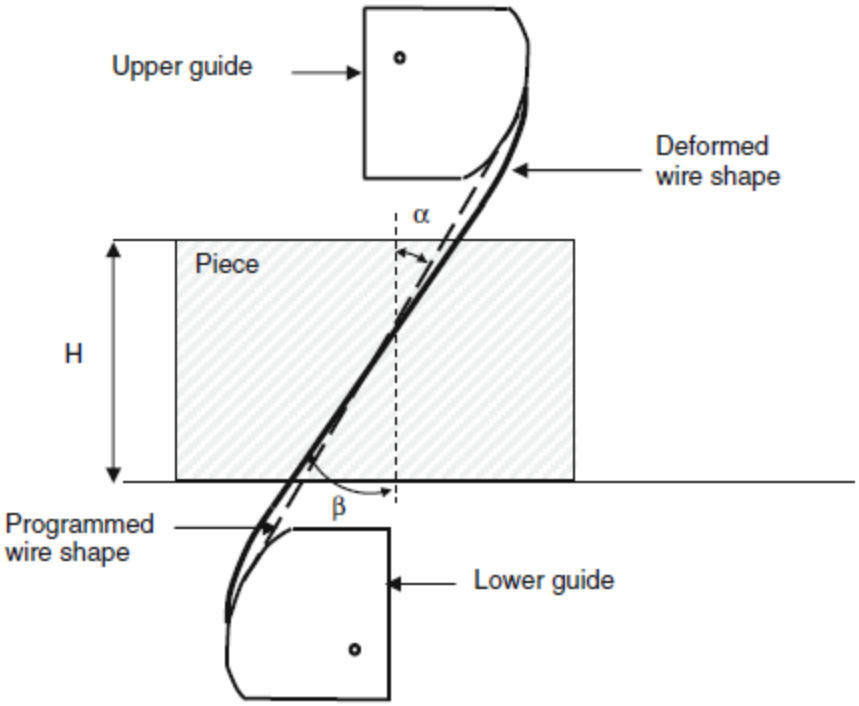


Figure 4.12: Theoretical and actual location of the deformed wire

Recent time, there many research work have been carried out with the effects of the forces developed on the wire during machining process [125, 126]. Plaza et al. [91] proposed a design of experiment methodology to study the influence of WEDM process parameters on the angular accuracy of taper cutting operations and influence of response variable related to geometrical problem and part thickness angle. Sanchez et al. [127] discussed an original contribution to the analysis of the factors that influenced angular error in taper cutting and developed of experimentalal and numerical model to predict error. Finally, Finite element simulation of mechanical behavior of a wire typically used for taper cutting was presented. Nayak et al. [128] presented a mathematical model using artificial neural network (ANN) to determine the relationship between response variable and output response. Finally, Bat algorithm is used to suggest the optimum parametric combination to minimize the angular error during taper cutting operation using WEDM operation. Sanchez et al. [90] presented a computer simulation software for analysis of angular error in taper during WEDM operation. The work material used was hard materials, such as those used in the tooling industry. The simulated result has been compared with the experimental result by the classical trial and error method, yielding good results. Nayak

et al. [129] highlighted a quantum behaved Particle Swarm Optimization (PSO) approach combined with maximum deviation theory to determine the optimum parameter setting during taper cutting on AISI D2 tool steel as work material. Jangra et al. [130] studied effects of response parameters on MRR and Surface roughness on carbide cobalt (WC-Co) composite as work material. The optimization of response output (MRR and surface roughness) was carried out using Gray Relation Analysis (GRA). Results, ANOVA showed that pulse-on time and taper angle were the most significant parameters for the multiple machining characteristics. Nayak et al. [131] reported an experimental investigation and optimization of different process parameter (part thickness, taper angle, pulse duration, discharge current, wire speed and wire tension.) during taper cutting of deep cryogenic-treated Inconel 718 using WEDM operation. Finally, process model was optimized using the bat algorithm which yielded good result of performance characteristics during taper cutting.

From the literature survey it has been observed that, inadequate investigations in case of taper cutting have been reported, with few attentions to optimize the response parameters of WEDM. It has been noted that few or none literature focusing on performance of zinc coated brass wire in taper cutting on Inconel 718 using WEDM has been reported. Therefore, the present study, an attempt has been made to discuss the effect of zinc coated brass wire as tool with various process parameters during taper cutting process on Inconel 718 in WEDM. Finally, the process model is developed using non-linear regression model which is optimized by Grey Wolf Optimizer (GWO) algorithm

### 4.2.3 Development of Mathematical model

Non-linear regression equation has been used for creating a relationship between the dependent variable and a set of independent variable(s) [122] [123]. The nonlinear regression can estimate models with random relationships between independent and dependent variables. The proposed mathematical model for response $Y_i$ has been represented as below:

$$Y_i = C \times X_1^a \times X_2^b \times X_3^c \times X_4^d \tag{4.16}$$

C represent as constant; $X_1$ represents as pulse-on time; $X_2$ represents as flushing pressure ; $X_3$ represents as wire tension ; $X_4$ represents as discharge currents and $a, b, c, d$ are the estimated coefficients of the said regression model.

## 4.2.4 Grey wolf optimization (GWO)

Grey Wolf Optimizer (GWO) is a metaheuristic search algorithm inspired by grey wolves (Canislupus) proposed by Mirjalili et al. [132], which simulates the social stratum and hunting mechanism of grey wolves in nature and based on three main steps of hunting: searching for prey, encircling prey and attacking prey. The flow chart has been depicted on Figure 4.13.

In case of mathematically model, these wolves are classified in four dominant strategies which are alpha (α), beta (β), delta (δ), and omega (ω) wolves [133].

a. Searching for prey

   The position of α, β and δ wolves, the grey wolves search for the prey. They diverge from each other to search for the prey and converge to attack the prey. It is observed that $|A|>1$ can force the wolves to search for a better prey. This divergence behavior refers to consideration or the global search of the GWO algorithm.

b. Encircling the prey

   Encircling the prey by the grey wolves can be expressed by the following equations

   $$D = \left|C.X_p(t) - X(t)\right|$$

   $$X(t+1) = X_p(t) - A.D,$$

   Where A and C are coefficient vectors which can be written as follows

   $$A = 2ar_1 - a,$$

   $$C = 2.r_2,$$

   The components of vector ‘a’ are linearly decreased from 2 to 0 with iterations and $r_1$ and $r_2$ are random vectors ϵ [0,1].

c. Hunting

Hunting behavior model of the grey wolves, the most dominant wolves are α (best fittest solution). Consequently, β wolves are second level of dominance in the group to help α in decision or other activities and δ wolves dominate ω wolves and shear information to α and β wolves. The following equations describe the hunting behavior:

$$D_\alpha = |C_1 X_\alpha - X|, D_\alpha = |C_2 X_\beta - X|, D_\delta = |C_3 X_\delta - X| \quad (4.17)$$

$$X_1 = X_\alpha - A_1.D_\alpha, X_2 = X_\beta - A_2.D_\beta, X_1 = X_\delta - A_3.D_\delta \quad (4.18)$$

$$X(t+1) = \frac{X_2 + X_2 + X_3}{3} \quad (4.19)$$

d. Attacking prey

The hunting process is terminated by attacking the prey when it stops moving. By mathematical model, decreasing the value of vector a from 2 to 0 with iterations. It is found that $|A| < 1$ can force the wolves to attack the prey. This behavior of attacking represents exploitation or local search of the GWO algorithm.

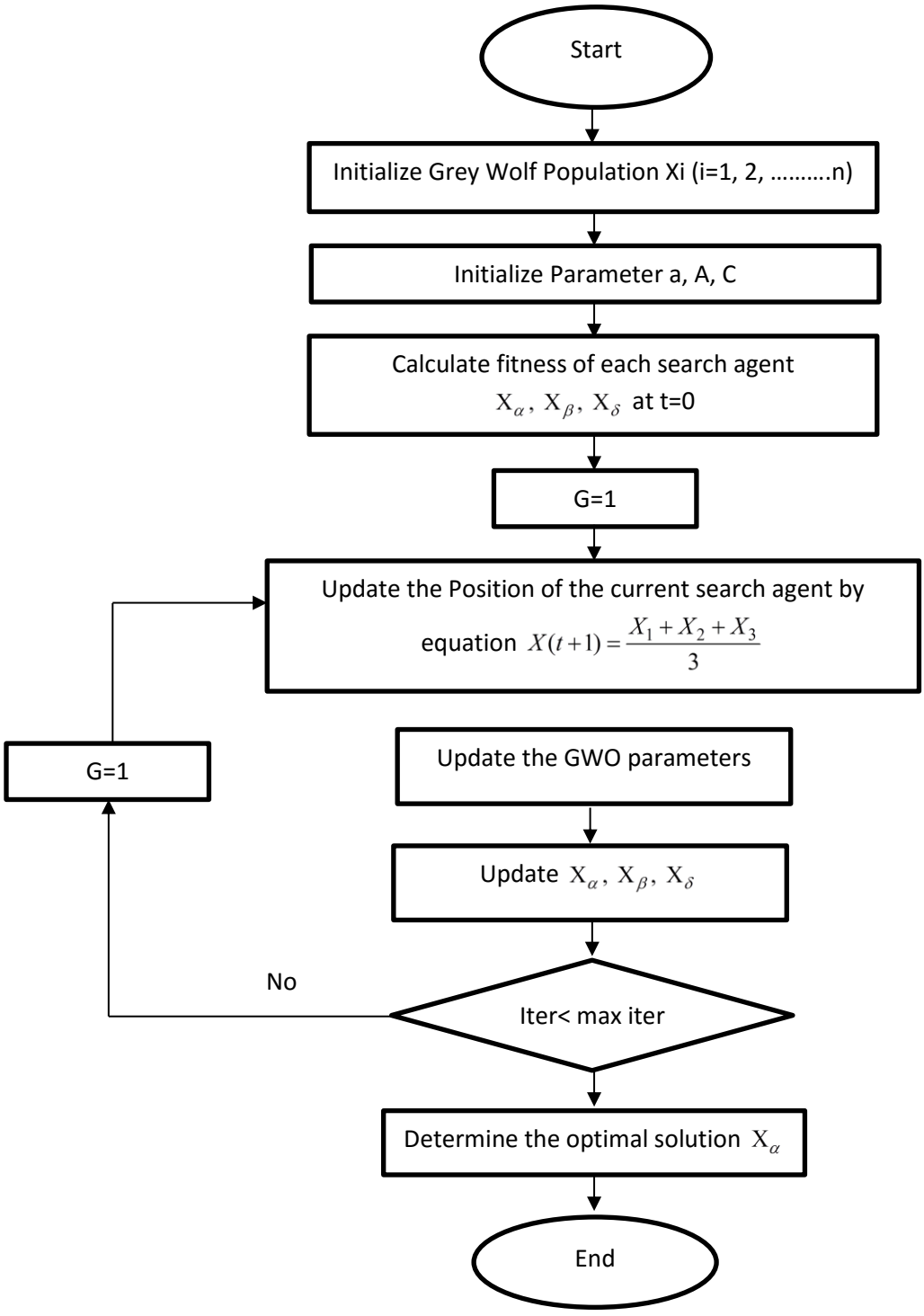


Figure 4.13: flow chart of Grey Wolves Optimization (GWO)

## 4.2.5 Experimentation

In the present study, experiments have been conducted on a CNC WEDM machine, [AGIE, SWITZERLAND]. Inconel 718 has been selected as work material with dimension (50mm × 10mm × 5mm).

### 4.2.5.1 Selection of process parameters

The selection process parameter has been given in Table 4.11. The experiments have been conducted to investigate the significant contribution of process parameters on machinability (in terms of angular error and surface roughness) during WEDM process. Pulse-on time, wire speed, wire tension and discharge current have been chosen as input process parameters. Initially the zinc coated brass wire electrode of diameter 0.2 mm has been used. Deionized water has been used as dielectric fluid. The pulse-off time and dielectric flow rate have been kept fixed as 50µs and 1.2 bars, respectively, throughout the experiments.

Table 4.11: process parameters and domain of variation:

| Control factors | Code | Unit | Level I | Level II | Level III |
|---|---|---|---|---|---|
| Taper Angle | A | Degree | 10 | 12 | 14 |
| Pulse on time | B | [µs] | 28 | 30 | 32 |
| Wire speed | C | [mm/s] | 95 | 115 | 135 |
| Wire tension | D | [N] | 8 | 10 | 12 |
| Discharge Current | E | [A] | 13 | 14 | 15 |

The process parameters and their levels were chosen based on the literature review significance and machining limitation. Plaza et al. [91] informed that taper angle are the most influencing variables in taper cutting using WEDM. Therefore, taper angle, pulse-on time, wire speed, wire tension and discharge current are considered were the input parameters.

The cutting speed ($C_s$) in mm/min has been directly obtained from digitally displayed on the computer screen during machining. The taper angles of all machined specimens have been measured using coordinate measuring machine (CMM) (spectra accurate). The surface roughness

(Ra) WEDMed surface of Inconel 718 has been measured using Talysurf (Talysurf 50 Taylor Hobson Ltd., UK). The surface texture and the finishing mechanism after WEDM process have been observed through FE-SEM (NOVA NANO SEM 450).

The angular error can be expressed in minute and calculated by the following formula [131]

$$Angular\ error = \theta - \phi$$

Where θ is programmed angle in the machined part and ϕ is the programmed angle obtained from machining. The geometry of the test part is shown in Figure.4.14.

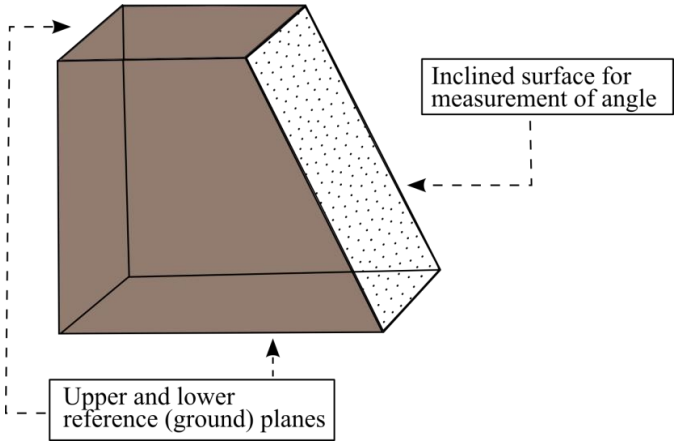


Figure 4.14: Specimen for measurement of angular accuracy.

## 4.2.6 Results and discussions

A 5-factor-3-level, $L_{27}$ orthogonal array has been selected for conduct the experiments and collection response data as shown in Table 4.12.

Table 4.12: design of experiment and collection response data

| Sl no. | A [$^o$] | B [μs] | C [mm/s] | D [N] | E [A] | Angular error [minute] | Ra [μm] |
|---|---|---|---|---|---|---|---|
| 1 | 1 | 1 | 1 | 1 | 1 | 13.80 | 2.84 |
| 2 | 1 | 1 | 1 | 1 | 2 | 17.40 | 3.48 |
| 3 | 1 | 1 | 1 | 1 | 3 | 21.24 | 4.20 |
| 4 | 1 | 2 | 2 | 2 | 1 | 13.02 | 3.02 |
| 5 | 1 | 2 | 2 | 2 | 2 | 21.00 | 3.14 |

| | | | | | | | |
|---|---|---|---|---|---|---|---|
| 6 | 1 | 2 | 2 | 2 | 3 | 25.20 | 3.20 |
| 7 | 1 | 3 | 3 | 3 | 1 | 12.60 | 3.00 |
| 8 | 1 | 3 | 3 | 3 | 2 | 17.76 | 3.10 |
| 9 | 1 | 3 | 3 | 3 | 3 | 22.20 | 3.40 |
| 10 | 2 | 1 | 2 | 3 | 1 | 20.40 | 2.56 |
| 11 | 2 | 1 | 2 | 3 | 2 | 23.40 | 3.10 |
| 12 | 2 | 1 | 2 | 3 | 3 | 24.60 | 4.10 |
| 13 | 2 | 2 | 3 | 1 | 1 | 12.60 | 3.20 |
| 14 | 2 | 2 | 3 | 1 | 2 | 15.00 | 3.55 |
| 15 | 2 | 2 | 3 | 1 | 3 | 19.80 | 3.80 |
| 16 | 2 | 3 | 1 | 2 | 1 | 37.20 | 3.04 |
| 17 | 2 | 3 | 1 | 2 | 2 | 40.80 | 3.50 |
| 18 | 2 | 3 | 1 | 2 | 3 | 43.20 | 3.73 |
| 19 | 3 | 1 | 3 | 2 | 1 | 13.80 | 3.00 |
| 20 | 3 | 1 | 3 | 2 | 2 | 18.00 | 2.94 |
| 21 | 3 | 1 | 3 | 2 | 3 | 21.00 | 2.80 |
| 22 | 3 | 2 | 1 | 3 | 1 | 35.40 | 2.88 |
| 23 | 3 | 2 | 1 | 3 | 2 | 31.80 | 3.20 |
| 24 | 3 | 2 | 1 | 3 | 3 | 28.80 | 3.71 |
| 25 | 3 | 3 | 2 | 1 | 1 | 16.80 | 3.85 |
| 26 | 3 | 3 | 2 | 1 | 2 | 17.52 | 4.10 |
| 27 | 3 | 3 | 2 | 1 | 3 | 27.60 | 4.40 |

Analysis of the results presented in Figure.4.15, leads to the conclusion that the $A_1B_2C_3D_1E_1$ provides the minimum Value of angular error, from Figure. 4.15 (a), show that increases the taper angle, angular error first increase then decreases because the wire and parameters of higher influence on angular error are related to part geometry, i.e., part thick ness and taper angle, with a smaller role of the EDM regime [127]. From the investigated of Analysis of variance (ANOVA); significance of each parameter with interaction is shown in Table 4.13.

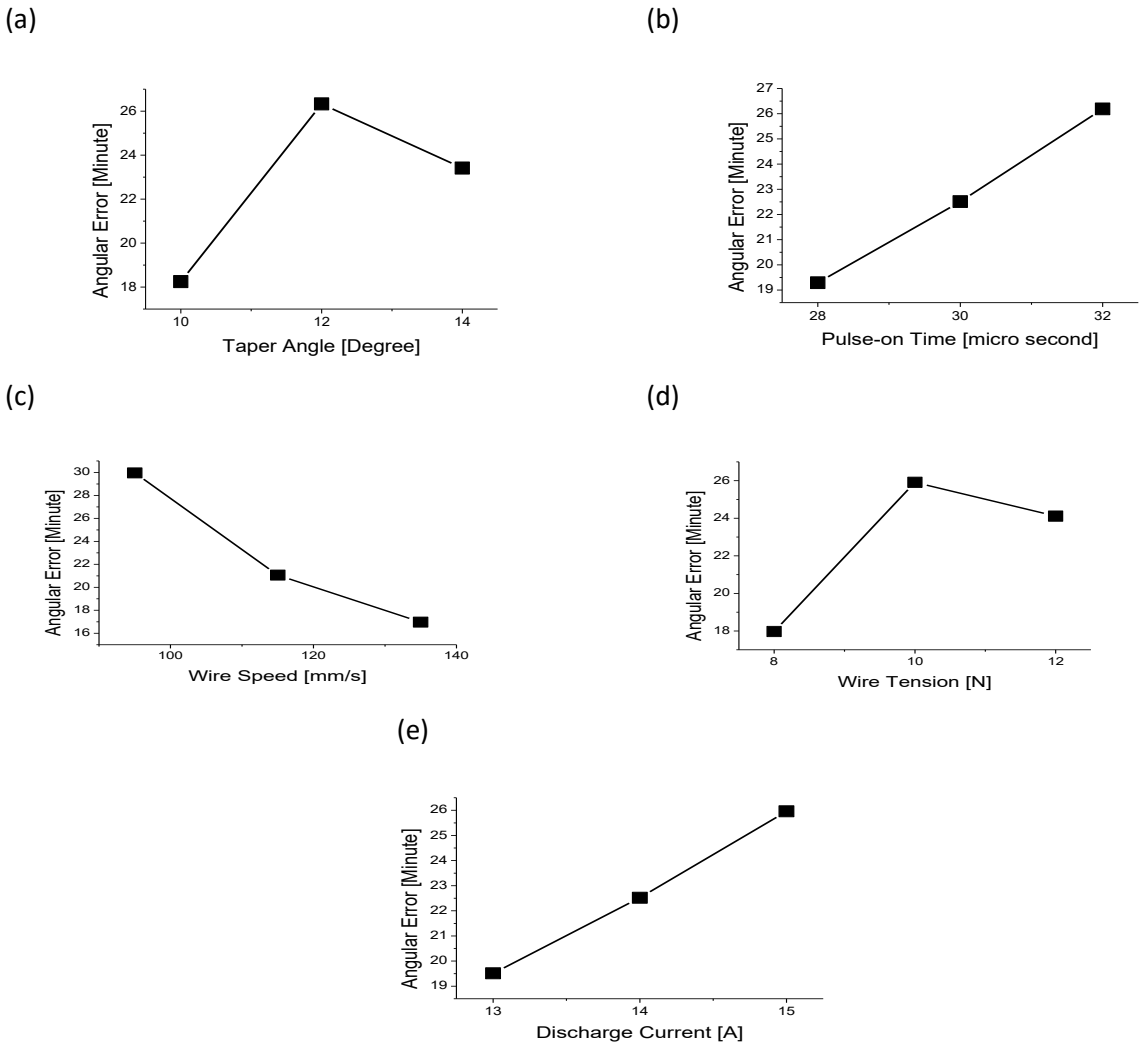


Figure 4.15: Main effect of control parameters on angular error

Table 4.13, has shown that taper angle (A), pulse-on time (B), wire tension (D) and discharge current (E) are the most significant parameters among others for angular error in WEDM.

Table 4.13: Analysis of Variance for SN ratios for angular error

| Source | DF | Seq SS | Adj SS | Adj MS | F | P |
|---|---|---|---|---|---|---|
| A | 2 | 22.948 | 22.948 | 11.4742 | 26.24 | <0.000 |
| B | 2 | 16.098 | 16.098 | 8.0491 | 18.40 | <0.000 |
| C | 2 | 96.373 | 96.373 | 48.1866 | 110.18 | 0.001 |
| D | 2 | 40.276 | 40.276 | 20.1378 | 46.05 | <0.000 |
| E | 2 | 53.830 | 53.830 | 26.9150 | 61.54 | 0.000 |

| | | | | | | |
|---|---|---|---|---|---|---|
| D*E | 4 | 5.902 | 5.902 | 1.4755 | 3.37 | 0.045 |
| Residual Error | 12 | 5.248 | 5.248 | 0.4373 | | |
| Total | 26 | 240.675 | | | | |

Similarly, the optimum parameter setting for minimum surface roughness has been shown by the main effect plot as shown in Figure. 4.16. The level of significant parameter setting is $A_1B_1C_3D_2E_1$, in which the minimum value of surface roughness is observed. ANOVA as shown in Table 4.14 shows that the taper angle (A), pulse-on time (B), wire tension (D) and discharge current (E) are the most significant parameters for surface roughness in WEDM. Referring to Figure 4.16(a) with increase the taper angle the surface roughness is also increase. The surface roughness also increases with increase in the pulse on time. The discharge energy becomes much more intense with increased in pulse on time; the explosion more powerful which deteriorates the surface finish [31].

(a)

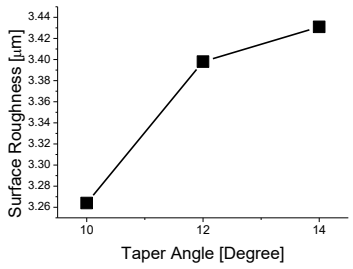


(b)

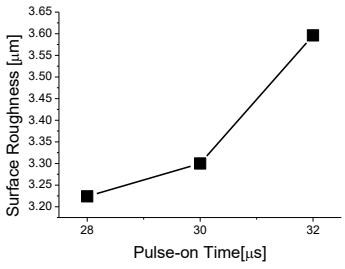


(c)

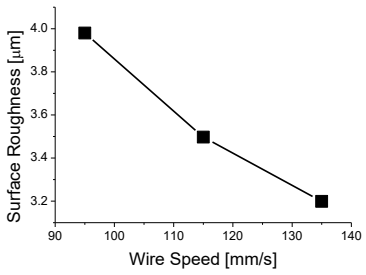


(d)

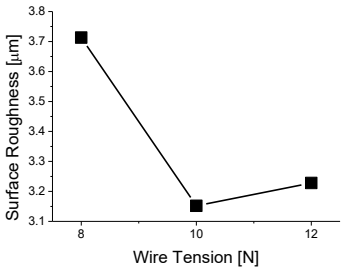

(e)

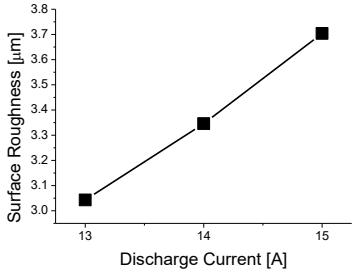


Figure 4.16: Main effect of control parameters on surface roughness

Table 4.14: Analysis of Variance for SN ratios for surface roughness

| Source | DF | Seq SS | Adj SS | Adj MS | F | P |
|---|---|---|---|---|---|---|
| A | 2 | 1.6161 | 1.6161 | 0.8080 | 6.04 | 0.015 |
| B | 2 | 3.3713 | 3.3713 | 1.6856 | 12.60 | 0.001 |
| C | 2 | 0.9319 | 0.9319 | 0.4659 | 3.48 | 0.064 |
| D | 2 | 8.5407 | 8.5407 | 4.2703 | 31.91 | 0.000 |
| E | 2 | 10.1697 | 10.1697 | 5.0848 | 38.00 | 0.000 |
| D*E | 4 | 0.4349 | 0.4349 | 0.1087 | 0.81 | 0.541 |
| Residual Error | 12 | 1.6057 | 1.6057 | 0.1338 | | |
| Total | 26 | 26.6701 | | | | |

### 4.2.6.1 Mathematical Modelling of Angular error and surface Roughness

$$\text{Angular Error} = 0.00470714 \times A^{0.324132} \times B^{2.23162} * C^{(-1.69173)} \times D^{0.688905} \times E^{2.45427} \quad (4.20)$$

$$\text{Surface Roughness} = 0.0257297 \times A^{0.225257} \times B^{0.720351} \times C^{(-0.0984095)} \times D^{(-0.382095)} \times E^{1.21424} \quad (4.21)$$

where, angular errors are minute and surface roughness are in µm.

### 4.2.6.2 Model accuracy test for Angular and surface Roughness

The first step of this present work, responses have been derived (for individual: angular error and Surface roughness) using non-linear regression analysis. The mathematical models have been based on controllable parameters. These models have been optimized individually using GWO algorithm in the selected parametric search space.

After careful examination of Figures (4.15-4.16), it has been observed that level of significant factors for angular error and surface roughness are $A_1B_2C_3D_1E_1$ and $A_1B_1C_3D_2E_1$ respectively. From the result, it has been noticed that the level of significant parameter setting for the angular error and surface roughness are conflicting. Therefore, there is no single parameter setting that could be suggested for the optimal setting for all the responses. Hence, there is a requirement to explore a responses strategy for optimization of this process.

Table 4.15: Results of single objective and multi-objective optimization for Zinc coated brass wire

| Optimization for | A | B | C | D | E | Z |
|---|---|---|---|---|---|---|
| Minimize the Angular error | 10 | 28 | 135 | 8 | 13 | 9.5172 |
| Minimize the surface roughness | 10 | 28 | 135 | 12 | 13 | 2.5630 |
| Multi-objective optimization | 10 | 28 | 135 | 8 | 13 | 1.9110 |

(a) (b)

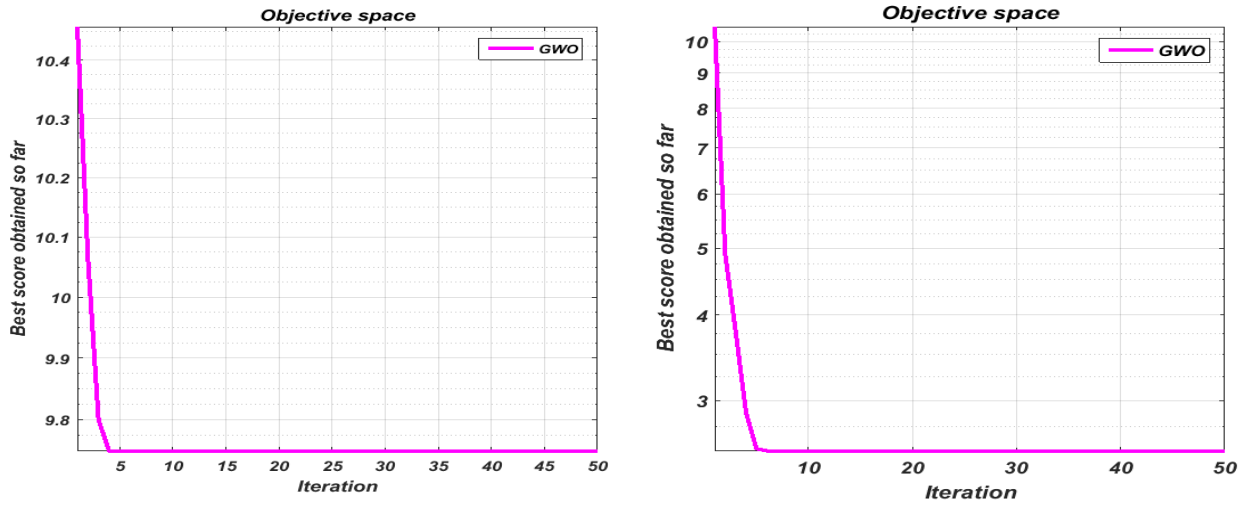


Figure 4.17: Convergence plot for optimizing using GWO for Zinc coated brass wire (a) Angular error (b) Surface roughness

Table 4.16: Results of different output response at optimal parametric combination for zinc coated brass wire

| A | B | C | D | E | Z | Angular error | Surface roughness |
|---|---|---|---|---|---|---|---|
| 10 | 28 | 135 | 8 | 13 | 1.9110 | 9.5172 | 2.5630 |

Table 4.17: Comparisons of performance between GA and WOA using Zinc coated brass wire

| Algorithm | Responses | | Optimization parametric combination | | | | Fitness value |
|---|---|---|---|---|---|---|---|
| | | A | B | C | D | E | |
| Genetic algorithm | Angular Error | 10 | 28 | 135 | 8 | 13 | 9.5341 |
| | Surface roughness | 10 | 28 | 135 | 12 | 13 | 2.5692 |
| | Z | 10 | 28 | 135 | 8 | 13 | 1.9146 |
| GWO | Angular Error | 10 | 28 | 135 | 8 | 13 | 9.5172 |
| | Surface roughness | 10 | 28 | 135 | 12 | 13 | 2.5630 |
| | Z | 10 | 28 | 135 | 8 | 13 | 1.9110 |

(a)

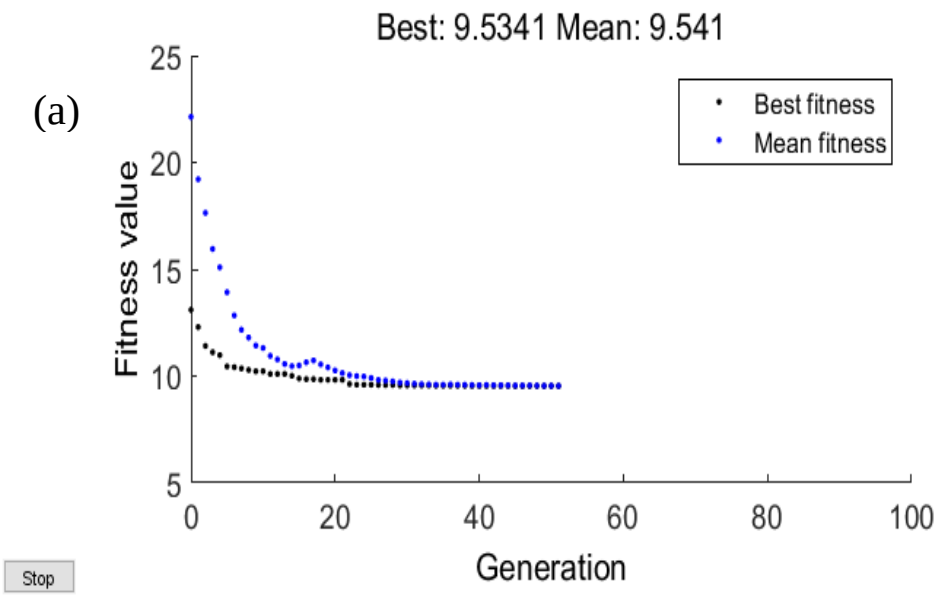
Best: 9.5341 Mean: 9.541
Best fitness
Mean fitness
Fitness value
Generation
25
20
15
10
5
0
20
40
60
80
100
Stop

(b)

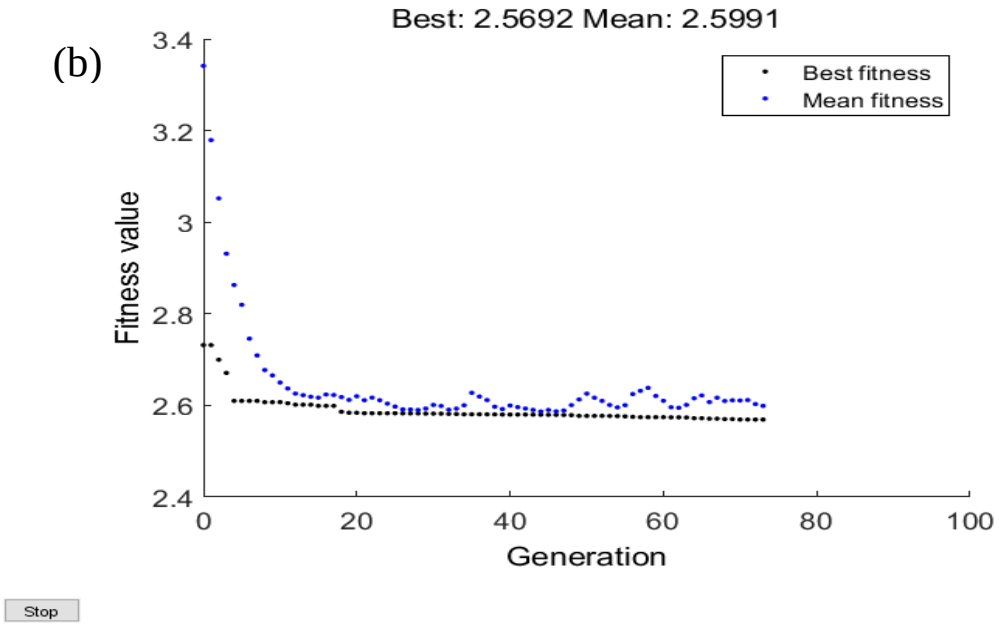
Best: 2.5692 Mean: 2.5991
Best fitness
Mean fitness
Fitness value
Generation
3.4
3.2
3
2.8
2.6
2.4
0
20
40
60
80
100
Stop

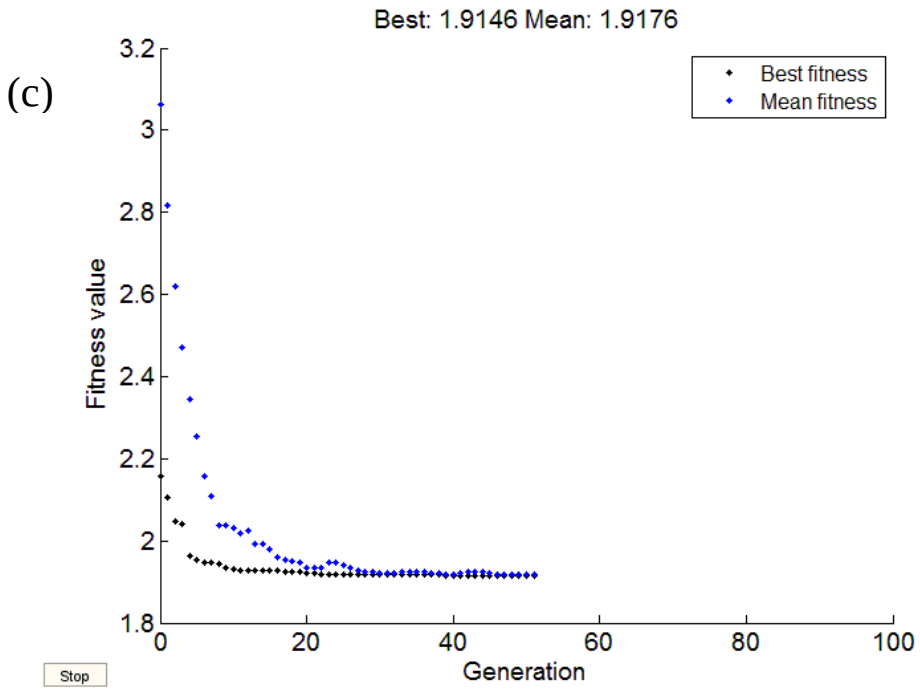


Figure 4.18: Convergence curve of fitness function using GA for (a) Angular Error (b) Surface roughness (c) MRR (d) Z

The performance result of GWO has been compared with that of Genetic Algorithm (GA). The results have been shown in Tables 4.17. The best fitness function for convergence curves of angular error; surface roughness and multi-objective have been shown in Figure 4.18 respectively. The best optimal value of the objective function found by GWO for angular error; surface roughness and multi-objective function are 9.5172, 2.5630 and 1.9110 respectively; whereas, objective function value found by GA for angular error; surface roughness and multi-objective function are 9.5341, 25692 and 1.9146 as shown in Tables 3.17; while considering initial parameter setting of GA as depicted in Table 3.18. From the value it has been observed that WOA provides better result compared to GA.

Table 4.18: Initial parameter setting for GA

| | |
|---|---|
| Population size | 50 |
| Maximum no. of generation | 100 |
| Crossover fraction | 0.8 |
| Mutation function | Constraint dependent |
| Selection function | Stochastic uniform |
| Crossover function | Scattered |
| Migration fraction | 0.2 |
| Elite count | 2 |

(a)

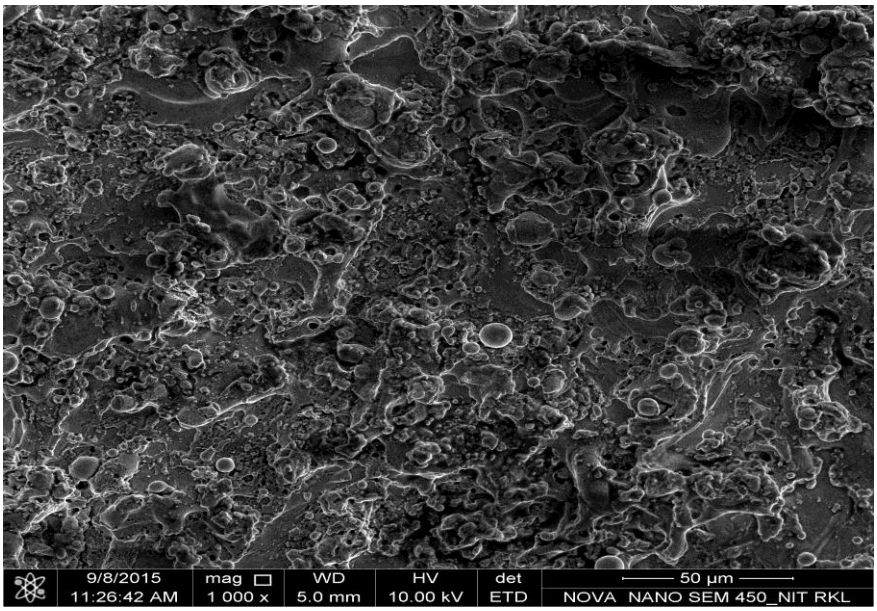


FESEM image of the WEDMed Inconel 718 using Zinc coated brass wire (5000x) (A1B1C1D1E1)

(b)

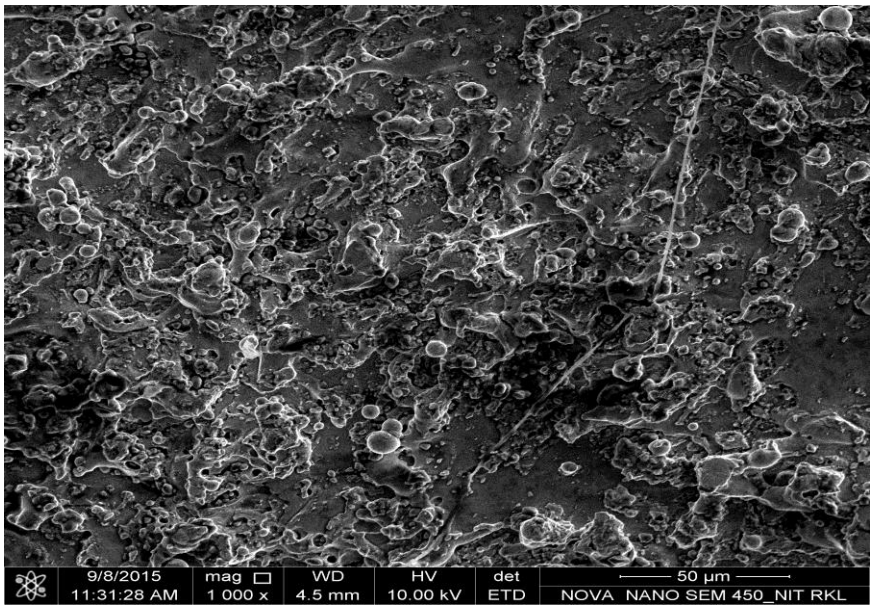


FESEM image of the WEDMed Inconel 718 using Zinc coated brass wire (5000x) (A2B3C1D2E2)

(c)

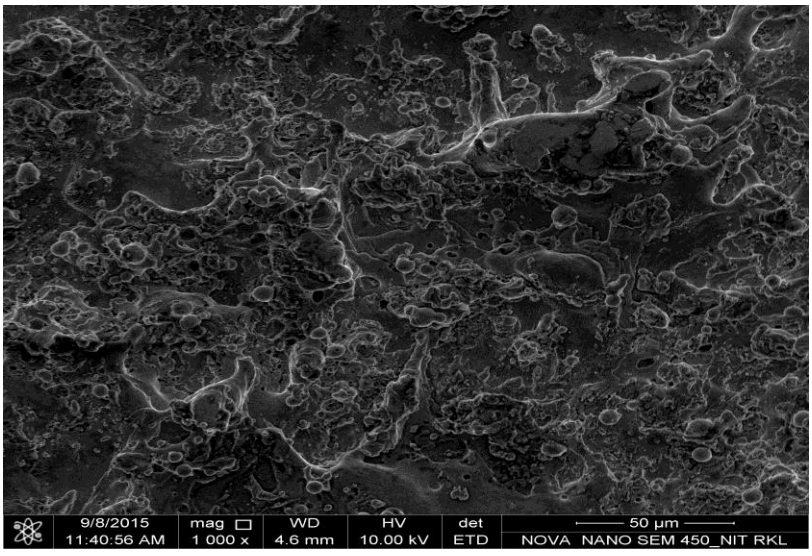


FESEM image of the WEDMed Inconel 718 using Zinc coated brass wire (5000x) (A3B3C2D1E3)

Figure 4.19: FESEM images of the machined surface of WEDMed Inconel 718

Figure 4.20(a-c) show the micrograph of Inconel 718 by Field Emission Scanning Electron Microscope (FESEM) (NOVA NANO SEM 450). Less number of craters and spherical shape particles were formed due to lower, taper angle ($10^{o}$), pulse on time (28 µs), wire speed (95 mm/s), wire tension (8 N) and discharge current (13 A) ( Figure. 4.20 (a)). Due to lower pulse-on

time and discharge current, the machined surface is impinged with less electrical discharge and may result in improved surface finish. Increasing the discharge current and pulse-on time (Figure 4.20 (b)), craters size, spherical shape particles and deterioration of surface roughness were found increases. These may be the places where individual discharge energies are able to infiltrate deep into the workpiece. It is possible that a high energy pulse vaporizes a large amount of metal on the initial discharge, taper angle ($14^o$), pulse on time (32 µs), wire speed (95mm/s), wire tension (10 N) and discharge current (14 A).

From Figure. 4.20 (c), at the higher discharge current (14 A), the impact of discharge energy on the surface of work piece becomes greater, and thus, resulting erosion leads to the increase in deterioration of surface finish. Some large molten particles are protruding and completely dislodged from the surface, which may happen due to higher pulse on time (30µs), discharge current (14 A) and modified flushing ability of zinc coated brass wire. Some micro spherical shape particles are observed which may be due to surface tension of molten material.

In this investigation, attempts have been made by GWO algorithm, to determine the optimal machining parameters settings in view of different process performance which yields in the context of WEDMed of Inconel 718. Initially attempts have been made for considering individual responses feature like angular error and surface roughness respectively. After the next step, aforesaid aggregated all the responses features to obtain the combined objective functions (Z) and finally optimized using GWO. Its results have also been compared with GA. From the results of GWO and GA, it has been observed that GWO showed better performance compared to GA.

### 4.2.7 Concluding Remarks

In this work, focuses on influences of process parameter in WEDM of Inconel 718 along with optimization of machining parameters are given. The mathematical models have been developed by using non-linear regression analysis for analysing the effect of process parameters such as such as Taper Angle, Pulse on time, Wire speed, Wire tension and Discharge Current. Angular error and surface roughness have been considered for appraisal of machining performance characteristics during taper cutting process. ANOVA tables have been used to justify the validation of the developed mathematical models (objective functions). The feasibility of the relatively new optimization technique called Grey Wolf Optimizer (GWO) has been tried.

Although the approach is applied to get optimal parametric combination, it can applied in any complex taper cutting for developing the process model.

# Chapter 5

# 5. Numerical thermal model for multi spark using WEDM operation

## *5.1 Coverage*

In the present study developed a thermal model using Finite Element Model (FEM) for the Wire EDM on the Inconel 718 as workpiece has been developed. An axisymmetric thermal model has been developed based on realistic assumptions using transient Gaussian heat flux distribution, time and energy-dependent spark radius to predict the thermal profile, Material Removal Rate (MRR), and residual stress. The MRR model has been validated with the experimental results. The overlapping approach has been adopted for solving the multi-spark problem. This is easy with co-relate with the experiments results.

## *5.2 Introduction*

In this demanding world by advanced technologies the WEDM has played an important role in non-traditional machining process, widely used in defenses, space, automotive industries. WEDM is a thermal erosion process whereby a desired shape and size is acquired using sparks. Material is removed from conductive material immersed in dielectric by a series of arbitrarily recurring sparks between wire tool and the workpiece. Furthermore to get high degree of accuracy and good surface finish make WEDM valuably.

Several studies have been carried out to determine optimal parameter setting for good surface finish on EDM process [134], [135], [136]. The literature on numerical modelling of WEDM is categorized as experimental and numerical or analytical modelling [137]. This present work is focussed on numerical modelling, the literature reports various two-dimensional heat flow models those have been discussed here.

Erden et al. [138] reported that a theoretical hypothesis to predict the behavior of materials for different energy function and obtained and optimum energy function for achieving maximum MRR. Azhiri et al. [139] have modeled the effect of process parameters such as pulse-on time,

pulse-off time, discharge current, gap voltage, feed rate and wire tension on surface roughness as process responses. Giridharan et al.[96] proposed the model for predicting the crater diameter based on anode erosion using wire electrical discharge turning (WEDT). Lok et al. [65] have reported that surface roughness and cutting have been decreasing with decrease pulse-off time. the surface roughness increasing with in pulse-on time, discharge current, wire tension, voltage, capacitance and feed rate. Tosun et al. [140] studied the effect of pulse-on time, dielectric pressure voltage and wire speed on crater depth and diameter of the wire. It has been reported that larger crater formation on wire takes place with increase in pulse-on time, wire speed and voltage and decreases with higher flushing pressure.

Salah et al. [141] developed a thermal model considering Gaussian-distributed heat source for EDM process. Marafona et al. [142] have developed an electro-thermal model based on joule effect using FEM. The numerical model have been compared with experiments [143].

Luo , Puri et al. and Han et al. [144], [75] ,[108] have modeled the wire supposing as structural beam with an equivalent force generated due to plasma channel acting on it. The stresses are developed on the wire due to the process parameter, wire vibration etc. Lastly error has been estimated during machining profile due to deformation

Banerjee et al. [145] estimated thermal profile of wire using finite differential method (FDM) for single spark. The modelling based on heat generation and convection heat transfers were taken into account with a constant convection heat transfer coefficient. Lastly included the multi-sparks with spark location selected randomly were modeled . Saha et al. [146] developed thermal model of cylindrical wire and solved the three dimensional transient heat transfer distribution with single spark for wire electrode. Han et al. [110] develop thermal model of cylindrical wire and solve the three dimensional transient heat transfer distribution with single spark for wire electrode. Das et al. [147] developed the thermal model and vibrational model for micro WEDM for single spark. Lastly, estimate with the multi-spark model for wire erosion rate was developed.

Lui and Guo [148] studied current modeling methods of EDM for single discharge. From the single discharge simulation is to predict stress due with the experimental. New modeling method accounting for massive random discharge was developed to simulate residual stress in die sinking EDM of the ASP 23 tool steel. Antar et al. [149] reported the high tensile residual stress

on the surface and low fatigue life on Udimet 720 using WEDM operation. Klink et al. [150] pointed out the residual stress distribution in the subsurface of ASP23 steel machined by WEDM. Reported result showed a high tensile residual stress within 30μm. Yang [151] used a molecular dynamics approach to simulate residual stress on Copper using EDM operation. Shabgard [152] develop a sequentially coupled model using ABAQUS to predict residual stress AISI H13 using EDM process.

From the literatures review it has been seen that many of research have been conducted on computation of the temperature distribution profile inside the wire electrode. Few amounts or No work has been reported on the estimate the temperature profile and residual stress on Inconel 718 using WEDM process. In this present study, crater formation on Inconel 718 to estimate material removal rate, thermal characteristics and residual stress on the workpiece has been investigated. No work has been reported on the multi-spark modelling and their effect on material removal rate and residual stress on Inconel 718 using WEDM process.

## 5.3 Theoretical model for predicting crater volume and erosion energy

### *5.3.1 Anode erosion model*

During the machining time of WEDM the spark process (discharge process), evaporate a very small amount of material from the workpiece gets evaporated. As number of sparks increases, a desired amount of material is removed. In the machining time the energy between wire and the workpiece is transformed into heat energy. In the erosion time, process parameter is discharge energy. It is required to find a correlation between erosion at the wire and the energy inputs at the anode and cathode zones, with due consideration to the latent heats of change of state. The assumptions in the analysis are as follows for predicting crater volume [96].

1. The analysis is made for a single spark.
2. The sizes of pulses are assumed to be normal and energy required to form a crater is same for all the pulses.
3. Discharge energy going to the workpiece is constant during pulses
4. The heat generated during discharge is transmitted into the workpiece by conduction. Neglecting other than heat transfer coefficients.

5. The chemical and physical properties of the workpiece is neglected during the phase change.
6. The workpiece is assumed to be homogeneous and isotropic
7. Initial temperature of the workpiece is assumed as 298K.

### *5.3.2 Thermal modeling using finite element method (FEM)*

In the WEDM process, the wire and workpiece are immersed in the dielectric (i.e., distilled water), and separated by a small gap, that gap control by the CNC program. A pulse voltage is applied between the wire and the workpiece in the presence of flushing pressure to melt the workpiece by the thermal process. Meanwhile, the material is removed by vaporizing explosion. When the electrons and positive ions reach the anode and cathode, they give up their kinetic energy in the form of heat [153]. In the WEDM process, the erosion mechanism is same as the of EDM process, there is only difference in the wire electrode is continuously travelling is used as the tool. However, in the WEDM process, the series of pulses are of short time with a highly transient discharge current [154]. For the thermal modeling of WEDM process, the heat transfer mode has assumed through convection process. For the predicting the crater volume the following prediction has made.

1. The heat source is assumed by the Gaussian flux distribution. The model has been assumed to be axisymmetric.
2. The insulated boundary is assumed of the workpiece which is far from the spark channel.
3. The flushing is assumed 100%.

### *5.3.3 Governing Equation*

This is the equation for calculation of transient temperature distribution with in workpiece. Heating of workpiece due to a single spark is assumed to be axisymmetric. The differential governing equation of thermal diffusion differential equation in an axisymmetric model is governed by the following

$$\rho C_p \left[\frac{\partial T}{\partial t}\right] = \left[\frac{1}{r}\frac{\partial}{\partial r}\left(K_r \frac{\partial T}{\partial r}\right) + \frac{\partial}{\partial z}\left(K_r \frac{\partial T}{\partial z}\right)\right] \quad (5.1)$$

where ρ is density, $C_p$ is specific heat, Kr thermal conductivity of the workpiece, T is the temperature, t is the time and r & z are coordinates of the workpiece.

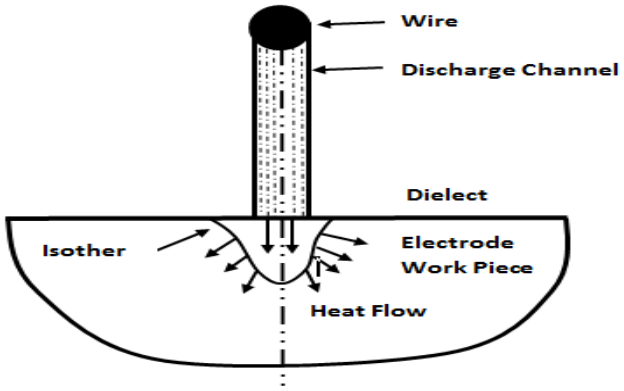


Figure 5.1 Spark channel configureration

### *5.3.4 Heat source*

The important parameters which need to be considered for predicting the crater volume are the fraction of heat input to the workpiece, type of the heat source and the physical properties of the material. Most of the researchers, [140, 155, 156] have considered had considered uniformly heat source in between a spark.

In the present work, a Gaussian heat distribution Equation 5.2 is assumed by [157] for better results over conventional cylindrical heat flux for die sinking EDM. This equation is modified to consider the effect of wire feed rate. An elliptical Gaussian heat flux distribution by [137] has been used in this work on WEDM (Equation 5.3)

$$Q(r)=\frac{4.57F_cVI}{\pi R^2}\exp\left(-4.5\frac{r^2}{R^2}\right) \tag{5.2}$$

$$Q(r)=\frac{4.57F_cVI}{\pi R^2}\exp\left(-4.5\left(\frac{r_x^{\,2}}{R_x^{\,2}}+\frac{r_y^{\,2}}{R_y^{\,2}}\right)\right) \tag{5.3}$$

where r is the radial distance from the axis of the spark, R is the spark radius, V is the voltage and I is the current and $H_i$ is heat input on workpiece.

### *5.3.5 Energy Distribution Factor*

During the WEDM, the discharge power is determined by the single discharge energy multiplied by discharge frequency. Figure 5.2 depicts the typical voltage and electrical current waveform. The current produced by the pulse generator has an equilateral triangle shape. The single discharge energy ( $\Delta E$ ) is given by the following equation [158]:

$$\Delta E = \int_{Pulse\_duration} \nu(\tau) i(\tau)\, d\tau = V_w \times K \times T_{on}^2 \tag{5.4}$$

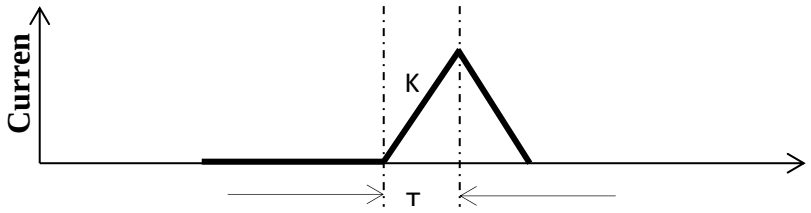


Figure 5.2 waveforms of voltage and current of a single discharge

Where, the rising sloping of the electrical current is K and the average working voltage is $V_w$

### *5.3.6 Total Energy Distribution*

Another parameter is energy distribution. It is important in the thermal modeling analysis of WEDM process. Joshi et al. [159] have suggested an energy distribution of 1-8% for workpiece and 18.3% for tool material using AISI W1 tool steel and graphite as the workpiece and tool material. In the present model, an energy distribution of 2-5% for workpiece and 3-8% for wire material has been recommended by employing Inconel 718 and brass as the work and tool material respectively comparing the experimental and numerical analysis.

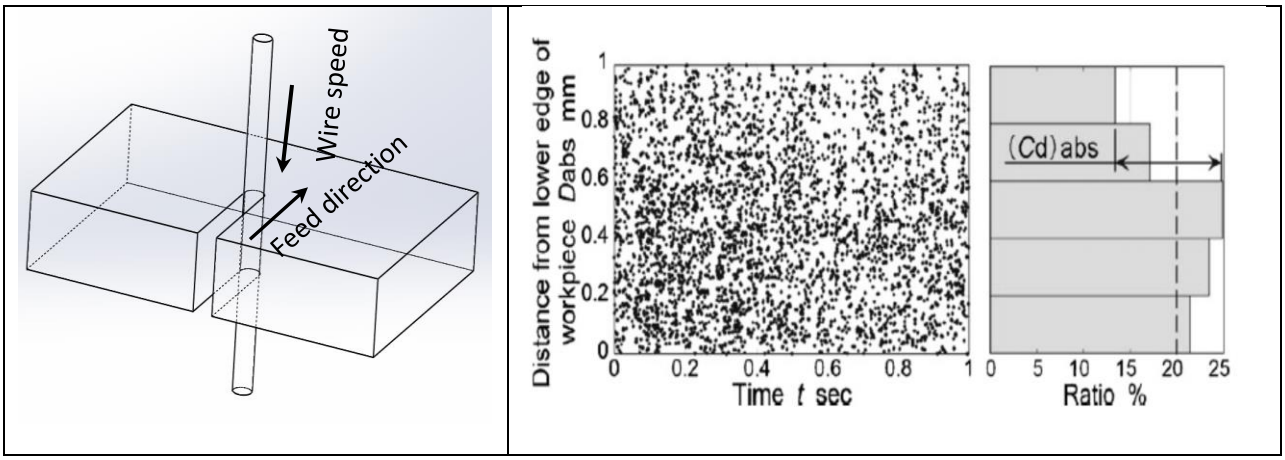


Figure 5.3 a) Wire EDM model b) Absolute spark location for 50V [160]

### *5.3.7 Sparks Location*

Okada et al. [160] investigated the effect of machining parameters, such as servo voltage, pulse-on time, wire running speed and other to predict the spark location along the length of the wire. Figure 5.3(b) shows absolute spark location with difference between the maximum frequency and the minimum one calculated from the histogram in order to quantitatively discuss the discharge concentration. Banerjee et al. [161] observed that the sparks occurred in a cluster in WEDM process. The crater is formation due to spark and some material gets deposited on the crater formation. This region at the inter-electrode gap very much small and probability of the next spark occurring near the periphery of the previous spark craters is more. Figure 5.4(a) shows the view of the spark on the workpiece along with the line Z-A-B-Y. AB is the initialization of the spark formed, the possibility of subsequently spark in predicted to be observed in the near region. The next subsequent spark is predicted on region ZA or BY.

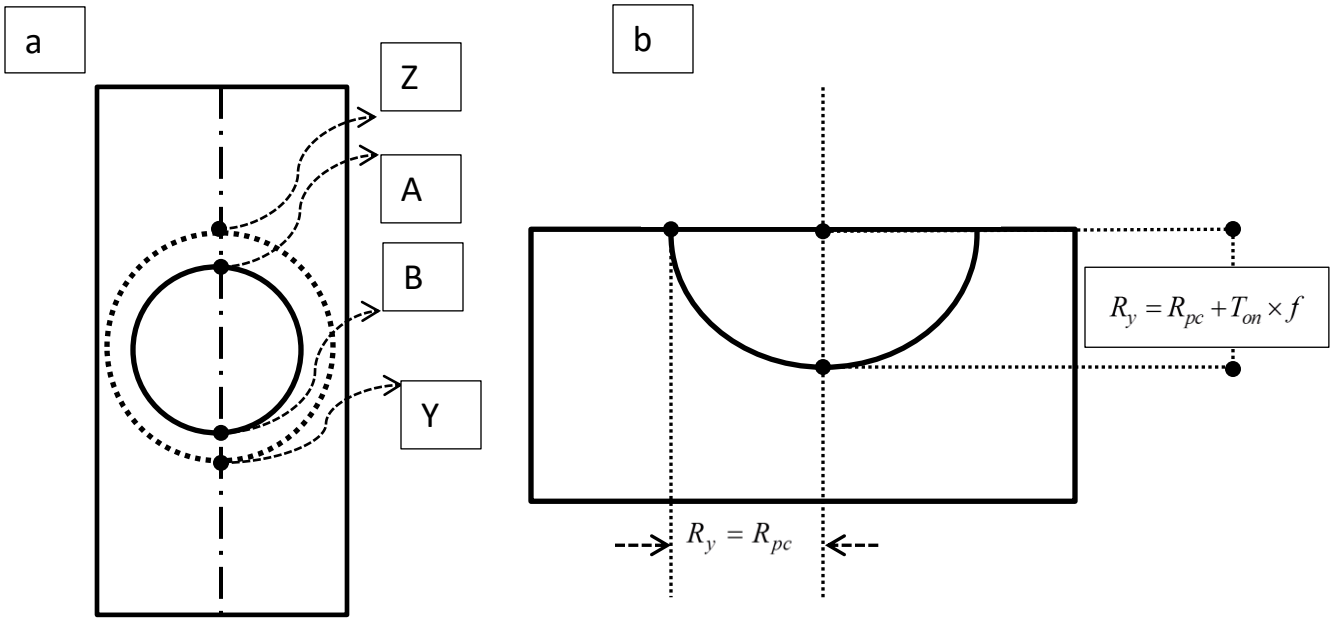


Figure 5.4 (a) location of subsequent spark (b) hemispherical footprint of spark. [137]

### *5.3.7 Spark Radius*

It is an important parameter in the thermal modeling of WEDM process. In practice, spark radius depends upon dielectrics, polarity and electrode materials [159], it is very difficult to measure experimentally, because spark radius is for very short pulse duration of in microseconds. During spark time, spark size dose not remain constant, its vary time to time [143]. According to Moulton [162] the spark theory on a wire EDM is basically the same as that of the vertical EDM process. In wire EDM, the conductive materials can be machined with a series of electrical sparks, which are produced between an accurately positioned moving wire (electrode) and the workpiece. High frequency pulses of AC or DC is discharged from the wire (electrode) to the workpiece with a very small spark gap through an insulated dielectric fluid. In particular, this radius is called the equivalent heat input radius, and it can be expressed as a function of the pulse current and the pulse-on time as shown below [134]

$$R(t) = 2.04 \times I^{0.43} \times T_{on}{}^{0.44} \tag{5.5}$$

Where $I$ is discharge current and $T_{on}$ is discharge time.

### *5.3.8 Boundary condition*

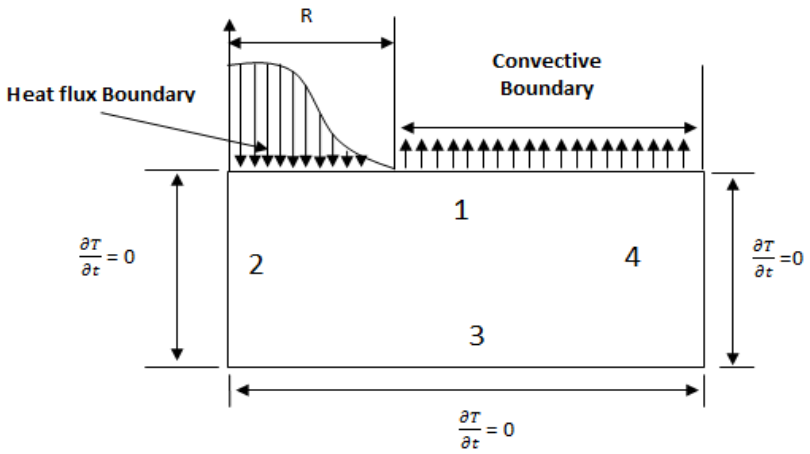


Figure 5.5 An axisymmetric model for the EDM process simulation

The workpiece is axisymmetric about z-axis, and small half-plane is cut from the workpiece with negligible thickness. The considered workpiece domain is shown in Figure. 5.5. The heat flux for a single spark is applied on the surface 1 up to R (spark radius). On the remaining surface 1, the convection heat transfer takes place due to the cooling effect caused by the dielectric fluid. As the surfaces 4 and 3 are far from the spark radius and also the spark has been made to strike for a very small amount, so no heat transfer conditions have been assumed on that surface. For surface 2, which is axisymmetric, the heat flux has been taken as zero.

1. For boundary surface 1

   Up to spark radius (R):

   $$K \frac{\partial T}{\partial z} = Q(r).$$

   Beyond Spark Radius R

   $$K \frac{\partial T}{\partial z} = h\,(T - T_0)$$

2. For boundary 4, 3, 2

   $$\frac{\partial T}{\partial z} = 0$$

where, h is the heat transfer coefficient between the workpiece surface and dielectric, Q(r) heat flux, $T_0$ is the initial temperature which is room temperature and T is Temperature.

### *5.3.9 MRR Efficiency*

The MRR efficiency is total molten material removed from the molten crater at end of the pulses, while the unremoved material solidifies vicinity in crater. Many of researchers, considered with 100% material removed in there modelling ([157], [163]). But in practically it is not possible to get or achieve 100% material removal efficiency because of its stochastic nature of machining process of EDM. The material removal efficiency's results for prediction of MRR with compared with the experimental results for electrodes is varied from 2 to 96% [143], from 10 to 20% [164], and from 0.3 to 10% ([165], [166], [167]). In this present work 8% has been taken for the metal removal efficiency.

#### *5.3.9.1 Convective heat transfer coefficient*

The heat transfer phenomenon in the WEDM process is complex and to predict the convection heat transfer coefficient ( $h_f$ ) is difficult for modeling. Many researchers have predicted the $h_f$ of 10000 W/m$^2$K, for good results [145], [168].

### *Steps of simulation for crater formations by APDL model*

Thermal modelling steps are as follows

- A two dimensional model of size 0.5 ×0.3 mm is developed for analysis.
- Model is created using PLANE 55 thermal solid element.
- Define workpiece material properties with fine mess.
- Initial temperature of the workpiece material is chosen as room temperature (298K).
- Heat flux applied at the spark radius (R) region as shown in Figure 5.5.
- Boundary condition applied as shown in Figure 5.5.
- Read result from the last is used set for nodal solution.
- Finish

### *5.3.10 Single spark model*

This numerical model on the workpiece based on single spark of dimension is 0.5mm ×0.3 mm. MRR ($mm^3$/min) is furnished using Equation 5.6.

$$MRR = \left( \frac{60 \times C_{Vol}}{T_{on} + T_{off}} \right) \tag{5.6}$$

where $C_{vol}$ is the material removed per discharge pulse, $T_{on}$ is discharge duration and $T_{off}$ is the discharge off time.

### *5.3.11 Multi-spark model*

The MRR occurred by series of sparks in WEDM process. The first sparks occurs, is assumed on the edge of the workpiece with flushing to remove the eroded material. The flushing also removes the debris and cools the region between the wire and the work piece during the pulse-off time.

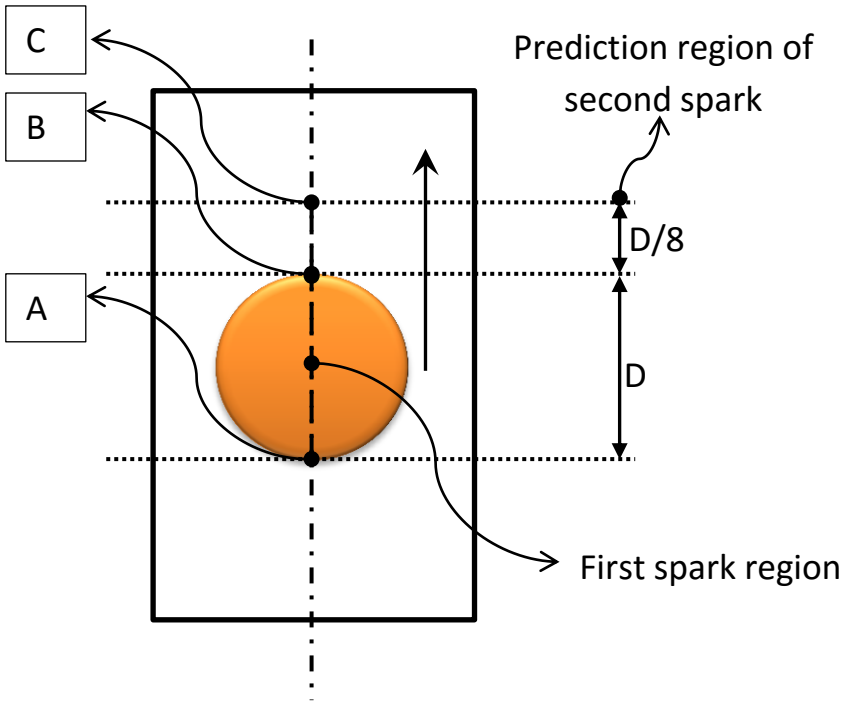


Figure 5.6 Region of second spark [137]

To estimate the exact location of second spark is very difficult task. Some researchers are observed that sparks occured in cluster Kunieda et al. [166] and Banerjee et al. [161]. assumed next spark occuring on the just on the periphery of the first spark.

Figure 5.7. indicates the assumed second spark occurs on the region of B and C. The region of A and B are assumed the first spark has been generated. D is the assumed diameter of first spark and assumed region B and C are located at the distance of D/8 [137].

During the second spark occurred, the crater formation would be overlapping on the first spark. Due to the overlapping, the MRR is lesser then the first spark. In practically, MRR occurs because of many over lapping craters are formed on the workpiece. Hence, MRR after the second spark is taken as an estimate for process.

To validate this model, an experiment has been conducted to validate this model. Inconel 718 has been chosen as workpiece.

### *5.3.12 Couple Thermo-Mechanical Approach*

The couple thermo-mechanical analysis is performed to simulate the residual stress. The coupled thermo-mechanical analysis is performed to simulate the residual stress. Figure 5.6 shows the boundary condition. All side surfaces and bottom surface are fixed to zero. The thermos-mechanical analysis is completed; the residual stress field is obtained.

#### ***Steps of simulation for Residual Stress by APDL model***

Thermal modelling steps are as follows

- Killing the element which is above the melting the workpiece.
- Apply thermal to structure analysis
- Apply boundary conditions for structure analysis in Figure 5.6
- Finish

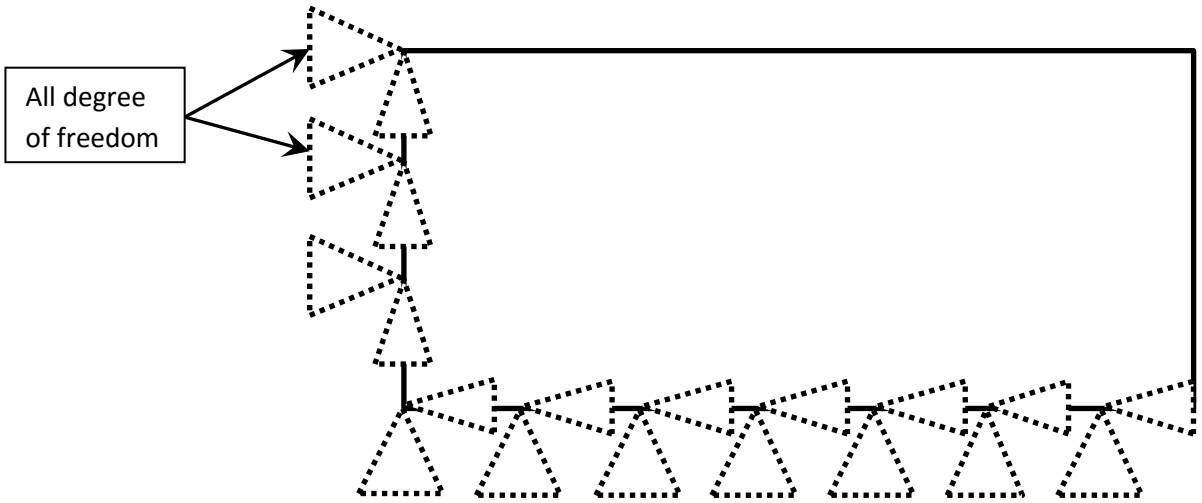


Figure 5.7 Boundary condition of structure model

### *5.3.13 Experimental Details*

To estimate the thermal model for MRR and Residual Stress of WEDM, the process parameters considered in this present work are pulse-on time, discharge voltage, current, wire speed and duty cycle. Pulse-off time, wire tension, flushing pressure and feed rate are have been kept fixed as 50μs and 1.2 bars, respectively, throughout the experiments. In this complexity process, it's very difficult to estimate the model of wire vibration and recast layer.

To validate the numerical model by ANSYS, it is compared with the experimental study using Table 5.2. Table 1.2-1.4 shows (Chapter 1) the properties of Inconel 718 as workpiece.

The experiments were furnished on a CNC WEDM machine. The manufacturer is AGIE, SWITZERLAND with axis travels as 350×250×256mm, the maximum workpiece dimension as 750mm×550mm×256mm, and the measuring resolution as 0.0001mm. The dimension of the work material (50mm × 20mm × 1mm) was used. A workpiece of 5 mm thickness and a 0.20 zinc coated brass wire were used in the experiment. During the experiment 15mm length was cut continuously.

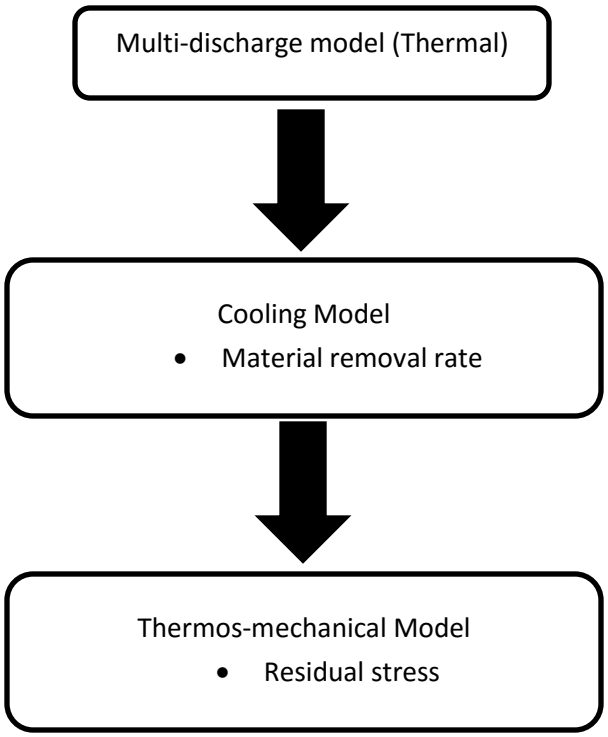


Figure 5.8 Methodology for residual stress modelling in WEDM

### *5.3.14 Results and Discussion*

The results are obtained for single spark and Inconel 718 as a workpiece. Temperature distribution in the workpiece has been shown in Figure. 5.8.

Table 5.1 Process parameters used to simulate the WEDM process

| Code | Parameters | Value | Units |
|---|---|---|---|
| A | Voltage | 60, 70, 80 | [V] |
| B | Discharge Current | 11, 15, 19 | [A] |
| C | Pulse-on Time ($T_{on}$) | 28, 30, 32 | [µs] |
| D | Wire speed | 80, 100, 120 | [mm/s] |
| E | Duty cycle | 80, 85, 90 | [%] |
| Pulse-off Time ($T_{off}$) | | 50 | [µs] |
| Room Temperature ($T_o$) | | 298 | [K] |
| Co-efficient of heat transfer of dielectric fluid ($h_f$) | | 10,000 | ($W/m^2K$) |

According to the Taguchi quality design of experiment, a $L_{27}$ orthogonal array design table with 27 rows (corresponding to the no of experiment) table was taken for experiments as shown in the Table 5.2. The number of observations under each combination of factors is one.

Table 5.2 Experimental design using $L_{27}$ orthogonal array and comparison of the estimated results with the experimental (**Coded form**)

| Sl. No | A | B | C | D | E | Numerical MRR ($mm^3$/min) | Experimental MRR ($mm^3$/min) | Experimental Surface Roughness (μm) | Numerical Residual Stress (GPa) |
|---|---|---|---|---|---|---|---|---|---|
| 1 | 1 | 1 | 1 | 1 | 1 | 0.023135 | 0.01851 | 2.90 | 1.63 |
| 2 | 1 | 1 | 1 | 1 | 2 | 0.031249 | 0.02260 | 3.03 | 1.69 |
| 3 | 1 | 1 | 1 | 1 | 3 | 0.032324 | 0.02586 | 3.08 | 1.75 |
| 4 | 1 | 2 | 2 | 2 | 1 | 0.032087 | 0.02727 | 3.15 | 1.68 |
| 5 | 1 | 2 | 2 | 2 | 2 | 0.032349 | 0.02828 | 3.05 | 1.70 |
| 6 | 1 | 2 | 2 | 2 | 3 | 0.034039 | 0.02883 | 3.35 | 1.72 |
| 7 | 1 | 3 | 3 | 3 | 1 | 0.030086 | 0.02727 | 3.50 | 1.74 |
| 8 | 1 | 3 | 3 | 3 | 2 | 0.035938 | 0.02875 | 3.48 | 1.78 |
| 9 | 1 | 3 | 3 | 3 | 3 | 0.030939 | 0.02635 | 3.27 | 1.82 |
| 10 | 2 | 1 | 2 | 3 | 1 | 0.028104 | 0.01984 | 3.10 | 1.68 |
| 11 | 2 | 1 | 2 | 3 | 2 | 0.026553 | 0.02124 | 3.11 | 1.73 |
| 12 | 2 | 1 | 2 | 3 | 3 | 0.029023 | 0.02242 | 3.17 | 1.68 |
| 13 | 2 | 2 | 3 | 1 | 1 | 0.029301 | 0.02344 | 3.10 | 1.71 |
| 14 | 2 | 2 | 3 | 1 | 2 | 0.035196 | 0.02976 | 3.20 | 1.74 |
| 15 | 2 | 2 | 3 | 1 | 3 | 0.040283 | 0.03223 | 3.60 | 1.78 |
| 16 | 2 | 3 | 1 | 2 | 1 | 0.039608 | 0.03249 | 3.20 | 1.73 |
| 17 | 2 | 3 | 1 | 2 | 2 | 0.041218 | 0.03297 | 4.13 | 1.68 |
| 18 | 2 | 3 | 1 | 2 | 3 | 0.041866 | 0.03349 | 3.53 | 1.68 |
| 19 | 3 | 1 | 3 | 2 | 1 | 0.029697 | 0.01816 | 3.60 | 1.65 |
| 20 | 3 | 1 | 3 | 2 | 2 | 0.026459 | 0.02117 | 3.60 | 1.69 |
| 21 | 3 | 1 | 3 | 2 | 3 | 0.029649 | 0.02372 | 3.90 | 1.68 |
| 22 | 3 | 2 | 1 | 3 | 1 | 0.031446 | 0.02516 | 3.50 | 1.65 |
| 23 | 3 | 2 | 1 | 3 | 2 | 0.027048 | 0.02164 | 3.40 | 1.72 |
| 24 | 3 | 2 | 1 | 3 | 3 | 0.025799 | 0.02224 | 3.20 | 1.63 |
| 25 | 3 | 3 | 2 | 1 | 1 | 0.025664 | 0.01973 | 4.15 | 1.70 |
| 26 | 3 | 3 | 2 | 1 | 2 | 0.030663 | 0.02613 | 4.20 | 1.72 |
| 27 | 3 | 3 | 2 | 1 | 3 | 0.035133 | 0.03131 | 4.40 | 1.72 |

### *5.3.14.1 Thermal model on Surface*

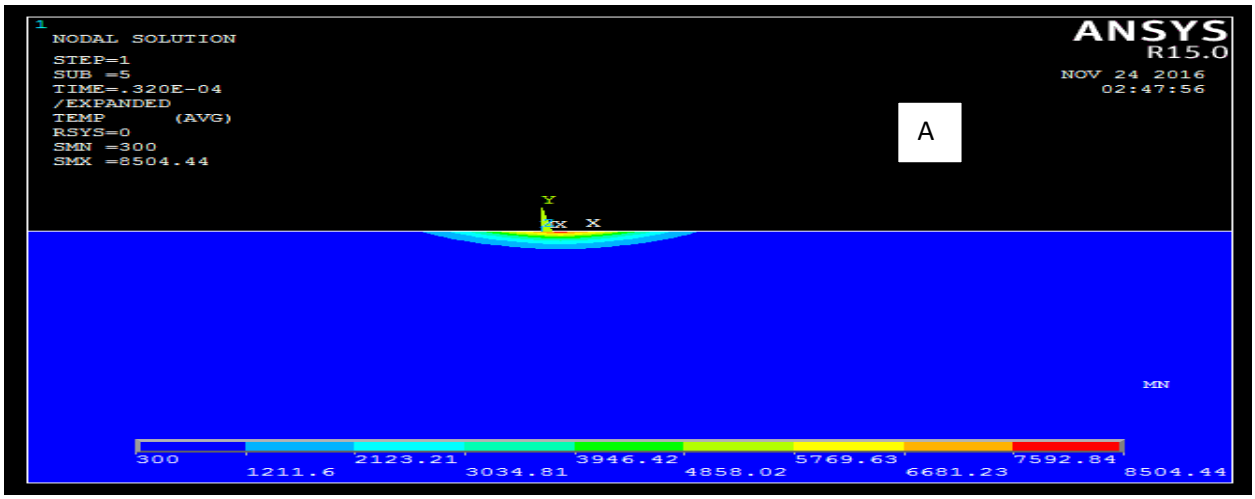


Figure 5.9 Single spark thermal contour of the workpiece (voltage 60V, discharge current 19A, pulse-on time 32µs, wire speed 120mm/s and duty factor 90%)

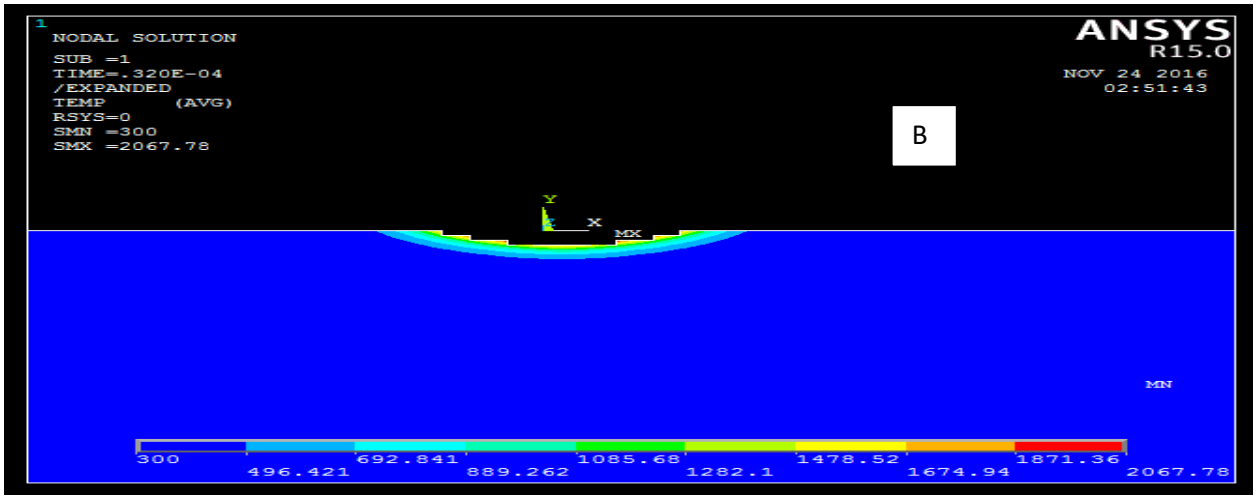


Figure 5.10 Crater profile of the workpiece (voltage 60V, discharge current 19A, pulse-on time 32µs, wire speed 120mm/s and duty factor 90%)

Figure 5.11 depicts representation graphically representation that the maximum temperature has been found on the tip of the workpiece. The temperature is going to decrease, when the workpiece region is far from the heat flux in radial direction.

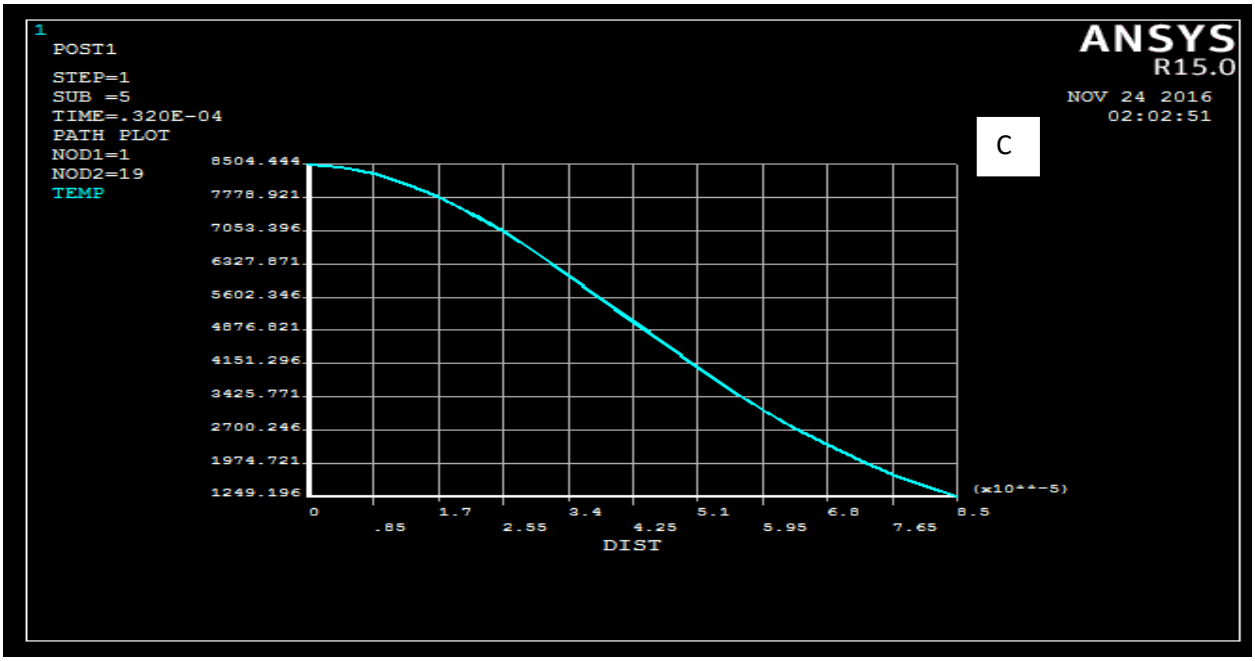


Figure 5.11 Graph obtained from Ansys [Radial crater distance(μm) vs Temperature (K)] (voltage 60V, discharge current 19A, pulse-on time 32μs, wire speed 120mm/s and duty factor 90%)

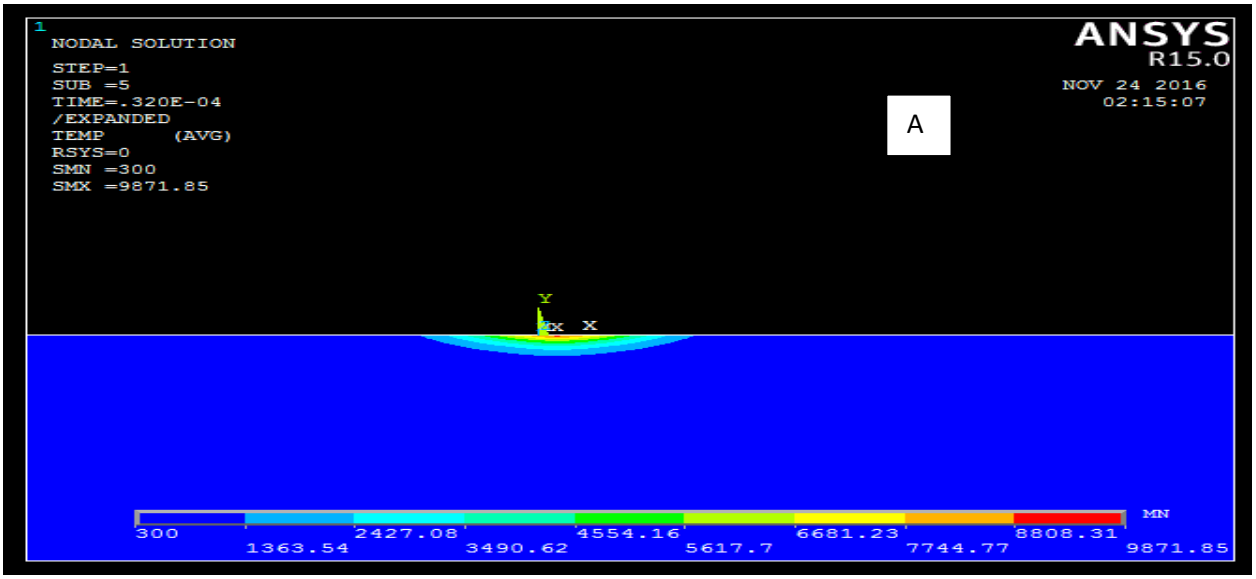


Figure 5.12 Single spark thermal contour of the workpiece (voltage 70V, discharge current 19A, pulse-on time 32μs, wire speed 120mm/s and duty factor 90%)

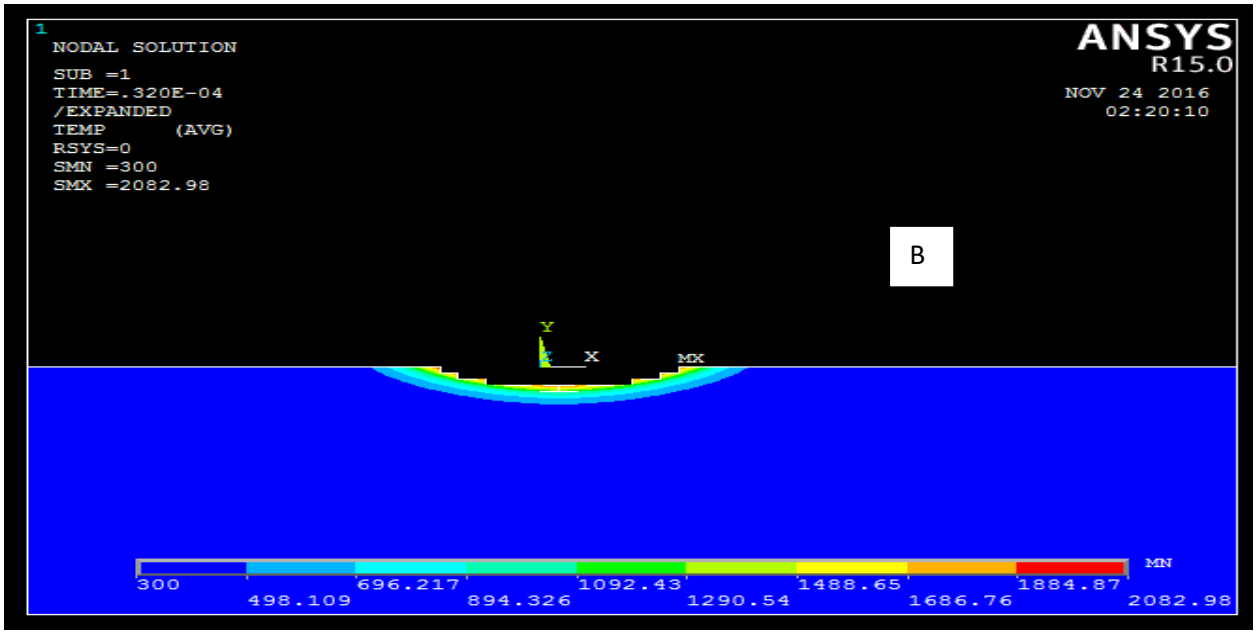


Figure 5.13 Crater profile of the workpiece (voltage 70V, discharge current 19A, pulse-on time 32µs, wire speed 120mm/s and duty factor 90%)

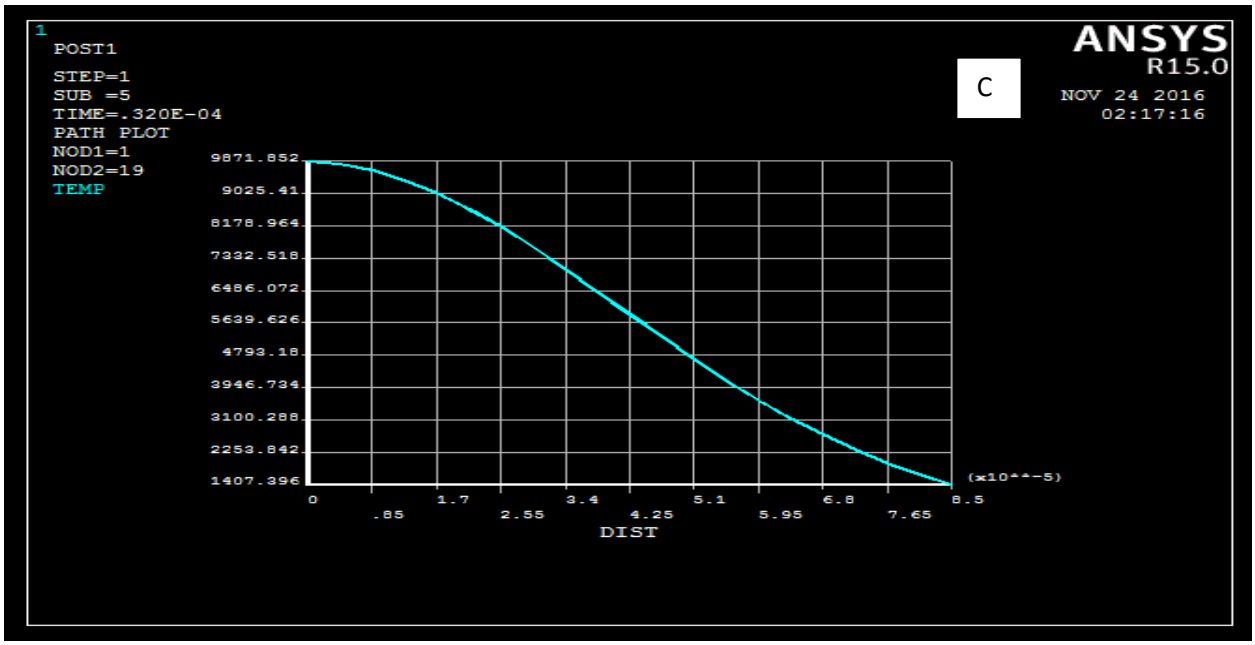


Figure 5.14 Graph obtained from Ansys [Radial crater distance(µm) vs Temperature(K)] (voltage 760V, discharge current 19A, pulse-on time 32µs, wire speed 120mm/s and duty factor 90%)

.

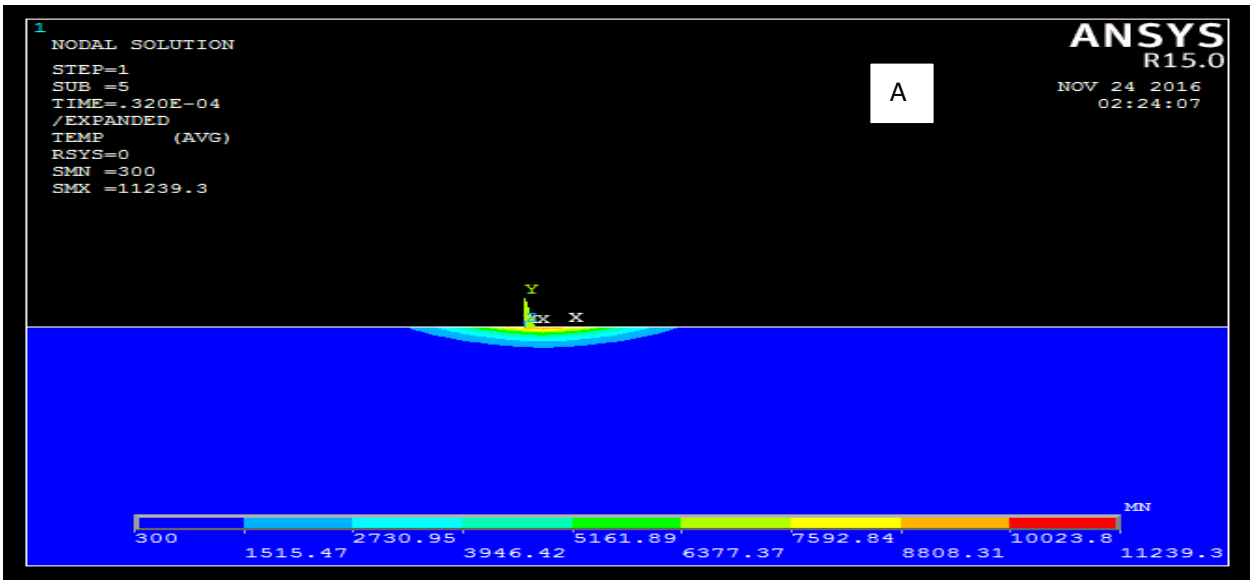


Figure 5.15 Single spark thermal contour of the workpiece (voltage 80V, discharge current 19A, pulse-on time 32µs, wire speed 120mm/s and duty factor 90%).

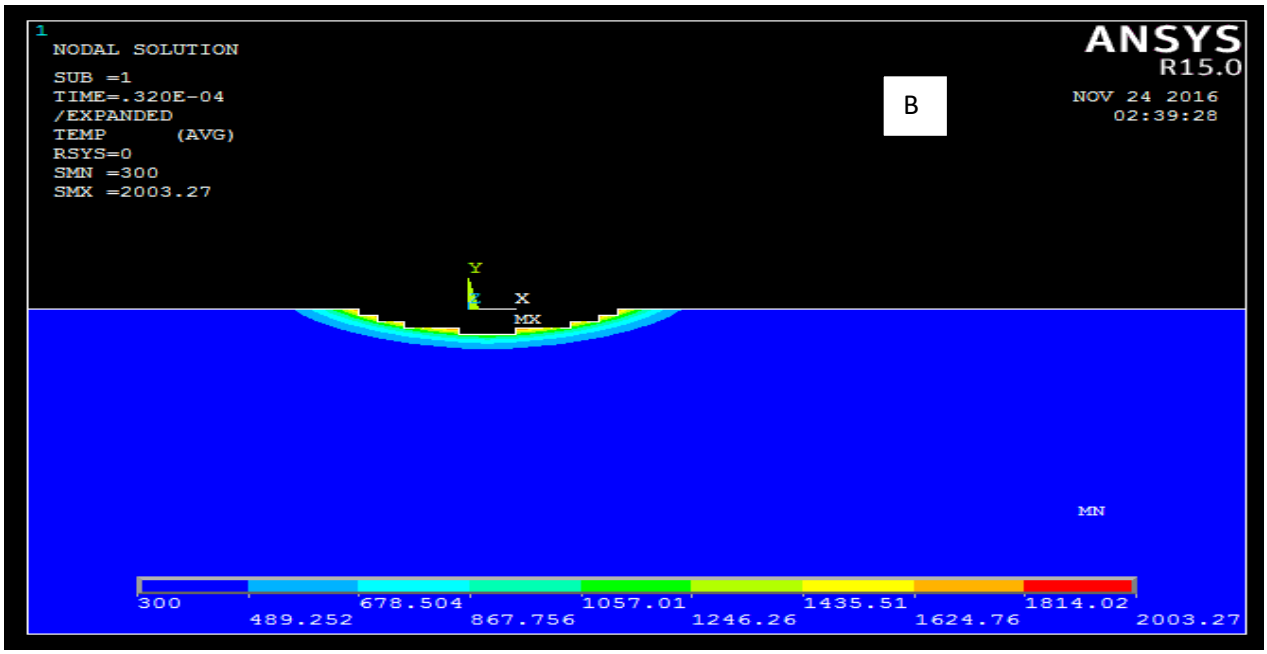


Figure 5.16 Crater profile of the workpiece (voltage 80V, discharge current 19A, pulse-on time 32µs, wire speed 120mm/s and duty factor 90%)

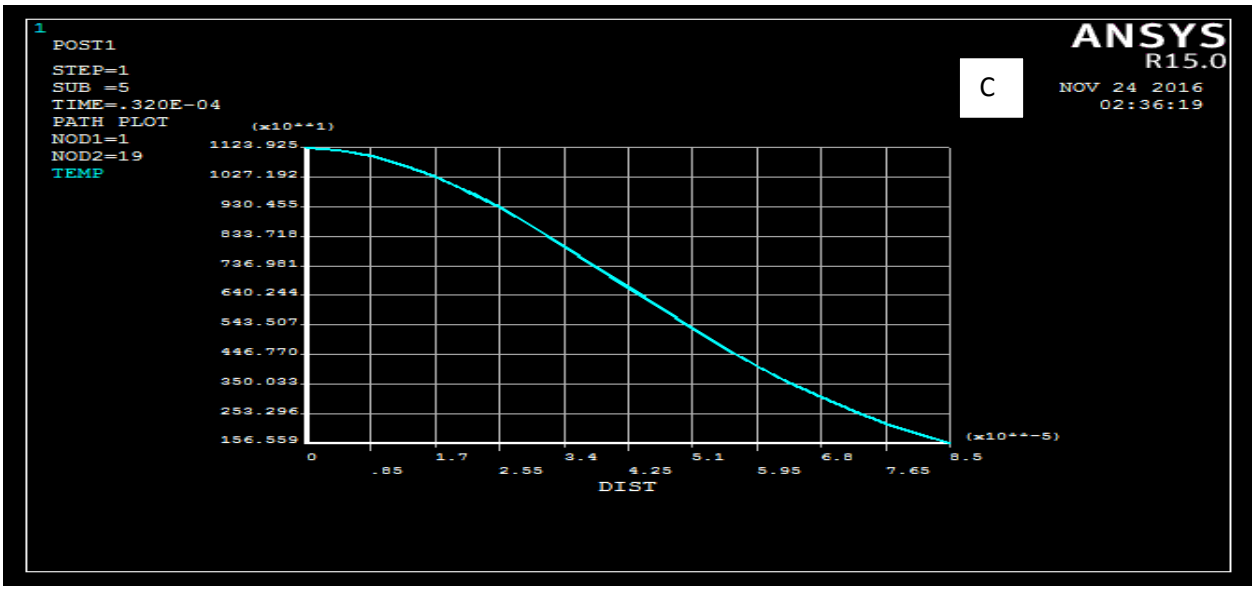


Figure 5.17 Graph obtained from Ansys [Radial crater distance(µm) vs Temperature(K)] (voltage 760V, discharge current 19A, pulse-on time 32µs, wire speed 120mm/s and duty factor 90%)

### *5.3.14.2 Residual stress in the subsurface*

Figure 5.18 shows thermos-mechanical model profile in the subsurface after single discharges. The stress on the workpiece as high 1.68 GPa on the top surface. The high stress obtained with 15µm below the top surface, and then gradually drops down to zero at the depth of 60µm.

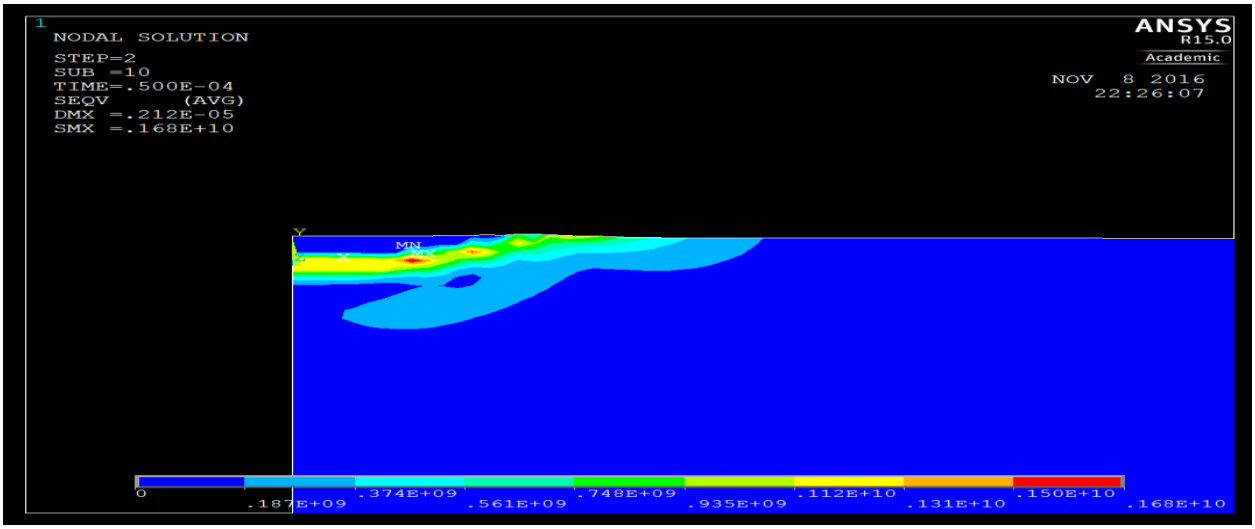


Figure 5.18 Residual stress in radial direction (voltage 80V, discharge current 19A, pulse-on time 32µs, wire speed 120mm/s and duty factor 90%)

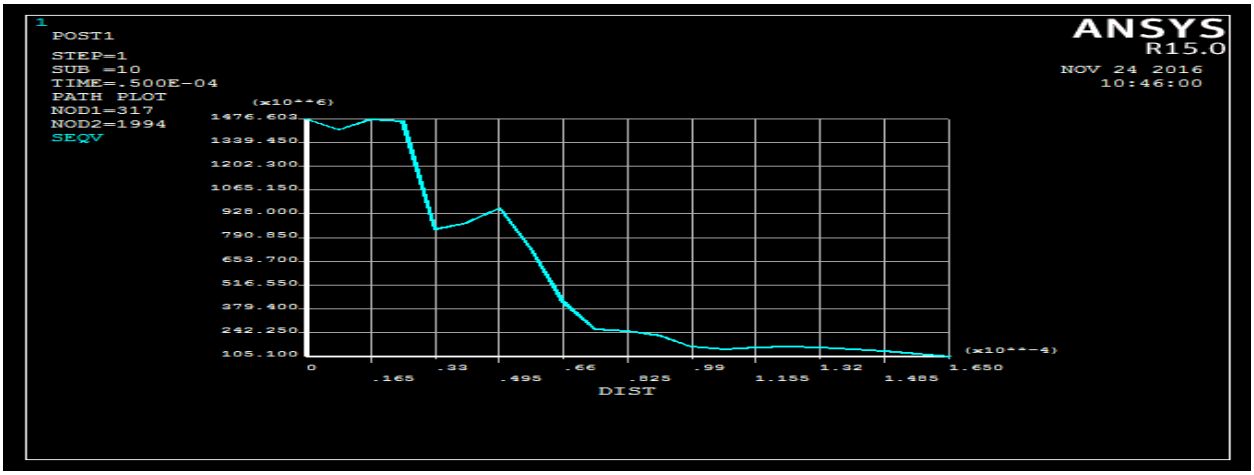


Figure 5.19 Graph obtained from Ansys [Radial crater distance(µm) vs Stress (MPa)] (voltage 760V, discharge current 19A, pulse-on time 32µs, wire speed 120mm/s and duty factor 90%)

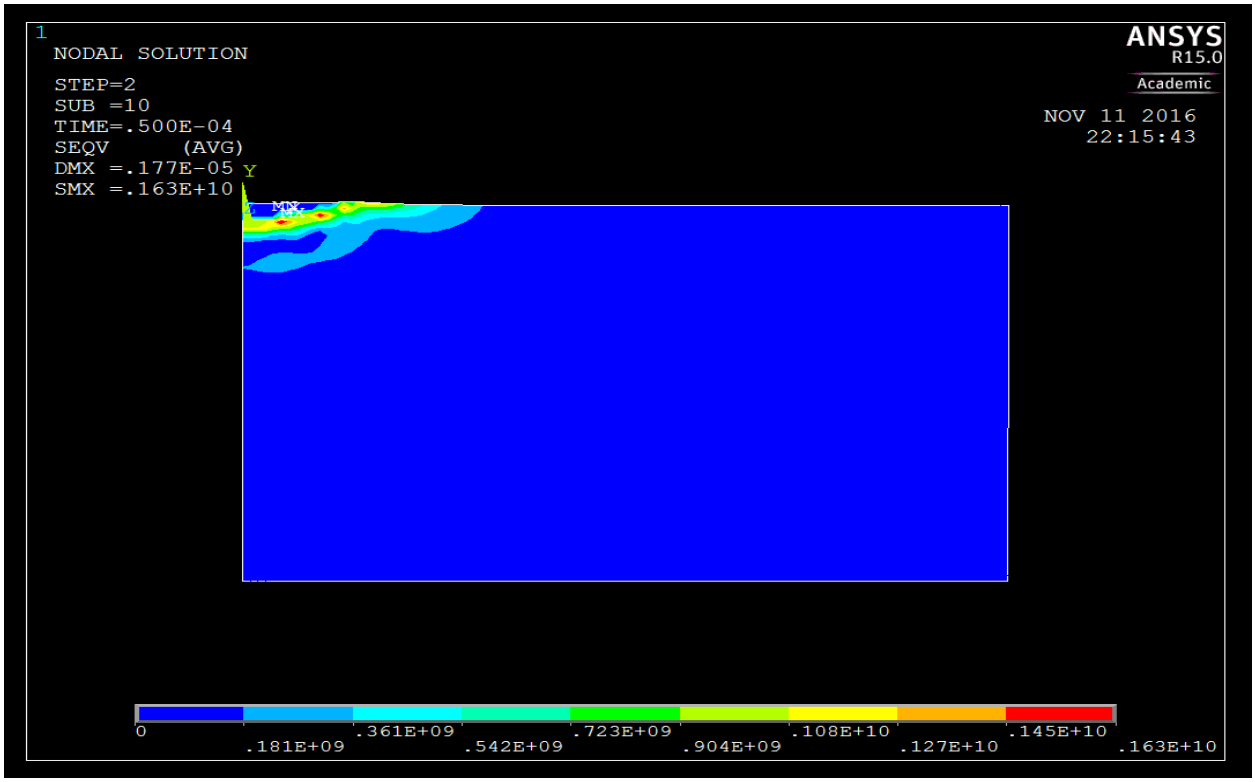


Figure 5.20 Residual stress in radial direction (voltage 60V, discharge current 19A, pulse-on time 32µs, wire speed 120mm/s and duty factor 90%)

Figure 5.19 show the residual stress remaining in the workpiece after the first spark. The compressive stress beneath the crater changes to tensile stress after completion of cooling. The stress is maximum at near the spark and minimum at away the spark region. Figure 5.18 show

graphically representation of process parameter as voltage 60V, discharge current 19A, pulse-on time 32µs, wire speed 120mm/s and duty factor 90%)

### *5.3.15 Parametric Studies*

The parametric studies have been carried out using the multi-spark model to predict the MRR using process parameters such as voltage, discharge current, pulse-on time, wire speed and duty factor.

Figures 5.20-5.21 shows the effect of duty cycle versus voltage and discharge current on MRR. It's seen that MRR is increasing with increase in voltage and discharge current with increase duty cycle. The voltage and discharge current generate more heat and that heat has been responsible of more material removal rate on the workpiece [169].

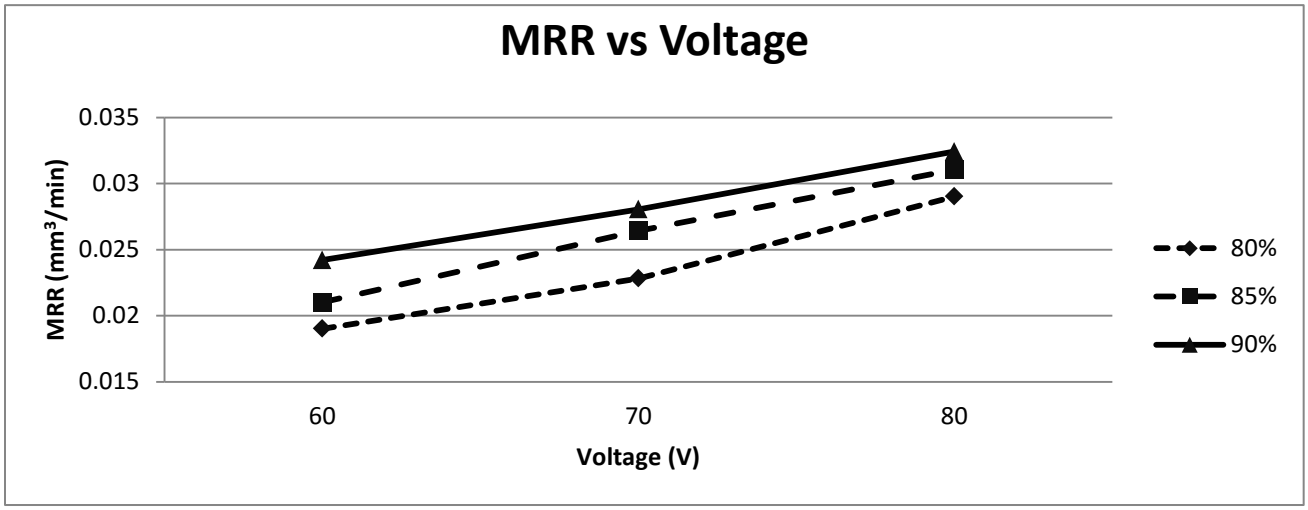


Figure 5.21 MRR vs Voltage

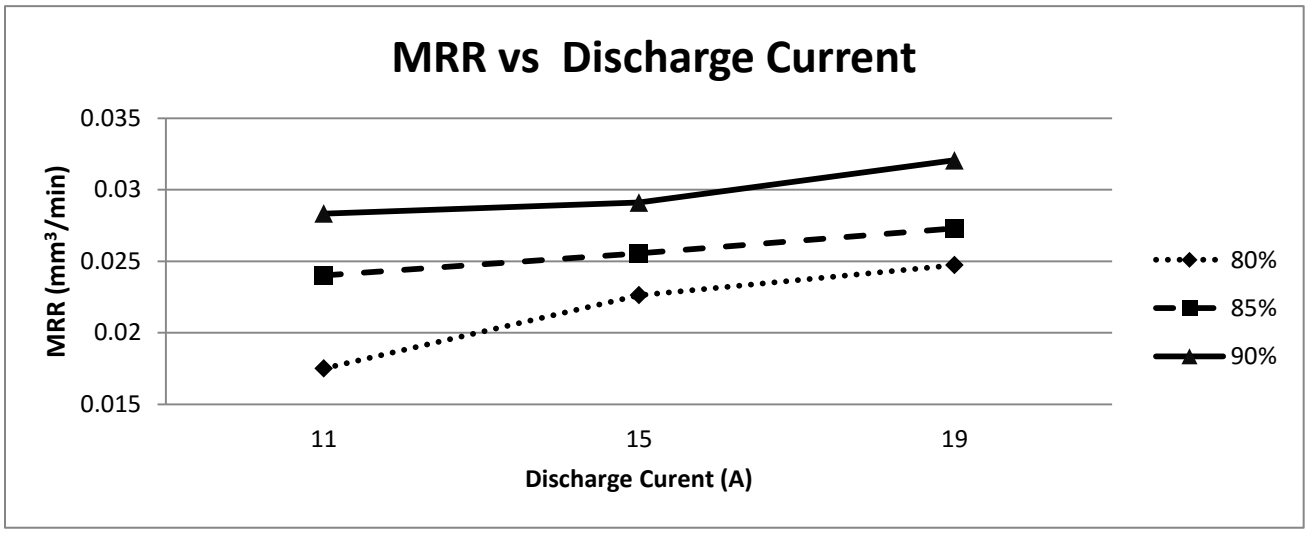


Figure 5.22 MRR vs Discharge current

Figure 5.22 shows that the effects the wire speed on MRR. With increase in the wire speed, the MRR also increases. Wire speed is a very important process parameter for increasing the MRR, because it's avoiding the localized high temperature which results in improving the cutting speed as well as prevent the wire brakeage. Wire speed is the very important parameter for FEM models in WEDM.

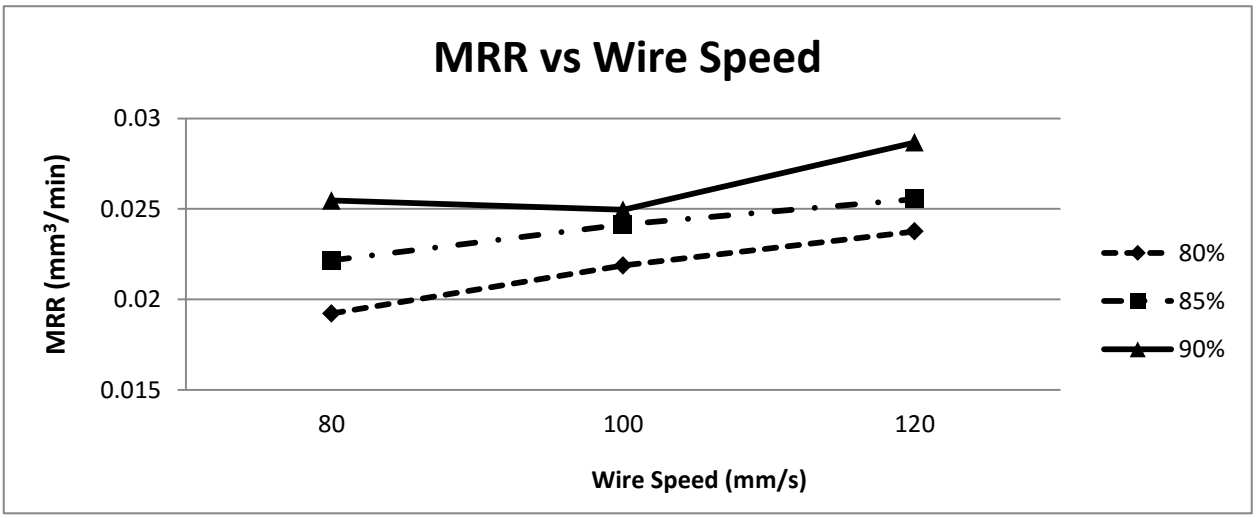


Figure 5.23 MRR vs Wire Speed

Figure 5.23 depicts that variation of MRR with pulse on time. MRR is increasing with increase in pulse-on time. Higher duty factor with pulse-on time increases the number of sparks per unit

time which maximizes the MRR. For the roughness cutting application, higher value of duty factor and pulse-on time can be used

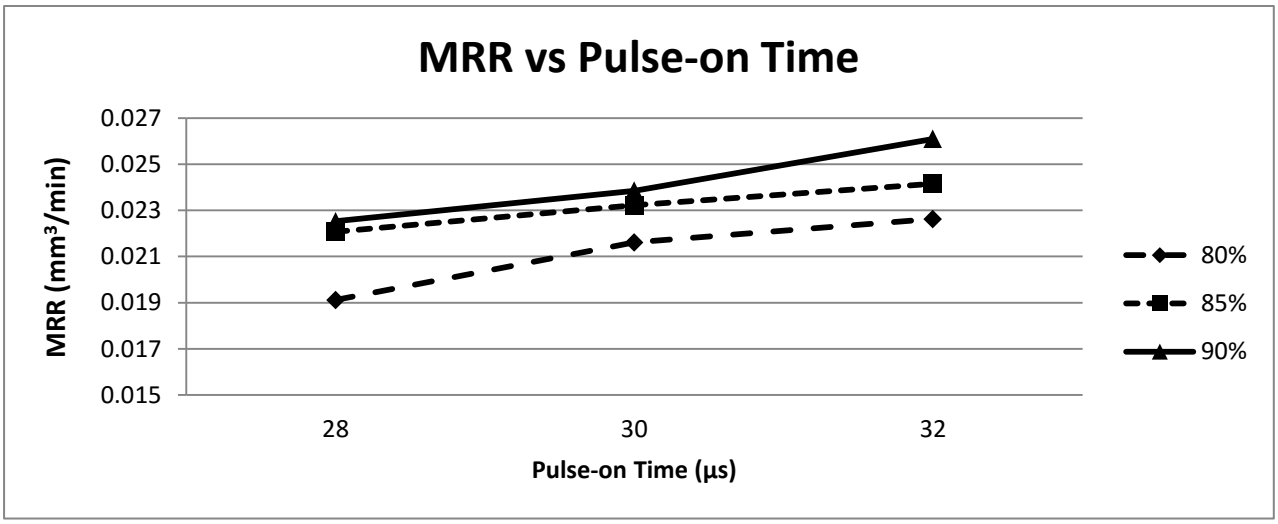


Figure 5.24 MRR vs Pulse-on time

Figure. 5.24 show the variation of MRR with pulse-on time. The MRR decreasing with increasing the discharge current, it's possibly the constant duty factor and decreasing the flux density. The similar trend is also displayed by Panda et al. [170] and Shahane et al. [137] .

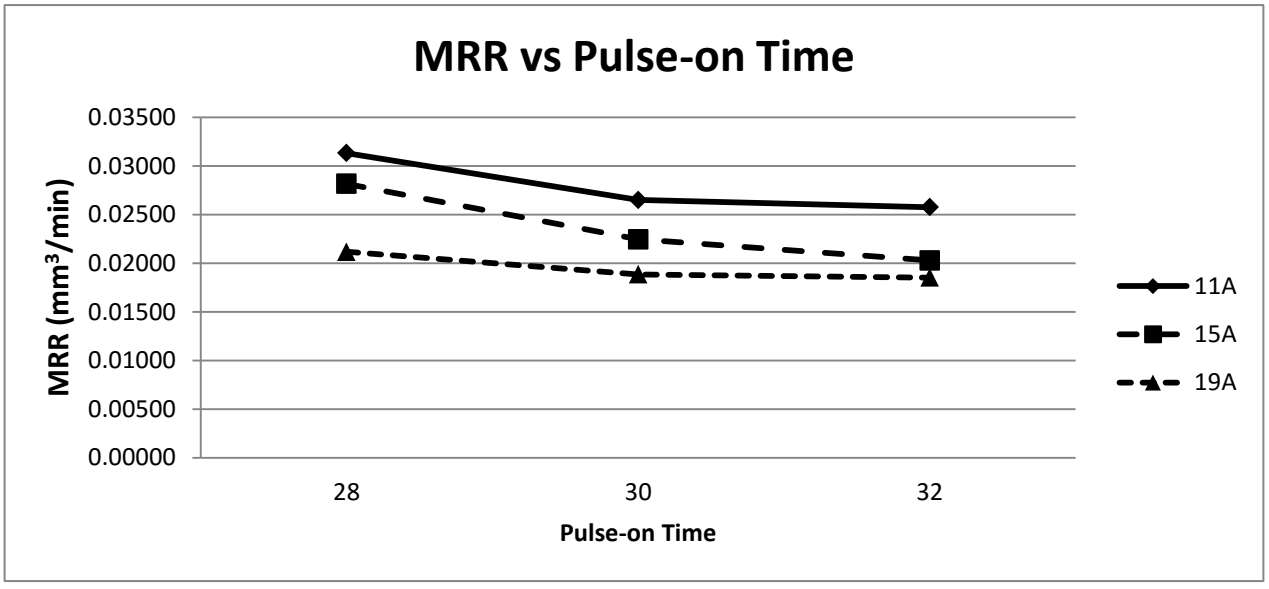


Figure 5.25 MRR vs Pulse-on Time

### *5.3.16 Concluding Remarks*

In this present work, WEDM multi-spark FEM model has been developed using ANSYS simulation software to predict the Material Removal Rate and residual stress on the workpiece. Models have been developed for single spark transient thermal heat transfer and modified with the multi-spark model.

***Thermal modelling***

- The numerical analysis result has been compared with the conducted experiments. It has been found that, the numerical analysis result has good agreement with the conducted experimental results. In this model many uncontrollable factors are affected such as Gaussian heat flux distribution, material properties and spark radius play critical role

***Residual Stress modelling***

- From the parametric studies it's have been observed that prediction of residual stress is helps the operators to go for robust machining operation. The maximum value of residual stress has been found in the subsurface instead of the top surface, which agrees with the different researchers conclusions. The low residual stress on surface attributed to the high surface roughness.

# Chapter 6

# 6. Conclusions, Thesis contributions and suggestions for Future work

## The contributions of the present dissertation have been summarized below.

- The present work provides a study on the influence of wire electrodes and effect of various process parameters on performance measures during different type of cutting such as straight cut, corner cut, V-shape cutting on Inconel 718 using WEDM process.
- Mathematical model has been developed using nonlinear regression model equation for analysis the effect of process parameters for obtaining better MRR, corner deviation and good surface roughness which improve the performance characteristics. A novel nature-inspired meta-heuristic optimization algorithm such as Whale Optimization Algorithm (WOA) has been used. The optimization results demonstrate that WOA is very competitive compared to Genetic algorithm on corner cutting.
- Evolutionary algorithm such as Gray Wolf Optimizer (GWO) has been used. These algorithms allow solving multi-objective and conflicting objective to be solved simultaneously. Using the non-linear regression find the better co-relation between the mathematical model and experimental on taper cutting have been found.
- A thermo-structure model finite element model (FEM) of WEDM process to predict the temperature distribution on Inconel 718 as workpiece. A new approach such as overlapping of multi-sparks has been adopted for finding out good agreement between numerical and experimental results. The residual stress has been predicted using this approach.

## Suggestions of future work have been pointed out below.

Based on the observation and finding in this study, the future works might be attempted to consider the other performance criteria proposed as follows:

- Heat affected zone, surface crack density and recast layer thickness of the machined surface have not been considered as process outputs. The effect of process parameter on these performance measures has not been studied.
- Present study mainly develops empirical models, optimization models and artificial intelligence models but mathematical or numerical approaches may be developed to substantiate the results obtained through experimental investigation.
- The present study is limited with the use of only brass wire and zinc coated brass wire electrode for different type of cutting.

# References


[1] M. Rahman, W. Seah,T. Teo, The machinability of Inconel 718, Journal of Materials Processing Technology. 63 (1997) 199-204.

[2] S. Datta,S. Mahapatra, Modeling, simulation and parametric optimization of wire EDM process using response surface methodology coupled with grey-Taguchi technique, International Journal of Engineering, Science and Technology. 2 (2010) 162-183.

[3] N. Tosun, C. Cogun,A. Inan, The effect of cutting parameters on workpiece surface roughness in wire EDM, Machining science and technology. 7 (2003) 209-219.

[4] R. Ramakrishnan,L. Karunamoorthy, Multi response optimization of wire EDM operations using robust design of experiments, The International Journal of Advanced Manufacturing Technology. 29 (2006) 105-112.

[5] A. Giridharan,G. Samuel, Modeling and analysis of crater formation during wire electrical discharge turning (WEDT) process, The International Journal of Advanced Manufacturing Technology. 77 (2015) 1229-1247.

[6] C. P. Mohanty, S. S. Mahapatra,M. R. Singh, A particle swarm approach for multi-objective optimization of electrical discharge machining process, Journal of Intelligent Manufacturing. (2014) 1-20.

[7] V. Aggarwal, S. S. Khangura,R. Garg, Parametric modeling and optimization for wire electrical discharge machining of Inconel 718 using response surface methodology, The International Journal of Advanced Manufacturing Technology. 79 (2015) 31-47.

[8] R. Ramakrishnan,L. Karunamoorthy, Performance studies of wire electro discharge machining (WEDM) of Inconel 718, International Journal of Materials and Product Technology. 35 (2009) 199-215.

[9] P. Kuppan, S. Narayanan,A. Rajadurai, Effect of process parameters on material removal rate and surface roughness in electric discharge drilling of Inconel 718 using graphite electrode, International Journal of Manufacturing Technology and Management. 23 (2011) 214-233.

[10] S. Abdulkareem, A. Ali Khan,M. Konneh, Cooling effect on electrode and process parameters in EDM, Materials and Manufacturing Processes. 25 (2010) 462-466.

[11] A. Golshan, D. Ghodsiyeh,S. Izman, Multi-objective optimization of wire electrical discharge machining process using evolutionary computation method: Effect of cutting variation, Proceedings of the Institution of Mechanical Engineers, Part B: Journal of Engineering Manufacture. (2014) 0954405414523593.

[12] J. Prohaszka, A. Mamalis,N. Vaxevanidis, The effect of electrode material on machinability in wire electro-discharge machining, Journal of materials processing technology. 69 (1997) 233-237.

[13] T. Muthuramalingam,B. Mohan, Influence of tool electrode properties on machinability in spark erosion machining, Materials and Manufacturing Processes. 28 (2013) 939-943.

[14] J. Kapoor, S. Singh,J. S. Khamba, High-performance wire electrodes for wire electrical-discharge machining, Proceedings of the Institution of Mechanical Engineers, Part B: Journal of Engineering Manufacture. (2012) 0954405412460354.

[15] S. Mahapatra,A. Patnaik, Optimization of wire electrical discharge machining (WEDM) process parameters using Taguchi method, The International Journal of Advanced Manufacturing Technology. 34 (2007) 911-925.

[16] S. Kuriakose,M. Shunmugam, Characteristics of wire-electro discharge machined Ti6Al4V surface, Materials Letters. 58 (2004) 2231-2237.
[17] D. Dauw,L. Albert, About the evolution of wire tool performance in wire EDM, CIRP Annals-Manufacturing Technology. 41 (1992) 221-225.
[18] J. Kapoor, S. Singh,J. S. Khamba, Recent developments in wire electrodes for high performance WEDM 2 (2010) 1-4.
[19] R. T. Yang, C. J. Tzeng, Y. K. Yang,M. H. Hsieh, Optimization of wire electrical discharge machining process parameters for cutting tungsten, The International Journal of Advanced Manufacturing Technology. 60 (2012) 135-147.
[20] R. Kern, TechTips Sinker Electrode Material Selection, EDM Today(July/August 2008 Issue), Reproduced with permission of the copyright owner. Further reproduction prohibited without permission.
[21] A. Ramamurthy, R. Sivaramakrishnan, T. Muthuramalingam,S. Venugopal, Performance Analysis of Wire Electrodes on Machining Ti-6Al-4V Alloy using Electrical Discharge Machining Process, Machining Science and Technology. 19 (2015) 577-592.
[22] C. Tzeng, Y. Yang, M. Hsieh,M. Jeng, Optimization of wire electrical discharge machining of pure tungsten using neural network and response surface methodology, Proceedings of the Institution of Mechanical Engineers, Part B: Journal of Engineering Manufacture. (2011) 09544054JEM2021.
[23] Y. Tarng, S. Ma,L. Chung, Determination of optimal cutting parameters in wire electrical discharge machining, International Journal of Machine Tools and Manufacture. 35 (1995) 1693-1701.
[24] M. Sadeghi, H. Razavi, A. Esmaeilzadeh,F. Kolahan, Optimization of cutting conditions in WEDM process using regression modelling and Tabu-search algorithm, Proceedings of the Institution of Mechanical Engineers, Part B: Journal of Engineering Manufacture. 225 (2011) 1825-1834.
[25] C.-T. Lin, I.-F. Chung,S.-Y. Huang, Improvement of machining accuracy by fuzzy logic at corner parts for wire-EDM, Fuzzy sets and systems. 122 (2001) 499-511.
[26] R. T. Yang, C. J. Tzeng, Y. K. Yang,M. H. Hsieh, Optimization of wire electrical discharge machining process parameters for cutting tungsten, The International Journal of Advanced Manufacturing Technology. 60 (2012) 135-147.
[27] R. Ramakrishnan,L. Karunamoorthy, Performance studies of wire electro discharge machining (WEDM) of Inconel 718, International Journal of Materials and Product Technology. 35 (2009) 199-215.
[28] R. Ramakrishnan,L. Karunamoorthy, Modeling and multi-response optimization of Inconel 718 on machining of CNC WEDM process, Journal of materials processing technology. 207 (2008) 343-349.
[29] W. Hsue, Y. Liao,S. Lu, Fundamental geometry analysis of wire electrical discharge machining in corner cutting, International Journal of Machine Tools and Manufacture. 39 (1999) 651-667.
[30] F. Han, J. Zhang,I. Soichiro, Corner error simulation of rough cutting in wire EDM, Precision engineering. 31 (2007) 331-336.
[31] J. Sanchez, J. Rodil, A. Herrero, L. L. De Lacalle,A. Lamikiz, On the influence of cutting speed limitation on the accuracy of wire-EDM corner-cutting, Journal of materials processing technology. 182 (2007) 574-579.

[32] F. Han, G. Cheng, Z. Feng,S. Isago, Thermo-mechanical analysis and optimal tension control of micro wire electrode, International Journal of Machine Tools and Manufacture. 48 (2008) 922-931.
[33] O. Dodun, A. M. Gonçalves-Coelho, L. Slătineanu,G. Nagîţ, Using wire electrical discharge machining for improved corner cutting accuracy of thin parts, The International Journal of Advanced Manufacturing Technology. 41 (2009) 858-864.

[34] D. Ghodsiyeh, A. Golshan,S. Izman, Multi-objective process optimization of wire electrical discharge machining based on response surface methodology, Journal of the Brazilian Society of Mechanical Sciences and Engineering. 36 (2014) 301-313.
[35] A. Golshan, D. Ghodsiyeh,S. Izman, Multi-objective optimization of wire electrical discharge machining process using evolutionary computation method: Effect of cutting variation, Proceedings of the Institution of Mechanical Engineers, Part B: Journal of Engineering Manufacture. (2014) 0954405414523593.
[36] D. Poroś,S. Zaborski, Semi-empirical model of efficiency of wire electrical discharge machining of hard-to-machine materials, Journal of materials processing technology. 209 (2009) 1247-1253.
[37] J. Prohaszka, A. Mamalis,N. Vaxevanidis, The effect of electrode material on machinability in wire electro-discharge machining, Journal of materials processing technology. 69 (1997) 233-237.
[38] M. Antar, S. Soo, D. Aspinwall, D. Jones,R. Perez, Productivity and workpiece surface integrity when WEDM aerospace alloys using coated wires, Procedia Engineering. 19 (2011) 3-8.
[39] A. Ramamurthy, R. Sivaramakrishnan, T. Muthuramalingam,S. Venugopal, Performance Analysis of Wire Electrodes on Machining Ti-6Al-4V Alloy using Electrical Discharge Machining Process, Machining Science and Technology. 19 (2015) 577-592.
[40] C. P. Mohanty, S. S. Mahapatra,M. R. Singh, A particle swarm approach for multi-objective optimization of electrical discharge machining process, Journal of Intelligent Manufacturing. (2014) 1-20.
[41] T. Muthuramalingam,B. Mohan, Influence of tool electrode properties on machinability in spark erosion machining, Materials and Manufacturing Processes. 28 (2013) 939-943.
[42] J. Kapoor, S. Singh,J. S. Khamba, Recent developments in wire electrodes for high performance WEDM 2 (2010) 1-4.
[43] D. Dauw,L. Albert, About the evolution of wire tool performance in wire EDM, CIRP Annals-Manufacturing Technology. 41 (1992) 221-225.
[44] S. Kuriakose,M. Shunmugam, Characteristics of wire-electro discharge machined Ti6Al4V surface, Materials Letters. 58 (2004) 2231-2237.
[45] R. Kern, TechTips Sinker Electrode Material Selection, EDM Today(July/August 2008 Issue), Reproduced with permission of the copyright owner. Further reproduction prohibited without permission.
[46] Y. Tarng, S. Ma,L. Chung, Determination of optimal cutting parameters in wire electrical discharge machining, International Journal of Machine Tools and Manufacture. 35 (1995) 1693-1701.
[47] M. Sadeghi, H. Razavi, A. Esmaeilzadeh,F. Kolahan, Optimization of cutting conditions in WEDM process using regression modelling and Tabu-search algorithm, Proceedings of

the Institution of Mechanical Engineers, Part B: Journal of Engineering Manufacture. 225 (2011) 1825-1834.
[48] N. Sharma, R. Khanna, R. D. Gupta,R. Sharma, Modeling and multiresponse optimization on WEDM for HSLA by RSM, The International Journal of Advanced Manufacturing Technology. 67 (2013) 2269-2281.
[49] Antar, M., S. Soo, D. Aspinwall, D. Jones and R. Perez 2011. "Productivity and workpiece surface integrity when WEDM aerospace alloys using coated wires." *Procedia Engineering* 19(3-8.
[50] Bharti, P. S., S. Maheshwari and C. Sharma 2012. "Multi-objective optimization of electric-discharge machining process using controlled elitist NSGA-II." *Journal of Mechanical Science and Technology* 26(6): 1875-1883.
[51] Cus, F. and J. Balic 2003. "Optimization of cutting process by GA approach." *Robotics and Computer-Integrated Manufacturing* 19(1): 113-121.
[52] Dabade, U. and S. Karidkar 2016. "Analysis of Response Variables in WEDM of Inconel 718 Using Taguchi Technique." *Procedia CirP* 41(886-891.
[53] Dey, S. and S. Chakraborty 2015. "Forward and Reverse Mapping for WEDM Process using Artificial Neural Networks." *Decision Science Letters* 4(3): 277-288.
[54] Dodun, O., A. M. Gonçalves-Coelho, L. Slătineanu and G. Nagîţ 2009. "Using wire electrical discharge machining for improved corner cutting accuracy of thin parts." *The International Journal of Advanced Manufacturing Technology* 41(9-10): 858-864.
[55] Golshan, A., D. Ghodsiyeh and S. Izman 2014. "Multi-objective optimization of wire electrical discharge machining process using evolutionary computation method: Effect of cutting variation." *Proceedings of the Institution of Mechanical Engineers, Part B: Journal of Engineering Manufacture*: 0954405414523593.
[56] Han, F., J. Zhang and I. Soichiro 2007. "Corner error simulation of rough cutting in wire EDM." *Precision Engineering* 31(4): 331-336.
[57] Hsue, W. and Y. Liao 1999. "A study of corner control strategy of wire-EDM based on quantitative MRR analysis." *International journal of electrical machining* 4(33-39.
[58] Kapoor, J., S. Singh and J. S. Khamba 2012. "High-performance wire electrodes for wire electrical-discharge machining." *Proceedings of the Institution of Mechanical Engineers, Part B: Journal of Engineering Manufacture*: 0954405412460354.
[59] Kapoor, J., S. Singh and J. S. Khamba 2010. "Recent developments in wire electrodes for high performance WEDM." *Proceedings of the world congress on engineering* 2(1-4.
[60] Kuriakose, S. and M. Shunmugam 2004. "Characteristics of wire-electro discharge machined Ti6Al4V surface." *Materials Letters* 58(17): 2231-2237.
[61] Mirjalili, S. and A. Lewis 2016. "The Whale Optimization Algorithm." *Advances in Engineering Software* 95(51-67.
[62] Mohanty, C. P., S. S. Mahapatra and M. R. Singh 2014. "A particle swarm approach for multi-objective optimization of electrical discharge machining process." *Journal of Intelligent Manufacturing*: 1-20.
[63] Padhi, P., S. Mahapatra, S. Yadav and D. Tripathy 2016. "Multi-Objective Optimization of Wire Electrical Discharge Machining (WEDM) Process Parameters Using Weighted Sum Genetic Algorithm Approach." *Journal of Advanced Manufacturing Systems* 15(02): 85-100.

[64] Prohaszka, J., A. Mamalis and N. Vaxevanidis 1997. "The effect of electrode material on machinability in wire electro-discharge machining." *Journal of Materials Processing Technology* 69(1): 233-237.
[65] Puri, A. and B. Bhattacharyya 2003. "An analysis and optimisation of the geometrical inaccuracy due to wire lag phenomenon in WEDM." *International Journal of Machine Tools and Manufacture* 43(2): 151-159.
[66] Sadeghi, M., H. Razavi, A. Esmaeilzadeh and F. Kolahan 2011. "Optimization of cutting conditions in WEDM process using regression modelling and Tabu-search algorithm." *Proceedings of the Institution of Mechanical Engineers, Part B: Journal of Engineering Manufacture* 225(10): 1825-1834.
[67] Sanchez, J., J. Rodil, A. Herrero, L. L. de Lacalle and A. Lamikiz 2007. "On the influence of cutting speed limitation on the accuracy of wire-EDM corner-cutting." *Journal of Materials Processing Technology* 182(1): 574-579.
[68] Sanchez, J. A., L. N. López de Lacalle and A. Lamikiz 2004. "A computer-aided system for the optimization of the accuracy of the wire electro-discharge machining process." *International Journal of Computer Integrated Manufacturing* 17(5): 413-420.
[69] Senthilkumaar, J., P. Selvarani and R. Arunachalam 2012. "Intelligent optimization and selection of machining parameters in finish turning and facing of Inconel 718." *The International Journal of Advanced Manufacturing Technology* 58(9-12): 885-894.
[70] Spedding, T. A. and Z. Wang 1997. "Parametric optimization and surface characterization of wire electrical discharge machining process." *Precision Engineering* 20(1): 5-15.
[71] Tarng, Y., S. Ma and L. Chung 1995. "Determination of optimal cutting parameters in wire electrical discharge machining." *International Journal of Machine Tools and Manufacture* 35(12): 1693-1701.
[72] Tosun, N. and C. Cogun 2003. "Analysis of wire erosion and workpiece surface roughness in wire electrical discharge machining." *Proceedings of the Institution of Mechanical Engineers, Part B: Journal of Engineering Manufacture* 217(5): 633-642.
[73] Yang, R. T., C. J. Tzeng, Y. K. Yang and M. H. Hsieh 2012. "Optimization of wire electrical discharge machining process parameters for cutting tungsten." *The International Journal of Advanced Manufacturing Technology* 60(1-4): 135-147.
[74] S. Plaza, N. Ortega, J. Sanchez, I. Pombo,A. Mendikute, Original models for the prediction of angular error in wire-EDM taper-cutting, The International Journal of Advanced manufacturing Technology. 44 (2009) 529-538.
[75] D. Dauw,I. Beltrami, High-precision wire-EDM by online wire positioning control, CIRP Annals-Manufacturing Technology. 43 (1994) 193-197; F. Han, M. Kunieda, T. Sendai,Y. Imai, Simulation on influence of electrostatic force on machining characteristics in WEDM, International journal of electrical machining. 7 (2002) 31-36.
[76] J. Sanchez, S. Plaza, N. Ortega, M. Marcos,J. Albizuri, Experimental and numerical study of angular error in wire-EDM taper-cutting, International Journal of Machine Tools and Manufacture. 48 (2008) 1420-1428.
[77] B. B. Nayak,S. S. Mahapatra, Trans Tech Publ A Hybrid Approach for Process Optimization in Taper Cutting Operation Using Wire Electrical Discharge Machining 619 (2014) 83-88.

[78] J. A. Sanchez, S. Plaza, L. Lopez de Lacalle,A. Lamikiz, Computer simulation of wire-EDM taper-cutting, International Journal of Computer Integrated Manufacturing. 19 (2006) 727-735.
[79] B. B. Nayak,S. S. Mahapatra, Springer A Quantum Behaved Particle Swarm Approach for Multi-response Optimization of WEDM Process (2014) 62-73.
[80] K. Jangra, S. Grover,A. Aggarwal, Simultaneous optimization of material removal rate and surface roughness for WEDM of WC-Co composite using grey relational analysis along with Taguchi method, International Journal of Industrial Engineering Computations. 2 (2011) 479-490.
[81] B. B. Nayak,S. S. Mahapatra, Optimization of WEDM process parameters using deep cryo-treated Inconel 718 as work material, Engineering Science and Technology, an International Journal. 19 (2016) 161-170.
[82] B. Ravani,J. Wang, Computer aided geometric design of line constructs, Journal of Mechanical Design. 113 (1991) 363-371.
[83] F. Cus,J. Balic, Optimization of cutting process by GA approach, Robotics and Computer-Integrated Manufacturing. 19 (2003) 113-121.
[84] J. Senthilkumaar, P. Selvarani,R. Arunachalam, Intelligent optimization and selection of machining parameters in finish turning and facing of Inconel 718, The International Journal of Advanced Manufacturing Technology. 58 (2012) 885-894.
[85] S. Mirjalili, S. M. Mirjalili,A. Lewis, Grey wolf optimizer, Advances in Engineering Software. 69 (2014) 46-61.
[86] C. Muro, R. Escobedo, L. Spector,R. Coppinger, Wolf-pack (Canis lupus) hunting strategies emerge from simple rules in computational simulations, Behavioural processes. 88 (2011) 192-197.
[87] C. P. Mohanty, S. S. Mahapatra,M. R. Singh, A particle swarm approach for multi-objective optimization of electrical discharge machining process, Journal of Intelligent Manufacturing. (2014) 1-20.
[88] R. T. Yang, C. J. Tzeng, Y. K. Yang,M. H. Hsieh, Optimization of wire electrical discharge machining process parameters for cutting tungsten, The International Journal of Advanced Manufacturing Technology. 60 (2012) 135-147.
[89] G. Selvakumar, S. Sarkar,S. Mitra, Experimental investigation on die corner accuracy for wire electrical discharge machining of Monel 400 alloy, Proceedings of the Institution of Mechanical Engineers, Part B: Journal of Engineering Manufacture. 226 (2012) 1694-1704.
[90] J. Sanchez, J. Rodil, A. Herrero, L. L. De Lacalle,A. Lamikiz, On the influence of cutting speed limitation on the accuracy of wire-EDM corner-cutting, Journal of materials processing technology. 182 (2007) 574-579.
[91] S. Sarkar, M. Sekh, S. Mitra,B. Bhattacharyya, Modeling and optimization of wire electrical discharge machining of γ-TiAl in trim cutting operation, Journal of materials processing technology. 205 (2008) 376-387.
[92] A. Puri,B. Bhattacharyya, An analysis and optimisation of the geometrical inaccuracy due to wire lag phenomenon in WEDM, International journal of Machine tools and manufacture. 43 (2003) 151-159.
[93] W. Hsue, Y. Liao,S. Lu, Fundamental geometry analysis of wire electrical discharge machining in corner cutting, International Journal of Machine Tools and Manufacture. 39 (1999) 651-667.

[94] M.-T. Yan,P.-H. Huang, Accuracy improvement of wire-EDM by real-time wire tension control, International Journal of Machine Tools and Manufacture. 44 (2004) 807-814.
[95] F. Han, J. Zhang,I. Soichiro, Corner error simulation of rough cutting in wire EDM, Precision engineering. 31 (2007) 331-336.
[96] A. Golshan, D. Ghodsiyeh,S. Izman, Multi-objective optimization of wire electrical discharge machining process using evolutionary computation method: Effect of cutting variation, Proceedings of the Institution of Mechanical Engineers, Part B: Journal of Engineering Manufacture. (2014) 0954405414523593.
[97] S. Kuriakose,M. Shunmugam, Characteristics of wire-electro discharge machined Ti6Al4V surface, Materials Letters. 58 (2004) 2231-2237.
[98] M. Antar, S. Soo, D. Aspinwall, D. Jones,R. Perez, Productivity and workpiece surface integrity when WEDM aerospace alloys using coated wires, Procedia Engineering. 19 (2011) 3-8.
[99] C. P. Mohanty, S. S. Mahapatra,M. R. Singh, A particle swarm approach for multi-objective optimization of electrical discharge machining process, Journal of Intelligent Manufacturing. (2014) 1-20.
[100] R. T. Yang, C. J. Tzeng, Y. K. Yang,M. H. Hsieh, Optimization of wire electrical discharge machining process parameters for cutting tungsten, The International Journal of Advanced Manufacturing Technology. 60 (2012) 135-147.
[101] J. Prohaszka, A. Mamalis,N. Vaxevanidis, The effect of electrode material on machinability in wire electro-discharge machining, Journal of materials processing technology. 69 (1997) 233-237.
[102] T. Muthuramalingam,B. Mohan, Influence of tool electrode properties on machinability in spark erosion machining, Materials and Manufacturing Processes. 28 (2013) 939-943.
[103] J. Kapoor, S. Singh,J. S. Khamba, Recent developments in wire electrodes for high performance WEDM 2 (2010) 1-4.
[104] D. Dauw,L. Albert, About the evolution of wire tool performance in wire EDM, CIRP Annals-Manufacturing Technology. 41 (1992) 221-225.
[105] R. Kern, TechTips Sinker Electrode Material Selection, EDM Today(July/August 2008 Issue), Reproduced with permission of the copyright owner. Further reproduction prohibited without permission.
[106] A. Ramamurthy, R. Sivaramakrishnan, T. Muthuramalingam,S. Venugopal, Performance Analysis of Wire Electrodes on Machining Ti-6Al-4V Alloy using Electrical Discharge Machining Process, Machining Science and Technology. 19 (2015) 577-592.
[107] C. Tzeng, Y. Yang, M. Hsieh,M. Jeng, Optimization of wire electrical discharge machining of pure tungsten using neural network and response surface methodology, Proceedings of the Institution of Mechanical Engineers, Part B: Journal of Engineering Manufacture. (2011) 09544054JEM2021.
[108] Y. Tarng, S. Ma,L. Chung, Determination of optimal cutting parameters in wire electrical discharge machining, International Journal of Machine Tools and Manufacture. 35 (1995) 1693-1701.
[109] M. Sadeghi, H. Razavi, A. Esmaeilzadeh,F. Kolahan, Optimization of cutting conditions in WEDM process using regression modelling and Tabu-search algorithm, Proceedings of the Institution of Mechanical Engineers, Part B: Journal of Engineering Manufacture. 225 (2011) 1825-1834.

[110] C.-T. Lin, I.-F. Chung,S.-Y. Huang, Improvement of machining accuracy by fuzzy logic at corner parts for wire-EDM, Fuzzy sets and systems. 122 (2001) 499-511.
[111] N. Tosun, C. Cogun,A. Inan, The effect of cutting parameters on workpiece surface roughness in wire EDM, Machining science and technology. 7 (2003) 209-219.
[112] R. Ramakrishnan,L. Karunamoorthy, Multi response optimization of wire EDM operations using robust design of experiments, The International Journal of Advanced Manufacturing Technology. 29 (2006) 105-112.
[113] Anand, K. (1996). "Development of process technology in wire-cut operation for improving machining quality." Total Quality Management 7(1): 11-28.
[114] Ayesta, I., et al. (2016). "Influence of the WEDM process on the fatigue behavior of Inconel® 718." International Journal of Fatigue 92: 220-233.
[115] Chalisgaonkar, R. and J. Kumar (2016). "Investigation of the machining parameters and integrity of the work and wire surfaces after finish cut WEDM of commercially pure titanium." Journal of the Brazilian Society of Mechanical Sciences and Engineering 38(3): 883-911.

[116] Dabade, U. and S. Karidkar (2016). "Analysis of Response Variables in WEDM of Inconel 718 Using Taguchi Technique." Procedia CIRP 41: 886-891.

[117] Galindo-Fernandez, M., et al. (2016). "The Prediction of Surface Finish and Cutting Speed for Wire Electro-Discharge Machining of Polycrystalline Diamond." Procedia CIRP 42: 297-304.

[118] Gökler, M. I. l. and A. M. Ozanözgü (2000). "Experimental investigation of effects of cutting parameters on surface roughness in the WEDM process." International Journal of Machine Tools and Manufacture 40(13): 1831-1848.

[119] Golshan, A., et al. (2014). "Multi-objective optimization of wire electrical discharge machining process using evolutionary computation method: Effect of cutting variation." Proceedings of the Institution of mechanical engineers, Part B: Journal of engineering manufacture: 0954405414523593.

[120] Gong, Y., et al. (2016). "Experimental study on surface integrity of Ti-6Al-4V machined by LS-WEDM." The International Journal of Advanced Manufacturing Technology: 1-11.

[121] Gong, Y., et al. (2016). "Experimental study on accuracy and surface quality of TC2 in LS-WEDM multiple cuts." Journal of the Brazilian Society of Mechanical Sciences and Engineering: 1-13.

[122] Goswami, A. and J. Kumar (2014). "Optimization in wire-cut EDM of Nimonic-80A using Taguchi's approach and utility concept." Engineering Science and Technology, an International Journal 17(4): 236-246.

[123] Han, F., et al. (2007). "Influence of machining parameters on surface roughness in finish cut of WEDM." The International Journal of Advanced Manufacturing Technology 34(5-6): 538-546.

[124] Hewidy, M., et al. (2005). "Modelling the machining parameters of wire electrical discharge machining of Inconel 601 using RSM." Journal of Materials Processing Technology 169(2): 328-336.

[125] Hsue, W., et al. (1999). "Fundamental geometry analysis of wire electrical discharge machining in corner cutting." International Journal of Machine Tools and Manufacture 39(4): 651-667.

[126] Huang, J.-T. and Y.-S. Liao (2003). "Optimization of machining parameters of wire-EDM based on grey relational and statistical analyses." International Journal of Production Research 41(8): 1707-1720.

[127] Ikram, A., et al. (2013). "Parametric optimization for surface roughness, kerf and MRR in wire electrical discharge machining (WEDM) using Taguchi design of experiment." Journal of Mechanical Science and Technology 27(7): 2133-2141.

[128] Kanlayasiri, K. and S. Boonmung (2007). "Effects of wire-EDM machining variables on surface roughness of newly developed DC 53 die steel: Design of experiments and regression model." Journal of Materials Processing Technology 192: 459-464.

[129] Kanlayasiri, K. and S. Boonmung (2007). "An investigation on effects of wire-EDM machining parameters on surface roughness of newly developed DC53 die steel." Journal of Materials Processing Technology 187: 26-29.

[130] Kozak, J., et al. (2004). "Machining of low electrical conductive materials by wire electrical discharge machining (WEDM)." Journal of Materials Processing Technology 149(1): 266-271.

[131] Kumar, A., et al. (2013). "Investigation of machining parameters and surface integrity in wire electric discharge machining of pure titanium." Proceedings of the Institution of mechanical engineers, Part B: Journal of engineering manufacture 227(7): 972-992.

[132] Kumar, A., et al. (2014). "Surface integrity and material transfer investigation of pure titanium for rough cut surface after wire electro discharge machining." Proceedings of the Institution of mechanical engineers, Part B: Journal of engineering manufacture 228(8): 880-901.

[133] Kumar, K. and S. Agarwal (2012). "Multi-objective parametric optimization on machining with wire electric discharge machining." The International Journal of Advanced Manufacturing Technology 62(5-8): 617-633.

[134] Kung, K.-Y. and K.-T. Chiang (2008). "Modeling and analysis of machinability evaluation in the wire electrical discharge machining (WEDM) process of aluminum oxide-based ceramic." Materials and Manufacturing Processes 23(3): 241-250.

[135] Kunieda, M. and C. Furudate (2001). "High precision finish cutting by dry WEDM." CIRP Annals-Manufacturing Technology 50(1): 121-124.

[136] Kuriakose, S. and M. Shunmugam (2005). "Multi-objective optimization of wire-electro discharge machining process by non-dominated sorting genetic algorithm." Journal of Materials Processing Technology 170(1): 133-141.

[137] Liao, Y., et al. (2004). "A study to achieve a fine surface finish in Wire-EDM." Journal of Materials Processing Technology 149(1): 165-171.

[138] Liao, Y., et al. (1997). "A study on the machining-parameters optimization of wire electrical discharge machining." Journal of Materials Processing Technology 71(3): 487-493.

[139] Lin, C., et al. (2002). "Optimisation of the EDM process based on the orthogonal array with fuzzy logic and grey relational analysis method." The International Journal of Advanced Manufacturing Technology 19(4): 271-277.

[140] Lin, J. and C. Lin (2002). "The use of the orthogonal array with grey relational analysis to optimize the electrical discharge machining process with multiple performance characteristics." International Journal of Machine Tools and Manufacture 42(2): 237-244.

[141] Mahapatra, S. and A. Patnaik (2007). "Optimization of wire electrical discharge machining (WEDM) process parameters using Taguchi method." The International Journal of Advanced Manufacturing Technology 34(9-10): 911-925.

[142] Mahapatra, S. S. and A. Patnaik (2006). "Parametric optimization of wire electrical discharge machining (WEDM) process using Taguchi method." Journal of the Brazilian Society of Mechanical Sciences and Engineering 28(4): 422-429.

[143] Mandal, A., et al. (2016). "Modeling and Optimization of Machining Nimonic C-263 Superalloy using Multicut Strategy in WEDM." Materials and Manufacturing Processes 31(7): 860-868.

[144] Mukherjee, R., et al. (2012). "Selection of wire electrical discharge machining process parameters using non-traditional optimization algorithms." Applied Soft Computing 12(8): 2506-2516.

[145] Muthukumar, V., et al. (2015). "An accelerated particle swarm optimization algorithm on parametric optimization of WEDM of die-steel." Journal of The Institution of Engineers (India): Series C 96(1): 49-56.

[146] Muthuraman, V., et al. (2012). "Influences of process variables during Wire Electric Discharge Machining of O1 steel." European Journal of Scientific Research 79(3): 2371-2377.

[147] Padhi, P., et al. (2016). "Multi-Objective Optimization of Wire Electrical Discharge Machining (WEDM) Process Parameters Using Weighted Sum Genetic Algorithm Approach." Journal of Advanced Manufacturing Systems 15(02): 85-100.

[148] Pasam, V. K., et al. (2010). "Optimizing surface finish in WEDM using the Taguchi parameter design method." Journal of the Brazilian Society of Mechanical Sciences and Engineering 32(2): 107-113.

[149] Plaza, S., et al. (2009). "Original models for the prediction of angular error in wire-EDM taper-cutting." The International Journal of Advanced Manufacturing Technology 44(5-6): 529-538.

[150] Puertas, I. and C. Luis (2003). "A study on the machining parameters optimisation of electrical discharge machining." Journal of Materials Processing Technology 143: 521-526.

[151] Puertas, I. and C. L. Perez (2003). "Modelling the manufacturing parameters in electrical discharge machining of siliconized silicon carbide." Proceedings of the Institution of mechanical engineers, Part B: Journal of engineering manufacture 217(6): 791-803.

[152] Puri, A. and B. Bhattacharyya (2003). "An analysis and optimisation of the geometrical inaccuracy due to wire lag phenomenon in WEDM." International Journal of Machine Tools and Manufacture 43(2): 151-159.

[153] Rajurkar, K. P. and W. Wang (1993). "Thermal modeling and on-line monitoring of wire-EDM." Journal of Materials Processing Technology 38(1): 417-430.

[154] Ramakrishnan, R. and L. Karunamoorthy (2006). "Multi response optimization of wire EDM operations using robust design of experiments." The International Journal of Advanced Manufacturing Technology 29(1-2): 105-112.

[155] Ramakrishnan, R. and L. Karunamoorthy (2008). "Modeling and multi-response optimization of Inconel 718 on machining of CNC WEDM process." Journal of Materials Processing Technology 207(1): 343-349.

[156] Sadeghi, M., et al. (2011). "Optimization of cutting conditions in WEDM process using regression modelling and Tabu-search algorithm." Proceedings of the Institution of mechanical engineers, Part B: Journal of engineering manufacture 225(10): 1825-1834.

[157] Saha, P., et al. (2008). "Soft computing models based prediction of cutting speed and surface roughness in wire electro-discharge machining of tungsten carbide cobalt composite." The International Journal of Advanced Manufacturing Technology 39(1-2): 74-84.

[158] Sanchez, J., et al. (2008). "Experimental and numerical study of angular error in wire-EDM taper-cutting." International Journal of Machine Tools and Manufacture 48(12): 1420-1428.

[159] Sanchez, J. A., et al. (2006). "Computer simulation of wire-EDM taper-cutting." International Journal of Computer Integrated Manufacturing 19(7): 727-735.

[160] Sarkar, S., et al. (2005). "Parametric analysis and optimization of wire electrical discharge machining of γ-titanium aluminide alloy." Journal of Materials Processing Technology 159(3): 286-294.